Kenady, Selene L. (2016) ***Geophysical explorations of archaeological shell matrix sites: evaluating geophysical techniques in determining the boundaries, structure and volume of buried shell deposits*****. PhD thesis, James Cook University.**

Geophysical Explorations of Archaeological Shell Matrix Sites: Evaluating Geophysical Techniques in Determining the Boundaries, Structure and Volume of Buried Shell Deposits

Selene L. Kenady

BA (Hons), MArchSci

A thesis submitted for the degree of Doctor of Philosophy, College of Arts, Society and Education, James Cook University, Cairns

December 2016

ACKNOWLEDGEMENTS

This thesis was made possible with the help of many people.

To begin with, there are those people who started me down the path of geophysics. The first and most pivotal was Lawrence Conyers (University of Denver) who started my training in ground-penetrating radar. Then thanks go to Ian Moffat (Flinders University) for further training in geophysical methods. Lastly thanks go to James Cook University (JCU) staff: Peter Ridd, James Whinney, Mel Boer and Sean Campbell for training me to use the electrical resistivity array held at JCU.

Thanks go to those who helped me in the field. Anna Kreij, Sarah Slater (and Alex), and Sean Ulm for helping with the site clearing, geophysical surveys and excavation at Thundiy in 2014. With further thanks to Emma Oliver and Daniel Rosendahl for site clearing and to Daniel for excavation help, and lastly Robin Twaddle for survey help in 2014. Thanks to Kelsey Lowe for survey guidance and mentoring in 2013. Thanks to Lincoln Steinberger for RTK surveying and subsequent map creation in both 2013 and 2014. Lastly a special thanks to Duncan Kelly for supporting us and sharing his country with us.

For help with the experimental site on the Cairns campus of JCU, I'd like to first thank the team from Cairns Ocean Products and the team from Preston Fresh for supplying the many, many, oyster shells that made this research possible. Further thanks go to Sean Ulm, Sarah Slater, Texas Nagel, Robin Twaddle, Christian Reepmeyer, Samantha Aird, Sam Lansdown, Redbird Ferguson, Emma Rehn, Djerami Callope, Alice Buhrich, Tanya Drury, Graeme Cotter, Brian Kenady, Joshua Neilson and the 2013 and 2014 AR3008 classes for helping dig big holes, shovelling sand and garden mix, and generally helping with the experimental trench set up. With extra thanks going to Helene Peck, Sarah Slater and Robin Twaddle for counting the first 5000 shells with me. A special thanks to Bev Rankine for feeding the hungry troops. And lastly, thanks to Paul Nelson (JCU) for loaning me the supplies and the know how to conduct the soil moisture content analysis for the experimental site, and to Shannon Todd (JCU) for advice and supervision operating the oven.

Thank you to the kind JCU staff that helped get me through the administrative details of a PhD: Dominique Sandilant, Sharyn Harrington, Mark Chong, and Maree Searston. Thanks also to those JCU staff that helped with my technological inquires: Christian Reepmeyer for helping with specific issues I was encountering in ArcGIS, Karen Joyce for allowing me to sit in on her ArcGIS subject and Margo Dean for saving me multiple times by finding ways to meet my odd technology needs. A special thanks also goes to Liz Tynan (JCU) for her academic writing seminar series, which improved my writing skills considerably.

Lastly and most personally, my thanks goes to the four people who made my PhD more bearable. The first is my husband, Brian Kenady, for being here for me. The second is

Anna Kreij for providing my day with joy during some very stressful field work. The third is Matt Leavesley who had to emotionally pick me up several times and reassure me that I was not as hopeless as I felt. The final person is Sean Ulm, for whom I am not eloquent enough to truly express just how much he has supported me nor how greatly that support has been appreciated.

CONTRIBUTION BY OTHERS

Scholarship Stipend:
This research was supported by an Australian Postgraduate Award Scholarship.

Project Funding:
This research was supported under Australian Research Council's Discovery Projects funding scheme (project number DP120103179).

Collaboration with Traditional Owners:
We acknowledge the Kaiadilt traditional owners of the South Wellesley Islands as research partners. The Kaiadilt Aboriginal Corporation collaborated in establishing the research framework for this project, which was formalised in an Agreement between the Kaiadilt Aboriginal Corporation and Kaiadilt Aboriginal Land Trust and James Cook University. This research was approved by the James Cook University (JCU) Human Research Ethics Committee (Human Ethics Approval Number: H4454).

Supervision:
Professor Sean Ulm (JCU) provided supervisory support covering research design, survey strategy and editorial assistance.

Professor Peter Ridd (JCU) provided supervisory support covering editorial assistance, survey strategy and training in the use of electrical resistivity as well as advice regarding the interpretation of survey results.

Dr Kelsey Lowe (University of Queensland) provided supervisory support covering editorial assistance, survey strategy and advice regarding interpretation of GPR results.

Dr Matthew Leavesley (University of Papua New Guinea) provided supervisory support covering editorial assistance.

Research Assistance:
Dr Lincoln Steinberger (University of Queensland) provided RTK mapping of the Thundiy field site and geophysical survey grid (2013 and 2014).

Dr Michelle Langley (Australian National University) and Professor Sean Ulm (JCU) provided stratigraphic section drawings for Thundiy.

Research Proposal:
Professor Lawrence Conyers (University of Denver) provided the initial research plan of creating a volume estimate for buried shell deposits.

Copyright Permissions:
Every reasonable effort has been made to gain permission and acknowledge the owners of copyright material. I would be pleased to hear from any copyright owner who has been omitted or incorrectly acknowledged.

Where figures or tables appear in the text without reference to a third party they have been produced solely by the Author.

Images were reproduced in this dissertation with permissions from corporate groups: Cambridge University Press https://doi.org/10.1017/S0003598X00084647, James Cook University, John Benjamins Publishing Company https://www.benjamins.com/#catalog/books/clu.18/main, Oxford Journals and the South Australian Museum.

Further corporate copyright permissions were obtained through Copyright Clearance Center, Inc. for: ABC-CLIO Inc., AltaMira Press, Elsevier http://www.sciencedirect.com/science/journal/xxxxx, John Wiley and Sons, Routledge: Taylor and Francis and Sage.

Copyright permissions from individual authors were obtained from: A. Best, C. Conyers, R.A. Dalan, T.J. Pluckhahn and V.D. Thompson.

RESEARCH CLASSIFICATION CODES

Field of Research (FoR)

210101 (Aboriginal and Torres Strait Islander Archaeology)	25%
210102 (Archaeological Science)	50%
040401 (Electrical and Electromagnetic Methods in Geophysics)	25%

Socio-Economic Objectives (SEO)

950503 (Understanding Australia's Past)	40%
970121 (Expanding Knowledge in History and Archaeology)	50%
970104 (Expanding Knowledge in the Earth Sciences)	10%

JCU Research Themes

People and Societies in the Tropics	100%

Keywords

Geophysics

Shell Matrix

Ground-Penetrating Radar

Electrical Resistivity

Australian

Archaeology

SUPPLEMENTARY DATA

Supplementary data including raw geophysical survey files can be found at:

http://dx.doi.org/10.4225/28/584755108d3dc

Statement of Access

I, the undersigned, the author of this thesis, understand that James Cook University will make the thesis available for use within the University Library and, by microfilm, photographic or digital means, allow access to users in other approved libraries. All users consulting the thesis will have to sign the following statement:

"In consulting this thesis, I agree not to copy or closely paraphrase it in whole or in part without the written consent of the author; and to make proper written acknowledgment for any assistance that I have obtained from it."

Beyond this, I do not wish to place any restriction on access to this thesis.

13 December 2016

(Signature) (Date)

Declaration of Sources

To the best of my knowledge, I declare that this thesis is my own work and has not been submitted in any form for another degree or diploma at any university or other institution of tertiary education. Information derived from the published or unpublished work of others has been acknowledged above and in the text and a list of references is given.

Every reasonable effort has been made to gain permission and acknowledge the owners of copyright material. I would be pleased to hear from any copyright owner who has been omitted or incorrectly acknowledged.

13 December 2016

(Signature) (Date)

ABSTRACT

Shell middens are a significant component of the Australian coastal archaeological record, however, they are notoriously difficult to research. Shell matrix sites are often large and structurally heterogeneous with complex formation histories. For large stratified shell matrix sites, the majority of the deposits are buried making the design of appropriate and representative sampling regimes challenging, as short of total excavation the population from which the sample was taken will never be fully understood. This study aims to address these sampling issues through the application of geophysical survey techniques to shell matrix sites, and by developing novel methods for creating three-dimensional models and volume estimates of buried shell deposits from these survey results.

An extensive literature review found only 22 published papers (representing 15 archaeological case studies) have applied geophysical surveys to shell matrix sites. Not one of these studies used geophysical methods to calculate volume estimates of the buried matrices or to create three-dimensional models of the deposits. Outside of archaeology, there have been studies (typically in glacial load research) which have attempted to create volume estimations from geophysical survey results. These studies have, however, typically not included ground truthing of results or calculated error values for the volume estimates.

This research has three primary aims: (1) to delineate and map buried shell matrix deposits in tropical Australian contexts; (2) to establish methods for transforming these survey results into volume estimates and three-dimensional models of the deposits; and (3) is to test the accuracy of these models and estimates. To achieve these aims two geophysical methods were chosen and compared; ground-penetrating radar (GPR) and electrical resistivity. These two geophysical methods were chosen, on the basis of the literature review, as being the most appropriate methods to meet the research aims. Both survey methods were employed under field and experimental conditions. Survey results were processed and then exported to Esri's ArcGIS suite of software for further processing, to create the three-dimensional models and volume estimates. Results from this modelling were then compared to the in-ground deposits to test their accuracy.

Survey and modelling results for the buried shell matrix deposits varied between geophysical method, and were dependent on the environmental conditions present on site. The electrical resistivity could not differentiate shell material from sand, but could differentiate shell from an organic-rich sediment. The GPR produced clearer, easier to interpret results under drier conditions, while the electrical resistivity produced them under wetter conditions. The modelled results showed more accurate three-dimensional representations of buried shell matrices could be created from the GPR, rather than the electrical resistivity surveys. Similarly, the volume calculations were highly accurate when based on GPR survey data, with an error margin on the estimates of 16%±11%, though it was found that small misinterpretations of the results can easily produce errors in excess of 50%. Volume calculations based on the electrical resistivity data were less accurate than the GPR and varied significantly depending on how the results were interpreted, meaning their overall error margin was significantly higher at 50%±29%. The geophysical survey results for this research also provided a greater understanding of the palaeolandscape on which the shell matrix at the field site was deposited.

In order to create accurate accounts of the archaeological record of coastal Australia it is vital that improved methods for characterising the variability of shell matrix sites are explored. The current research addressed this issue by evaluating the capabilities of two geophysical survey techniques in investigating buried shell matrices, and by developing methods for transforming the survey results into three-dimensional models and volume estimates. These methods provide a way to greatly improve sampling regimes in shell matrix research by providing an understanding of the buried deposits before excavation takes place. The methods also provide information in their own right, allowing for a better understanding of the size and shape of buried matrices, and the palaeolandscapes on which they were deposited.

TABLE OF CONTENTS

LIST OF FIGURES

LIST OF TABLES

ABBREVIATIONS

ΔR	Regional offsets for marine reservoir ages
Ɛ	dielectric permittivity
σ	electrical conductivity
μ	magnetic permeability
Ω-m	Ohm-meter
χ	Low field mass
χfd	Frequency dependence of susceptibility
3D	Three-dimensional
AC	Alternating current
AGI	Advanced geosciences Incorporated
AMS	Accelerator Mass Spectrometry
ANSTO	Australian Nuclear Science and Technology Organisation
ArcGIS	Aeronautical reconnaissance coverage geographic information system
BP	Before present
cal BP	Calibrated years before present
CSV	Comma-separated values
CVM	Caesium vapour magnetometer
DC	Direct current
EM	Electromagnetic induction
ESRI	Environmental systems research institute
FS	Field specimen
GHz	Gigahertz
GPR	Ground-Penetrating Radar
GPS	Global positioning system
GSSI	Geophysical survey systems incorporated
Hz	Hertz
I	Current
JCU	James Cook University
K	Volume susceptibility

kHz	Kilohertz
LiDAR	Light imaging, detection and ranging
mA	Milliampere
MNI	Minimum number of individuals
MHz	Megahertz
NISP	Number of individual specimens
Ohm-m	Ohm-meter
R	Resistance
RDP	Relative dielectric permittivity
RMS	Root mean square error
RTK	Real time kinematic
SI	Volume susceptibility
STP	Shovel test pit
SU	Stratigraphic unit
TARL	Tropical archaeology research laboratory
TIN	Triangular Irregular Network
TLS	Terrestrial laser scanning
V	Volt
WoRMS	World Register of Marine Species
X	Mass susceptibility
XU	Excavation unit

1 INTRODUCTION

1.1 INTRODUCTION

Current archaeological understandings of the Indigenous history of Australia exhibit gaps both temporally and spatially, with biases towards particular site types and geographical regions of Australia. Ulm (2013) argues there needs to be a refocusing of Australian archaeology on creating more detailed local and regional chronologies, and to accomplish this he suggests finer grained methodologies are required. While improved methodologies for sampling, chronological control and taphonomy are necessary to address the central concerns of all detailed archaeological work, this thesis focuses on issues of sampling, specifically in relation to shell matrix research.

Existing archaeological knowledge of Indigenous Australia is based on small samples taken from immense landscapes. This methodology requires large assumptions to be made in order to construct a cohesive story, but despite this limitation small sample sizes are common in Australian archaeology. Langley *et al.* (2011) reviewed the excavation practices employed at Pleistocene sites in Australia and New Guinea, and found the average excavated area consisted of four squares measuring either 1m by 1m or 50cm by 50cm, to around 100cm in depth. Further analysis found the total excavated volume from a single site dropped from an average of 10.27m³ to only 2.61m³ after 1990. Langley *et al.* argue that while unduly large excavation is not desirable, improved and perhaps expanded sampling regimes are required to reveal more of the complexity of Pleistocene societies in Sahul (Australia and New Guinea).

In 2002, Ulm summarised all prior excavations of shell middens from the southeast Queensland coast. This study detailed 62 excavations, however both the estimated site area and the area excavated was known for only 39 of these sites. These 39 excavations ranged from the years 1965 to 2001 and were by eight different archaeologists. Of these, one was fully excavated, while 13 represented excavations of between 1 and 80% of the total estimated site. The other 25 excavations represented less than 1% of the estimated site, of which 18 actually represented less than 0.1%. Similarly, a survey of recent literature showed that out of 27 sites only nine represented an excavation of 1% or more of the overall estimated site size, the maximum being 33%. This was based on five articles which shared both their excavation size and estimated site size; Ulm 2006a;

Harrison 2009; Morrison 2013; Shiner *et al.* 2013 and Rosendahl *et al*. 2015. Seven of these excavations were salvage archaeology, where larger excavations could reasonably be expected, yet only one of these seven excavations equalled as much as 1% of the total site size. Of the 18 excavations representing less than 1% of the site, eight represented less than 0.1%. While the site size estimates may not be fully accurate, they do suggest only tiny fractions of overall sites are being excavated. This is not an exhaustive survey, but the results indicate the popularity if not predominance of small sample sizes in Australian shell matrix research.

Sampling inadequacies in Australian archaeology are not only due to small samples in large sites but also in the types of sites sampled. Langley *et al.* (2011) and Ulm (2013), point out an existing bias towards creating chronological frameworks for the Indigenous history of Australia based on rockshelter deposits (e.g. Barker 2004:57; Lourandos and David 1998; Lourandos 1997; Mulvaney and Kamminga 1999). Ulm (2013) further asserts this bias is so prevalent that even in coastal regions typified by open shell matrix sites, chronologies are still based on rockshelter sequences. This bias is primarily one of open sites verses sheltered (or closed) sites. Shell matrix sites, though dominant in coastal environments, are typically open sites exposed to environmental disturbance, and are often considered to lack the stratigraphic integrity and well stratified, long chronological sequences which rockshelters offer. While this can be true of a single shell matrix, matrices taken together from across a region can provide extensive regional chronologies (Faulkner 2008).

Shell matrix sites are a vital part of the Australian archaeological record, and by improving the manner in which these sites are researched more accurate local and regional chronologies could be produced. Appropriate sampling regimes can be difficult to design as Australian shell matrix sites vary considerably. Shell deposits can range from small surface scatters consisting of a few shell valves to immense shell mounds exhibiting complex stratification in deposits containing billions of shells and archaeological features like burials and hearths. Researchers are faced with the problem of determining what sample size and location will characterise the population from which the sample is taken without unduly costing time and resources (Reitz and Wing 2008:113). For large-scale sites with deeply stratified deposits representing long-term site use, sampling strategies must attempt to determine what constitutes a representative sample while dealing with a population (overall site) about which little is known

(Claassen 1998:100). With a better understanding of the size and structure of a buried matrix, a more representative sampling and dating regime can be facilitated, allowing for excavated samples to be characterised in reference to an overall population.

The research aims of this thesis are to address these sampling issues in shell matrix studies by using geophysical survey techniques to map the structure and boundaries of buried shell deposits. These geophysical surveys will allow for greater insight into the size and shape of buried matrices thus creating a better understanding of the population from which samples are being taken.

1.2 BACKGROUND AND RATIONALE

Shell matrix sites are a major component of the Indigenous Australian archaeological record but are difficult to study owing to their complex depositional and taphonomic histories in dynamic environments. In 2001 Smith ended her summary of shell midden analysis with the somewhat dispiriting sentiment that:

> The key issues for midden analysts are still those of Worsaae in the nineteenth century … The history of midden analysis is, therefore, not a story of increasing knowledge about the past so much as an increasing recognition of the complexity of processes creating archaeological deposits in general (Reproduced with permission of ABC-CLIO, from Smith 2001; permission conveyed through Copyright Clearance Center).

The complexities of these depositional and post-depositional processes have challenged shell matrix research, but with modern scientific advances and multidisciplinary approaches the field is advancing and new knowledge is becoming available. Roksandic *et al.* (2014) point out how a multitude of different disciplines have been applied to shell matrix site analyses in recent years: micromorphology, geochemistry, biological anthropology, palaeobotany, ethnoarchaeology, zooarchaeology, geoarchaeology, and biogeochemistry. Interdisciplinary approaches to shell matrix sites have also led to the wider use of isotope analysis, sclerochronology and microstratigraphic, phytolith, pollen and foraminifera studies, as well as improved dating methods. These interdisciplinary studies have proven of great benefit to shell matrix research, aiding in understandings of site formation and use patterns.

Geophysical surveys represent another interdisciplinary method which could prove beneficial to shell matrix research, but which has been underutilised to date. The research in this thesis aims to enhance the methodology for sampling and investigating shell matrix sites via the use of geophysical surveys. Before exploring those aims however, it is important to situate the rationale guiding this study within the history of shell matrix research and geophysical survey use in archaeology. The following sections provide succinct summaries of these histories. The first section (Section 1.2.1) summarises archaeological shell matrix research, focusing particularly on prior research into sampling issues. The second section (Section 1.2.2) reviews the history of geophysical research in archaeology while the final section (Section 1.2.3) looks at geophysical research focusing specifically on shell matrix sites and 3D volume analyses of buried matrices.

1.2.1 Shell Matrix Research in Archaeology

In the 1820s shell middens were first recognised to be of scientific interest (see Claassen 1998 for a detailed history). Since then, shell middens have been investigated for the information they provide, which has raised questions regarding their nature and how to best study them. The first question/issue encountered in the 1820s, and still encountered today, was in establishing whether the shell matrix in question is anthropogenic or a natural accumulation of shell. After a shell matrix has been identified as cultural there are another three basic issues which need to be addressed: how to define the type of matrix it represents, what taphonomic processes have impacted the stratigraphic integrity of the site, and how to best sample the site. Each of these issues will be briefly looked at to provide a background to shell matrix research, concluding with a more detailed look at sampling issues as they are the primary focus of this research.

There has been wide debate about how to distinguish a natural from an anthropogenic shell matrix (see Attenbrow 1992; Coutts 1966; Erlandson and Moss 2001; Gill 1948; Henderson *et al.* 2002; O’Connor and Sullivan 1994). The consensus is that they can be distinguished by certain visual criteria (see Table 1.1). However, these diagnostic characteristics need to be applied with care and in relation to one another as contradictory evidence can occur. For example, Attenbrow (1992:19) found charcoal inclusions may occur in natural shell matrix sites while articulated bivalves may not, and that burnt shell, artefacts and fauna variability may be absent from anthropogenic matrices, and Ulm (2006a:84-85) found the inclusion of articulated bivalves to be common in some anthropogenic matrices.

Table 1.1 Characteristics of natural versus anthropogenic shell middens (after Henderson *et al.* 2002; Martindale *et al.* 2009:1568; O'Connor and Sullivan 1994:22-23; Rosendahl *et al.* 2007).

Diagnostic Characteristic	Natural Shell Matrix	Anthropogenic Shell Matrix
Anthropogenic artefacts (e.g pottery, stone tools, carved shell)	Absent	Present
Evidence of burning (e.g. charcoal, burnt wood, blackened shells hearth features)	Absent	Present
Stratification of deposits	Distinct stratification	Rough or absent stratification
Edible faunal variability including land-based fauna	Low	High
Non-edible marine life as well as shell grit and pumice	Present	Absent
Shell species and size variability	High	Low (Edible species at edible sizes)
Shell fragment variability	Low	High
Friction smoothing of shell fragments	Present	Absent
Articulated bivalves	Present	Absent
Shell packing	Dense	Loose
Black organic sediment	Absent	Present
Foraminifera	<50/100g	>1000/100g

The task of distinguishing natural from cultural shell deposits can be further complicated by the deposition of cultural shell on top of natural shell matrices, as found by O'Connor and Sullivan (1994:25) during their study of the southern Kimberley region in Australia. For these sites, and for sites which are otherwise visually difficult to differentiate, experimental works such as foraminifera studies (which look at micro-organisms prevalent in marine environments) have provided new criteria for distinguishing between natural and cultural shell accumulations (see Nagel et al. 2016; Rosendahl et al. 2007). By examining foraminiferal densities, natural and cultural shell deposits can be differentiated. This method is a valuable tool not only for sites where visual identification is difficult and where cultural shell has been located on top of natural shell, but also for sites where mixing has taken place between natural and anthropogenic shell matrices.

Once a shell matrix has been identified as cultural in origin, the next identification issue is in defining what is meant by the researcher when referring to the 'shell midden.' As Claassen (1991:252) pointed out, the common use and misuse of the term 'shell midden' has made the term semantically meaningless, leading to efforts to distinguish types and definitions of shell-bearing sites (see Bowdler 1983; Claassen 1998; Waselkov 1987). Differentiation of shell matrix sites is typically based on a combination of factors such as size, shape, internal characteristics and site use, as based on discernible patterns in a given region. However, observing these differences in order to characterise site types can be complicated by factors like erosion or the removal of shell material by anthropogenic means and by the full complexity of the buried deposit not being understood (Gutiérrez-Zuasti *et al.* 2011).

For this dissertation, distinctions between cultural site types are unnecessary as the work focuses on general research methodology, and is not site specific. The functionally neutral term 'shell matrix site' as suggested by Claassen (1998:11) is adopted for this research and defined broadly as *intentional anthropogenic shell accumulations* (Balbo *et al.* 2011). As Balbo *et al.* (2011) explain, this inclusive definition covers all types of shell midden sites regardless of their size, shape, chronology, formation or geographical location. Though using a broad definition of shell matrix sites this study is primarily concerned with shell sites which include buried deposits, and not sites limited to surface scatters, though no semantic distinction has been made to address this as it is purely a point of practical consideration with the geophysical investigation of buried shell deposits requiring buried deposits.

The term 'shell matrix site' is further used in this dissertation to include both natural and cultural shell deposits. Natural deposits will, however, be differentiated from anthropogenic shell matrices through definition as chenier or beach ridge, depending on the formation of the matrix. A chenier is a ridge of muddy sandy material deposited on top of a coastal plain by storm-surges which often includes molluscan shell material. By comparison, a beach ridge is a relict ridge built up along the shore by wave action typically consisting of sand or shingle material (see Otvos 2000 and Bird 2008 for full definitions).

With theoretical issues of identification and definition out of the way, shell research encounters two universal practical issues. The first issue is how to best sample a site, the second is how to assess site integrity due to taphonomic impacts. While research projects usually settle on a sampling strategy before investigating the stratigraphic integrity of a site, these issues are considered here in reverse order. First taphonomic issues will be briefly noted, followed by a more in-depth examination of sampling issues as they are the theme of this thesis.

Taphonomic attenuation of a shell matrix can introduce problems not only in interpreting the archaeological record of a site, but also in defining what type of matrix the site represents. There are multiple sources that contribute to taphonomic processes at shell matrix sites, from decomposition and bioturbation to various forms of marine erosion and subsequent cultural processes. Open coastal sites can be destroyed or modified by tidal inundation (see O'Connor 1989) or by cyclones (see Bird 1992, 1995; Przywolnik 2002; Rowland and Ulm 2012); though these processes can also serve to make older sites visible. Subsequent destructive cultural processes can include site cleaning and the placement of burials or post holes by descendant groups, or large-scale transformations such as looting, industrial development and resource mining by later cultural groups and excavation by archaeologists (see Ceci 1984). Shell matrix exploitation around the world has led to sites which no longer represent primary deposits, but are instead semi-primary or secondary and sometimes even completely depleted. In defining these site types it is important to identify their exploitation (Ceci 1984).

The last issue representing a primary and universal problem for shell matrix sites is in sampling. Discussion surrounding sampling for shell matrix sites is fairly unanimous in its assessment of the situation: sampling shell matrix sites presents complex considerations so the only way to create appropriate sampling regimes is to tailor them to meet specific research aims (see Ambrose 1967; Claassen 1998; Bowdler 2014; Waselkov 1987). Some research has attempted to quantifiably address sampling issues in shell matrix research. O'Neil (1993), Poteate and Fitzpatrick (2013), and Treganza and Cook (1948) all excavated large proportions of shell matrix sites in order to establish the sampling size and/or strategy required to produce an accurate understanding of the shell population of the entire matrix. While Bailey (1975) and Greenwood (1961) focused on how much of the excavated shell material needed to be analysed in detail to accurately characterise the overall sample.

This prior research has differed in approach and results. Treganza and Cook (1948) excavated an entire shell mound site (48,631kg of dry material) concluding that 15 to 30 samples of 0.5-2kg were statistically sufficient in representing the more prevalent mound content with an error margin of ±5%. This meant as little as 7.5kg or 0.015% of the total site could be a representative sample for high density components. For less prevalent components of the mound 2,063 samples were required to achieve a standard error of ±5%, meaning as much as 4,126kg of material or around 8.5% of the total site may be needed to characterise rarer material.

O'Neil (1993) took a different approach, excavating approximately 63% of a shell matrix while aiming to characterise site use and chronology. The size of the matrix was calculated based on depth measurements taken from excavation and horizontal boundaries were estimated based on the darker colour of the midden soil compared to surrounding soils. O'Neil claimed a satisfactory understanding of the site use and chronology was not obtained until approximately 50% of the shell matrix had been excavated. O'Neil admits it was purely by chance the research aims were not fully met sooner or even later than the 50% mark, suggesting there can be no one sample size appropriate for all sites.

Most recently, Poteate and Fitzpatrick (2013) excavated and analysed a 25m² area within a larger midden matrix. By using this 25m² area as the full population and dividing it into smaller samples (1m by 1m excavation squares), they could investigate how different sampling strategies affected the results of various quantitative measurements. These measurements included species count, weight, minimum number of individuals and number of individual specimens present. The authors found that with a single 1m² excavation there was a 24% chance that at least one of the quantitative measurements would experience an error and no longer be representative of the overall site. If two non-consecutive 1m squares were sampled the error rate dropped to 4.67%, then to 0.09% for three non-consecutive squares and to 0% with four. Conversely, they found the error rate increased when squares were located adjacently, changing from 4.67% for two separated 1m by 1m squares to 7.5% for two adjacent squares (a 2m by 1m area) and similarly from 0.09% for the three non-consecutive squares to 3.33% for three consecutive squares. Poteate and Fitzpatrick determined that 16% of a given surface area, sampled in non-consecutive excavations, should produce a sample representative of the whole population. The authors note this strategy would not, however, ensure accurate representation of changes between stratigraphic layers.

Rather than characterising site population, Greenwood (1961) and Bailey (1975) looked at what constitutes the minimal sub-sample required (for detailed laboratory analysis) to characterise the larger excavated sample. Greenwood (1961) conducted methodological experiments from which he concluded that 500g of sieved shell, per 4-inch excavated level, constituted an adequate sample. It is unclear what percentage of the overall shell this sample represented, however, as values for only one level were presented in the paper: for this level the total shell sample was 1110g making a sample of 500g around 45% of the total. In his paper, Bailey (1975) recommended a sampling strategy in which the bulk material from each 10cm excavation unit (for a $1m^2$ pit) was bagged evenly in 50cm x 20cm plastic bags, usually resulting in about 12 bags. Of these 12 bags two or three bags, representing approximately 12-20kg worth (or 16-25% of the overall material) were considered an adequate representation of the total unit for further laboratory analysis.

The varying results of these studies illustrates just how difficult it is to create sampling regimes which appropriately characterise a shell matrix, and how different research aims can have a major impact on what constitutes an ‘appropriate’ sample. All of the studies made sure to note that the samples they found appropriate, for the site being studied, may not be appropriate at another site. These methods are therefore impractical as a way of addressing sampling issues in shell matrix research, and new methods need to be established. The first and most significant difficulty in constructing appropriate sampling regimes is in understanding the full scope of the matrix. Only three studies have attempted to address how to best calculate the volume of a shell matrix.

In 1948, Treganza and Cook attempted to create a volume calculation for the shell mound they excavated. First they tried an estimate based on the shape of the deposits.

Initially they thought the mound was shaped like the segment of a sphere with a maximum height of 92cm and a radius of 533cm, making the volume 41.45m³. However, during further excavation they found the shape was closer to a cone which would change the volume estimate to 27.36m³. Ultimately Treganza and Cook decided estimates based on geometric shapes were all bound to be wrong, as the deposits did not conform to simple geometric patterns. Next the authors attempted a volume estimation through density determinations, in which the dry weight of the material was compared to the volume taken out of the ground. From this method they calculated a volume of 29.92m³, concluding 30m³±10% would be a reasonable estimate for the matrix volume.

Sorant and Shenkel (1984) proposed a method to address the problem, encountered by Treganza and Cook, of calculating the volume of irregularly shaped shell matrices. Sorent and Shenkel argued that while the detailed analysis of samples had increased many times over since Teganza and Cook's 1948 study, the ability to extrapolate the sample data to a total site universe remained at the same level. Sorent and Shenkel proposed their volume calculation method as a means of elucidating total site volume based off contour maps. Shenkel (1986) went on to refine the calculation methods involved, but the basic problem of mapping buried deposits remained, so this method added little to shell matrix research. While the detailed analysis of shell matrix samples has continued to develop, with new scientific methods, the ability to place those samples in a site universe has remained largely unimproved since 1948.

Modern research has moved away from determining what constitutes an adequate sample and on to investigations of alternate sampling methods, in order to provide greater insight into the buried matrix. These alternative methods are aimed at providing preliminary data such as establishing the boundaries of shell matrix deposits, recovering dateable material, and investigating the internal stratigraphic structure of the buried matrix. The preliminary samples can in this way provide insight into the buried matrix, allowing for subsequent excavations to be placed within an understanding of how they represent the site as a whole (Martindale *et al*. 2009). These methods commonly include bucket auguring and/or percussion coring, employed most frequently in the Pacific North-West of North America (e.g. Cannon 2000a, 2000b, 2013; Martindale *et al*. 2009; Whittaker and Stein 1992).

Cannon (2000a) employed a combination of bucket-augering and coring to investigate shell matrix sites in order to better understand the regional context in which they exist. Over 60 years of archaeological investigations (up until 2000 when the paper was published) in the Heiltsuk territorial claims region (covering approximately 10,000km^2 in British Columbia, Canada) only 16 of 334 recorded shell matrix sites were subject to investigation. By employing coring and augering as a cost- and time-effective alternative to excavation Cannon aimed to create a broader regional context in which to place Namu, one of the few previously well researched and documented sites. By comparing the results of analysed bucket-auger material with prior test excavations at Namu, Cannon found the auger samples provided an accurate indication of overall trends in salmon fishing intensity (the focus of her research). Coring was used to investigate stratigraphic variation between matrix sites and to obtain uncontaminated material for radiocarbon dating, while bucket-augering provided larger samples which could be analysed in the laboratory to assess the fauna content of the matrices. An additional 16 sites were investigated in this manner, essentially doubling the amount of analysed shell matrix sites in the region (see also Cannon 2000b, 2013).

Martindale *et al.* (2009) built on the work of Cannon (2000a, 2000b) employing percussion coring, but not auguring, to investigate shell matrix boundaries. Martindale *et al.* felt the auger was undesirable as it mixed the deposits during retrieval and so focused solely on the percussion coring. Their research aims included retrieving samples for radiocarbon dating and mapping the subsurface of large complex shell matrix sites. Percussion coring provided a system by which stratigraphically intact samples large enough to permit content analysis (though compaction of sediments will occur), could be obtained and stored for transport in remote and challenging landscapes with dense vegetation. Percussion coring had the added benefit of being able reach the required depths (up to 8m) to access the culturally sterile fill underlying the shell matrix deposits.

It is widely agreed there can be no single sampling model ideal for all shell matrix sites and research regimes. There can, however, be methods of site investigation which provide a better basis from which to create the desired sampling model. These alternative sampling methods are vital as they can provide a greater understanding of how small-scale excavation results fit within the overall site, without the time and expense of major excavation. Coring and auguring regimes have shown success in providing insight into buried shell matrices, even in remote landscapes with dense vegetation. However these methods are still destructive, require interpolation between cores and as Cannon (2013) points out, auguring is not sufficient for intra-site investigations of larger features such as living areas, burials or artefact analysis.

The advancement of recovery methods and analytical processes in shell matrix research has led to intensive excavation and post-excavation procedures. These procedures make sampling extensive deposits a large investment in time and resources, and sampling at the regional scale becomes largely infeasible for a single research project (Bailey *et al.* 2013). Bailey (1975) reasons that a single cubic meter of dense shell matrix can potentially contain a tonne of material representing up to 100,000 mollusc shells, so even modest matrices can consist of shell counts in the millions and represent hundreds of tonnes of material. In light of this, it is not surprising large-scale sampling regimes are rarely implemented in Australian archaeology as the large extents and depths of many Australian middens make such excavation infeasible as well as hugely expensive, time consuming and destructive.

The detailed recovery of small samples may maximise the information obtained from the sample while minimising damage, but are these tiny samples truly representing the overall population when they represent less than 0.1% of a site? With such small samples, their placement within the overall matrix and thus their representativeness of the matrix becomes of paramount importance. However, with no real understanding of the buried deposits these samples are often placed probabilistically into the densest areas of cultural material accumulation visible at the surface. As Ulm (2006a:38) notes "A key problem with this strategy is the assumption that visible concentrations of cultural material are an accurate indicator of intra-site diversity and not simply a product of differential visibility."

As Bowdler (2014:380) remarks "In the end, your interpretation is only as good as your analysis, which is only as good as your sample." This PhD thesis proposes a greater understanding of the overall deposit may be obtained by using geophysical techniques to map buried shell matrices. Such knowledge will facilitate more representative sampling of the site, allowing in turn a more representative dating of the site. As Roksandic *et al.* (2014:xiv) note in regards to shell matrix sites, a multidisciplinary approach is the only way to competently deal with the complexity of shell matrix sites.

Geophysical surveys represent just such a competent multidisciplinary tool in investigating the past, but are underutilised in Australia in general and in shell matrix research worldwide. This study aims to improve the ways in which shell matrix sites are analysed by researching and experimenting with the use of geophysical methods in the investigation of shell-bearing sites.

1.2.2 Geophysics in Archaeology

Geophysical surveys are a relatively recent introduction to archaeological investigation. Aside from Augustus Pitt Rivers using a mallet as a basic acoustic locating device in the 1890s (Clark 1990:11), the first recorded use of a geophysical survey in archaeology has been traced back to an unpublished equipotential survey conducted by M. Malamphy at Williamsburg, Virginia, USA in 1938 (Bevan 2000). Commonly though, the field of archaeo-geophysics (the practice of applying geophysical techniques to archaeological deposits) is considered to have begun almost simultaneously on opposite sides of the world in 1946, when electrical resistivity was employed by R.J.C. Atkinson in England and by H. Lundberg in Mexico (Hesse 2000). The field did not become more widespread until the advent of micro-computers in the 1980s and the rise of compact, cheaper systems in the 1990s (Gaffney 2008). Even today the field of archaeological geophysics is still fairly new with constant improvements being made to the instrumentation and data processing software.

Globally the use of geophysical surveys in archaeology has varied. England has seen a long history of geophysicists and archaeologists working together, enabling the United Kingdom (UK) to become a world leader in the application of geophysical surveys on archaeological sites. Comparatively, the routine use of geophysical surveys in archaeology is far more limited outside the UK. Even the United States of America (USA), despite being a leading manufacturer of geophysical survey equipment, falls far behind the UK in archaeological applications of geophysical surveys. In 2003, Kvamme compared geophysical survey numbers in the UK to their use in the USA, finding nearly 10,000 surveys had been undertaken in England alone during the twentieth century (data taken from Gaffney 2001 as cited in Kvamme 2003:436) as compared to 550 surveys for both North and South America during the same period (data taken from Bevan 2000).

The spread of geophysics in archaeology globally, has been limited by a notorious history of expensive failures. These failures often went unanalysed and were not typically reported in the published record, so little was gained from these experiences in terms of research practice. However, professional discourse passed around the stories of failure which at times discouraged the application of geophysical surveys at archaeological sites. The failures were frequently due to incorrect data collection or processing by inexperienced technicians, as well as the use of methods in unsuitable conditions or in attempting to locate features the techniques were not capable of delineating (Conyers and Leckebush 2010). Cheetham (2008) claims this misuse of the geophysical methods by archaeologists is due in part to the lack of communication between geophysicists and archaeologists outside of the UK. These failures along with the expense associated with geophysical surveys have resulted in many archaeologists declining to incorporate geophysical surveys into their research plans.

Despite their slow emergence, geophysical surveys in archaeology have seen a growing popularity in the past two decades. Archaeo-geophysics professionals have seen a change in the prevailing attitude of caution, in regards to geophysical survey use, to a more optimistic and experimental use. Television series like *Time Team* and *Time Team America* have popularised geophysics in archaeology, creating a demand for geophysical techniques among those engaging archaeologists in the public sector and among university archaeology intakes. Universities in the UK, North America and parts of Europe have responded to this demand by adding geophysical instruction to the standard scientific archaeology curriculum (Lowe 2012).

Australia has been particularly slow and erratic in applying geophysical surveys in archaeology. Interest in the use of geophysical techniques is growing in Australia, but remains far behind international standards (Lowe 2012). Where growing interest has spurred universities to purchase geophysical equipment, it is typically spread across different faculties with few staff members trained to operate the equipment; if these staff members move to another university the equipment may be left in storage unused. Gibbs and Gojak (2009) and Lowe (2012) point to limited access to equipment and a lack of trained operators as having held back the growth of the field. Lowe (2012) asserts that crucial training and support from university archaeology departments is lacking.

With poorly trained operators and few examples of successfully applied geophysical surveys in Australia, it is understandable that Australian archaeologists remain sceptical about their capabilities. Though interest in archaeological geophysics has gained momentum in the 2000s there are still few courses and little support for practitioners available in Australia. Gibbs and Gojak (2009) state that many historical archaeologists in Sydney, with prior experience of geophysical techniques, claimed they would not employ them again based on a combination of expense and dissatisfaction with the results. Other archaeologists reported to Gibbs and Gojak a failure to see the relevance of the techniques to their sites/research interests. Lowe (2012) further proposes the lack of geophysical survey application in Australian contexts is due to a prevailing view that geophysics is only good for historical archaeology and is therefore not useful with the subtle archaeological record of Indigenous Australians.

A literature review revealed 15 geophysical surveys of Australian sites. While twelve of the surveys did focus on Indigenous Australian sites, eight of these were unmarked burials of which five were historical Indigenous cemeteries (i.e. institutional cemeteries such as missions or prisons). A total of 10 out of the 15 surveys were aimed at locating unmarked burials of some description. While this was not a comprehensive search or analysis of the literature on Australian archaeo-geophysics, the results did show an immediate bias towards surveying unmarked burials over other site types. This implies there are significant biases among archaeologists and/or those people employing archaeologists in Australia, to use geophysical techniques simply as grave detectors. Geophysical surveys need to be promoted in Australia as being applicable to Indigenous sites, relevant to the research questions of researchers, and useful for more than detecting unmarked graves. We are currently at the forefront of a change in Australian archaeological geophysics. More universities are investing in equipment, and training courses are becoming available, though sporadically. If Australian archaeology is to keep up with international projects it is important a push be made to add to the current international research aims and discourse.

The current international discourse for archaeological geophysics is one of moving away from the simple prospection aims of early surveys and towards creating original knowledge about sites. Many proponents of archaeo-geophysics have strongly articulated that it is time to stop limiting surveys to feature location and move them towards becoming research methods in their own right, using the unique capabilities of geophysical techniques to test hypotheses and answer questions which can only be answered via remote sensing (see Annan 2002; Aspinall *et al.* 2008: Conyers 2009; Conyers and Leckebusch 2010; Dalan 2008; Gaffney 2008; Hargrave *et. al.* 2002).

There is also a small international push to situate geophysical surveys into larger theoretical frameworks. Thompson *et al*. (2011) argue archaeo-geophysics has failed to be more widely integrated into the design and research objectives of research projects, being applied as a 'post-hoc method' or afterthought, because the field has failed to situate itself within any larger theoretical framework. Thompson *et al*. suggest grounding geophysical research in landscape archaeology, specifically in theories of persistent places: looking at how humans make decisions around site use through time. The authors further suggest exploring these changes in site use via four categories, including, identifying any changes in construction of the built environment, the continuity or discontinuity of site use, natural versus cultural modifications and lastly, regional trends in site construction and use.

This push away from simple prospection does not mean the use of geophysical surveys to locate buried features of interest will diminish. One of the greatest strengths of archaeo-geophysics lies in surveys acting as both fast subsurface mapping to aid excavation planning and also as an alternative to wider, costly and destructive, excavation (Gaffney 2008). This is a significant service as excavation is becoming increasingly more expensive and time consuming, with many researchers now reluctant to conduct large-scale excavations due to ethical and conservation considerations.

1.2.3 Geophysical Investigation of Shell Matrix Sites

There have been very few applications of geophysical survey techniques to shell matrix deposits (this includes both archaeological and geological papers). As late as 2000, Neal and Roberts were advocating for the use of GPR to investigate coastal archaeological sites above the salt water line. Neal and Roberts point out how little research has actually been done in this area, even though studies have confirmed the potential of GPR at coastal sites. The literature review conducted for this thesis found a total of only 22 published papers which apply geophysical surveys to the investigation of shell matrix sites. These 22 papers represent 15 archaeological case studies and a further 3 geological studies. The papers can be divided into two broad types, those which focus on prospection and those which focus on site formation (see Chapter 2 for a full review of the papers).

For archaeology just over half of the studies focused on prospection, aiming to locate either the buried boundaries of shell matrix deposits or features within the shell matrix. A total of 10 articles were found to focus on this topic (two of these papers covered different aspects of the same study), all of which were archaeological in nature and covered a range of geophysical methods. The geophysical methods included ground-penetrating radar (GPR), magnetometry, electrical resistivity, magnetic susceptibility, seismic refraction and electromagnetic induction (EM).

Twelve papers were published focusing on using geophysical surveys beyond prospection, to examine shell matrix site formation and the landforms on which they were deposited. Nine of these were archaeological, out of which three are different papers addressing the same study with the same methodology so of the 12 papers only seven archaeological case studies are represented. The final three papers come from geological studies of shell matrix chenier sites. For these 12 papers the geophysical methods are confined to GPR, magnetic susceptibility, electrical resistivity and terrestrial LiDAR. The geology surveys all employ GPR and show great success with their results.

While multiple studies addressed locating buried shell deposits, features within the deposits and site formation, only one study quantified the deposits. This study was by Larsen *et al.* (2015) and utilised terrestrial LiDAR to investigate and quantify shell mounds. LiDAR is limited, however, as it cannot differentiate between shell matrices and surrounding deposits, nor can it look at buried deposits but only the mounded matrix above the surrounding ground plane. Outside of shell matrix research there have been efforts to create volume estimates for buried matrices from geophysical survey results, however only one of these can be tied to archaeological research. Aside from the terrestrial LiDAR these volume estimates have all employed GPR and electrical resistivity. A total of 16 papers were examined for the literature review, of which, only four ground truthed the results and only seven provided error margins on their estimations; two of these papers both ground truthed and provided error margins. The term “ground truth" is used here and throughout this thesis to refer to the practice of substantiating and/or calibrating results obtained by remote sensing, with information obtained from direct observation (Hargrave 2006:269).

The research proposed in this dissertation addresses the paucity of prior research by employing a holistic approach to the geophysical investigation of shell matrix deposits. The study attempts to both replicate the prospection viability of these methods in Australian shell matrix contexts, as well as going beyond prospection to add to understandings of site formation history. The research will also address a gap in the literature by experimenting with a new application of geophysical survey, this experimental stage will attempt to use geophysical techniques to calculate the volume and create 3D models of buried shell matrix deposits.

1.3 AIMS OF RESEARCH

This study uses geophysical methods to define the size and shape of buried shell deposits and the palaeolandscape on which they were deposited. A key research aim is to contribute to the methodology of both shell matrix research and archaeo-geophysics by developing methods for calculating the volumes of buried shell deposits. These volume estimations will be the first attempt at employing the methods in shell matrix research and one of only a few in any area to compare the volume estimations to the real in-ground results. While creating volume estimations for buried deposits, based on geophysical data, is becoming fairly popular (particularly for glacier ice-load studies) few have attempted to test the validity of the estimations created. These aims will be met by comparing two methods, ground penetrating radar and electrical resistivity, in two settings: an experimental site constructed on the Cairns campus of James Cook University (JCU) and a field site in the Gulf of Carpentaria, Queensland.

By utilising geophysical methods to survey shell matrix sites, this research makes contributions to several bodies of under-represented research. By surveying shell matrix sites with geophysical methods, this research will be adding to a small base of published papers utilising geophysical methods to investigate shell deposits. By surveying in tropical Australian contexts, this research will be adding to the small body of papers published utilising geophysics in Australia in general, and the even smaller amount based in tropical Australian contexts. Lastly, as mentioned above, by applying these methods to shell matrix sites for the first time, this study will be adding a new aspect to the published research in creating volume calculations of buried matrices from geophysical survey data.

The primary aims of this research are in improving sampling methods in shell matrix studies and creating new knowledge through geophysical survey. By creating a better understanding of the extent of buried shell deposits the methods proposed in this study aim to provide a basis on which to build and implement better sampling regimes. The methods will create new knowledge by mapping the boundaries of shell matrix sites as well as the palaeolandscapes on which they have been formed and by calculating the volume of the deposits.

The aims of this research will be met by addressing three main research questions:

1. Can geophysical surveys accurately delineate and map the extent of buried shell matrix deposits in northern Australian contexts?
2. Can volume estimates and 3D models of the buried shell matrix be created based on the data obtained from the geophysical surveys and what methods are required to do so?
3. How accurate are these models and the volume estimates created from them?

By investigating the exploratory capabilities of these methods in both field and controlled experimental settings, this research addresses crucial gaps in the current literature and in issues surrounding inadequate sampling of shell middens. Such research will not only benefit our understanding of midden deposits but also of the wider archaeological record of Australia.

1.4 Survey Sites

The survey sites were chosen for several different practical reasons. The experimental site was chosen on a basis of convenience and availability, being set up in an area on campus previously used by archaeology staff for a different purpose. As the site was experimental and the shell matrix was going to be artificially created, the main concern was location and not site content. The field site, however, was chosen because of the appropriateness of the shell matrix as well as the availability of previously secured funding as part of a larger research project. The field site, Thundiy, is a large matrix known to extend to depths of approximately 40cm. The isolation of the field site on an island in the Gulf of Carpentaria, means many of the disturbance problems experienced by shell matrix sites in more populated areas are not an issue here. The site also benefits from a protective stand of mangroves, which will have sheltered it from some of the worst weather elements. The site has, however, been sporadically affected by the use of 4WD vehicles along the crest of the ridge since the 1980s which has contributed to the fragmentation of shell at the surface.

1.5 Thesis Overview

This first chapter introduced the current research, establishing both the aims and rationale driving the study. The rationale behind this current research was established as addressing sampling problems in shell matrix research, which have far reaching consequences in Australian archaeology and our understanding of the archaeological past. The current research also adds to two areas with a paucity of geophysical applications: Indigenous Australian sites and archaeological shell matrix sites. The aims of the current research were established as improving sampling methods for shell matrix research as well as obtaining new knowledge, by investigating the proposed methods' ability create volume calculations, three-dimensional models and to establish palaeolandscapes for buried shell matrix sites. A brief look at the backgrounds for the two main study areas for this research (shell matrix research and archaeo-geophysics) was also undertaken.

Chapter Two reviews prior research utilising geophysical methods to investigate shell matrix sites. As mentioned in Chapter One, this research is scarce so all papers found relating to both archaeological and naturally formed shell matrix sites were included for detailed review. The review also establishes a gap in the literature, with no published papers that create volume estimates for buried shell deposits via geophysical survey. However, where geophysical methods have been utilised to establish volume calculations for non-shell matrices, they will be reviewed for their ability to methodologically inform the current research.

Chapter Three details the methodology, presenting the geophysical techniques utilised for this research as well as the unique methodology employed. Two geophysical methods were chosen for this study based on the results of the literature review in Chapter Two. The two methods chosen for this research, ground penetrating radar and electrical resistivity, are outlined including a review of commonly encountered problems and how they were addressed in this research. This chapter also details the general geophysical survey design as well as the data processing steps for each method, and for the creation of the 3D models and volume estimates of the buried deposits. The site specific survey methodology employed for the field and experimental sites is presented in their respective chapters (Chapters 4 and 5).

Chapters Four and Five present the two case studies, consisting of the field site and the experimental site, and the results of their geophysical surveys. Chapter Four introduces the field site, Thundiy, describing its archaeological history and environmental context. The results of both the geophysical surveys and excavation completed on site are also presented and discussed in this chapter. Chapter Five details the set-up of the experimental site and its environmental context as well as the results obtained from successive geophysical surveying under different conditions.

The last chapter, Chapter Six, presents a general discussion of the results and the conclusions reached. Chapter Six reviews the results for both the field and experimental sites analysing what worked and what did not, as well as comparing the two methods employed. The aims of the current research are then revisited and evaluated with regards to how they were met, as well as an evaluation of the viability of creating volume estimates for buried shell deposits based off geophysical survey results. Lastly, this chapter recaps the limitations encountered and establishes the direction of future research.

2 LITERATURE REVIEW

2.1 INTRODUCTION

Geophysical survey methods have increasingly shown their value in archaeological applications. Starting out as prospection tools, geophysical surveys are now routinely employed to reveal important aspects of depositional history and site formation. The application of geophysical surveys to archaeological shell matrix sites is, however, still in the exploratory phases. Geophysical surveys are rarely used in the investigation of shell matrix sites and the best techniques for doing so are still being established. This is the case even though electrical resistivity surveys were conducted at the British Camp Site in 1986-7 (as reported by Dalan *et al.* 1992, in the seminal work *Deciphering a Shell Midden* edited by J.K. Stein), and the first modern digital GPR systems were tested on archaeological shell middens in the late 1990s (Arnold *et al.* 1997). Even in Australian archaeology, which has historically lagged behind other regions in the use of geophysics, magnetometer surveys were being tested on shell middens in the 1970s (Connah *et al.* 1976). In order to further the use of geophysical surveys in relation to shell matrix sites, this study takes up the challenge where others have left off. To better understand where previous studies have left us, a critical review of the key literature is undertaken in this chapter. The basis of the research model applied in this thesis, including limitations, methods, and areas for further research, is then generated based on the information obtained through the critical review.

The limited number of published studies using geophysical methods to investigate shell matrix sites means each paper can be discussed in detail below. The following review is the result of an exhaustive literature search (limited to English language sources) focusing on the history of geophysical research into shell matrix sites for both archaeology and geology. For clarity, the review is divided into three sections based on research focus: prospection, site formation and volume calculations. These three areas are then further subdivided by technique: GPR, electrical resistivity, electromagnetic induction, terrestrial laser scanning, magnetometry and magnetic susceptibility. First, however, a short introduction and review of the history and methods of the geophysical techniques is conducted to provide a background understanding of the field.

2.2 HISTORY OF RESEARCH

The notion of using geophysical methods to ascertain what lies beneath the surface of the ground has been around since the 1890s when Augustus Pitt Rivers described his use of *bosing*, a very basic form of acoustic location using a mallet to identify soil disturbance (Clark 1990:11). The field did not develop, however, until after World War II. The 1940s saw the main advent of electrical resistivity in archaeology, followed a decade later by electromagnetic induction (EM), magnetic susceptibility, and magnetometry. GPR did not join the field of archaeological applications until the 1970s.

Steady progress was made through the 1950s to the 1980s, with instruments being refined and improved. The next leap in advancements came with the introduction of micro-computers in the 1980s. By the 1990s, the incorporation of micro-computing to geophysical instrumentation was common, allowing greater and faster data collection. During the 1990s the cost of geophysical instrumentation also fell, instigating more widespread use (Cheetham 2008). From the 2000s geophysical surveys have been undergoing another form of advancement, with instrumentation being developed that integrates global positioning systems, multi-method systems, and large mechanised multi-array platforms (Cheetham 2008). For more detailed information on the history and methodology of the techniques see Clark (1990), Scollar *et al.* (1990), Gaffney and Gater (2003), and Conyers (2012).

2.3 DESCRIPTION OF METHODS

The following sections provide a brief summary of how each geophysical method works. The methods are discussed in the order in which they were incorporated into archaeology: starting with electrical resistivity and ending with GPR. A more detailed review of the methodology for GPR and electrical resistivity is provided in the next chapter (see Section 3.3).

2.3.1 Electrical Resistivity

Electrical resistivity measures the resistivity (resistance over one cubic meter or Ω-m) values of the material through which an electrical current is passed (Reynolds 2011:289). To overcome resistance problems created in measuring resistivity values for the subsurface (such as soil often being a poor conductor combined with the small contact point created by an electrode), four electrodes are required for each resistance reading. A known electrical current is passed between two current electrodes (AB or CC) and the resulting voltage field or potential gradient is then sampled between two potential electrodes (MN or PP) (Clark 1990:28). As the ground is not homogenous, a kind of average of the true resistivity encountered between electrodes is created, known as 'apparent resistivity' (Scollar *et al.* 1990:313). By measuring resistance changes, electrical resistivity surveys can detect sediment change and disturbance, cultural objects, rocks, bedrock and ground water.

Electrical resistivity surveys utilise the four required electrodes in a range of configurations. Commonly used are Wenner, Twin Probe, Double Dipole and Schlumberger (Clark 1990:38), while Square arrays have allowed for rapid vehicle-powered surveys (Cheetham 2008). The use of electrodes allows for surveys in fairly dense vegetation. Survey results will, however, be adversely affected by extreme topography, such as a steep hill or ditch which create anomalies in the data, and very dry ground, which inhibits the current from traveling between electrodes. Surveys are usually collected in grids made up of transects as is typical across geophysical methods. The depth penetration obtained during surveying is roughly proportional to the spacing between electrodes. To create a detailed vertical depth profile of the subsurface, known as a pseudosection, an array of many electrodes (set in a line) is required. The array still only employs four electrodes to take any one reading, but by changing the four active electrodes, moving them further and further apart, the array gains deeper and deeper readings which are compiled into a single vertical profile. Reynolds (2011:293) advises it is best to plan for an electrode separation at least twice, preferably more than three times the desired depth penetration, to allow for around 50% of the current to pass through any interfaces or features of interest encountered at the desired depth. Three-dimensional surveys are created by running consecutive transects in a grid, the resulting pseudosections are then complied to create a 3D block of data. Horizontal surveys are made by using just the four required electrodes, two of which are moved along transects in the desired survey area, so the same depth is achieved across the entire site.

2.3.2 Magnetic Susceptibility

Magnetic susceptibility is the measured response of a material to an induced low magnetic field (making it an active technique). The degree to which the material can be magnetized is measured and expressed as either mass susceptibility (X) or volume susceptibility (K). The magnetic field induced can be varied and applied under diverse frequencies and temperatures allowing for the determination of the mineral composition, concentration, and grain size of the dominant magnetic carrier in the sample (Dalan and Banerjee 1998). Magnetic susceptibility can be used for prospection, to establish occupation boundaries and delineate large features and modified terrain (such as pits and ditches). Magnetic studies can also contribute to understandings of site formation and post-depositional processes. Studies conducted have gained insight into erosion processes, floodplain deposits, correlating stratigraphic layers across a region, and determining pedogenic regimes including past weathering and climatic variations (Dalan and Banerjee 1998).

Magnetic susceptibility studies are typically conducted in the laboratory but can also be made in the field. For laboratory studies samples are first taken in the field, either from cores or preferably from the cleaned stratigraphic sections of an excavation. Ideally, samples are large (100g-500g) to guard against the possible anomalous inclusion of a few highly magnetic grains (Scollar *et al.* 1990:403). Field studies, conversely, can be conducted in the typical grid survey system common to other geophysical methods. Field surveys can be made using a balanced AC (alternating current) susceptibility bridge, or with EM instruments via either a probe or without direct ground contact. However, these instruments can only measure volume magnetic susceptibility (K) which is imprecise (it does not account for inclusions, compaction or water content of sediments), and are limited in the depth they can reach as well as being unable to examine changes occurring with depth (Dalan and Banerjee 1998).

2.3.3 Magnetometry

A magnetometer reads fluctuations in the Earth's magnetic field caused by the presence of localised magnetic anomalies. Iron-rich features (i.e. rotting organic material, human-made objects, or changed magnetic signatures due to burning) will have a differing magnetic signature to the surrounding soil. Magnetometry has two instrument types: one measures total magnetic field intensity while the other measures the magnetic field's component on the vertical axis. Proton magnetometers are the most common choice for total intensity measurements, while the fluxgate gradiometer is commonly used for the vertical axis (Nishimura 2001).

Magnetometer surveys are often conducted in the commonly used grid-and-transect system. Because they do not need to connect to the ground, magnetometer surveys can be conducted over rough terrain at a walking pace, with some systems capable of being towed by vehicles up to 30km/hr (Cheetham 2008). Dense tree cover can cause problems for magnetometer surveys, as the instruments need to be held as vertical as possible; tipping the sensors to avoid branches can cause anomalies in the data. Sensors are standardly 50cm apart, which allows for an effective depth reading to only 1.5m. To take readings at greater depths the sensors have to be moved further apart, which would quickly inhibit the operators' ability to maintain the vertical orientation of the instrument and to conduct a smooth walking pace during surveying (Nishimura 2001).

2.3.4 Electromagnetic Induction

Electromagnetic induction (EM) works by generating a primary electromagnetic field which responds to the presence of conductive material in the subsurface. The electro-magnetic field is produced by a wire coil and responds to the conductive materials by creating a secondary magnetic field which is then detected and recorded (in siemens) by another coil. The instrument can provide information similar to electrical resistivity, magnetometry and magnetic susceptibility; this is done by varying the instruments' coil orientation and then recording both the in-phase and out-of-phase responses (Cheetham 2008).

Surveys for EM require no ground contact, so like magnetometry they can be conducted on rough terrain. As the technique records the inverse of resistivity it is often used as a non-contact resistivity survey with the benefit of operating in very dry conditions, although EM, unlike resistivity, is subject to interference from external magnetic fields (Nishimura 2001). Survey results are dependent upon the frequency (kHz) used and the coil orientation and separation. Survey depth penetration is correlated to the distance between the transmitting and receiving coils, the greater the distance between coils the greater the depth penetration but the lower the resolution. A coil spacing of 50cm will survey to 30cm, while a separation of 1.5m will reach to a depth of 1m but the magnetic response will be limited to locating objects which consist of several kilograms of metal (Scollar *et al.* 1990:549).

2.3.5 Ground-Penetrating Radar

Ground-penetrating radar propagates an electromagnetic wave from a transmitting antenna, after the wave has been reflected off changes (objects and differing sediment) in the subsurface, it is then recorded by a receiving antenna. Radar waves attenuate as they travel, but how fast they attenuate in the ground is based on both the medium through which they travel and the frequency (MHz) at which they are transmitted. Higher frequency wavelengths penetrate only the shallow subsurface but they detect small objects, while low frequency antennas reach much greater depths but will only discern larger objects.

Ground-penetrating radar data is collected by moving the antenna over the ground to create profiles which consist of thousands of individual reflections (Conyers 2004:11). Surveys require the antenna to be in as direct contact as possible with the ground and are therefore hampered by dense vegetation or rough terrain. Surveys are typically conducted by laying out grids and pulling or pushing the GPR along transects. Transect spacing varies depending on the desired resolution of the survey. During data processing the profiles are first filtered then analysed. The profiles can be individually analysed or complied to create 3D blocks from which time-slices (horizontal slices at different depths) can be taken.

2.4 PROSPECTION

Geophysical surveys in archaeology were first used simply as site location methods, so it is unsurprising that prospection was earliest and most common application of geophysical methods to archaeological shell matrices. Ten studies, utilising six different geophysical methods, were found which focused on geophysical prospection and shell matrix sites. Five of these methods will be discussed: magnetometry, magnetic susceptibility, EM, GPR, and electrical resistivity (for clarity they have been broken down by method, see Table 2.1). Seismic refraction was employed on one occasion, however this method will not be discussed as it is not commonly used in archaeology and there are no other cases available for comparison. Magnetic susceptibility was discussed only once in these prospection papers, but as it was utilised in understanding the magnetometry results in Connah *et al.*'s (1976) magnetic study it will be analysed in conjunction with magnetometry.

Table 2.1 Breakdown of archaeological prospection focused publications by geophysical technique.

Publication	Magnetometry	Magnetic Susc.	EM	GPR	Electrical Res.	Seismic Ref.
Connah *et al.* (1976)	x	x				
Dalan *et al.* (1992)	x				x	x
Arnold *et al.* (1997)	x			x		
Thompson *et al.* (2004)	x		x	x	x	
Moffat *et al.* (2008)	x		x			
Rodrigues *et al.* (2009)			x	x		
Santos *et al.* (2009)			x			
Lowe (2010)					x	
Berzins *et al.* (2014)	x			x		
Arias *et al.* (In Press)	x					

2.4.1 Magnetometry and Magnetic Susceptibility

Magnetometry is quick and relativity easy to use and interpret, because of this it has commonly been used for archaeological prospection. Clark (1990:69) called fluxgate gradiometers the "workhorse – and the racehorse – of British archaeological prospecting." Kvamme (2003) also praises the applicability of magnetometry surveys to archaeological sites by stating "Magnetometry surveys are probably the most productive prospecting method employed in archaeology; it is almost as if nature designed archaeological sites to be made visible by the magnetic variations they exhibit." In light of these views it is unsurprising that seven of the 10 studies devoted to testing the reliability of geophysical prospection in relation to shell matrix sites, employed magnetometers. Of these seven, five compared magnetometers with other geophysical methods while two focused solely on magnetometry.

Magnetometry has shown limited success in locating shell matrix sites, with four of the seven studies being deemed unsuccessful by the authors. Dalan *et al*. (1992) and

Thompson *et al.* (2004) both found their magnetometry results unsatisfactory; unfortunately, in both publications the magnetic survey results were dismissed without discussion. Dalan *et al.* felt their results to be inconclusive and moved onto other methods, while after initial field processing Thompson *et al*. discarded the magnetic survey as it was felt to be less viable than GPR and electrical resistivity. The decision by Thompson *et al.* to discard magnetometry was reported to be mainly due to time constraints and was not discussed further, allowing no analysis of the potential of the method. Having furnished no details, little can be gained from these studies. More, however, can be learned from Moffat *et al.* (2008) who tested their G-856 proton precession magnetometer on an area with several known features, and Berzins *et al*. (2014) who excavated and took sediment cores to further investigate the results of their magnetometer survey.

Moffat *et al.*'s (2008) survey covered an area which included a known re-burial, shell midden and several hearths in northwest Queensland. A 50m by 50m grid with transect spacing of 1m was laid out and readings were collected at intervals of five seconds. Neither the hearths nor midden were located, but the location of the re-burial did show a response. The authors suspect the 1m spacing was not sufficient, as the magnetic survey failed to reliably locate the hearth features which were expected to show a strong magnetic response due to burning. Connah *et al.* (1976) note that insufficient survey spacing is problematic for magnetometry. To locate a magnetic anomaly Connah *et al.* suggest several readings must be taken within its influence, so if prospecting for a hearth (about 1m in diameter) sampling every 0.1m is required to accurately locate the feature. Connah *et al.* explain this is due to weak archaeological magnetic anomalies in Australian contexts, which can be obscured by fluctuations in the Earth's magnetic field or by magnetic mineral content in the soil if only one reading is made within the influence of the anomaly. With Moffat *et al.* sampling every 5 seconds, the data frequency would depend entirely on how fast the surveyor was walking, so it is impossible to determine from the data reported whether they were sampling along the transect frequently enough to detect hearth features. However a transect spacing of 1m being employed to search for features typically 1m in diameter is probably too large. The authors themselves declare their failure to accurately locate features was due to survey layout, and suggest a transect spacing of 0.1 to 0.2m would be required to detect hearth features in open contexts. The authors further note their use of handheld GPS rather than static grid lines may have been a negative factor in the spatial accuracy of the survey. This is particularly relevant as their magnetometry survey results showed several anomalies which corresponded quite well with known hearth features, but were offset.

Berzins *et al.* (2014) investigated a shell matrix composed of freshwater bivalves situated near Lake Burtnieks in northern Latvia. The site, known as Rinnukalns, had been extensively excavated in the 1800s and after this it was considered unlikely that further excavations would be able to locate undisturbed sections of shell matrix. However, three subsequent smaller excavations were successfully carried out in 1895, 1913 and lastly in 1943. In 2011 two geophysical surveys were carried out at the site to investigate the possibility of any remaining undisturbed deposits. The first survey examined the edges of the remaining mound with magnetometry (employing a Ferrex DLG 4.032.82 array of 6 fluxgate magnetometers). The second survey employed GPR as discussed below in Section 2.4.3. The results of the magnetometry survey showed an area of potential archaeological interest around the south-eastern margins of the mound area. However, further investigation found it was not shell matrix deposit, though the sediment in this area did appear to be anthropogenic, consisting of humic deposits containing charcoal.

Sitting in neither the successful nor unsuccessful category is the study presented by Arias *et al.* (In Press) who looked at two shell middens in the Sado valley in southern Portugal. The shell matrix sites are located on sandy deposits, and are difficult to distinguish at the surface, being relatively flat areas with accumulations of shell fragments. Magnetometry surveys were employed to help establish shell matrix boundaries and to pinpoint any features of interest within. The surveys were conducted using a 5 channel Magneto® magnetometer within a grid which had been laid out with a total station. The survey results found correlations between small anomalies and anthropogenic features, and further delineated an area believed to represent the shell matrix present at one of the two sites. However, at the time of publication the research team had not yet excavated to establish if this interpretation was correct.

Magnetometry surveys were successfully applied in two of the published studies. In the first study Connah *et al.* (1976) pioneered the use of magnetometry in the context of open Australian sites. The authors employed a proton precession magnetometer in 1974 to survey a linear midden known as Stuarts Point along the lower Macleay River, aiming to delineate the edges of the buried deposit. Mining surveyors had previously made test cuts into the shell deposits, and Connah *et al.* cleaned and recorded these sections to be used as control data for the surveys. The first survey consisted of two transects 30m apart taken at right angles to the long axis of the midden close to the recorded section, with readings taken at 0.5m intervals. A second more detailed survey was made later in the year, with 10 transects placed across the midden at 0.25m intervals and readings taken at 0.25m intervals. The survey results showed a clear magnetic response which matched the midden matrix (see Figure 2.1). These results were replicated for another midden site at Clybucca, 10km inland from the present coastline. The Clybucca survey consisted of a single transect taken with readings every 0.5m; again there was a pronounced magnetic anomaly which matched excavated sections on site.

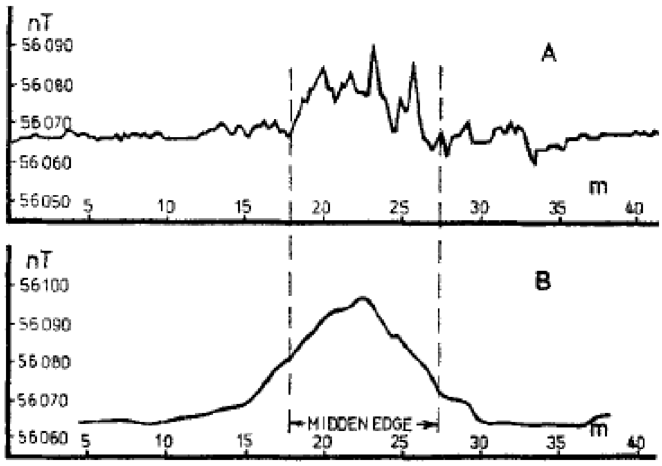

Figure 2.1 Magnetometry results from Stuarts point: (A) Unfiltered total field magnetic profile recorded 5cm above the midden surface. (B) Profile after a 30 point box-car integration (Reproduced with permission of John Wiley and Sons, from Connah *et al.* 1976:152; permission conveyed through Copyright Clearance Center).

Magnetic susceptibility tests were conducted in the field at Stuarts Point by Connah *et al.* (1976) using a Bison susceptibility bridge. Samples were taken from the cleaned section, and results revealed the surrounding sand and unburnt shell of the midden had virtually no susceptibility. The burnt zones (hearths) in the section showed enhanced magnetic susceptibility while the humus layer accumulated over the midden had the highest susceptibility on site. These results indicate while the midden matrix itself could not be detected, an associated anomaly in the magnetometry results was indirectly caused by the midden, due to the increased fertility of the buried material and subsequent increased humus accumulation. While burning from hearth areas was a contributing factor in the magnetic anomaly observed, the increased response from the humus allowed delineation of the midden's boundaries.

The second study to successfully employ a magnetometer as a prospection tool at a shell matrix site was Arnold *et al.* (1997). This study focused on finding features within the midden rather than the midden itself. Employing a caesium vapour magnetometer (CVM) two sites were surveyed on Santa Cruz Island, California, USA. For the first site, Morse Point, two 20m by 20m grids were established with 0.5m transect spacing. The site exhibited clear depressions in the surface, thought to indicate house floors, the CVM survey results exhibited correlating anomalies (see Figure 2.2). At the second site, Prisoners Harbour, two grids were surveyed. The first grid, 8m by 14m, was previously excavated and included a known house structure. The second grid, 7m by 9m, may have been part of the large-scale trenching of the 1920s. Strong rectangular anomalies were visible in the data over the locations of previous excavations, and several anomalies from an unidentified source were detected.

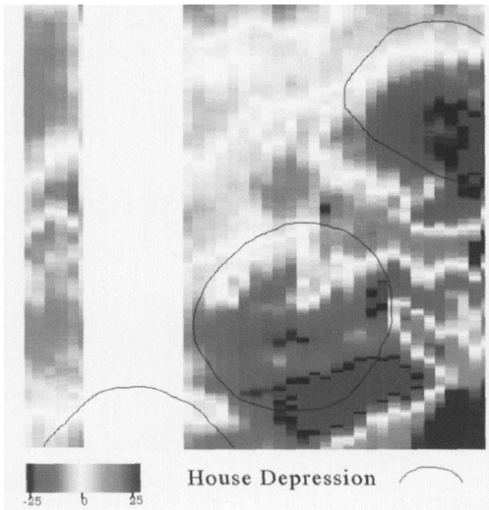

Figure 2.2 Magnetometry results from Morse Point with location of surface depressions marked (Reproduced with permission of Cambridge University Press, from Arnold *et al.* 1997:164).

These studies show the potential of magnetometry, it is relatively easy and quick to use, but there are difficulties in working with magnetic surveys and shell material. The magnetic susceptibility of unburnt shell is extremely low, so surveys rely on burnt shell material and organic humus present in the shell matrix to signal the presence of the midden itself. Surveys searching for features within a shell matrix site such as house floors or hearths, where burning is likely to have occurred are more likely to be successful, and so magnetometry surveys have a relevant place in the study of shell matrix sites. They do not, however, meet the demands of this study as they cannot be reliably used to create maps of buried deposits or delineate the subtleties of the landscapes buried beneath them.

2.4.2 Electromagnetic Induction

Electromagnetic induction, like magnetometry, is well-represented as a prospection tool being employed in four of the seven papers (see Table 2.1). As with magnetometry there were successes and failures with regards to the results produced by the EM surveys. Unfortunately Thompson *et al.* (2004), as they did with the magnetic results, field-processed the EM data and discarded it without further explanation, in favour of using GPR and electrical resistivity as the more viable detection methods for shell matrices. As mentioned above, with no further information there is no way of evaluating their results and learning from them.

Like Thompson *et al.* (2004), Moffat *et al.* (2008) also produced inconclusive results for EM, though more can be learnt from their paper. Their EM survey used a Geophex GEM-2 and ran the same 50m by 50m grid with 1m transect spacing their magnetic survey used (Section 2.4.1), but with a rate of 10 readings per second. Like the magnetometry survey results, the authors concluded neither the hearths nor the midden were detected in the EM survey results, but the reburial was detected at certain frequencies. It is hard to evaluate this conclusion, however, as they do not show all the frequencies for the EM; only the highest frequency data is displayed and it shows no evidence of an anomaly in the location of the re-burial.

The EM data presented in the paper is used to illustrate the presence of an anomaly in the northeast corner of the grid. Moffat *et al*. interpret this anomaly to be the weathered bedrock present at the surface in this location, but their site map shows other exposed bedrock outcrops within the survey grid which are not represented in the EM data. Interestingly the feature which coincides solely with the anomaly in the northeast corner of the grid is the midden (see Figure 2.3). No reasons are given for why the authors thought the exposed bedrock and not the midden material was the source of the EM anomaly. Personal communication with the lead author (Ian Moffat 2014) failed to clarify this point; with Moffat dismissing the entire study as too spatially coarse and inaccurate to be worthy of attention, but agreeing EM surveys over midden deposits would be worth exploring.

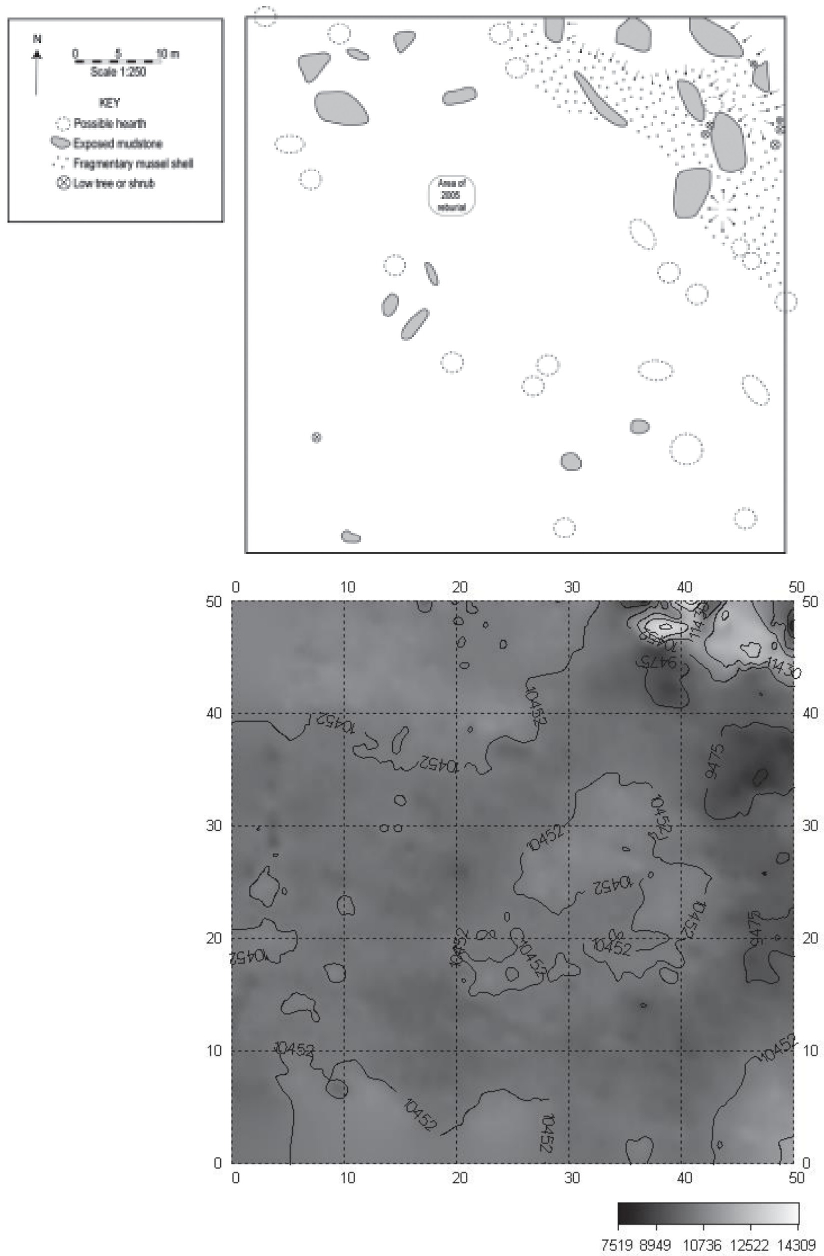

Figure 2.3 Site plan and high frequency (47975 Hz) electromagnetic induction results for a site in remote northwest Queensland (Reproduced with permission of Routledge: Taylor and Francis, from Moffat *et al.* 2008:62; permission conveyed through Copyright Clearance Center).

Successful EM studies of shell matrix sites include two papers from research conducted in Santa Caterina State, Brazil and one conference paper from New York, USA. The conference talk was given at the 42nd Annual Meeting of the North-Eastern Section of the Geological Society of America by Steinberg *et al.* (2007). Steinberg *et al.* outline their research comparing the results of standard shovel test pits (STP) with EM. On Shelter Island, New York, they used a Geonics EM31 conductivity meter with 1m line spacing and 0.5m data collection over 0.5ha, and located two small dense shell middens the STP had missed. These middens were 3m in diameter and approximately 0.45m thick. The data obtained from this study could not be assessed as an associated paper was never published (John Steinberg, pers. comm., 2014) and so this study was not included in Table 2.1, but the reported results do suggest that EM could be successful in locating shell matrix sites.

The two Brazilian studies were interested not in the location and boundaries of shell matrix sites, but in finding features of interest within already known midden deposits. The studies were published by the same team and back-to-back in the same issue of the *Journal of Archaeological Science*. The first paper (Rodrigues *et al.* 2009) covered several sites, mainly focusing on GPR use with the exception of combining GPR and EM results at the Santa Marta IV site. The second paper (Santos *et al.* 2009) focused on EM at Santa Marta IV. Both studies employed a Geonics EM38, which has two coils 1m apart allowing for both horizontal and vertical dipole readings contiguously. The vertical dipole allows for 1.5m depth analysis, while the horizontal allows for 0.75m.

Rodrigues *et al.* (2009) surveyed a 10m by 5m grid, running 5m transects every 0.5m and taking data readings every 0.5m. These readings were corrected for instrumental drift (caused by ambient temperature variation) by using a base station. They found an anomaly of high magnetic susceptibility and low conductivity in the EM data which coincided with a high amplitude anomaly in the GPR profiles (see Figure 2.4). This anomaly upon excavation was found to be a hearth feature. Their interpretation of the low conductivity region associated with the hearth feature is questionable. The low conductivity is by no means clearly associated with the hearth location, unlike the results from the GPR and the magnetic data from the EM.

The second paper addresses the EM surveys and the Santa Marta IV site in more detail (Santos *et al.* 2009). Two grids were surveyed, Grid 1 was 25m by 10m (11 profiles were taken), and Grid 2 was 20m by 5m (6 profiles taken), both were run north/south with 1m transect spacing, and data readings were collected at 0.5m intervals. A base station was again established for drift correction, and the terrain was mapped using a total station. Irregularities were discovered in the conductivity data obtained which corresponded with terrain changes; the higher the elevation (thus further from the shallow water table) the lower the conductivity (see Figure 2.5).

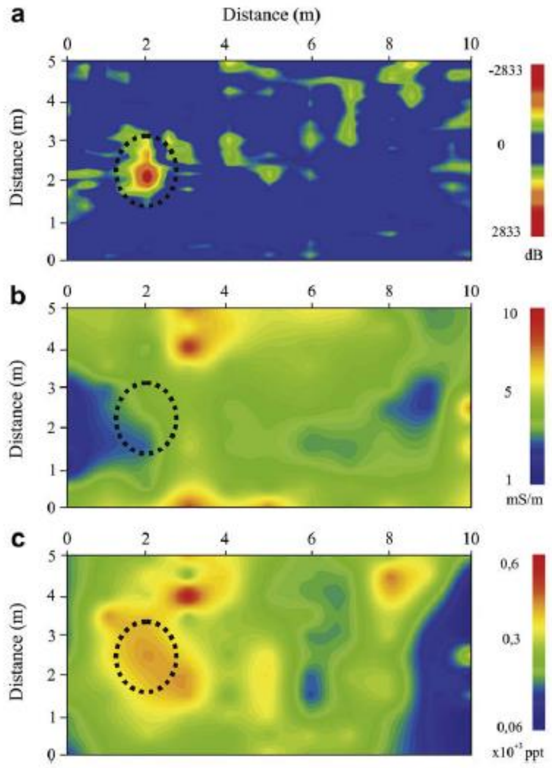

Figure 2.4 Depth slices taken at 1.125m from Santa Marta IV; (a) GPR survey results, (b) electrical conductivity results from EM survey, and (c) magnetic susceptibility results from EM survey (Reproduced with permission of Elsevier, from Rodrigues *et al.* 2009:2084; permission conveyed through Copyright Clearance Center).

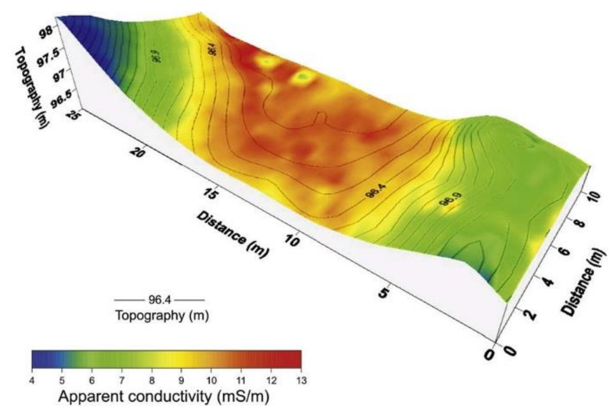

Figure 2.5 EM survey of Grid 1 at Santa Marta IV showing topographically corrected conductivity results (Reproduced with permission of Elsevier, from Santos *et al.* 2009:2092; permission conveyed through Copyright Clearance Center).

The simple nature of the correlation between elevation and conductivity allowed the authors to create and use a linear model to remove the topographic effects of the survey. The magnetic data was not affected by the water table and thus was not corrected. The removal of these topographic effects from the conductivity results allowed the authors to pinpoint an anomaly previously almost obscured in Grid 1, but observable in the magnetic profile (see Figure 2.6); excavation found this anomaly to be a hearth feature. Two low conductivity anomalies observable in the data were dismissed because they were not observed in the magnetic survey and were therefore considered as having no archaeological potential. This is unfortunate, it would have been interesting to see what caused the anomalies. For Grid 2 conductivity anomalies related to the topography were not as prevalent as they were in Grid 1, but the correction was still applied in case a lower water table was present; the resulting correction showing little difference. Grid 2 displayed a strong magnetic and conductive anomaly which upon excavation was revealed as a concentration of ceramic material.

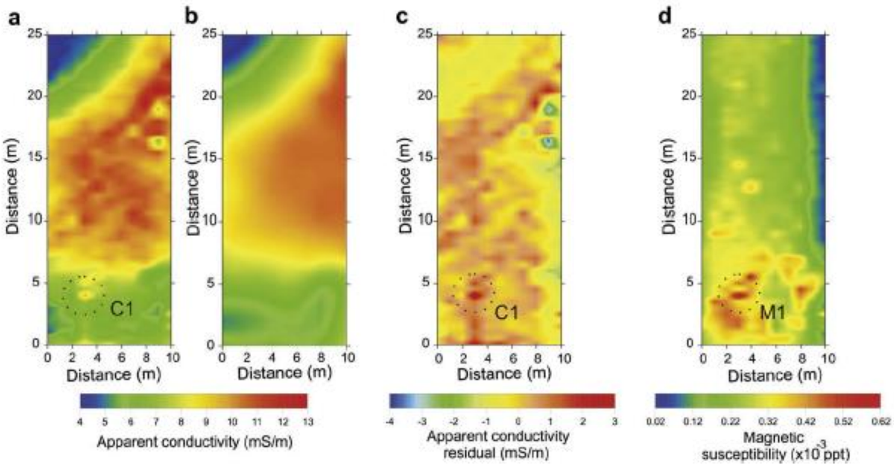

Figure 2.6 EM survey results for Grid 1 at Santa Marta IV: (a) raw conductivity results, (b) conductivity anomalies produced by topography, (c) filtered conductivity results and (d) magnetic results (Reproduced with permission of Elsevier, from Santos *et al.* 2009:2093; permission conveyed through Copyright Clearance Center).

The EM surveys, like the magnetometry surveys, show potential for use on shell matrix sites, particularly in relation to locating features within shell deposits. However, because the design of the instrument only permits shallow subsurface investigation, its potential is limited, and unsuitable for the research aims of this study. A lesson can be taken away from these prior studies in the importance of careful planning, applying appropriate survey grid layout and transect spacing. The failures of Moffat *et al.* (2008) and the successes of Rodrigues *et al.* (2009) and Santos *et al.* (2009) are salient. Where Moffat *et al.* used handheld GPS with a few guide tapes to track their survey, Rodrigues *et al.* and Santos *et al.* laid out grids and mapped them with a total station. Perhaps less important than the structured layout of the survey grid, but still important, is the transect spacing. Both Moffat *et al.* and Santos *et al.* used 1m transect spacing to search for features approximately 1m across, and where Moffat *et al.* failed, Santos *et al.* succeeded, though it is likely the 1m transects employed by Santos *et al.* missed features as well. Santos *et al.* also clearly illustrated the importance of accounting for water table effects in conductivity results; as conductivity is the opposite of resistivity these results can be translated to electrical resistivity as well.

2.4.3 Ground-Penetrating Radar

GPR has great potential as a prospection method for locating and identifying features of interest within shell matrix sites. However, GPR surveys are represented in only four, less than half, of the prospection focused papers (see Table 2.1). Conversely, it is the favoured tool for studies investigating shell matrix site formation processes, present in nine out of 11 papers (see Table 2.2 in Section 2.5). It is likely researchers prefer the quicker and thus less expensive geophysical methods when it comes to questions of prospection, with GPR data processing being too time consuming. Comparatively questions of site formation are more complex to answer and the level of detail provided from GPR results becomes highly desirable.

The first of the four studies reporting the use of GPR at shell matrix sites, looked at locating house floors and burials within shell deposits. Arnold *et al.* (1997) experimented with both magnetometry (as discussed above) and GPR to locate these features. Similarly to the magnetometry, GPR was deployed at both the Morse Point and Prisoners Harbor sites on Santa Cruz Island, California, USA. A GSSI SIR-10 was used with an antenna frequency centred in the range of 100-500MHz. For Morse Point two 20m by 20m grids were surveyed with 1m transect spacing. The GPR results for Morse Point contained several clearly defined planar anomalies interpreted as house floors as well as two hyperbola anomalies interpreted as possible burials. The article includes two profiles to illustrate the presence of a house floor, one filtered and one unfiltered (see Figure 2.7). The unfiltered profile presented is far clearer than the filtered one; the authors do not state what filters they used to process the profiles but clearly they were inhibitive to interpretation.

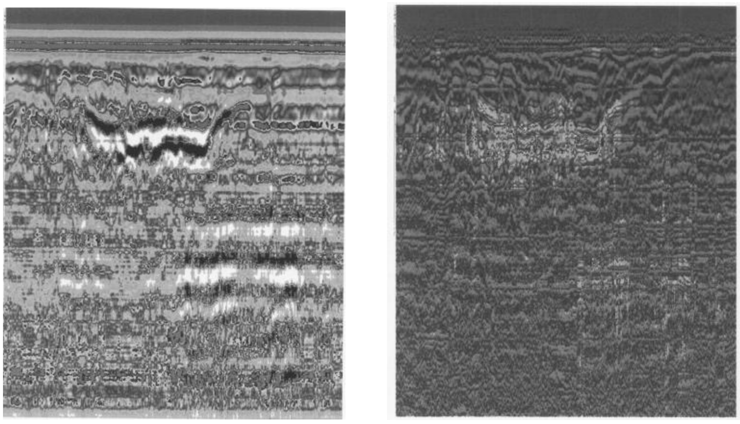

Figure 2.7 GPR profile from Morse Point showing a planar anomaly thought to be a compacted house floor: (left) unfiltered data, (right) filtered data. Profiles are 20m long and 40ns or 1.5m to 2m in depth (Reproduced with permission of Cambridge University Press, from Arnold *et al.* 1997:165-166).

The survey at the Prisoners Harbor site was also conducted in two grids: one 8m by 14m and one 7m by 9m with 1m transect spacing. As mentioned for the magnetometry results, one of these grids contained an area of prior excavation which is represented as a rectangular anomaly in the GPR data (see Figure 2.8).

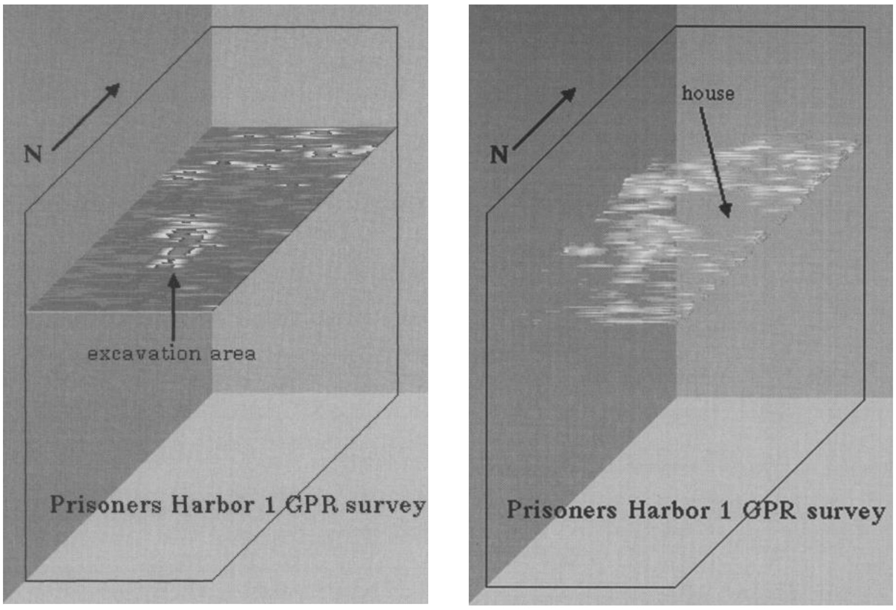

Figure 2.8 GPR depth slices from Prisoners Harbor; (left) square high amplitude anomaly thought to be earlier excavation, (right) circular low amplitude anomaly thought to be house floor (Reproduced with permission of Cambridge University Press, from Arnold *et al.* 1997:162-163).

The surveys also detected a known house floor at this site, but unlike the compact clay floor at Morse Point which created a strong planar reflection in the profiles this floor created a circular gap in the three dimensional data sets produced (see Figure 2.8). The gap was theorised to be created by the low reflectivity of the house floor compared to surrounding deposits. This response was thought to be due to the house floor being made up of sandy deposits allowing greater water drainage compared to surrounding sediments.

The second paper describes the Thompson *et al.* (2004) study in which magnetometry and EM were discarded in favour of electrical resistivity and GPR. The study site was located on Sapelo Island, Georgia, USA, and consisted of three large shell ring mounds and many smaller non-ring mounds. The study aimed to determine which deposits the shell ring mounds formed from, to re-locate and map the spatial extent of mounds whose location had been lost, identify features of interest within the shell deposits, and to investigate the structure of the mounds. The stated aim of going beyond just prospection to investigate site formation was at this stage unsuccessful. An electrical resistivity survey was selected for locating the lost ring mounds and is described in the next section. For investigating the internal structure of the shell ring mounds and any features of interest within them, the survey employed a GSSI SIR 2000 GPR with a 400MHz and a 300MHZ antenna. Grids of 20m by 20m were established on and around Ring III and GPR transects were run every 0.5m, as well as 3m wide transects over sections of Ring I. Numerous circular anomalies were found ranging in size from 5m to 10m, thought by the authors to be the remains of archaic domestic structures (similar to those found nearby on the mainland). There was, however, no ground truthing to verify this interpretation of the data.

The third paper, by Rodrigues *et al.* (2009), employed a GSSI SIR 3000 with a 200MHz antenna at three sites on the coast of Santa Catarina, Brazil. Their aims were to identify archaeological features of interest such as lithic materials, ceramics, burials and hearths, as well as to characterise and differentiate archaeological layers within the shell deposit. All the GPR data was collected with a 0.04m trace interval and in continuous mode, but survey layout varied. For Jabuticabeira II, GPR profiles were run with irregularly spaced lines. For Santa Marta IV, two grids were surveyed with transect spacing of 0.5m. Encantada III was also surveyed as a grid but with transect spacing of 1m. A total station was used for topographical corrections, and data was filtered using time-zero correction (trace position corrected for air-wave travel), time filtering (band-pass to remove unwanted frequencies), time-varying gains (to compensate for energy losses owing to absorption and scattering), and time-depth conversion (nanoseconds to depth based on a common-midpoint velocity analysis). The profiles illustrated in the article are very distinctive, showing effective processing which produced clear results.

The GPR results for the Rodrigues *et al.* (2009) study were indicative of great success in locating the boundaries of, and features of interest within, the deposit. At Jabuticabeira II they found a very clear delimitation which marked the boundaries of the shell deposit (see Figure 2.9). At Santa Marta IV the GPR profiles showed strong sub-horizontal reflectors which marked the base of the shell mound as well as an anomalous high amplitude response, which was found to be an area of burnt material from fire hearths. Further anomalies (hyperbolic reflections) were found to be a burial, a collection of ceramics, and a dense area of shell (see Figure 2.10). For Encantada III, once again the shell mound base was clearly observable in the GPR data as well as a hyperbolic reflector which upon excavation turned out to be a silicified tree root (see Figure 2.11).

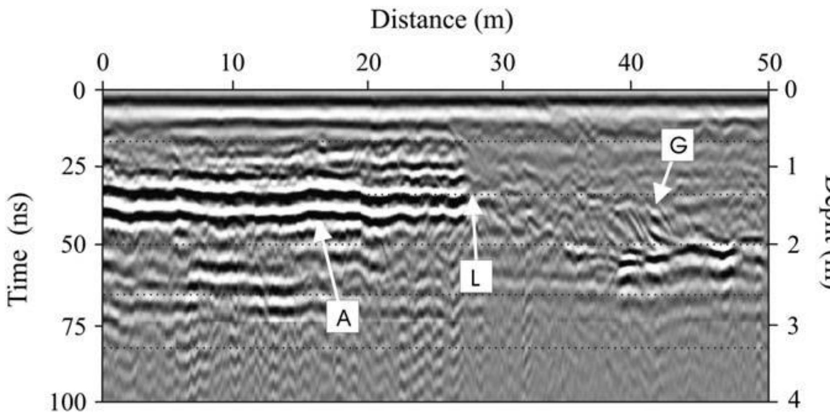

Figure 2.9 GPR profile from Jabuticabeira II: (A) archaeological shell deposit, (L) boundary between shell and surrounding geological region and (G) geological region (Reproduced with permission of Elsevier, from Rodrigues *et al.* 2009:2084; permission conveyed through Copyright Clearance Center).

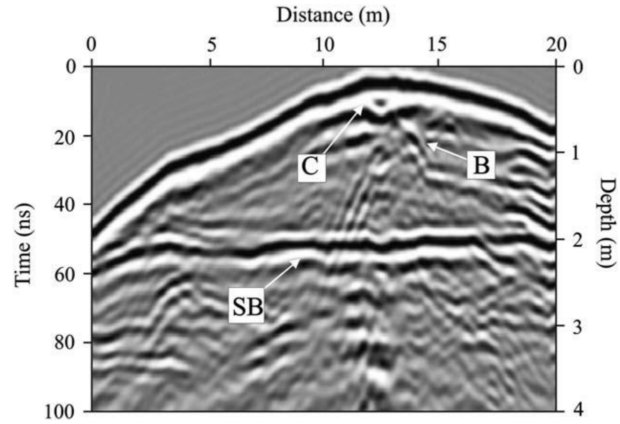

Figure 2.10 GPR profile from Santa Marta IV: (C) hyperbolic anomaly representing an accumulation of carbonate shell, (B) hyperbolic anomaly representing a burial and (SB) a planar anomaly representing the base of the shell deposits (Reproduced with permission of Elsevier, from Rodrigues et al. 2009:2085; permission conveyed through Copyright Clearance Center).

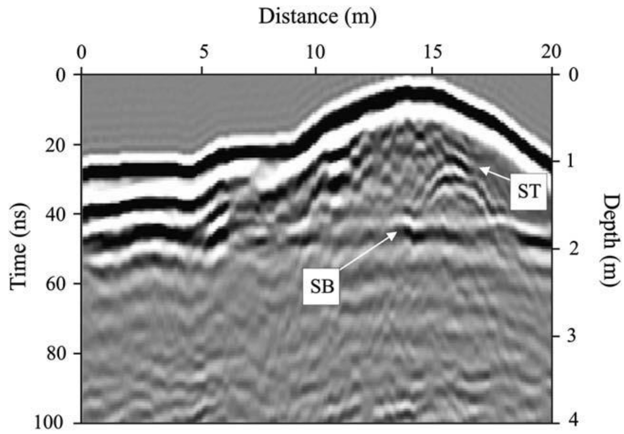

Figure 2.11 GPR profile from Encantada III: (ST) hyperbolic anomaly representing a silicified tree root and (SB) a planar anomaly representing the base of the shell deposits (Reproduced with permission of Elsevier, from Rodrigues et al. 2009:2086; permission conveyed through Copyright Clearance Center).

The reported results of the Rodrigues *et al.* (2009) study focus on the successful location of archaeological features within the shell deposits and the deposit boundaries. While a stated aim of the paper was defining and characterising stratigraphic layering within the archaeological deposits, this aspect of the data was largely ignored. Jabuticabeira II showed distinctive stratigraphic layering yet no analysis is made, while a general statement about the stratigraphy in the analysis of Encantada III is covered in one sentence. For Santa Marta IV there is some mention of the stratigraphic units present, but mostly in relation to computer modelling of results, rather than actual analysis of the site. Interestingly the GPR profiles show markedly different characteristics in the archaeological deposits of Jabuticabeira II, which exhibits multiple strong planar reflections, and the other two sites, which exhibit a homogenous zone with hyperbolic anomalies above a single planar anomaly representing the shell mound base. Excavation photographs clarify these results, with Jabuticabeira II exhibiting dense shell deposits while the other two sites consist of sandy sediment with areas of organic humus and shell inclusions.

The fourth and final paper was the second survey conducted at the Rinnukalns site in northern Latvia and presented in the paper by Berzins *et al.* (2014). Their stated aim was to locate any areas of undisturbed shell matrix within the already extensively excavated site. This survey employed a GSSI SIR-20 with a 400MHz antenna to examine what remained of the mound itself (the edges had been surveyed via magnetometry as presented in Section 2.4.1). A total of eight survey lines were run, spaced out over the mound area, five of which ran north/south with the final three running east/west across the site. The GPR survey results located an area of potential interest, with a subsurface anomaly along line 4 indicating the existence of horizontally layered deposits (see Figure 2.12). Subsequent excavation revealed this anomaly was indeed an area of intact shell matrix.

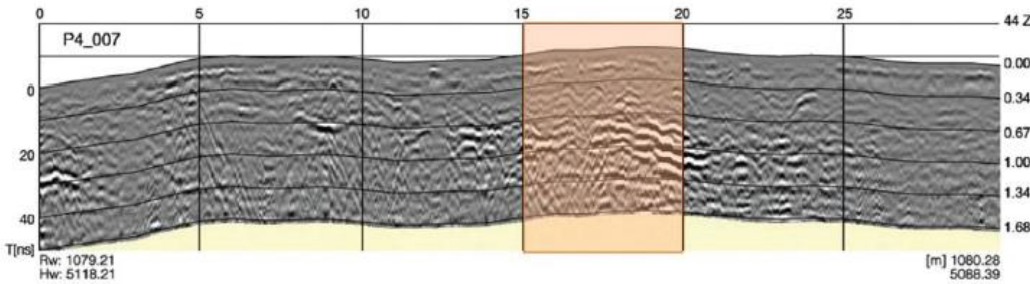

Figure 2.12 GPR profile for Line 4 at Rinnukalns, the highlighted segment shows the area excavated (Reproduced with permission of Cambridge University Press, from Berzins *et al.* 2014:721).

Difficulties have been experienced in employing GPR surveys at archaeological sites, and studies are only recently starting to move away from sites which guarantee a successful survey. As noted at the start of this section, GPR has great potential for use as a prospection tool in relation to shell matrix sites, yet studies and applications are few. Even Conyers' seminal 2012 manual *Interpreting Ground-Penetrating Radar for Archaeology* has very little information in its shell midden section; only two cases are presented, the first was an already published study while the second case study was otherwise unpublished and so minimal it was not added to the list in Table 2.1. The first, and main, case study mentioned is a summary of one of Thompsons' later studies at the Crystal River Complex in Florida. This study is detailed in the next section based on three papers published by the research team (Pluckhahn *et al.* 2009, 2010; Thompson and Pluckhahn 2010). The second case study consists of a brief mention of a midden found during bridge construction on the Tennessee River. The GPR results showed a distinct planar reflection with many small hyperbolic reflections between non-reflective units (see Figure 2.13). Amplitude maps created from the survey results show the feature to be linear and running parallel to the natural levee west of the river channel (see Figure 2.14). Excavation discovered this planar feature to be a 20cm to 25cm thick shell midden sitting on a distinct buried soil horizon (Conyers 2012:162-163).

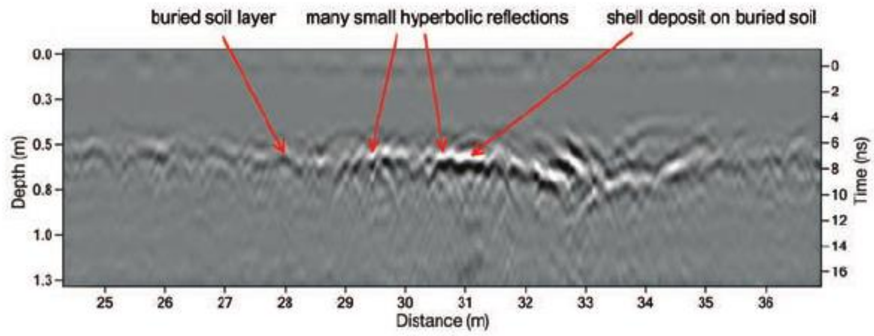

Figure 2.13 GPR profile of Tennessee River Site, showing a planar anomaly made up of many small hyperbolic reflections representing the buried shell matrix (Reproduced with permission of L.B. Conyers, from Conyers 2012:163).

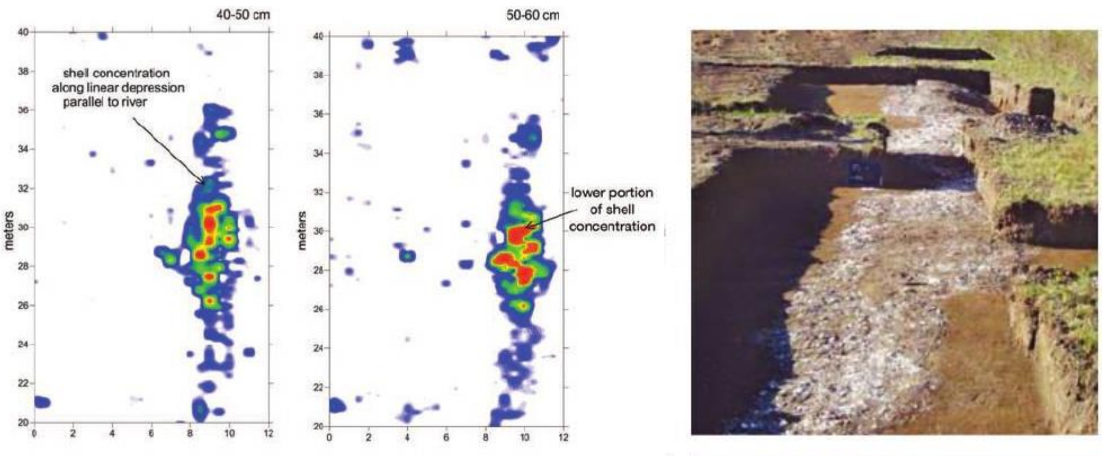

Figure 2.14 GPR amplitude map of shell deposits at Tennessee River site (left), and (right) excavation showing the shell deposits (Reproduced with permission of L.B. Conyers, from Conyers 2012:164).

The work appears to have been conducted for the Georgia Department of Transport (by Shawn M. Patch) though unfortunately no further interest or publications (aside from the mention in Conyers 2012) appear to have resulted from the initial work. The above description and GPR results could have been used to create boundaries for identifying shell middens in the surrounding region. With these identifying boundaries a follow up study could have been conducted along the Tennessee River's banks, aimed at locating buried shell middens and allowing insight into regional subsistence patterns.

The use of GPR to both delineate boundaries of shell matrix sites and to locate features within them, has been proven viable through these studies. The results vary markedly depending on the surrounding sediment, the shell concentration and the shell volume. The Thompson *et al.* (2004) study showed the advantage of utilising multiple geophysical techniques together; electrical resistivity was used for locating the shell mounds (discussed in more detail in the next section) while GPR was used to focus on locating features of interest within the mounds. Unfortunately the anomalies identified in the results and interpreted as house floors were not excavated, and so remain anomalies. While geophysical surveys provide valuable information about a site they typically do not provide definitive results by themselves, secondary evidence to back up interpretations made based off geophysical survey results is required with the best method being some form of ground truthing.

2.4.4 Electrical Resistivity

Electrical resistivity is even less prevalent than GPR as a prospection tool in shell matrix studies, being represented in only three of the seven publications. The first study was one conducted by Dalan *et al.* (1992) at the British Camp site on San Juan Island, Washington, USA. The authors employed an ABEM SAS-300 earth resistivity meter and conducted both vertical and what they refer to as horizontal profiles, though their horizontal profiling was in single transects, not grids, and more closely resembled a shallow vertical profile. To take the vertical soundings the authors employed a Schlumberger array, this array maintains two closely spaced potential electrodes (MN or PP) while moving the outer two current electrodes (AB or CC) further and further apart, to get deeper soundings over the one point. The soundings taken were then linked together to create two section profiles, similar to a pseudosection but with data interpolated between soundings. One transect was run parallel to a wave cut-bank present on site, while the other was run perpendicular to the bank. For the perpendicular section (see Figure 2.15) they obtained data both in summer when the ground was very dry and late winter/early spring when the water table was high and ground quite wet. They found that while the resistivity values changed, by comparing the relative (and not absolute) changes in resistivity, the results matched. The transects for the horizontal profiles obtained results which matched well with the vertical soundings, and allowed for mapping the boundaries of the midden deposits at those particular transect locations. The site was then augured to ground truth the results; as they did not auger and sound in the same locations they found two points where there were differences between the auger results and the interpreted midden deposits. Subsequent checks verified this was due to the interpolation between soundings not due to problems with the results of the resistivity surveys.

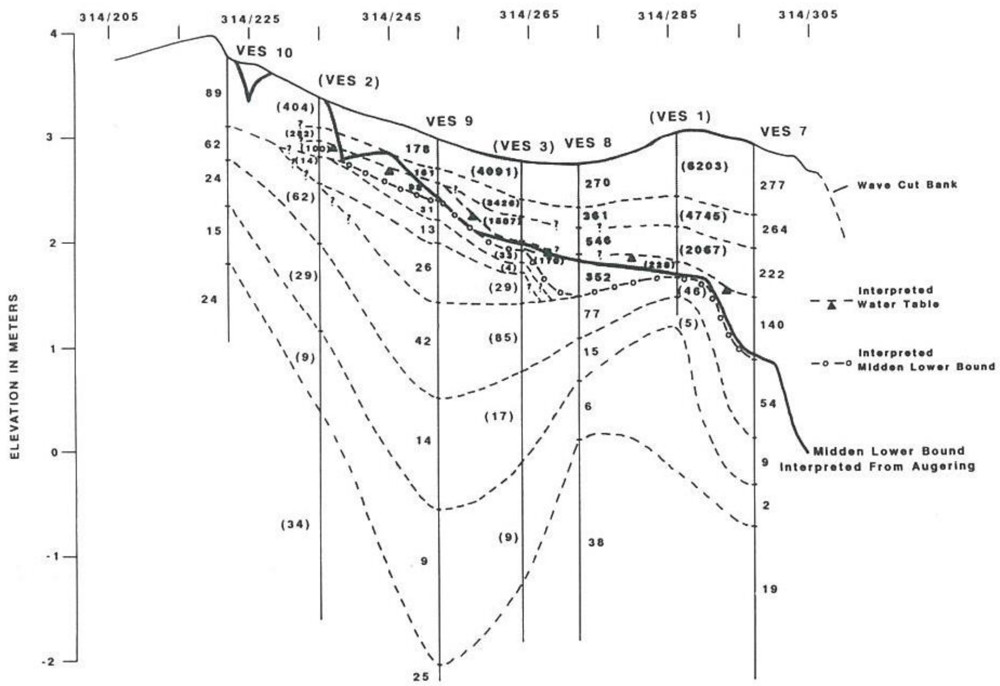

Figure 2.15 Vertical soundings 1-3 and 7-10 from the British Camp site (Reproduced with permission of Elsevier and R.A. Dalan, from Dalan *et al.* 1992:50).

Between VES 2 and VES 9 (see Figure 2.15) a relatively straight line was interpolated as the midden boundary, while coring showed it to dip dramatically between those points. At VES 8 there is also a discrepancy between the interpolated midden boundary based on auguring and the boundary based on electrical sounding, but once again the auger core was taken 4m away from VES 8. Survey designs based on interpolation between soundings are bound to produce some inaccuracy, however, the associated loss in accuracy could be worth the savings in time and cost depending on how great the error is. For this survey the loss did not seem excessive, but a more thorough investigation of the error range would enhance the results of the study.

The second paper is Thompson *et al.* (2004), who trialled four geophysical methods for their study. As mentioned above the Magnetometry and EM were quickly discarded, but the electrical resistivity was deemed useful for large-scale horizontal surveys. The authors found the shell highly resistant compared to the surrounding sandy matrix, and so used the resistance meter to locate the mounds. The exact locations of two of the three larger mounds on Sapelo Island had been lost due to deflation, caused by removal of shell material for use as road fill. To locate the rings, grids of 20m by 20m were laid down from a baseline. The placement of these grids were based on field observations, as well as historical records and prior archaeological work. The survey was conducted using an RM15 resistance meter in a twin probe array, this layout allows for a fast horizontal survey of the shallow subsurface. Readings were taken in 0.5m intervals along transects spaced at 1m. The survey results were successful in locating clearly defined rings of higher resistance indicating shell deposits (see Figure 2.16).

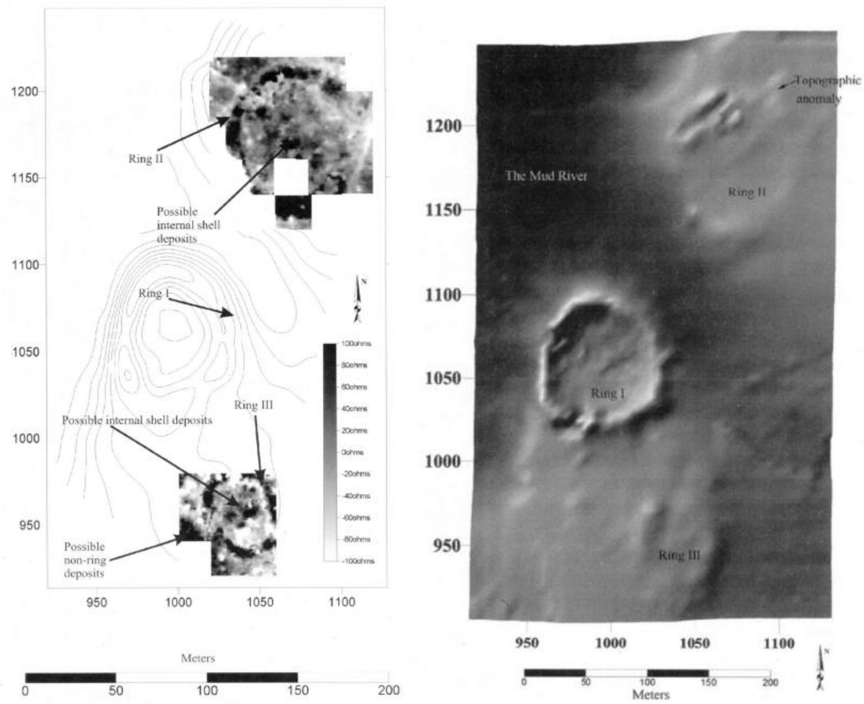

Figure 2.16 Sapelo Shell Ring Complex; (left) resistivity results, (right) topographical survey results (Reproduced with permission of V.D. Thompson, from Thompson *et al.* 2004:197).

The resistivity results were then used to guide a topographic survey using a total station (see Figure 2.16). The topographic map produced was used to provide complementary data to the resistivity results, adding further evidence for the location of the rings. The combination of topographic and resistivity surveys provided compelling evidence for the location of the rings without the need for ground truthing. The third publication was a draft report on work conducted at Bay Cove and Oak Grove in Mississippi, USA presented by Lowe (2010). The surveys were conducted using a twin probe electrical resistivity array (a TR Systems Resistance meter) with a probe separation of 50cm. While identifying shell matrix boundaries was not the aim of the research, the survey results found regions of higher resistance in the results related to areas on the ground with exposed shell matrix.

Resistivity like GPR has great potential as a prospection tool in relation to shell matrix sites, though little has been done with it. Interestingly these methods are being applied, though minimally, in answering questions about shell matrix site formation, while magnetometry and EM surveys while popular for prospection are less suited to answering larger questions about site structure or formation and drop out of the studies. This is likely due to their limited ability in creating three dimensional maps of the subsurface. The next section will, therefore, see the focus move from magnetometry and EM to electrical resistivity and GPR.

2.5 Site Formation

In moving beyond prospection, there are 12 papers published which use geophysical surveys to establish depositional history and site formation processes for shell matrix sites. Of the 12 papers nine are archaeological, but three of these detail the same case study; Pluckhahn *et al.* (2009); Pluckhahn *et al.* (2010); and Thompson and Pluckhahn (2010). Beyond archaeology, in geology, three more papers have been published investigating site formation in shell cheniers. The geophysical survey methods employed in these site formation studies consist mainly of GPR and electrical resistivity. However, Terrestrial Laser Scanning (TLS or Terrestrial LiDAR) is employed in one published study and magnetic susceptibility is used to analyse excavated sediment in another (see Table 2.2). These papers will be broken down by geophysical method and discussed separately.

Table 2.2 Breakdown of site formation focused publications by study focus and geophysical technique.

Publication	Archaeological Study	GPR	Electrical Res.	Magnetic Susc.	TLS
Chadwick and Madsen (2000)	Yes	x			
Neal *et al.* (2002)	No	x			
Thompson (2007)	Yes		x		
Pluckhahn *et al.* (2009)	Yes	x	x		
Thompson and Pluckhahn (2010)	Yes	x	x		
Pluckhahn *et al.* (2010)	Yes	x	x		
Dougherty and Dickson (2012)	No	x			
Weill *et al.* (2012)	No	x			
Rosendahl *et al.* (2014)	Yes			x	
Larsen *et al.* (2015)	Yes				x
Rodrigues *et al.* (2015)	Yes	x			
Pluckhahn *et al.* (2016)	Yes	x			

2.5.1 Magnetic Susceptibility

Magnetic susceptibility was used by Rosendahl *et al.* (2014) to investigate site integrity and to distinguish cultural from natural site formation processes. Three study sites were investigated on Mornington Island in the Gulf of Carpentaria, Australia. The study employed a Bartington MS3 Magnetic Susceptibility Meter with a MS2B Dual Frequency (460 and 46000Hz) lab sensor, and conducted low field mass (χ), volume susceptibility (SI), and frequency dependence of susceptibility (χfd) measurements. Measurements were taken from excavations at three sites: Guttapercha which was a 1m^2 excavation, and Mala Katha and Munburlda which were 50cm^2 excavations. The results found that increases in χ and χfd coincided with both increased anthropogenic remains and finer grained sediments, leading the authors to argue that increases in the magnetic susceptibility values are indicative of cultural changes. The authors claim that the rising and falling cycle of magnetic enhancement present at Guttapercha (see Figure 2.17) and Mala Katha, but not at Munburlda which peaks and then drops off, is therefore illustrative of multiple occupation phases. Rosendahl *et al.* then argue for the stratigraphic integrity of the sites based on the decreasing sediment size and magnetic susceptibility values with depth, as well as distinct colour changes between stratigraphic units.

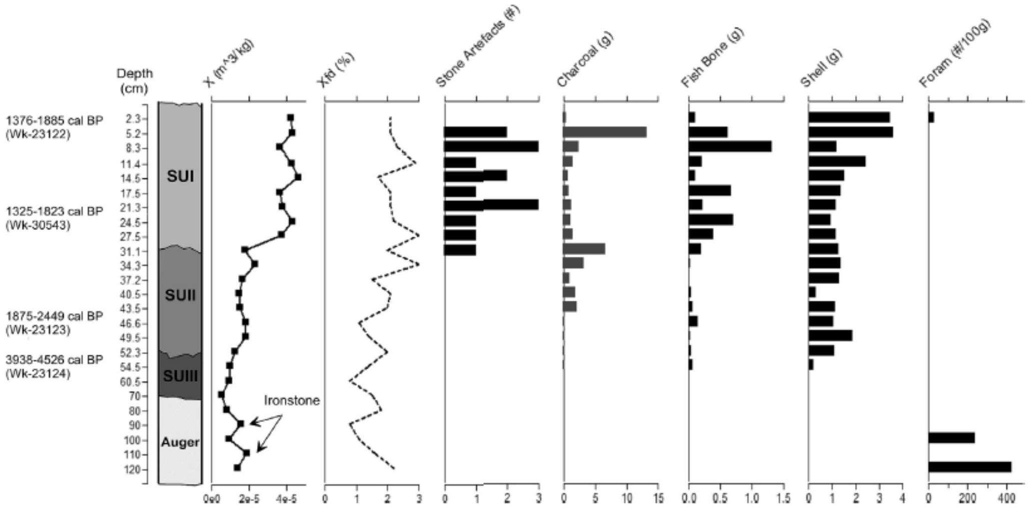

Figure 2.17 Combined geophysical and geoarchaeological results for Guttapercha (Reproduced with permission of Elsevier, from Rosendahl *et al.* 2014:26; permission conveyed through Copyright Clearance Center).

This paper shows the potential of magnetic susceptibility in investigating site formation for shell matrices, but unfortunately the arguments presented are hard to follow, requiring the reader to make assumptions about the results rather than clearly specifying the authors' interpretations. For example, it is never clearly stated the rising and falling cycle of magnetic enhancement is the basis for their interpretation of multiple occupation phases at Guttapercha and Mala Katha. The authors leave the connection to be made by the reader, first asserting that multiple occupation phases can be inferred from the results for Guttapercha and Mala Katha but not from Munburlda, then later noting that prior research has found a correlation between high χ values with occupational layers and low values with culturally sterile fill.

Contemporary research trends in magnetic susceptibility (see Dalan 2008) illustrate the vital role it can play in understanding site formation and post-formation processes. However, for the aims of the current study it could provide only complementary data as it cannot be utilised to produce an estimate of volume for buried shell deposits which is a pivotal aim of this research.

2.5.2 Terrestrial Laser Scanning

Larsen *et al.* (2015) employed Terrestrial Laser Scanning (TLS) or terrestrial LiDAR, as a non-invasive and time saving method to investigate shell mounds. The survey looked at shell mounds around Weipa in Queensland, Australia, aiming to characterise the size and shape of 51 mounds, 28 of which were radiocarbon dated based on samples from excavations taken from the centre of the mounds. The shell mounds were scanned, then post-processing of the results targeted the removal of vegetation and other obstructions leaving only the mounds in the scans. The TLS results were combined with airborne LiDAR results, so the mounds could be mapped into their surrounding landscapes. Eleven morphological variables were used to quantify the mounds, including volume (see Section 2.6 for further discussion of this).

By combining these morphological characteristics with radiocarbon dates taken from each mound, temporal and spatial variability between mounds could be investigated. The study found older mounds tended to be flatter than younger mounds, with the exception of mounds whose accumulation ceased then recommenced. This was an expected result given that weathering and compaction leads to landforms decreasing in height over time. Further correlations between mound form and spatial location found that mound material tended to spread along ridges rather than up or down slope, though the most elongated mounds were located not along ridges, but close to the shore away from the ridges. These results showed both natural and cultural processes have impacted upon the morphology of the mounds and need to be considered together.

This method of investigating shell mounds showed great potential for gaining an insight into regional formation patterns and mound variability. The method is restricted, however, as the laser reflects off surfaces and can map only mounded deposits giving no insight into the subsurface. This method could not be used on buried shell matrix sites and is thus not desirable for this current research.

2.5.3 Ground-Penetrating Radar

Chadwick and Madsen's (2000) study is the earlier of only two archaeological case studies to utilise GPR in investigating the depositional history of shell matrix sites. Employing a PulseEKKO IV with a 100MHz antenna they surveyed a shell matrix site on Cape Henlopen, Delaware, USA. Their survey applied both the common-offset method (transmitter and receiver are moved along the profile at a constant interval) and the common-midpoint method (transmitter and receiver are moved outwards incrementally from a midpoint). Three single transects (using common-offset) were run across the mound, two ran parallel with the third running perpendicular to the first two. A common midpoint profile was obtained to establish velocity (for depth conversion) where two of the three common-offset lines intersected on site. Traces were collected every 0.25m and processing included stacking and automatic gain control. The study aimed to both map the buried shell deposits and to understand the paleoenvironment in which the shell midden had been laid down.

The buried shell deposits were mapped based upon their presence on the surface, and the continuation of associated reflections in the GPR profiles occurring directly beneath the surface scatters. Chadwick and Madsen assessed alternative possibilities for these reflections but ultimately argued for their representing the shell deposits. These deposits, as based on the GPR results, were mapped to between 1.5m and 2.1m in depth. Nearly circular in shape, the deposits covered approximately 250m² reaching 20m across at its greatest width. The authors go on to interpret all the anomalous features of the GPR profiles based on educated guesses regarding coastal morphology for the region. It is hard to say how accurate these interpretations are in the absence of ground truthing (see Figure 2.18).

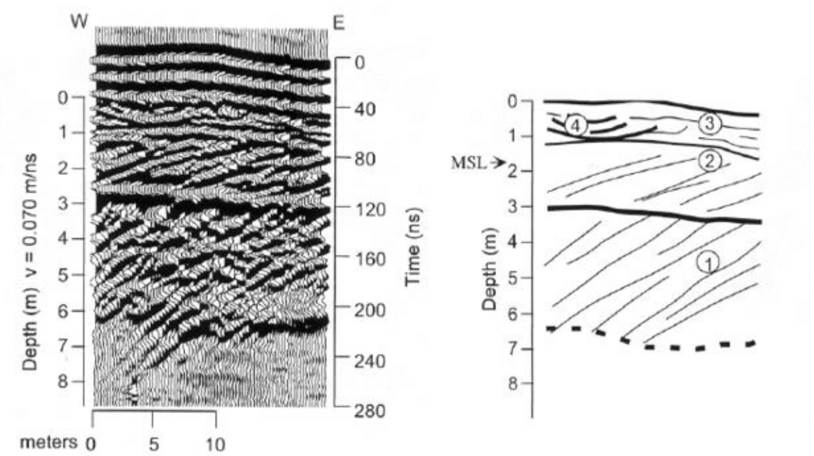

Figure 2.18 GPR profile (left) and interpretation (right): (4) shell deposits, (3) dune, (2) spit, (1) spit platform, (MSL) present mean sea level (Reproduced with permission of John Wiley and Sons, from Chadwick and Madsen 2000:772; permission conveyed through Copyright Clearance Center).

To address their aim of establishing the palaeoenvironment in which the shell midden was formed, Chadwick and Madsen created an isopach map of the base of the midden deposits. This map was then taken as a representative estimate of the palaeotopography of the site. The authors then argued that estimations of the prior local sea-levels could be made based off this palaeosurface. By assuming the past tidal range was proportional to the present, the authors calculated that with the site currently 1.26m below mean high water and the base of the site approximately 0.11m above present mean sea-level, the prior mean sea-levels for the site would have been at least 1.15m below present. However, these arguments and site interpretations fail to be more than conjecture without ground truthing.

The second study to use GPR in investigating shell matrix site formation was at the Crystal River complex in Florida, USA, it is detailed in three papers (Pluckhahn *et al.* 2009, 2010; Thompson and Pluckhahn 2010). The study utilised both GPR and electrical resistivity (discussed in Section 2.5.4) to investigate the shell mounds on site. For the GPR survey, the team employed a SIR 3000 with a 400MHz antenna. Varying grid sizes were deployed based on the mound being surveyed, but transect spacing was always 0.5m. GPR-SLICE and GPR Viewer software were used to process the data. Several areas were surveyed: Mounds H, K and A as well as Feature B (Pluckhahn *et al.* 2009, 2010; Thompson and Pluckhahn 2010). The site consists of six mounds including two burial mounds and four platform mounds (see Figure 2.19), the largest being over 9m tall. There is also a curvilinear mound thought to be a simple shell midden rather than intentional mound structure (Thompson and Pluckhahn 2010). The study aimed to map internal structures and/or stratigraphic layers to better understand the developmental sequence of the site. Further aims were to provide insight into the scale and rapidity of landscape modification present, and to locate past excavations and assess the impact of various historic site uses like house construction and mining.

On Mound H two anomalies thought to be prior excavations were located in the profiles. The authors argue for the interpretation of these anomalies as prior excavations, based on their appearance being consistent with expected GPR results for excavations and on their location in the general vicinity of prior excavations. The GPR profiles illustrating these anomalies, one in Grid 2 from the summit of Mound H (see Figure 2.20) and one in Grid 3 from the ramp area of Mound H (see Figure 2.21), do show what appear to be a straight-sided gaps in the sediments. However, additional horizontal time slices of the grids would have provided a greater insight into whether or not these features are excavation trenches.

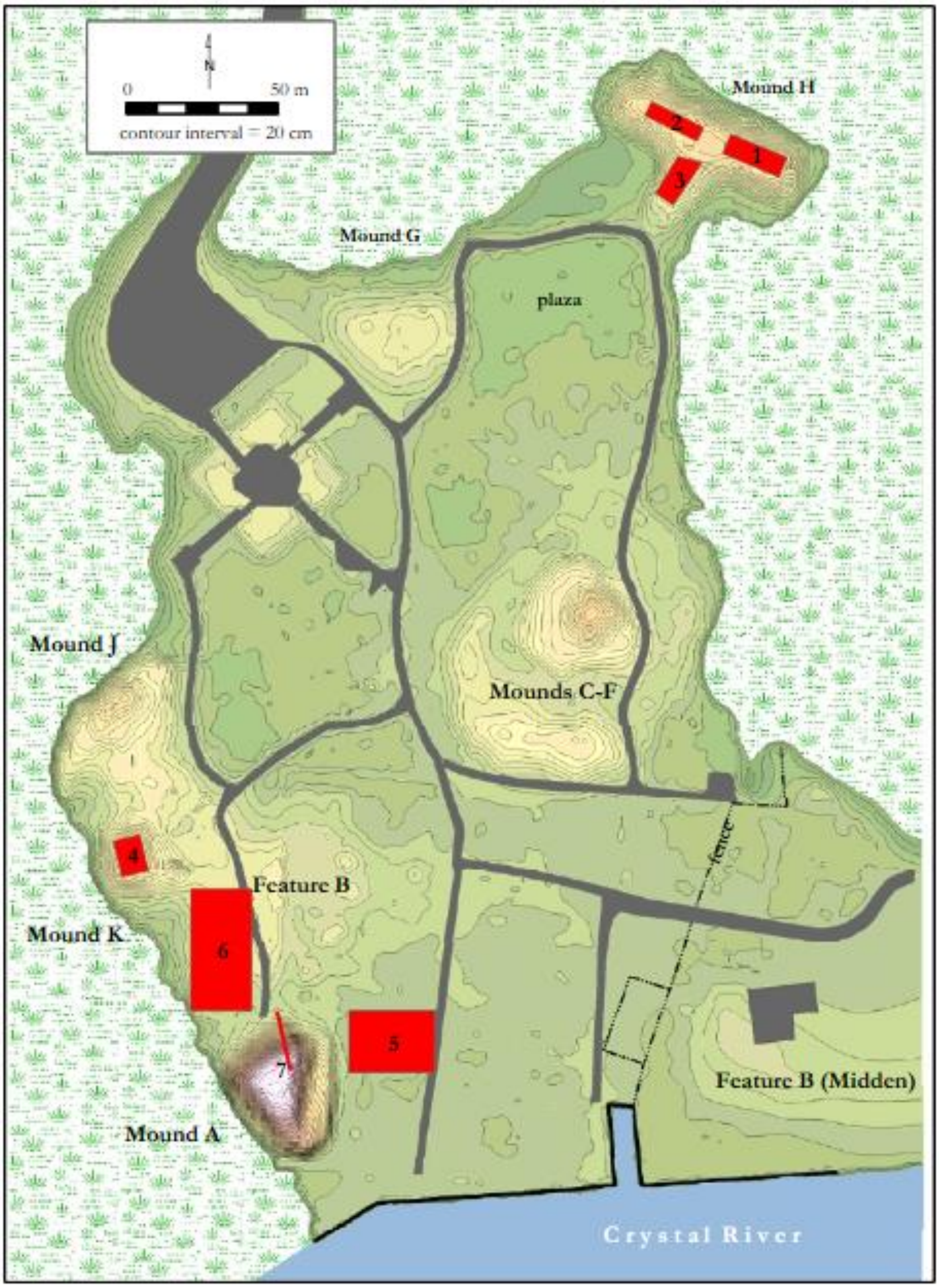

Figure 2.19 Topographic map of Crystal River Complex with GPR grid locations (Reproduced with permission of V.D. Thompson and T.J. Pluckhahn, from Pluckhahn *et al.* 2009:45).

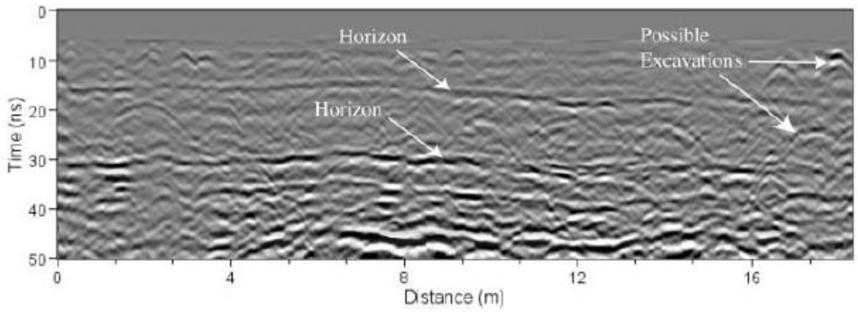

Figure 2.20 GPR profile showing buried horizons and possible prior excavation in Grid 2 on Mound H (Reproduced with permission of Routledge: Taylor and Francis, from Thompson and Pluckhahn 2010:45; permission conveyed through Copyright Clearance Center 45).

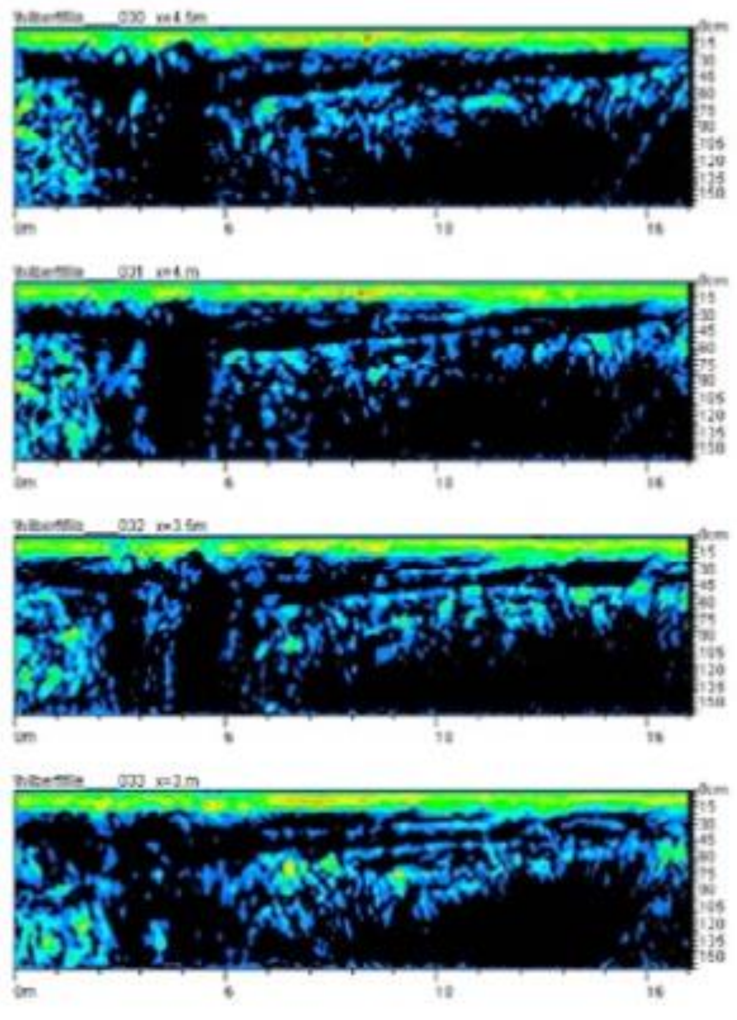

Figure 2.21 GPR profiles from Grid 3 on Mound H, showing a large low amplitude anomaly on the left-hand side extending across several transects, interpreted as a possible prior excavation (Reproduced with permission of V.D. Thompson and T.J. Pluckhahn, from Pluckhahn *et al.* 2009:49).

Further anomalies present in the profiles included buried horizons (see Figure 2.20) and large highly reflective anomalies the authors suggest could be either a collapsed structure or limestone blocks. The authors suggest the mound was constructed in at least three stages based on the buried horizons, claiming these survey results match photographs from prior excavations which show layers of dense shell and layers of sandy deposits (Pluckhahn *et al.* 2009, 2010; Thompson and Pluckhahn 2010).

For Mound K the GPR data exhibits a dense highly reflective subsurface, considered to be indicative of high-density shell deposits (see Figure 2.22). The authors further suggest a lack of visible layering in the deposits is indicative of a more rapid single phase construction compared to Mound H (Pluckhahn *et al.* 2009, 2010; Thompson and Pluckhahn 2010), however it is common for anthropogenic shell matrix sites to exhibit a general lack of internal stratigraphy. It is possible this site, though created in multiple phases, is lacking the sandy layers responsible for the buried horizons in Mound H. It is also possible the site was indeed created in one event, but without further evidence the lack of visible layering in the deposits is not enough proof to confirm a single phase construction.

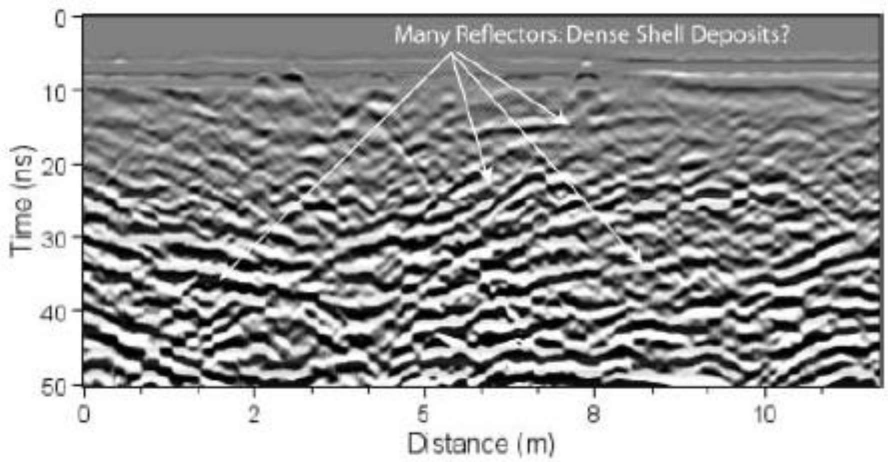

Figure 2.22 GPR profile showing the highly reflective deposits thought to be dense shell material from Grid 4 on Mound K (Reproduced with permission of Routledge: Taylor and Francis, from Thompson and Pluckhahn 2010:46; permission conveyed through Copyright Clearance Center).

The last two areas surveyed were Mound A and Feature B. The GPR survey for Mound A consisted of both a grid and a single transect and was deemed inconclusive. The grid area survey was aimed at trying to identify the remnants of a ramp for Mound A. The survey results failed to find enough evidence of formal structure for a definitive interpretation. The single transect (marked as Grid 7 on the topographic map, see Figure 2.19) ran from the peak of the mound down to the base. The GPR data for this transect showed a highly reflective fill, which along with the observation of high shell content in exposed areas on the mound, was concluded to indicate high shell content for the mound fill. An anomaly in the profile situated at the base of the mound showed a curved lens of more reflective material over less reflective material (see Figure 2.23). This was tentatively (with the need for further investigation) suggested to be evidence of a dome or conically shaped mound stage constructed of less reflective fill (Pluckhahn *et al.* 2009:56). The GPR profile for this transect had not been topographically corrected, it is possible with correction that the upward curve of the mound may flatten out the seemingly curved lens. Instead of representing a domed mound stage, the anomaly may represent the demarcation of a prior land surface with mound construction fill on top of it; topographically correcting the profile would help clarify this anomaly. However, even though their Pluckhahn *et al.* (2010) paper did present a topographically corrected profile, little was clarified (see Figure 2.24). The authors presented only the first 10m of the profile, while the anomaly occurred in the last 7-8m of the 18m profile. The authors still reference the same curved lens area as being visible on the right hand side of the profile, but this area of the profile appears to be missing.

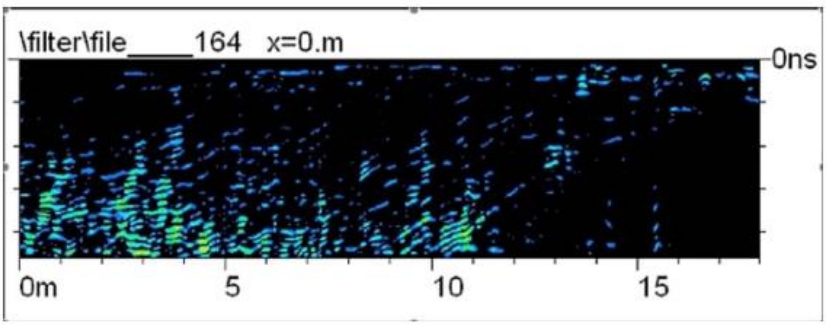

Figure 2.23 GPR profile showing highly reflective deposits thought to be dense shell material and the "curved lens" anomaly from Grid 7 on the slope of Mound A (Reproduced with permission of V.D. Thompson and T.J. Pluckhahn, from Pluckhahn *et al.* 2009:54).

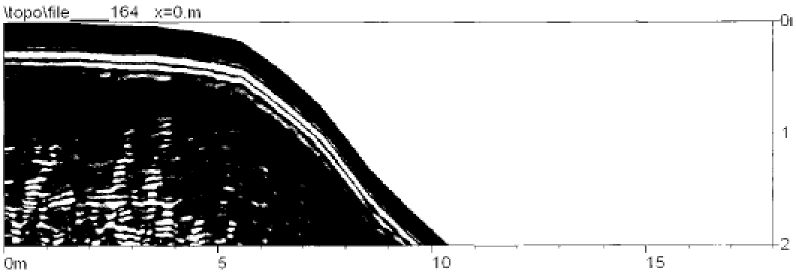

Figure 2.24 **GPR profile showing the highly reflective deposits thought to be dense shell material from Grid 7 on the slope of Mound A (Reproduced with permission of Routledge: Taylor and Francis, from Pluckhahn *et al.* 2010:172; permission conveyed through Copyright Clearance Center)**

For Feature B (Grid 6, see Figure 2.19) the authors interpreted the highly reflective anomalies in the profiles to be an area of dense midden material to a depth of around 40cm (see the first four time slices of Figure 2.25).

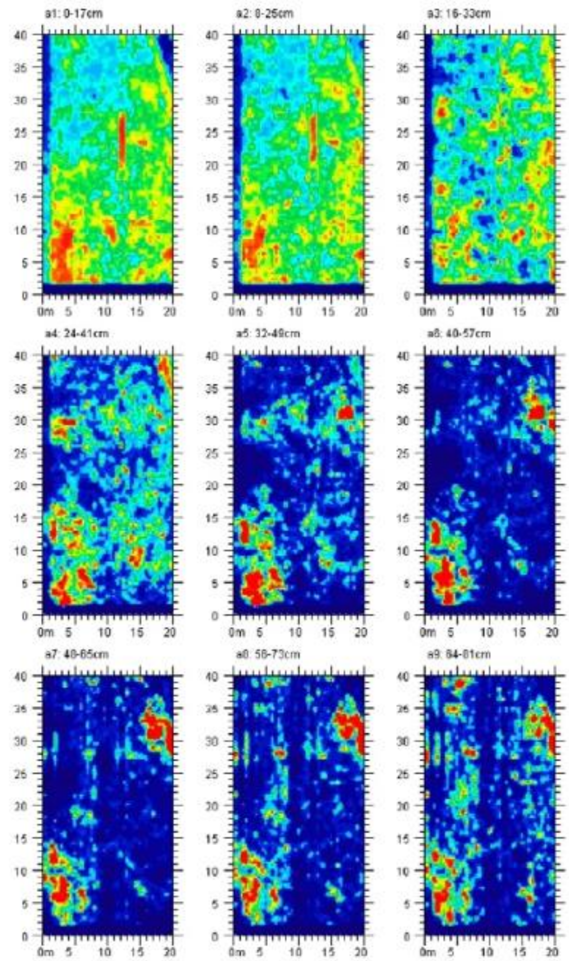

Figure 2.25 **GPR (horizontal) depth slices of Grid 6 from Feature B (Reproduced with permission of V.D. Thompson and T.J. Pluckhahn, from Pluckhahn *et al.* 2009:53).**

Coring confirmed that these reflective anomalies in the profiles were indeed shell deposits. Below the area of dense shell, lenses of discrete high amplitude anomalies, possibly midden material, were observable in the profiles. These discrete piles were thought to potentially be the result of back filling from prior excavation as the anomalies were present from the surface down (Pluckhahn et al. 2009:51). In Thompson and Pluckhahn (2010) the authors argue that because the GPR results are significantly different from those obtained for Mounds H and K, the feature should be considered a midden rather than a planned mound. While the GPR results for Feature B are indeed different from Mound H and K, so too are the results from Mound K different from Mound H, making this a poor rationale for deciding Feature B is a midden and not planned architecture. No other reasons are given, nor is any reference to this argument made in either of the other papers.

While some of the interpretation of results may raise questions, the GPR data collected from the Crystal River Complex was significant. The results showed clearly definable sedimentary units and areas of dense shell deposits, which were verified with cores taken from the edge of Mound J, Feature B and from the region of the possible ramp for Mound A. While not showing conclusive evidence for their site interpretations beyond the shell deposits, the authors did demonstrate the viability of their methods. The work was let down by omissions in the data presented. A horizontal slice of Grids 2 and 3 from mound H would have helped assess whether the anomalies in the profiles were prior excavations, while showing all of the topographically corrected profile for Grid 7 would have helped establish whether or not the curved lens anomaly was a prior domed mound phase.

Thompson and Pluckhahn continued their use of GPR to investigate site formation in later research. Looking at a site complex on Roberts Island, located just downstream from the Crystal River Complex, Pluckhahn *et al.* (2016) employed a GPR (SIR-3000 with a 400MHz antenna) survey alongside excavation to present evidence for classifying the shell complex as a stepped pyramid. A GPR transect was run from the summit to the base of Mound A at the Roberts Island Complex. This profile revealed a series of shallow anomalies which were found to match closely to a series of horizontal and vertical surfaces found during excavation. These surfaces and corresponding anomalies in the GPR profiles were interpreted by the authors as evidence of a stepped construction to the mound.

The last archaeological study to employ GPR in analyses of site formation and history is a follow on study by Rodrigues *et al.* (2015). The research looks again at the Jabuticabeira II site, integrating the results of GPR surveys with sedimentological analyses based on sediment columns collected by auger drilling. The integration of sedimentological results with the GPR allowed for the characteristic stratigraphic layering present on site to be identified, meeting the stated aims of the earlier research paper, Rodrigues *et al.* 2009 previously discussed in Section 2.4.3. The combined sedimentology and GPR survey results allowed for an identification of four radar-facies (a group of related reflections in a radar profile). These facies represented the archaeological deposit making up the mound at Jabuticabeira II (RFA1), a soil (RFS3), as well as two sedimentary deposits representing palaeolandscapes (see Figure 2.26). The two sedimentary deposits were from a palaeolagoon (RFS1) and a palaeodune deposit (RFS2). This analysis allowed for the shell matrix to be placed in physical and chronological relation to the palaeolandscape it was built on.

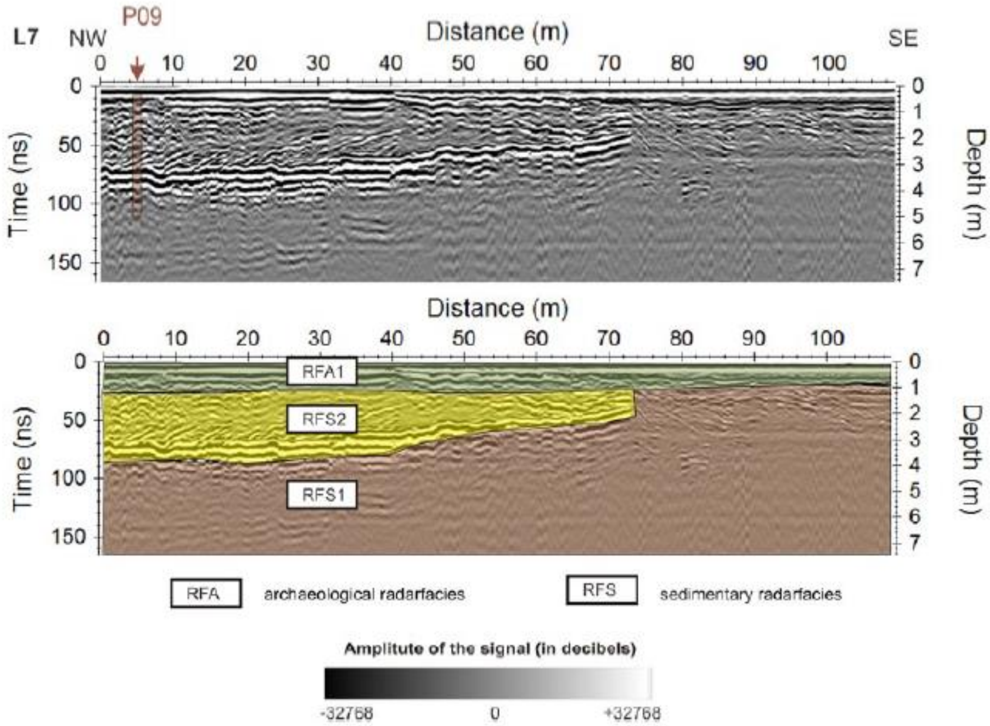

Figure 2.26 GPR profile of Jabuticabeira II (above) showing the location the sediment core (P09) and an interpretation (below) of the radar-facies based on the sedimentological analysis (Reproduced with permission of Sage Publishing, from Rodrigues *et al.* 2015:1262; permission conveyed through Copyright Clearance Center).

Moving beyond archaeology to geology, three more studies report the use of GPR in answering questions about shell matrix site formation. These studies present complex interpretations of coastal morphology based on the GPR results which will not be discussed in detail here as they are not archaeological in nature, though they do indicate the applicability of employing GPR to investigate site formation. The three studies will be analysed in relation to the results obtained and the methods used to obtain them.

The first, a paper by Neal *et al.* (2002), employed a PluseEKKO 1000 with a 900MHz antenna on a shell chenier on the Essex Coast, UK. The survey team conducted 40 transects, using a common mid-point survey for time/depth conversions. Single profiles were used rather than grids, with transects run both along and across chenier ridges. Neal *et al.* provided a comprehensive account of the processing applied to the data which included a low-frequency de-wow filter, two-dimensional F-K migration, a horizontal average of three traces and an automatic gain control with a maximum limiting value of between 50 and 150. At each site ground truthing was attempted using trenches or cores. The authors reported excellent correspondence between the stratigraphy visible in the trenches and the GPR reflection profiles. The GPR profiles were clear and the demarcation of stratigraphic units by the authors, as based on anomalies, could reasonably be expected to be replicable by others (see Figure 2.27).

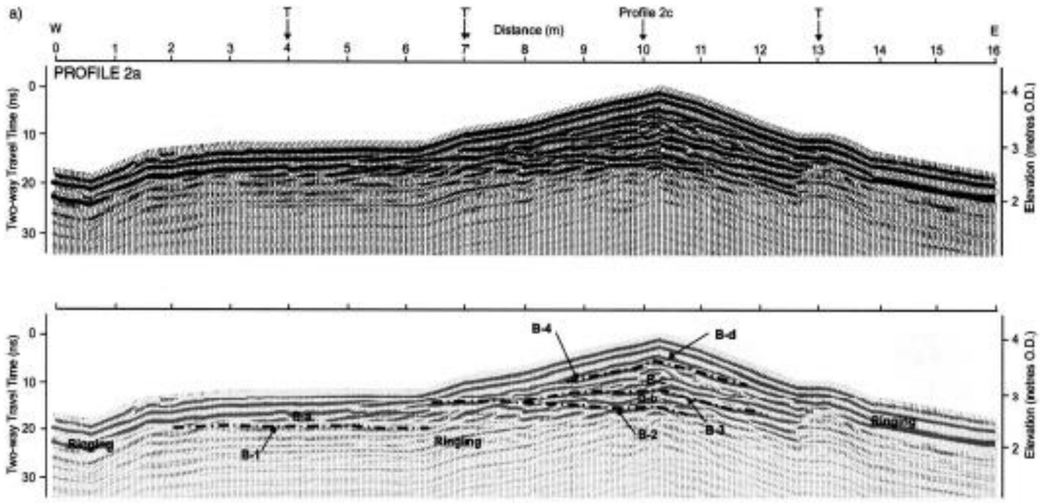

Figure 2.27 GPR profile (above) and stratigraphic interpretation (below) (Reproduced with permission of Elsevier, from Neal *et al.* 2002:451; permission conveyed through Copyright Clearance Center).

The Neal *et al.* study from 2002 was not retested and expanded upon until 2012 by Weill *et al.*, who investigated shell cheniers in Mont-Saint Michel Bay in France. The

Weill *et al.* study employed a GSSI GPR with 400MHZ, 900MHz, 1.6GHz and 2.6GHz antennas. The survey was conducted in both widely spaced transects to produce an overall image of the site and in grids to investigate the cheniers in finer detail. No three dimensional or horizontal results from the grids are presented in the paper. The first inspection of the study site was made with the 400MHz antenna, but subsequently most of the data obtained was with the 900MHz antenna. Only a few transects were made with the 2.6GHz for very fine surface stratigraphy, while the 1.6GHz was sometimes employed as a compromise between the 900MHz and the 2.6GHz. Velocity analysis was conducted by hyperbola fitting and then confirmed with ground truthing. Weill *et al*. included a detailed description of their processing steps which involved applying a high-pass and low-pass filter for each antenna, time-zero position adjustments for each trace, a low frequency 'dewow' filter, kirchhoff migration and deconvoluation to remove multiples, and lastly a band-pass filter and a constant gain were also applied to the signal. The authors supply photographs which directly compare trench results with GPR profiles from the 400MHz and the 1.6GHz antennas (see Figure 2.28). These results clearly show a positive correlation between the results obtained in the GPR profiles and the stratigraphic units observable in the trench section. Further interpretations of stratigraphic units made by Weill *et al.* are clearly distinguishable as based on the anomalies observed in the GPR profiles (see Figure 2.29).

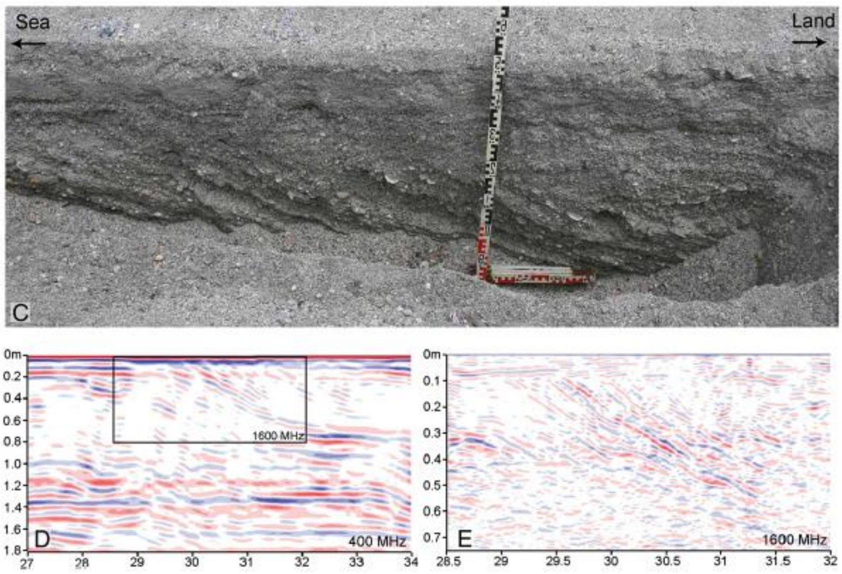

Figure 2.28 Ground truthing trench with related GPR profiles taken using (D) a 400MHz antenna and (C) a 1600MHz antenna (Reproduced with permission of Elsevier, from Weill *et al.* 2012:179; permission conveyed through Copyright Clearance Center).

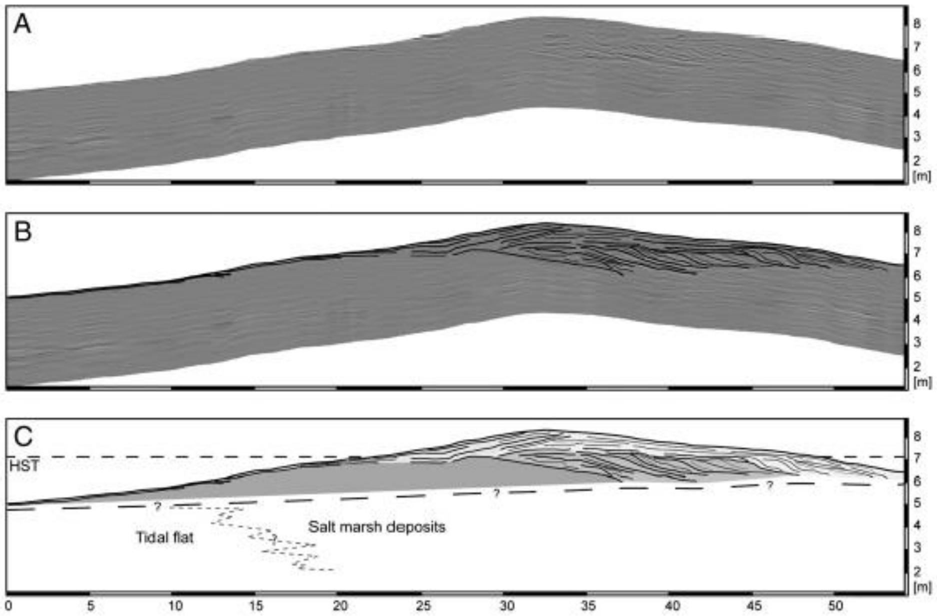

Figure 2.29 GPR profile taken using a 900MHz antenna: (A) Processed profile (B) Interpreted stratigraphy and (C) Profile showing high spring tide (HST) water level (Reproduced with permission of Elsevier, from Weill et al. 2012:180; permission conveyed through Copyright Clearance Center).

The third paper, by Dougherty and Dickson (2012), is also a follow on study of the 2002 Neal *et al.* paper, looking at the Miranda chenier plain in the Firth of Thames, New Zealand. Seven kilometres of profiles were collected in two transects from shell ridges 2km wide by 8.5km long, using an SIR 2000 with a 200MHz antenna. Each survey transect was taken twice, once at 100ns and once at 150ns. Processing and depth conversion were achieved using RADAN 6.5 software. The GPR data was only minimally processed as the authors found further processing produced negligible results. Ground truthing was conducted using drainage ditches which exposed the local stratigraphy as well as hand-auger coring. The GPR profiles presented in the paper show clear stratigraphic boundaries, however the authors' interpretation of the stratigraphy as represented in the GPR profiles is rudimentary (see Figure 2.30). The low resolution of the 200MHz GPR data and the rudimentary interpretation of the stratigraphic units appear to be sufficient for this coastal morphology study, but may lack the required definition for an archaeological study of a shell matrix site.

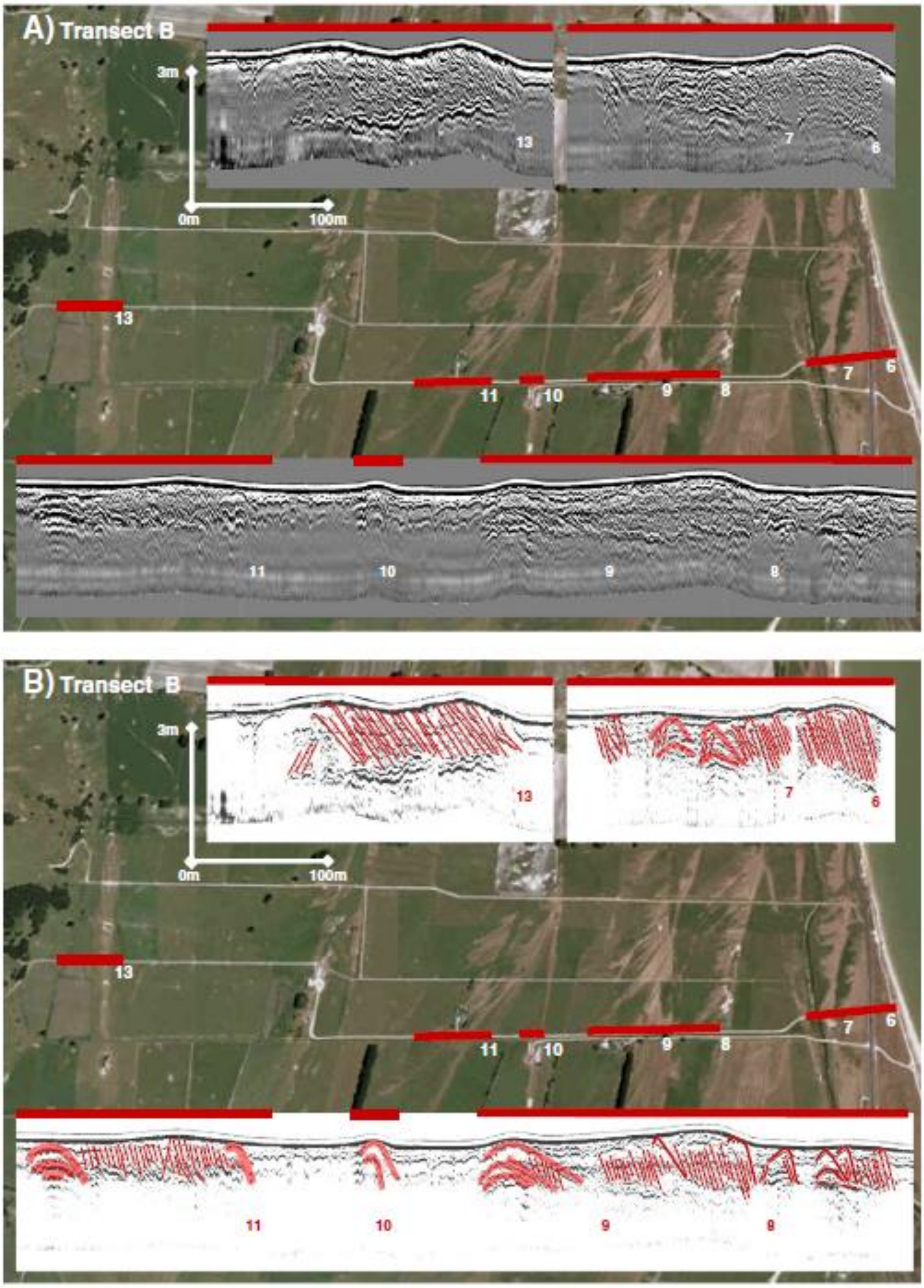

Figure 2.30 GPR profile taken using a 200MHz antenna: (A) processed profile and (B) Interpreted stratigraphy (Reproduced with permission of Elsevier, from Dougherty and Dickson 2012:64; permission conveyed through Copyright Clearance Center).

From a comparison of the GPR profiles and results presented in these studies, it appears the ideal antenna frequency range is between 400MHz and 900MHz. The higher resolution appears to be invaluable in interpreting shell matrix sites, though some depth is still required, making anything higher than a 900MHz almost pointless. Transect spacing of 0.5m provides effective results for a detailed investigation of shell matrix deposits. The different studies showed that what constitutes appropriate processing of the data can vary considerably depending on the site and the study aims. Ground truthing in some form was shown to be necessary for ensuring the results are being accurately interpreted. The three papers on the Crystal River Complex also showed the importance of making sure interpretations can be confirmed by the data displayed in the paper.

2.5.4 Electrical Resistivity

There are four papers which utilise electrical resistivity to investigate site formation processes for shell matrices. Three of these papers (as mentioned for the GPR results in Section 2.5.3) cover the results of a large study at the Crystal River Complex in Florida, USA. All four of these papers included Victor D. Thompson as a lead researcher/author. Thompson began his investigations into using electrical resistivity in studying shell matrix site formation in his 2004 Thompson *et al.* paper on the Sapelo Island shell ring complex (discussed in Section 2.4.4). This study fell short in its aim to investigate site formation and succeeded only in using the geophysical techniques for prospection. Thompson did, however, return to Sapelo Island to finish what he had started.

In 2007 Thompson added additional electrical resistivity surveys (made again using a Geoscan RM15 resistance meter) to Ring III of the Sapelo Island shell ring complex. This time both horizontal and vertical profiling was employed, though the vertical profiling is not reported in the paper. The resistivity survey results appeared to indicate areas of higher and lower shell density around the rings, as indicated by higher and lower resistance values; this interpretation was then confirmed by excavation (see Figure 2.31). Thompson strategically utilised the resistivity survey results to both interpret the site and to place excavation test pits for detailed site investigation. The research found that areas with high shell density had low ceramic concentrations, while the areas between these high density shell concentrations were composed of occupational midden, pottery and organic humus. Thompson argued the evidence suggested shellfish was being processed in discrete areas next to households so that rings, like Ring III, were being formed unintentionally via the gradual accumulation of shell. This study exemplifies the applicability of using geophysical surveys to help answer questions about site formation processes.

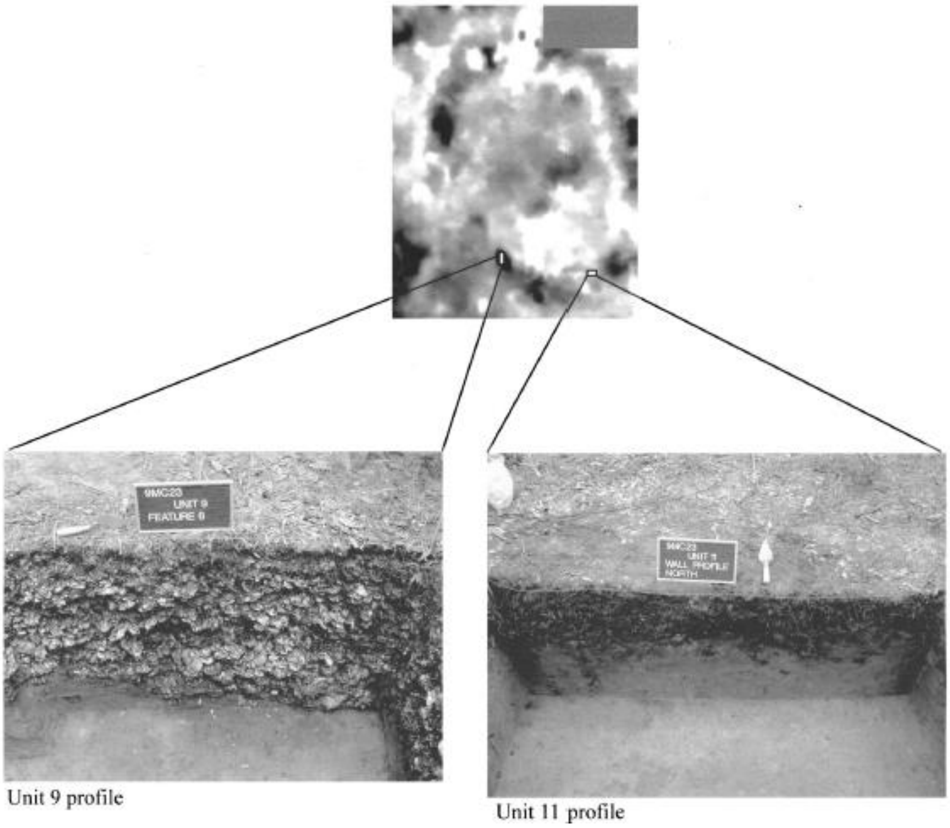

Figure 2.31 Electrical resistivity results and associated excavation profiles: (Left) showing the relationship between higher (darker) resistivity results and dense shell deposits, (Right) showing the relationship between lower (lighter) resistivity results and sparse shell deposits (Reproduced with permission of V.D. Thompson, from Thompson 2007:101.).

As mentioned, Thompson was also part of the team investigating shell mounds at the Crystal River Complex in Florida, USA. This study also employed a Geoscan RM15 resistance meter in a twin probe array. A total of 51 grids were surveyed with 1m transects and 0.5m electrode spacing, of which 49 were 20m by 20m grids while two were 20m by 10m grids (Pluckhahn *et al.* 2009, 2010). ArcheoSurveyor was used to process the results, which were first reviewed raw, then de-spiked and filtered using a high pass filter, and lastly the data was enhanced by smoothing and interpolating the values (Pluckhahn *et al.* 2010). The main aims of the surveys were to establish the history of disturbance on site. The authors also used the survey to evaluate whether or not the complex had a central plaza.

There had been some speculation over the existence of a central plaza with Bullen (1965, cited in Pluckhahn *et al.* 2009, 2010; Thompson and Pluckhahn 2010) suggesting the ground between Mounds G, C-F and H could be a plaza. This theory was tested using a resistance survey to investigate the area. The results were supportive of the theory but not conclusive. The survey showed one spot of high resistance theorised by the authors to potentially be one of the large posts typical of plazas or a buried stelae (see Figure 2.32). The area is otherwise relatively clear of high resistivity features, which the authors argue indicates a lack of domestic occupation, though ground truthing would have aided this interpretation as a core of the area could have confirmed or denied the apparent lack of occupational deposits. The area is low lying and it is possible the apparent lack of high resistance features could be due to ground water lowering the overall resistance values.

Figure 2.32 Electrical resistivity results from the possible plaza area: (3) high resistance anomaly thought to be a potential stelae (4) higher resistivity anomaly and (5) edge of Mound C (Reproduced with permission of V.D. Thompson and T.J. Pluckhahn, from Pluckhahn *et al.* 2009:41).

A large portion of Mound G was surveyed in an attempt to locate an excavation conducted in the 1960s, the exact location of which was unknown. A linear feature observable in the resistivity data was taken to be the excavation, this feature was cut back into another linear section made by a bulldozer (see Figure 2.33). The bulldozer cut was mapped by Bullen in the 1960s (cited in Pluckhahn *et al.* 2009:40) as running almost directly north-south, the same orientation as the anomaly. The only argument made for the interpretation of this anomaly as the prior excavation was that Bullen may have cleaned up a section of the bulldozer cut. Mound G was not entirely surveyed so it is unknown if any other linear anomalies would have turned up. In Pluckhahn *et al.* (2009) the possible excavation is recorded as 20 by 20 feet, compared to Bullen's report (in a letter cited in Pluckhahn *et al.* 2009:40) that his excavation measured 10 by 20 feet. However, further references to the same pit made by Bullen in two unpublished manuscripts (Bullen 1960, 1965 cited in Pluckhahn *et al.* 2009:40) claim it was 15 by 15 feet. The possible excavation is larger than either of the sizes reported by Bullen, but the discrepancies in Bullen's reporting make it hard to rule out the possibility of this anomaly representing the actual excavation.

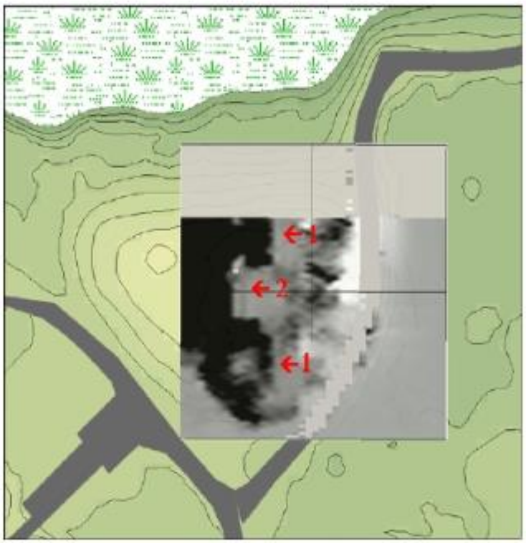

Figure 2.33 Electrical resistivity results from Mound G: (1) straight line high resistance anomaly thought to be a bulldozer cut and (2) linear low resistivity feature cut into higher resistivity deposits thought to be prior excavation (Reproduced with permission of V.D. Thompson and T.J. Pluckhahn, from Pluckhahn *et al.* 2009:40).

Mounds J and K were not included on maps made during the first excavation on site in 1903, they have previously been theorised to have been made by bulldozers after 1903. In Thompson and Pluckhahn (2010) the authors argue the sub-linear features observable in the resistivity surveys for Mounds J and K are evidence of purposeful construction (see Figure 2.34). The authors state that the features are clearly defined and not smeared as may be expected from bulldozer-deposited piles. This is not an entirely convincing argument as bulldozers can be used to create precise mounds. Furthermore the data itself, while showing a distinctive line in the resistance anomalies for Mounds J and K, also shows a smearing of resistance beyond the linear features contradicting Thompson and Pluckhahn's claims. However the 2009 report (Pluckhahn *et al.*) mentions a photograph taken in the 1960s showing large well-established trees growing on the mounds, which would indicate they had not been made by bulldozer in the recent past, and may have been missed by previous surveys in the dense vegetation.

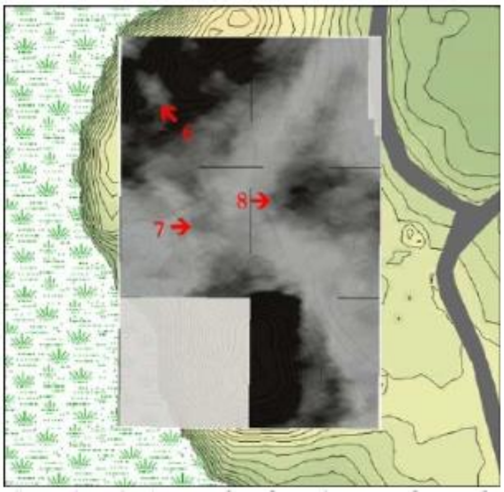

Figure 2.34 Electrical resistivity results from Mounds J and K: (6) low resistance anomaly in Mound J, (7) linear higher resistivity anomaly and (8) higher resistivity anomaly associated with rising ground (Reproduced with permission of V.D. Thompson and T.J. Pluckhahn, from Pluckhahn *et al.* 2009:42).

For Mounds C-F only the edges were investigated, as they had previously been excavated and then reconstructed. Thompson and Pluckhahn (2010) claim their results show a small portion of Mound C may be original deposits, though they give no reasoning for this claim and make no indication of what area they think is intact. This argument is not made in either of the other two papers. Without knowing what area is being referred to and on what evidence they are basing their supposition it is impossible to assess the veracity of the claim.

Feature B was the last area to be analysed for historical disturbance and for the presence of any remaining intact deposits. The authors argue several portions of Feature B are intact, though it has been segmented by historical disturbances (see Figure 2.35). Interestingly, Pluckhahn *et al.* (2009:43) note that the areas of higher resistance they consider to be due to increased shell material also correspond to areas of higher topographic relief, indicating this increased resistance could be related to water table levels instead.

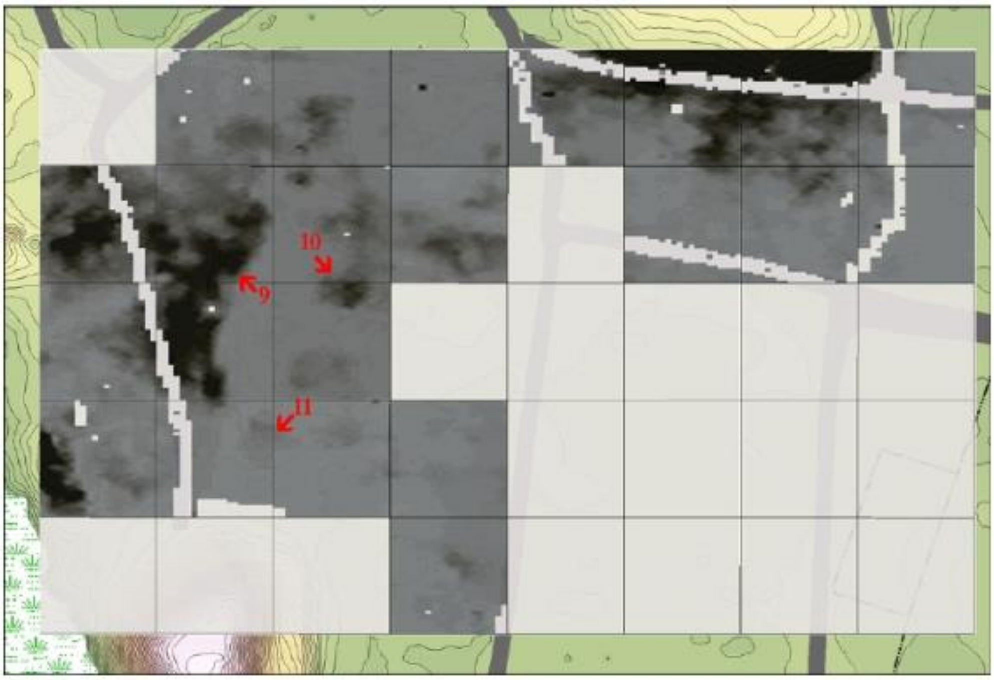

Figure 2.35 Electrical resistivity results from Feature B: (9, 10, and 11) higher resistivity anomalies thought to be indicative of midden deposits, but also associated with rising ground (Reproduced with permission of V.D. Thompson and T.J. Pluckhahn, from Pluckhahn *et al.* 2009:43).

Three cores were taken within the area surveyed with electrical resistivity, these were Cores 3 to 5 for the study (see Figure 2.36). Core 3 showed the expected result, being positioned within one of the 'intact' areas of Feature B it indeed contained a high shell content. Core 4 was taken as a control core from an area on a 'slight rise' with no major anomalies (low resistivity values); according to their topographic map (see Figure 2.37) the rise in this area was at a similar height to Core 3 and about 20cm lower than Core 5. Core 4 in fact found a high shell content similar to Core 3, however the core hit the water table about 20cm closer to the surface here than at Core 3. While the water table was not reached directly due to an 'impenetrable root' (at 123cm deep) the authors noted the section was becoming distinctly wetter; comparatively, the water table for Core 3 was reached at 150cm depth. Core 5 was excavated from an area of higher resistivity, it contained similar shell content for the first 30cm as Cores 3 and 4 but then significantly less shell than the other two cores for the sections covering 30cm to 60cm and 60cm to 120cm (Pluckhahn *et al.* 2009:60-63). With a 0.5m spacing between electrodes the results should be averaging the subsurface content down to 50cm, for which Cores 3 and 4 had around three times the shell content compared to Core 5, yet Core 4 exhibited low resistance while Core 5 showed a high resistance. Core 5 interestingly did not hit the water table until 180cm, and as noted above, was about 20cm higher in elevation to Cores 3 and 4. The data from the cores appears to show a strong correlation between resistivity values and the water table.

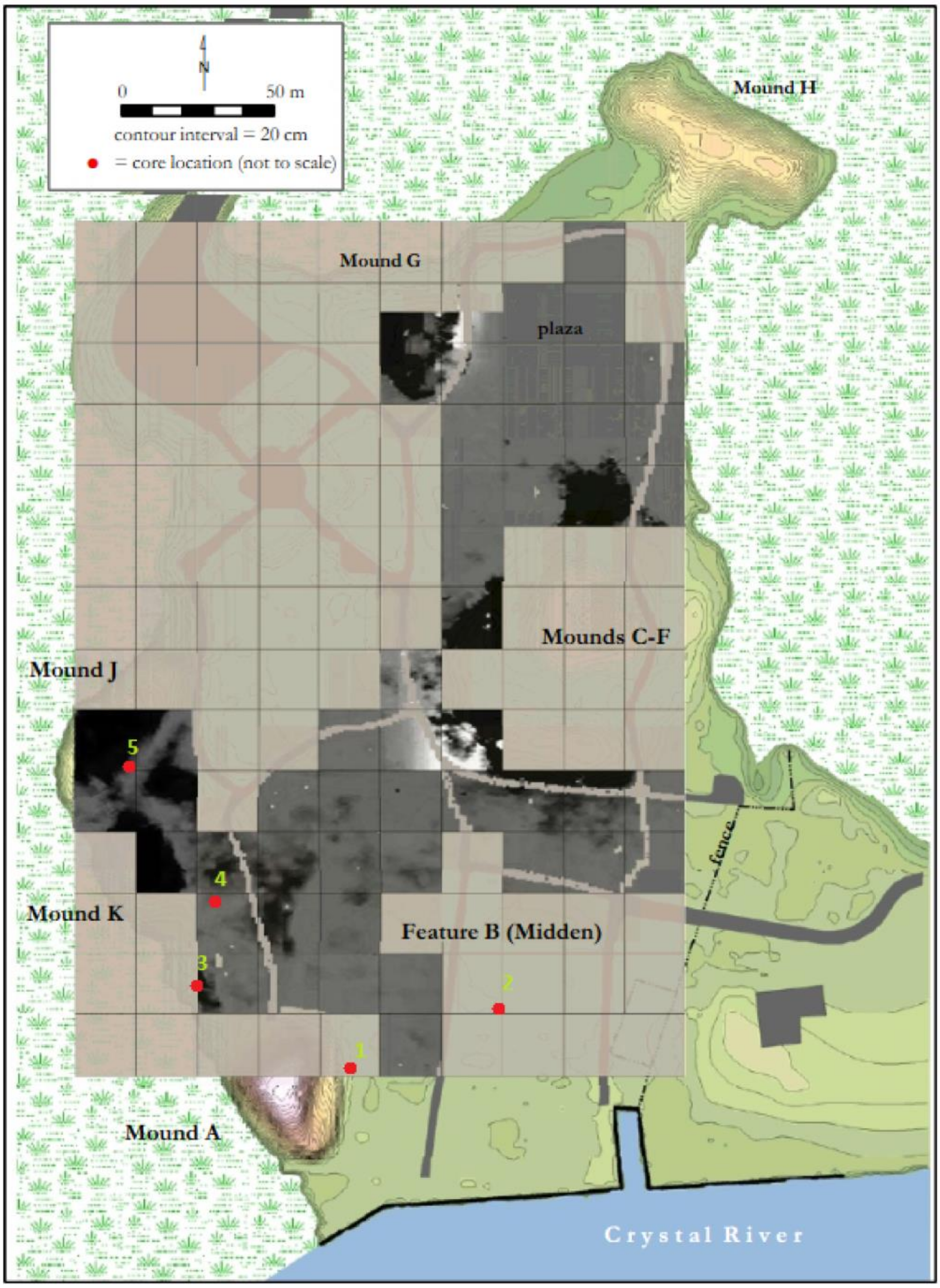

Figure 2.36 Electrical resistivity results and core locations for Crystal River Complex (Reproduced and modified with permission of V.D. Thompson and T.J. Pluckhahn, from Pluckhahn *et al.* 2009: Figures 3.3 p.39 and 4.3 p.58 were combined to create this figure).

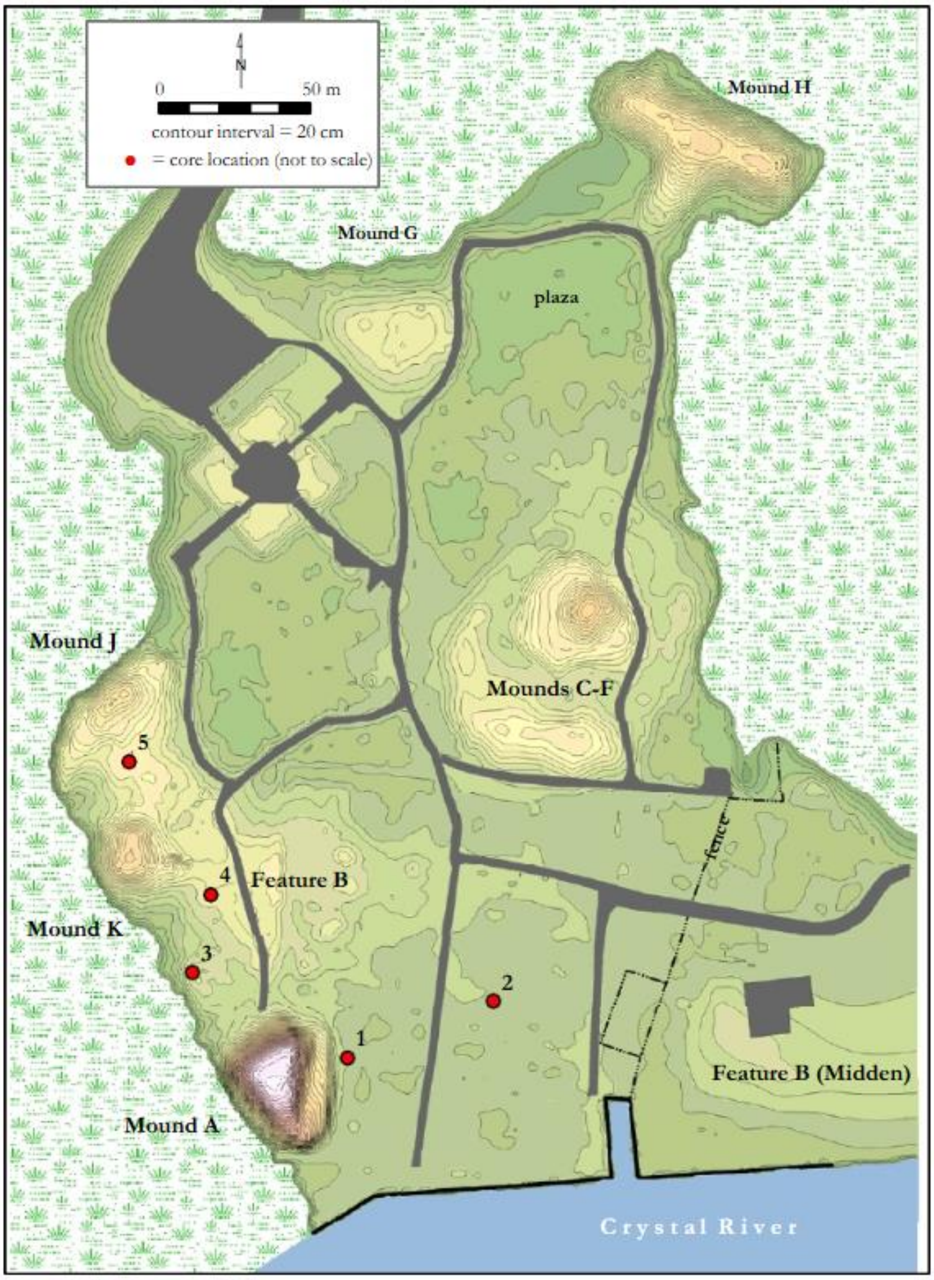

Figure 2.37 Topographic map showing Core locations for Crystal River Complex (Reproduced with permission of V.D. Thompson and T.J. Pluckhahn, from Pluckhahn *et al.* 2009:58).

When factoring in topography it is possible the resistance readings for the plaza area, a particularly low-lying section of the site, are being influenced by the water table. There is a high correlation across the site between the areas of high resistivity and the areas of increased topographical height. However several anomalies present do not match this pattern. The first is the possible excavation on Mound G. This region of low resistivity is not related to low-lying topography which along with the very straight lines present for the anomaly, makes it highly likely to be the product of human removal of shell from the mound; though whether this was via excavation or the industrial removal of shell is hard to determine without the entire mound being surveyed. The second anomalous area is between Mounds J and K. This area shows a lower resistivity path cut through high resistivity anomalies. The path is fairly straight sided and in an area of high topographical relief, pointing to the possibility of it being caused by historical removal of shell rather than the water table. Lastly there is an area to the south side of Mounds C-F showing a high resistivity response in a low-lying area, a core of this region would be informative and would have had minimal impact on the site. This study could have benefited greatly from the type of linear model Santos *et al.* (2009) used to remove the topography/water table effects for their EM conductivity survey.

These studies show the immense potential of electrical resistivity in surveying shell matrices and elucidating information about site formation. However, with only two studies utilising electrical resistivity, both of which are by the same lead researcher, it is hard to derive best practice guidelines for electrical resistivity surveys of shell matrix sites. The main lessons from these papers are in designing surveys and providing sufficient justification for interpretations. The Crystal River papers (Pluckhahn *et al.* 2009, 2010; Thompson and Pluckhahn 2010) leave the reader questioning the author's interpretations due to gaps in the survey coverage of the mounds and also due to a lack of supporting reasons for their interpretations. It should be noted that gaps in site coverage do not always destabilise site interpretations, some gaps are present in the resistivity surveys for Thompson *et al.* (2004) and the results do not suffer for it. The Crystal River results also showed the importance of accounting for the water table when dealing with electrical resistivity surveys.

2.6 Calculating Volume from Survey Data

While the studies discussed above report on a range of geophysical approaches applied to the investigation of shell matrix sites, only one study attempted to quantify the deposits. Larsen *et al.* (2015), calculated volume for shell mounds using Terrestrial LiDAR. This method created a highly detailed map of the mound surface from which vegetation and other obstructions were removed during post-processing. A 3D model of each mound was created using a Triangular Irregular Network (TIN), which had been created from the scanned data and placed above a ground reference plane which was defined in the field. The mound perimeter and the ground reference plane were defined qualitatively in the field via visual inspection. Volume was then calculated from the 3D model. This system, while beneficial, is open to sources of error with the boundaries of the shell mounds and the ground surface plane being defined by visual inspection. More importantly, this method does not account for any mound material occurring below the ground surface plane. In order to find a method which can calculate volume for subsurface shell matrix deposits, techniques which probe the subsurface are required.

To find methods of creating volume calculations for buried deposits, we need to move outside archaeology and beyond shell middens. Published studies attempting to use geophysical survey data to create volume calculations of buried deposits can be separated into those using GPR and those applying electrical resistivity. Interestingly, the research focus of the volume calculations differs between GPR and electrical resistivity. GPR is used mainly for environmental studies concerning the loss of glacier ice and beach sand, while electrical resistivity is used for industrial purposes such as mining and dredging. No rationale is provided in any of the studies for the choice of geophysical method, so it can only be speculated upon. Perhaps the lengthier time involved in processing GPR and thus the potentially higher costs associated with it make it unsuitable for commercial interests. Conversely, perhaps the more detailed results of GPR make it the more desirable tool for environmental studies.

At the commencement of this research only nine papers were found which specifically created volume calculations from geophysical data and each one was going to be analysed in detail. However, since the commencement of this dissertation, it has become common to use GPR surveys as a method of creating volume calculations for glacier ice loads, so rather than detail all the recently published papers a selection of them will be looked at as a bulk group and analysed only in terms of basic methods.

2.6.1 Ground-Penetrating Radar

GPR has been used to create volume estimations of glacier ice, sand and water. As mentioned above, the most common application is in using GPR surveys to create volume estimations for glacier ice, which is aimed at enhancing the monitoring of environmental change in glacier loads. Eight papers were examined that look at quantifying glacial loads (Ai *et al.* 2014; Baojuan *et al.* 2015; Binder *et al.* 2009; Colucci *et al.* 2015; Navarro *et al.* 2014; Prinz *et al.* 2011; Wang *et al.* 2014 and Yde *et al.* 2014). While the methods vary in small details these papers all tend to run sporadic

GPR transects, aimed at covering the length and breadth of the glacial area, and are mapped with some form of GPS. The areas between these sporadic profiles are then interpolated using kriging (a common statistical technique) and two Digital Elevation Models (DEM) are created, typically in ArcGIS, one of the surface of the glacier and one of the bedrock. These two DEM are then used to create volume calculations of the ice load. None of the papers verified the accuracy of their results via any form of ground truthing. While GPR does work exceedingly well in icy conditions, there are inherent error margins in interpreting GPR profiles and without any form of error check there is no assurance the machine is working or being operated correctly, or that profiles are being interpreted correctly. Five of the papers made efforts to statistically analyse error margins for the GPS and GPR system measurements. GPS error margins will vary depending on the system and method used, while GPR error margins are prevalent in things like converting two-way travel-time to depth measurements and in topographic migrations. There were also more complex sources of error often only mentioned in passing which can occur during interpretation, such as tracking the source of multiple reflections or estimating the actual boundary of a glacier where it is obscured due to snow patches and debris. Navarro *et al.* (2014) present one of the most thorough error margin estimations, from which they concluded the volume estimates for the glaciers studied amounted to 4-8% of their total volume. Baojuan *et al*. (2015) and Wang *et al.* (2014) looked at system error and came up with low ranges (1.18% and 1.2-5% respectively). While Ai *et al*. (2014) and Binder *et al.* (2009) both experienced significant errors (20-50%) in their kriging interpolation due to sparse data sets and errors in spatially locating the survey results.

Kristiansen (2013) also looked at ice loads, but this was conducted under slightly different conditions and for different reasons. Kristiansen attempted to make 3D models which included volume estimates of snow and ice accumulation for a perennial snow patch (essentially a stationary glacier). The perennial snow patch studied was Kringsollfonna in Norway. The project was designed to assist the Snow Patch Archaeology Research Cooperation (SPARC). SPARC’s main aim is to locate artifacts in ice and snowdrifts as they become visible due to melting. To assist this aim, Kristiansen created 3D models of the internal structures of the snow patch by combining GPR data (collected using a Mala 500MHz antenna) with Real Time Kinematic (RTK) data in Esri’s ArcGIS software suite. The primary aim of Kristiansen’s thesis was to detail the process he employed to map the GPR data into 3D models in ArcScene; from which an understanding of the internal structure of the snow patch (snow as compared to ice) and volume estimations of various stratigraphic layers could be obtained. After processing the GPR survey data in Reflex 2D Quick, Kristiansen employed Microsoft Excel, ArcMap and ArcScene to transform the survey results into a 3D model. Using the *pick* function in Reflex to single out velocity changes which signalled two layers (one of snow and one of ice) in the GPR results, Kristiansen then exported the 'picks' as an ASCII file to Excel. The 'picks' were then assigned georeferencing information, and saved in a format that could be imported into ArcGIS. The georeferencing information had to be generated in ArcMap as due to technical difficulties Kristiansen was unable to connect the RTK to the GPR during survey. The Excel files of the georeferenced 'picks' were imported into ArcMap and transformed into TIN (triangular irregular network) models which were then imported into ArcScene. In ArcScene the TINs were used to create 3D polygons of the snow and ice layers from which volume estimations were created.

There were three other papers employing GPR to create volume estimations for substances other than ice. The first was Sambuelli and Bava (2012), who created a bathymetric map of a lake based on GPR results and calculated the lake volume from it, comparing the results against official lake volume estimations. While the last two papers looked at calculating volume for beach sand. Van Heteren *et al.* (1996) examined a coastal barrier system in Saco Bay, Maine, USA, using a 120MHz antenna. The results were ground truthed using auger cores and a time/depth conversion was calculated from this. The results were made into a detailed isopach map from which the volume was calculated using ArcGIS. The results included a 5% margin of error to account for possible over- or under-estimation of the sand volume beyond the reach of the GPR, and a 10% margin of error to compensate for velocity miscalculations. How these particular error figures were decided upon is not explained. Dickson *et al.* (2009) examined beach sand erosion on the South Island of New Zealand. Eighteen sites were surveyed with a pulseEKKO 100; the study trialled multiple antennas, including a 100MHz, 200MHz, 225MHz, 450MHz and 900MHz, but only the results from the 200MHz antenna were displayed in the article. RTK and established survey marks were used to record surface topography. Surveys were limited on the seaward side by several meters due to attenuation of the signal with the incursion of saltwater; to mitigate this as much as possible surveys were completed at low tide. The results were ground truthed in multiple ways, including observation of a stream-cut that was also imaged by radar and excavation at nine of the sites. Beach volume was calculated by using polygons whose upper surface was measured by the RTK survey and whose lower boundary was measured from the GPR survey. The landward edge was constrained by cliffs or by the boundary between barrier sediments and substrate, while the seaward edge was left open where surveying had to stop, with sediments below the water level left out of the volume calculation.

These studies all calculated volume by creating isopach, DEM or TIN maps of the deposits. The top of the deposit was mapped topographically with some form of GPS system while the base was mapped from the GPR results. While there are reported margins of error for half the studies the results are rarely tested against reality, with only four of the studies ground truthing their results.

2.6.2 Electrical Resistivity

The use of electrical resistivity to calculate volume has, as mentioned, been for industrial purposes. The most recent of the three papers (Tetegan *et al.* 2012) does not actually create an explicit volume calculation but rather a volume percentage. The study hypothesises rocks will create noise in the resistivity data which can be used to calculate what percentage they make up of the overall sediment content. Tetergan *et al.* set up three grids with varying rock fragments visible on the surface. Transects were run at 2m and 4.8m with three arrays of varying spacing: 0.6m, 1.2m and 2.2m, allowing for horizontal profiles at differing depths. The grids then underwent a visual estimation for the rock fragments present on the surface and test pits were excavated and quantitatively analysed. The test pits were applied to only two of the three grids, one of which received 18 test pits the other nine. Initial results showed the resistivity surveys to contain white noise, so areas with rock content of 15% or below were discarded as they would produce overestimations. With this study aiming to create a content percentage rather than an outright volume calculation it fails to provide useful information for the research being undertaken in this dissertation.

The second paper is by Nowroozi *et al.* (1997), who investigated a quarry in the state of Virginia, USA. The study aimed to map the remaining gravel deposits in the quarry area. Nowroozi *et al.* conducted 14 Schlumberger soundings and 4 horizontal profiles, using a Wenner array with four electrode spacings: 0.7m, 4m, 7m and 10m. The resistivity data was ground truthed with two test soundings taken close to the quarry wall so the local stratigraphy could be compared to the resistivity data. The results of this comparison showed the resistivity data closely matched the *in situ* sections. The target gravel was highly resistive compared to the weathered alluvium beneath it, so a minimum target of 10,000Ω-m was created. Anything at or above 10,000Ω-m was considered to be F3 gravels, and anything below to be weathered alluvium. Nowroosi *et al.* first created an isopach map of apparent resistivity contours based on the survey results. Using the isopach map, a grid of 100m x 100m cells was overlain and approximate thickness was assigned. Where cells covered more than one isopach contour the lower value was assigned, to give an under-estimation rather than an over estimation of the yield. These cells were then used to calculate the volume of the gravel deposits and from this a yield in metric tons was created. For a more accurate estimate they suggested more closely spaced data points would be required.

The last paper is by Rucker *et al.* (2011), who used resistivity to calculate the dredgable volume of sediments in the Panama Canal. Rucker *et al.* conducted a resistivity survey which covered 50km of waterway with parallel transects 25m apart. These transects were located using GPS. A bathymetry survey was also conducted with an echo sounder, and a probe test produced water temperature and conductivity data. To reach the required depths, electrodes were spaced 15m apart along 170m of cable towed behind a boat, with readings taken approximately every 3.77m. The resistivity results were compared with bore-hole logs to ground truth them. The resistivity data results found a wide variability in the conductivity of the alluvial fill sediments, thought to be due to more or less sand or clay content. While the resistivity results could not reliably discern particular deposits, the alluvial fill of the canal bottom fell between the ranges of 40-250Ω-m. Everything between these ranges was then assumed to represent alluvial fill, which can be suction dredged, and everything outside this range would require other means of dredging. The authors do not mention exactly how their data was synthesised in order to create volume calculations, although for one length of the river they do show a horizontal resistance map they created for the canal bottom.

The basic methods presented by these studies is the same as those presented by the GPR studies: create isopach maps of the deposits then calculate the volume based off the maps. The study conducted by Nowroosi *et al.* (1997) was clear, concise and easy to follow; of the electrical resistivity papers it provided the most insight into how a calculation of volume can be conducted, though it was not as detailed as Kristiansen's (2013) GPR study.

2.7 SUMMARY

The prior studies reviewed in this chapter demonstrate the worth of geophysical methods in investigating shell matrix sites. They have successfully been shown to delineate features of archaeological interest within shell deposits, as well as being able to map boundaries and in some cases the internal stratigraphy of shell matrix sites. The application of volume calculations to shell matrix sites has, however, been overlooked. Where it has been addressed in other geophysical research it has been done with little verification of the accuracy of the results. This study will attempt to address this gap by applying volume calculations (based on geophysical surveys) to shell matrix sites, and by testing the accuracy of the results with an experimental set-up.

The study will combine the successful methods reported by others with lessons learnt from prior failings. The prior research showed successes in combining geophysical surveys to provide complimentary data sets. Fine transect spacing (0.5m) provided detailed results while the use of grids in combination with GPS systems provided accuracy in locating surveyed features within the ground. Past failures illustrated the problems that can occur when proper grid control is not achieved, and when the survey design employed fails to meet the research aims. Failure to appropriately ground truth results was a problem for several studies and left their interpretations open to question. Through both the failure and success of different studies, the importance of accounting for topographical and water table effects in the geophysical results was demonstrated. This study will employ GPR and electrical resistivity as the most viable methods in producing volume estimations of buried matrices.

This study found the processing steps detailed by Kristiansen (2013) to be an invaluable insight into how to transform geophysical data into volume estimates and 3D models in ArcGIS. Kristiansen's research was conducted for a Master's Thesis and was published online in Norwegian. In order to read the thesis it was first translated to English via Google Translate. There were difficulties with the translation, but much of the information and many of the basic processing steps in ArcGIS were decipherable and will be used as the basis of the methods employed for this study. Kristiansen's methods were developed specifically for GPR and will need to be modified in order to allow electrical resistivity results to be converted to volume estimates and 3D models as well.

3 METHODS

3.1 INTRODUCTION

This thesis employs two geophysical survey methods to investigate shell matrix sites under both experimental and field conditions. The research design allows for controlled scientific experiments to test the accuracy of the results obtained as well as a test of the methods under real world conditions. Both the experimental and field sites were surveyed using GPR and electrical resistivity. The field site was located on Bentinck Island in the Gulf of Carpentaria, while the experimental site was set up on the Cairns campus of James Cook University (JCU). The experimental site consisted of two trenches with differing sediments, to simulate sites in differing environmental conditions, into each of these trenches were placed two distinct shell deposits. The first experimental shell matrix consisted of a shell deposit buried in coarse washed sand to simulate the type of environmental conditions common to many northern Australian shell matrix sites. The second experimental shell matrix was placed in an organic-rich soil simulating another common environmental condition in which shell matrices are found elsewhere in Australia and around the world. The methods for both the general use of GPR and electrical resistivity as well as the specific survey methods employed for this research are described below. Following this, the data processing steps employed to clean up the GPR and electrical resistivity survey data are described. Then lastly the methods developed specifically for this research, to create 3D models and volume calculations of the buried matrix, are presented.

3.2 PERMISSIONS AND FUNDING

This research was conducted as part of a larger project supported under the Australian Research Council's Discovery Projects funding scheme (DP120103179). As part of this project an agreement was made between JCU and The Kaiadilt People, as represented by the Kaiadilt Aboriginal Corporation and the Kaiadilt Aboriginal Land Trust, which covered research conduct and intellectual property rights. Fieldwork was conducted in collaboration with, and with the consent of, The Kaiadilt People. The surveys conducted on Bentinck Island as part of this thesis are subject to the agreement made between JCU and The Kaiadilt People. This thesis and any publications produced from it are bound by the agreement and require clearance by The Kaiadilt People.

3.3 GEOPHYSICAL METHODS

Based on extensive research (see Chapter 2), GPR and electrical resistivity were chosen as the geophysical techniques best fitted to meet the needs of this research. These techniques produce results which should allow for an estimation of the volume of buried shell deposits within a site as well as broader site investigation. The following subsections detail the theoretical principles underlying GPR and electrical resistivity.

3.3.1 Ground-Penetrating Radar

Radar waves (a type of electromagnetic wave) are produced when an oscillating electric current is applied to a conductive medium. The oscillation of the electric current back and forth through the conductive medium produces a subsidiary magnetic field resulting in conjoined oscillating electrical and magnetic fields (see Figure 3.1). The conjoined fields generated from this process make up the electromagnetic wave which then propagates outwards.

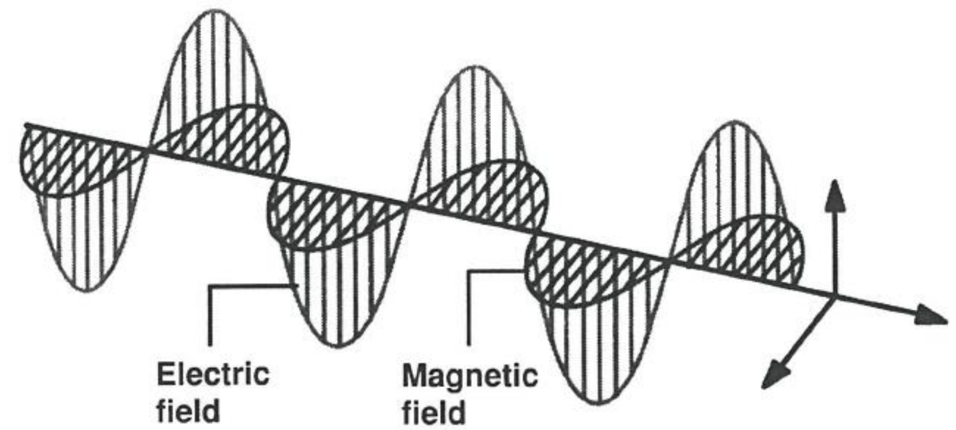

Figure 3.1 Diagram of an electromagnetic wave: exhibiting the conjoined oscillating electrical and magnetic fields which feed off each other during propagation (Reproduced with permission of AltaMira Press from Conyers 2004:24; permission conveyed through Copyright Clearance Center).

Radar waves for GPR are produced by an antenna, the simplest form of which is a copper wire or plate (the conductive medium) through which is passed the oscillating electric current. The frequency of the oscillation, measured in hertz (Hz), typically in the range of megahertz (MHz), is what dictates the wavelength of the radar wave propagated. Higher oscillation frequencies (above 300,000MHz) result in shorter wavelengths measuring less than a millimetre, while lower frequencies (below 300MHz) result in longer wavelengths measuring more than a metre. The propagation of radar waves occurs in all directions so modern GPR antennas are shielded to direct the waves downward into the subsurface.

Electromagnetic waves of differing wavelengths make up a variety of common phenomena. At the higher frequency end of the electromagnetic spectrum, well beyond the operating frequencies of GPR, are x-rays, visible light, ultraviolet, and infrared radiation, for which wavelengths are measured in fractions of millimeters. At the lower end of the electromagnetic spectrum, commonly ranging between 10MHz to 1000MHz, are the frequencies of many modern communication systems: cellular phones, radios, pagers and television transmissions, as well as GPR antennas. Because the frequency of GPR antennas (particularly antennas between 500MHz and 1000MHz) overlap with common communication devices they are subject to interference, making it particularly important not to carry or operate a cellular phone near a GPR antenna (Conyers 2004:24).

Electromagnetic waves will not decay on their own and will travel infinitely if they fail to encounter a medium which absorbs or reflects them. If, however, the electromagnetic waves encounter a medium which interferes with either the electric or magnetic component of the field, propagation will cease and the wave will die (Conyers 2004:23). For the electromagnetic waves produced by GPR there are two factors which determine how the energy will respond once it enters the subsurface: the electromagnetic properties of the subsurface material through which the wave is traveling and the wavelength of the radar waves produced. Longer GPR wavelengths (those measuring up to several metres) will travel deeper in the ground but reflect only off larger objects. Shorter wavelengths (measuring a few centimetres up to a metre) are prone to attenuating faster but will reflect more readily owing to lesser changes and smaller objects in the subsurface (Conyers 2004:23-24). Table 3.1 shows the theoretical vertical resolution obtainable for different wavelengths in different media; this is a maximum resolution, actual field conditions can be expected to result in less resolution than the theorised values.

Table 3.1 Theoretical vertical resolutions for three frequencies in two media; basic soil and bedrock such as limestone (Reproduced with permission of John Wiley and Sons, from Reynolds 2011:544; permission conveyed through Copyright Clearance Center).

	Antenna frequency (MHz)		
	120	500	900
Soil			
Wavelength (cm)	62.5	15	8
Resolution (cm)	15.6	3.75	2
Bedrock Wavelength (cm)	92	22	12
Resolution (cm)	23	5.5	3

The speed at which radar waves can be propagated and the rate at which they attenuate is also based on the composition and water content of the subsurface media (*Reynolds 2011*:539). Electromagnetic waves are influenced by the magnetic permeability (μ), dielectric permittivity (Ɛ) and electrical conductivity (σ) of the medium through which they are traveling. These factors are typically measured as a relative dielectric permittivity (RDP) value which is the measure of a material's capacity to store, then transmit, an applied electrical charge from an electromagnetic field, taking both magnetic permeability and electrical conductivity into account (Conyers 2004:45). RDP works as a measure of how well radar energy will travel to depth. The RDP is inversely related to radar travel velocity: the higher the RDP the slower the radar energy will travel (see Figure 3.2) and can be used to convert travel-times to depth (Conyers 2004:45-46). Slower traveling radar waves, created by higher RDP values, result in greater vertical resolution but also greater attenuation, thereby decreasing depth penetration (Reynolds 2011:548). RDP values vary from 1.0003 (typically rounded to 1) in air up to 88 in highly saline seawater. Most field conditions will exhibit RDP values in the range of 3-25 under dry conditions. Water has a particularly high RDP, even freshwater is at 80, meaning the addition of water to a medium will significantly raise the RDP value (Conyers 2004:47).

Freshwater itself will not attenuate the radar signal, but radar energy can pass through water only slowly (Conyers 2004:45-46). Radar waves do not attenuate in freshwater because the conductivity values are so low, at 0.5 mS/m (millisiemens per metre).

Conversely, seawater has a conductivity value of 3000 mS/m which will quickly attenuate radar waves. This is because the more electrically conductive the media through which the radar wave is travelling the faster the electrical component of the radar wave is conducted away, leading to the dissipation of the wave (Conyers 2004:50).

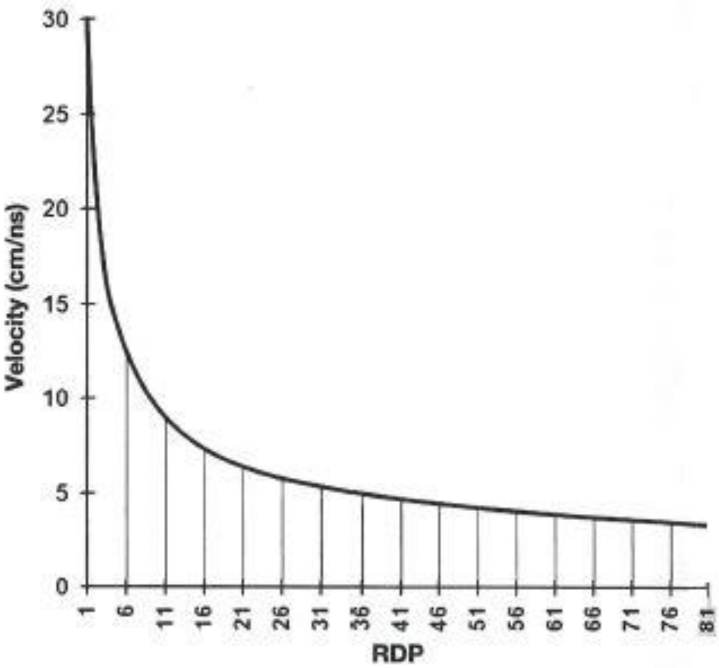

Figure 3.2 Graph showing the inverse relationship between relative dielectric permittivity (RDP) and the travel velocity of radar waves (Reproduced with permission of AltaMira Press from Conyers 2004:46; permission conveyed through Copyright Clearance Center).

As noted in Chapter 2, GPR profiles are a record of the electromagnetic waves which have been produced by the transmitting antenna and have bounced back off changes in the subsurface to be recorded by the receiving antenna. These waves are bounced back to the antenna due to changes in the RDP values between two materials encountered in the subsurface. The greater and more sudden the RDP change, the greater the amount of radar energy reflected will be, which will result in more prominent reflections recorded in the profiles (Reynolds 2011:539). If RDP changes happen gradually with depth then the reflection profiles will show little to no response; the change in RDP between two materials must happen relatively suddenly to be recorded as reflections (Conyers 2004:48).

3.3.1.1 Limitations of Ground-Penetrating Radar

There are several common complications, due to the manner in which radar waves are propagated and reflected, which required consideration during this study. As GPR profiles are purely a record of the reflection of radar waves, it is important to understand the typical anomalies produced by these common complications so they are not misinterpreted as geological or archaeological features. These common complications are produced by ground coupling, scattering and focusing of waves, background noise and air waves. Each of these complications and the anomalies they produce in the radar profiles are briefly considered here, along with their effect on this research and how they were mitigated.

The first complication, ground coupling, is the effect of the electromagnetic wave transitioning from the air around the antenna into the ground (Conyers 2004:68). This transition between the air and the ground directly beneath the antenna is one of the most prominent and sudden changes in RDP values encountered in a profile. Around 40% of the electromagnetic wave propagated is reflected at this interface between antenna and ground surface, creating high amplitude planar reflections in the profiles. The strong reflections created by this change in RDP will affect approximately the first 30cm of the profile produced; saturating the signal and obscuring features (Nishimura 2001). This complication was unavoidable in the data produced for this study and was particularly prevalent in the profiles produced at the field site due to the uneven surfaces encountered, which reduced coupling between the antenna and the ground surface. To minimise the effect of these reflections as much as possible the field site was extensively cleared of surface vegetation before surveying to reduce coupling losses. Post-acquisition processing targeted at removing some of the anomaly was also employed and applied to both the field site and the experimental site data (see Section 3.5.1).

When ground coupling is lost completely due to the antenna bouncing off surface obstructions like rocks or grass tufts, the resulting amplitude change creates a distinctive anomaly in the data. Coupling loss anomalies were only an issue for the field site and as mentioned, clearing was employed to minimise their occurrence. The distinctive appearance of coupling loss, along with field notes and careful observation, enabled recognition of these particular anomalies where they occurred in the GPR profiles.

The next common complication, the focusing and scattering of radar waves, is a product of the way radar waves behave when encountering subsurface features which are either curved or oriented on a different angle to the antenna. Scattering (reflection of radar waves away from the antenna) occurs when a planar reflective feature is angled away from the antenna on the surface, or when a reflective subsurface feature is convex in relation to the surface. Scattering results in either no return signal or a low amplitude signal. Conversely, if the reflective feature is angled towards the antenna on the surface, or the feature is concave with respect to the surface, the radar waves will be focused and more than usual will return to be recorded by the receiving antenna. Focusing will result in high amplitude reflections in the data (Conyers 2004:73).

The anomalies created by scattering and focusing are more likely to occur in the results from the experimental site (where we put in a straight-sided square pit), but these will be easily interpretable as the layout of the subsurface is known. For the field site, features such a tree roots and beachrock could cause focusing or scattering. These potential complications were factored into the analysis of the results. The location of tree roots were mapped based on surface tree locations so they could easily be identified in the profiles. Since the beachrock is known, through prior excavations, to be representative of the old land surface and to generally align to the same orientation as the current surface it should cause minimal focusing or scattering.

The last two common, anomaly producing, complications for GPR are two types of above ground interference. The first type of above ground interference is background noise, which is produced by external electromagnetic energy of similar frequency to the antenna being employed. Background noise, as discussed in the above section, is particularly concerning for antennas in the 500MHz to 1000MHz range as cellular phones, radios, pagers and television transmissions all operate within this band. External electromagnetic noise will produce a high amplitude response in the data, which can obscure any reflections originating in the subsurface (Conyers 2004:72). Background noise is not a problem for the field site, for while a 500MHz antenna was employed the remote location means there are no transmitters of any kind nearby and cellular phones do not receive reception. The experimental site is not located near any large transmitters, so as long as cellular phones are removed when the GPR is in operation background noise should not be a problem.

The second type of above ground interference is air waves, which are produced by large objects on the surface. Surface objects such a trees, buildings, cars, even livestock or people have been known to cause air waves in GPR profiles. These air waves are formed from radar energy traveling out to the sides of the antenna and hitting the object. This process creates a straight line high amplitude reflection which appears to be dipping, due to the movement of the antenna by the operator, in the profile (Conyers 2012:85).While air waves are easy to identify in the data owing to their uniform appearance, they are unlikely to occur in this study for two reasons: the sites surveyed have little in the way of surface objects (only occasional trees at the field site) and modern small antennas are typically well-insulated, so radar waves are unlikely to escape to the sides. Furthermore, Conyers (2012:85) only reports air waves being generated from antennas of 400MHz or lower, so they are unlikely to occur with the 500MHz antenna employed in this study.

3.3.2 Electrical Resistivity

To understand the methodological basis of electrical resistivity a basic understanding of how an electrical current behaves when traveling through a medium is required. For an electrical current (I) to travel through a conductor, an electrical potential difference or voltage (V) is applied; the size and rate at which this current travels is then dependent upon the resistance (R) encountered within the conductor (Clark 1990:27). According to Ohm's Law, resistance is equal to the potential difference across a resistor divided by the current passing through it or $R = \frac{V}{I}$ (Reynolds 2011:290). Resistivity (ρ) is a resistance over distance, this is measured in the Ohm-meter (Ω-m) which is the resistance of a 1m cube of material when 1 volt is applied to opposite faces (Clark 1990:27), or $\rho = \frac{VA}{IL}$ (Ω-m) where A is the cross-sectional area and L is length of the material (Reynolds 2011:290).

An electrical current is essentially the movement of charged particles, typically electrons and ions (Clark 1990:27). If a direct current (DC) was utilised for electrical resistivity it would create a phenomenon known as polarisation. During polarisation, current carrying ions with positive or negative charges are attracted to their contrasting positive or negative electrodes where they accumulate and repel similarly charged ions thereby obstructing conduction. By applying alternating current (AC) instead, the constant reversing of current direction prevents the accumulation of charged ions. AC also has the benefit of allowing the resistivity array to disregard any electrochemical currents which could be produced by interaction between the electrodes and soil electrolytes (creating a battery effect) or by naturally present telluric currents. Electrical resistivity arrays are typically run off batteries (such as car batteries) so the control system for the array must first convert the DC supplied from the battery into an AC, before running it through the electrodes (Clark 1990:29).

To make resistance measurements of the ground, electrodes must be inserted into the surface (just enough to make adequate contact). With the ground being a semi-infinite medium (it has only one boundary, the surface) the current is otherwise unconfined and spreads away radially. Electrical current will travel in the path of least resistance, so when encountering a buried high resistance feature it will attempt to travel around the feature taking a longer but less resistive path. This process results in a reduction of current (I) density at the location of the high resistance feature which in turn results in an increase in the potential gradient (V). An increased potential gradient (V/I =R) will result in an increased resistance value or positive anomaly in the data. Conversely a low resistance feature will attract current, lowering the potential gradient in its location and resulting in a negative anomaly in the data (Clark 1990:37). This process of the current deflecting around or moving towards different resistivities means the resistivity values obtained no longer accurately reflect a *true resistivity* but rather a composite of the resistivities encountered, known as an *apparent resistivity* (Scollar 1990:313).

Electrical resistivity surveys are sensitive to the array selected and the manner in which it is employed. The most popularly employed arrays are the Wenner, double-dipole, twin-probe and Schlumberger. The twin-probe array was designed specifically for archaeology and has been employed extensively by archaeologists. Guides aimed at explaining the basics of archaeological geophysics tend to focus on the twin-probe array with little to no mention of other array types (e.g. Somers 2006 and Oswin 2009). However the twin-probe system does not lend itself to vertical profiling as it was designed for horizontal mapping at a set depth, so after some initial testing, the twin-probe was dismissed for use in this research. The Wenner and Schlumberger electrical resistivity arrays are able to produce higher vertical resolution (Reynolds 2011:295). These arrays are considered to be unsuitable for narrow archaeological features, being more suited to larger geological features involving horizontal layering (Clark 1990:37). The double-dipole array is sensitive to shallow features and exhibits high sensitivity to lateral resistivity variations at depth (Reynolds 2011:295). This sensitivity to shallow lateral features is due to the current probes being located together restricting current penetration (Clark 1990:44). The double-dipole array exhibits less sensitivity to orientation than the Wenner or Schlumberger arrays (Reynolds 2011:298), see Figure 3.3 for current flow diagram. For this research a double-dipole array was employed. This choice was made for two main reasons: availability of equipment and the sensitivity exhibited by double-dipole to shallow features. This sensitivity was desirable for the current research as prior excavation showed the archaeological deposit at the field site to occur in the upper 40cm of the subsurface (Nagel *et al.* 2016).

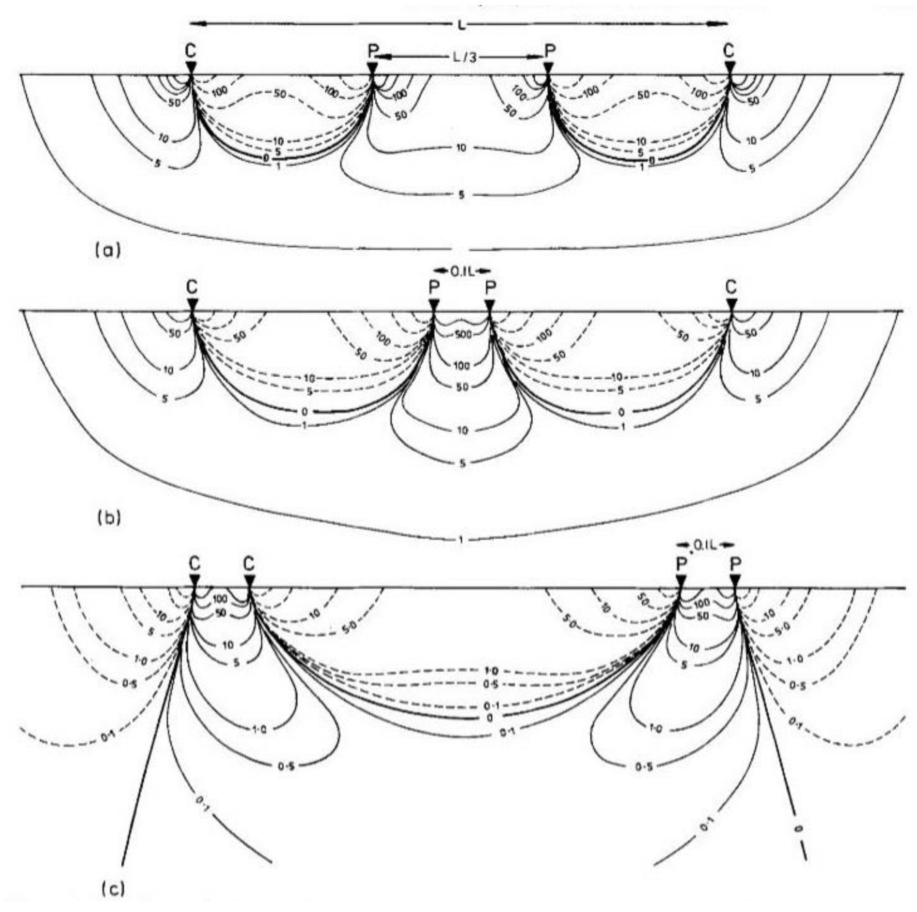

Figure 3.3 Sub-surface current flow for three popular electrical resistivity array configurations: (a) Wenner, (b) Schlumberger and (c) dipole-dipole. Contours represent the relative contribution of each region of the sub-surface to the total potential difference measured by the potential electrodes, with broken lines marking negative contours (Reproduced with permission of Oxford Journals, from Barker 1979:125).

3.3.2.1 Limitations of Electrical Resistivity

Electrical resistivity surveys are prone to several common problems which can produce errors in the results. As noted in Chapter 2, topography and moisture content can cause issues. Surveys over ditches or hillocks will cause the current to be concentrated or dispersed, creating anomalies in the data (Scollar 1990:349). The survey grids employed in this research did not exhibit significant topographic changes, so topographic anomalies should be minimised. The majority of the survey was conducted at such a fine scale the results did not reach the water table. However, there was one survey transect from the field site which was completed with 5m electrode spacing, this line was both topographically corrected and interpreted with reference to the water table present on site. Seasonal moisture content effects were investigated via results produced under different conditions at the experimental site on the JCU campus (see Section 5.4.1 for more details).

The most common problem encountered when using electrical resistivity in the field is electrode contact resistance. When contact resistance becomes anomalously high, the current applied by the array can fall to zero resulting in a failed measurement. High contact resistance is common for dry sand, gravel and frozen material. High contact resistance can be minimised in two ways: by using extra electrodes at right angles to the main line of the array and by applying a water or saline solution. Using extra electrodes is unsuitable, however, when the current electrode separation is small as this can produce errors in the results (Reynolds 2011:308). This study works with dry sand at the field site and sand of varying moisture levels in the experimental site. With sand being a poor electrical conductor, large volumes of saline water were employed in the field to reduce contact resistance. As salting the ground could inhibit the GPR results, freshwater was applied to the electrodes instead of salt water at the experimental site; this was not deemed necessary for the field site because of the large scale of the GPR survey compared to the limited electrical resistivity survey areas. Extra electrodes were not employed as they were likely to produce errors in the results due to the small electrode spacing (25cm) used during surveys for this research.

Errors in electrical resistivity data can also occur due to differences in electrode placement. Small errors may be produced due to insertion depth differences, however significant errors may be produced by the misalignment of electrodes along the line of the survey transect. Misalignment errors can be reduced by employing larger electrode spacing; conversely they will be compounded when employing small spacing. Prior research (Aitken 1974 as reported in Clark 1990:58) found it is better to laterally displace the electrodes if encountering an obstacle than to alter their linear separation from the other electrodes. With relatively clear sites being surveyed for this study, purposely misaligning electrodes was not required. However, strict transect control was required with the small electrode separation employed. Survey lines were established with Real Time Kinematic (RTK) satellite navigation, then marked by string lines which stayed in place for the duration of the survey. Electrodes were located with the use of a tape measure. Survey transect lines were meticulously replicated across all survey grids so the results would be spatially aligned.

3.4 Geophysical Survey Design

The geophysical survey was designed in two main parts. As mentioned previously, the first part of the survey design consisted of an actual field site to test the geophysical methods in real world conditions, while the second part comprised an experimental setup to allow for controlled analysis of the results produced. These sites and the survey methods employed at each are discussed in detail in their respective chapters (see Section 4.5 of Chapter 4 and 5.4 of Chapter 5). For both sites the geophysical instruments employed consisted of a MALÅ GeoScience GPR, utilising a 500MHz shielded antenna with the Ramac XV monitor and the X3M control box, and an Advanced Geosciences, Inc. resistance meter consisting of a MiniSting™ control unit and Swift™ electrode cable with 28 electrodes. Standard settings were applied to the GPR and electrical resistivity systems for both the fieldwork and the experimental work.

For the electrical resistivity array, the standard settings consisted of max cycles of 2, meaning the instrument will cycle through each reading twice and then average them. The current was set to 200mA since it automatically downgrades if required (Advanced Geosciences, Inc. 2003:39-40). The system was also set to 200 volts, but for the field site and the sand-filled trench of the experimental site this was increased to 400 volts to help combat the contact resistance. All lines were run through a contact resistance test first to make sure the electrodes were in proper contact with the ground and not experiencing too much resistance. Any electrodes experiencing difficulties were adjusted and retested before the actual survey readings were taken.

The GPR system was standardly set so the number of samples was 1016. The samples allotted dictates how many digital readings will be taken to record one trace of the reflected wave, the more samples the higher and more accurate the resolution. The longer the time window is open or the higher the frequency antenna, the larger the number of samples required to adequately characterise the reflected wave (Conyers 2004:87-88). The trace stacking was set to four, meaning a digital average of four consecutive reflection traces was made into one composite trace; this is done to remove reflection waveforms created by bumps or dips in the ground during collection (Conyers 2004:88-89). While filters such as background removal and low pass can be set in the field they are not recorded in the data and serve only to enhance profile visualisation on the monitor during collection (this is an aspect specific to Mala GPR systems).

3.5 Data Processing and Volume Calculation

The complexity and intensiveness of data processing varies based on the geophysical methods employed and the research questions addressed. For GPR the data are subject to effects known as noise, multiples, snow and horizontal banding which can all obscure reflections created by the features the researcher is seeking to locate. These extraneous effects need to be filtered out during processing. Raw GPR data are also typically collected without accurate depth scales, which then need to be created during the processing stage (Conyers 2004:119). While electrical resistivity data requires comparatively less processing than GPR data it still requires the removal of any anomalous data points as well as inversion. All geophysical methods also require topographical corrections when varying topography is encountered during survey. For this study topographical corrections were only necessary to enhance interpretation for some of the field site data, but when the survey data were moved to ArcGIS topographical corrections were applied to all data points to increase the level of accuracy for the volume calculations.

The following sections (3.5.1 and 3.5.2) will detail the general processing undertaken for the GPR and electrical resistivity data at both the field and experimental sites. Following this, section 3.5.3 will discuss in detail the volume calculation method employed for this study, as processing the data to create volume estimates is a novel technique in investigating shell matrix sites. The specific methods employed in this study were developed based on prior literature that utilised GPR and electrical resistivity to create volume estimates for other (non-shell) buried deposits (as discussed in Section 2.6 of Chapter 2).

3.5.1 Ground-Penetrating Radar

For processing, the MALÅ files were imported into Reflexw. The files were initially *time-cut* to the top 100ns to remove extraneous depth beyond the point of total signal attenuation. The raw data files for the fieldwork extend to over 300ns due to user error with the MALÅ: the antenna had been set to *deep* (by other users) and lack of familiarity with the MALÅ system meant this settings error was not detected until the survey results were compared with prior test files recorded in the field. Investigation into this matter found a sub-setting had been missed: not only did the correct antenna need to be selected, but then it needed to be re-selected to set its parameters as either *Shallow*, *Medium* or *Deep*. This does not affect the depth penetration the antenna is achieving, just the time window shown, which in this case resulted in unnecessary profile depth where the signal was already fully attenuated. Further data processing included the following list and was conducted in this order: *Subtract mean* (also called *dewow*) to remove inherent low-frequency bias in the data. *Static correction* (move to negative times) to remove the time delay so the profile begins at ground level. *Manual gain (y)* was then employed to better visualise the results and to counteract the weakening of the signal strength with depth, and *background removal* to remove some of the constant horizontal banding noise common to radar profiles. A *bandpass filter (butterworth)* was utilised to remove unwanted frequency noise; any noise below 300MHz or above 1000MHz was removed. Then a *Kirchhoff 2D-velocity migration* and a *time-depth conversion* were completed based on a *hyperbola* (or *velocity*) adaption. The velocity migration attempts to track the reflection and diffraction energy back to its source and thus adjust the reflectors to their true position (Sandmeier 2012:325). Time-depth converts the time axis into a depth axis based on velocity distribution as assessed from the velocity adaption and was confirmed with ground truthing. Lastly, where required, the radar profiles were topographically corrected (see Figure 3.4 for processing flow).

With the files fully processed the *pick* function in Reflexw was used to mark the deposit boundaries. The pick function records the x, y and z coordinates of the selected location as well as the amplitude. For the field site I marked the top of the beachrock in Transect C, while both the top of the beachrock and the base of the cultural shell deposit were discernible in Transects A/B. The depth of the deposits for Transects A/B and C were ‘picked’ every 1m across the survey lines (see Section 4.6.2 of Chapter 4 for images). The ‘picks’ for each profile were then exported as ASCII columns files; the separate survey lines for each transect were compiled in Microsoft Excel and each ‘pick’ was georeferenced based on information generated from ArcMap. Results were saved as CSV (comma delimited) files for import into ArcMap. The process for the experimental site was much the same except the ‘picks’ were created every 25cm and both the top and bottom of the deposit had to be ‘picked’ then exported as two separate files as the deposit was fully buried: one set of files marking the top of the deposit in each survey line and one marking the bottom (see Section 5.5.1 of Chapter 5 for images). To achieve highly accurate results, specially georeferenced points (points with x and y coordinates based on UTM coordinates) were created in ArcMap for ‘picks’ where the deposit began or ended more than 1cm off the 25cm grid marks.

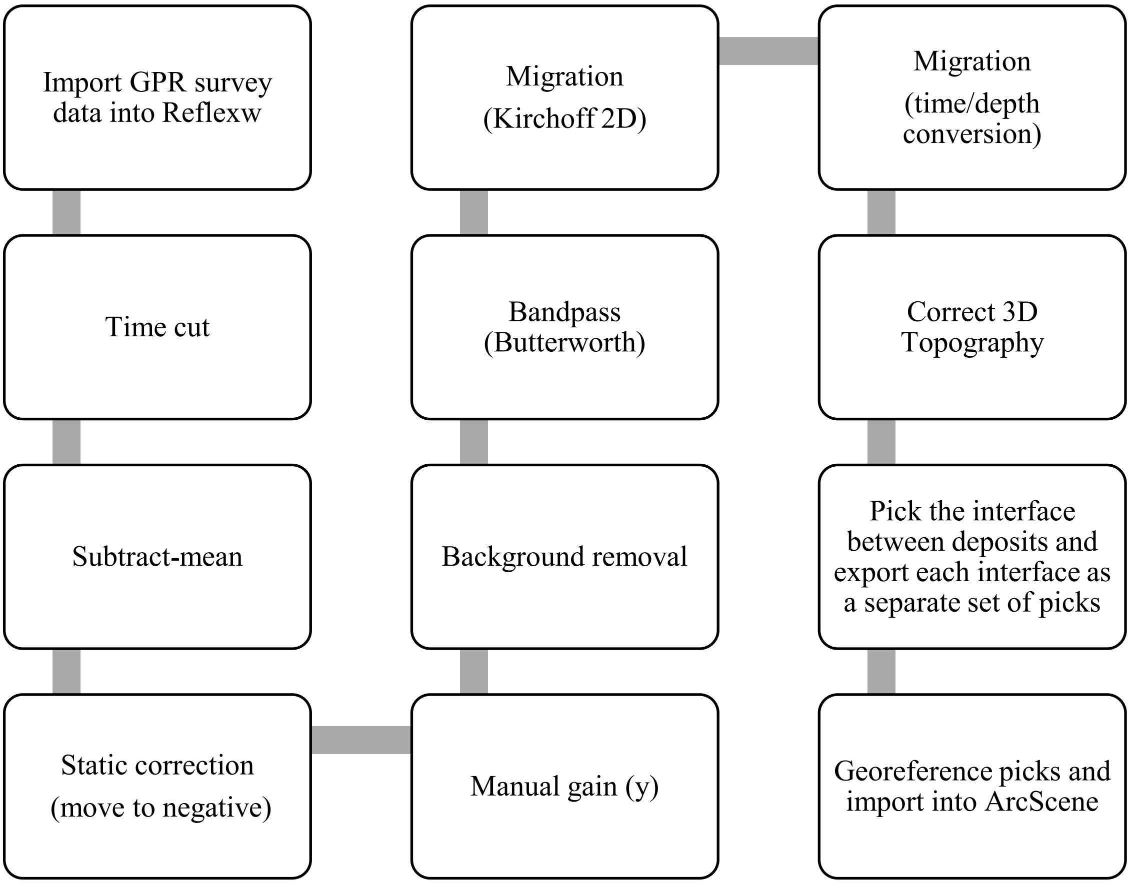

Figure 3.4 Data processing workflow for GPR survey data.

3.5.2 Electrical Resistivity

The electrical resistivity files were initially inverted and viewed in the field (for both the field site and the experimental site) before being fully processed with AGI EarthImager software in the laboratory. The resistivity files were edited for noisy data points and bad electrodes, removing any which were found in order to improve the inversion results. Topography files were then loaded if required (many of the resistivity grids did not require topographical correction for interpretation because they were short lines in flat areas) and the inversion was run a second time. The inversion process attempts to convert the apparent resistivity results into true resistivity values through inverse modelling. The settings employed for this research consisted of standard initial settings as recommended by Advanced Geosciences, Inc. (2009:54-57), then two different sets of resistivity inversion settings.

The first inversion settings employed were to compensate for the large errors encountered in the results obtained from the fieldwork and the sand-filled experimental trench. These settings consisted of increasing the maximum Root Mean Square (RMS) error to 5% as well as increasing the *smoothness* and *damping* factors to 100 to compensate for the large amount of noise in the data. RMS error is an average of the data misfit between the recorded resistivity values and the modelled true resistivity values of the inversion; a single erroneous data point can lead to a large error, so any ‘bad’ points are removed during processing before inversion. Lastly, the *suppress noisy data* command was turned on to reduce noise. These are the suggested settings for processing noisy data in the EarthImager2D manual (Advanced Geosciences, Inc. 2009:62-64). The fieldwork results were subjected to extensive editing of electrodes to remove erroneous or ‘bad’ data points before inversion.

The second group of inversion settings were tailored to the survey results obtained from the organic sediment-filled trench. These settings did not utilise the *suppress noisy data* command and reduced the RMS error to 3% and the *smoothness* and *damping* factors to 10, which are the standard recommended settings (Advanced Geosciences, Inc. 2009:60-63). As the data obtained from the organic sediment-filled trench was good, the removal of erroneous data points was not required. After inversion, the resistivity results were then scaled so the contour levels were uniform across the different results. A scale range of 1Ω-m to 25,000Ω-m was chosen as best representing the resistivity values of the shell. The fully processed inversion results were then saved as an image and a text file (see Figure 3.5 for processing flow).

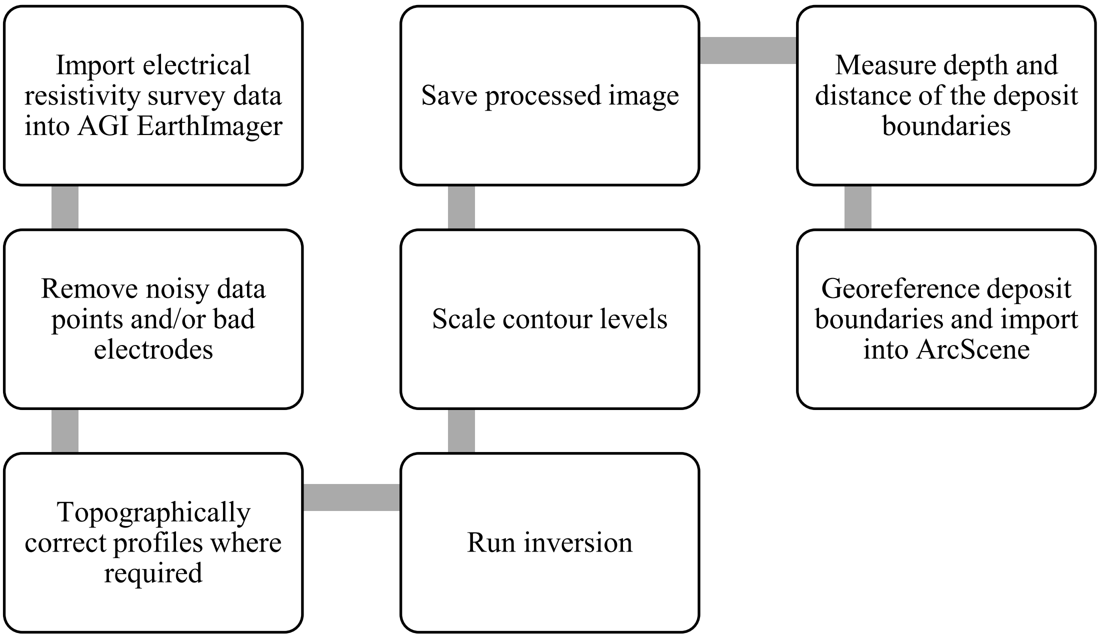

Figure 3.5 Data processing workflow for electrical resistivity survey data.

The only interpretable electrical resistivity results, in terms of calculating the volume of the shell deposit and creating 3D models, were from the organic rich Trench 2 of the experimental site. It was initially hoped to use the saved text files to narrow down the results to just the highly resistive shell material, thereby creating a consistently replicable and quantitative method of extracting the shell deposit values from the rest of the inversion results, but this could not be accomplished. Instead, the shell deposit was singled out of the processed results via a method similar to the ‘pick’ system in Reflexw. The processed pseudosections were gridded manually over the area of the shell deposit based on the distance markers supplied on the inversion image, then the ‘picks’ were marked on the image and the depth and distance was measured off the grid for each ‘pick’. ‘Picks’ were placed on the 25cm survey marks where possible. When the ends of the deposit fell outside the 25cm marks, specially georeferenced points were created for them in ArcMap as was done with the GPR results (see Section 5.5.2 of Chapter 5 for images). These ‘picks’ were recorded in Microsoft Excel and georeferenced based on information generated in ArcMap, they were then saved as CSV files and imported into ArcScene (the top and bottom of the deposit were imported as separate files).

3.5.3 Three-Dimensional Mapping and Volume Calculation

Calculating a volume estimation of the deposit required using both ArcMap 10.2.1 and ArcScene 10.2.1 to complete the different functions in mapping the deposits. While there were several basic ArcGIS functions employed to complete the volume calculations, some tools and processes employed were the result of extensive problem-solving. This problem-solving was done by scouring the abundant help forums for Esri's ArcGIS software to find the right tools to assist with the more obscure processing requirements. Processing in the ArcGIS software was similar for Thundiy and the experimental site, the main differences being in relation to the creation of surface data. Thundiy had been mapped extensively with the RTK while the experimental site was mapped with basic GPS points and dumpy levels. The RTK recorded highly accurate x, y and z values for the field site, while the two experimental trenches only had GPS points with variable error (±5m). To create accurate topographical information for these trenches, georeferenced points were created in ArcMap and assigned z values based on dumpy level readings and approximate height above sea-level information. The RTK points for Thundiy and the updated GPS points for the experimental site were then imported into ArcScene and used to create a triangulated irregular network (TIN) of the surface topography of each site.

Neither the RTK nor the GPS was connected to the GPR or electrical resistivity array during survey, so survey lines needed to be manually georeferenced to locate them accurately within the survey grids in the ArcGIS software. To accomplish the georeferencing, the RTK and GPS data were imported into ArcMap where a new *point feature* file was created to record the desired survey points. This 'point feature' file was then assigned x and y coordinates before being imported into ArcScene to add z values. The z values were allocated from the surface topography TINs for the sites. These z values may not always perfectly represent the surface of the sites in reality as they were created by the algorithm employed to create the overall TIN (in the case of an ArcGIS TIN this is the Delaunay triangulation method), but for small-scale areas and with good quality source data the results will be high-precision. The georeferenced survey lines were exported as a text file from the attributes table of the 'point features' file. The full x, y and z values were used to topographically correct some of the GPR files from Thundiy while the x and y values were used to georeference the 'picks' created from the

GPR profiles in Reflexw, as well as those recorded manually from the electrical resistivity inversion images.

The georeferenced ‘picks’ were then imported into ArcScene and employed to create a second TIN, and where more than one boundary was being represented a third TIN was made based on the deposit boundaries. The TINs were then used to create volume calculations for the deposit by using the *surface difference* tool in ArcScene. Two TINs are input into the surface difference tool which then creates a third surface demarcating whether each corresponding triangle of the first TIN is above, below or equal to the second TIN (Esri 2012); from these measured differences the volume is calculated and can be found in the attribute table. The volume estimation was at this stage fully complete, however to better visualise the deposits, a 3D polygon model was created using the *extrude between* tool (see Figure 3.6 for processing flow). Unfortunately these images cannot be exported from ArcScene with a scale bar, north arrow or key, as ArcScene, unlike ArcMap, has no *layout view*.

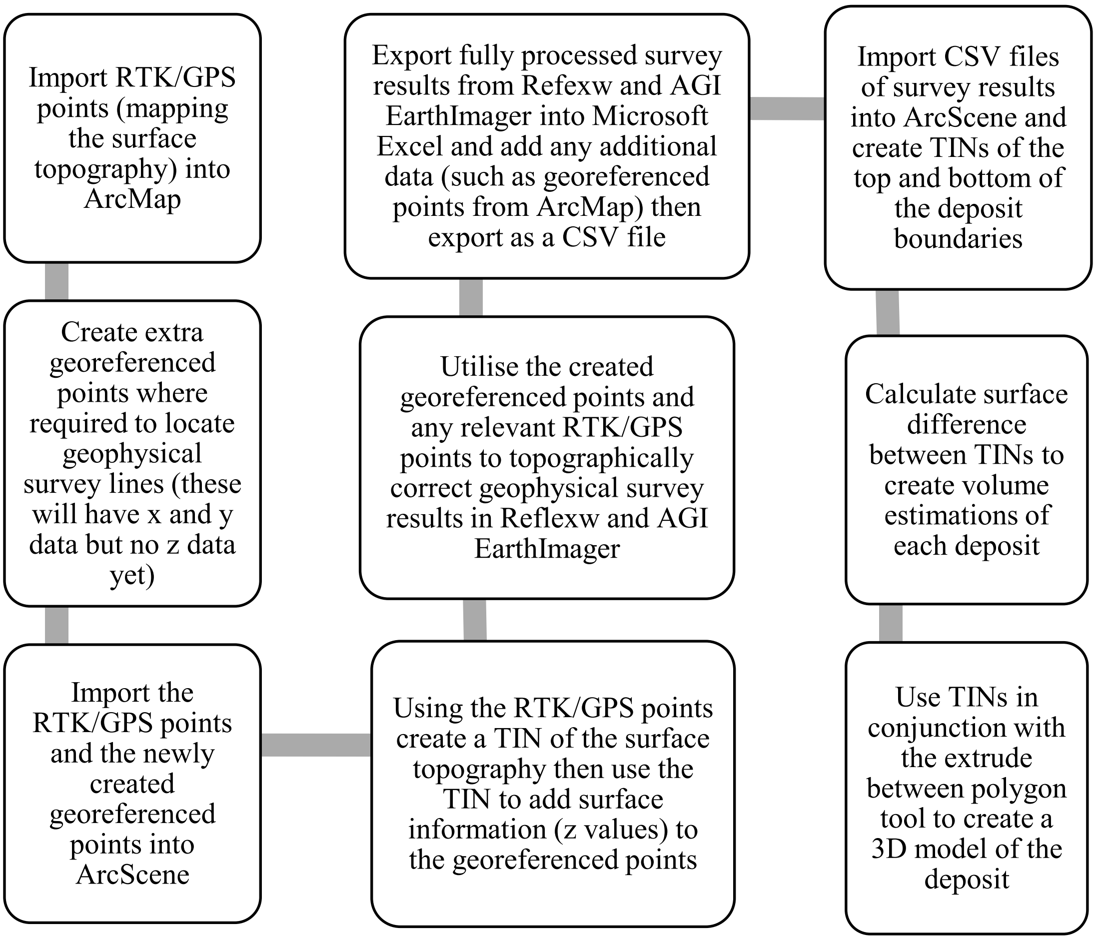

Figure 3.6 Data processing workflow for ArcGIS and ArcScene.

3.6 Methodological Limitations

One of the main limitations experienced during this research was the location of the field site. With the field site in a remote and difficult to access location there were strict funding and time limitations on the work. Further limitations were encountered in accessing the geophysical equipment. Both the GPR system and the electrical resistivity array are shared between JCU campuses (Cairns and Townsville, located 347km apart by road) and in the case of the electrical resistivity array also shared between university faculties (with the array belonging to the College of Science, Technology and Engineering). Initially the experimental site had been designed to serve two main functions: to allow for volume calculations of a known deposit and to create an understanding of the type of environment likely to be encountered in the field so the best methodology to employ could be determined. Unfortunately the bulk of the experimental work did not occur until after the fieldwork, which meant the fieldwork did not benefit from lessons learnt during surveys of the experimental site. Failure to fully survey the experimental site before the field season was due to a lack of access to the electrical resistivity array. However, with hindsight the fieldwork methodology was robust and appropriate; the only noted improvement would have been to shift some of the time spent collecting electrical resistivity profiles into collecting more GPR data.

3.7 Summary

While standard methodological practice was implemented for the geophysical surveys in this study, the application of those methods and the data processing methodology employed were both novel. By employing the recommended methodology for geophysical surveys as set out by practitioners of archaeological geophysics such as Conyers (2004), Clark (1990), Scollar *et al.* (1990), Nishimura (2001) and Oswin (2009), this study avoided the common mistakes made by other researchers. Failure to ground truth, to account for topographical influences or to achieve proper grid control were the most commonly occurring methodological oversights exhibited in prior research, each of which were addressed in the methodological design of this study. Unfortunately not all mistakes were avoided, and as Conyers and Leckebusch (2010) point out: many of the mistakes which lead to inconclusive survey results are due to inappropriate technique choice and/or data collection and processing. This study found the sand and shell were too close in their resistivity values for the electrical resistivity to differentiate them. The closely matched resistance values for the sand and shell made electrical resistivity an inappropriate technique for the task of differentiating them, although, interpretable results were obtained in the field from the longer survey transects (with 1m and 5m electrode spacing) which looked at the larger site composition. Overall, the research design ensured most sources of error were avoided and interpretable results were collected.

4 FIELD SITE: THUNDIY

4.1 INTRODUCTION

Thundiy (also spelt Tondoi) is a large archaeological shell matrix complex on the northern end of Bentinck Island in the southern Gulf of Carpentaria, Queensland, Australia. The aims of the fieldwork conducted at Thundiy were to test the selected geophysical methods (GPR and electrical resistivity) in real world conditions. The fieldwork also aimed to contribute new knowledge to an existing research project investigating the shell deposits present on site. Preliminary site inspection and survey planning at Thundiy was conducted in July 2013, the geophysical surveys then took place in a single field season the following year, from 7-23 July 2014.

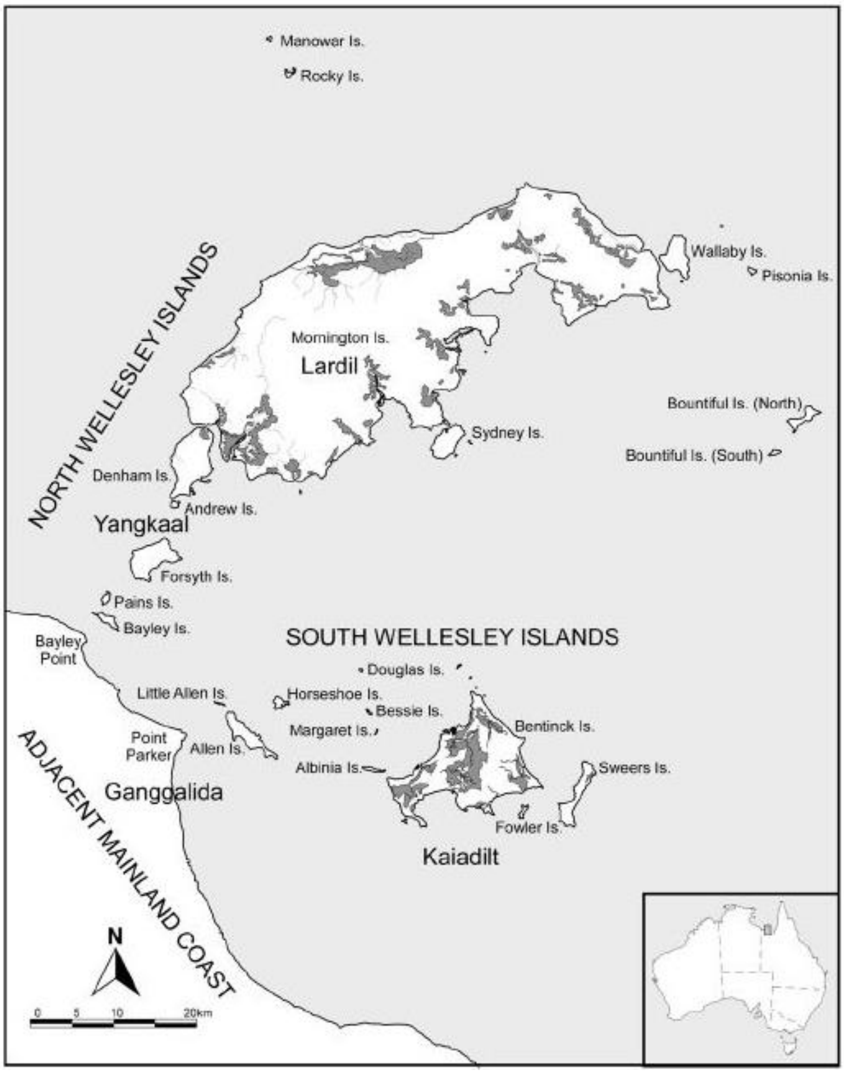

Figure 4.1 Wellesley Islands and adjacent mainland coast (Reproduced with permission of A. Best, from Best 2012:2).

Bentinck Island is part of the Wellesley Islands. The Wellesley archipelago consists of 23 islands of which Bentinck is the second largest at c.150km² or 180km² if surrounding reefs and sandbanks are included. The Wellesley Islands are divided into a North and South group. The North Wellesley Islands are split between two cultural groups the Lardil and Yangkaal while the South Wellesley Islands, of which Bentinck Island is part, belongs to the Kaiadilt (Figure 4.1).

Bentinck Island is currently occupied on a seasonal basis as medical and educational facilities are all located on the larger Mornington Island. A small outstation is located on the southeast corner of Bentinck Island at Nyinilki (also spelt Njinjilki) and until early 2015 was occupied year-round by a caretaker employed by the Kaiadilt Aboriginal Corporation. This outstation served as accommodation during fieldwork. To access the Thundiy field site from the outstation at Nyinilki (see Figure 4.2) equipment and field-crew were transported by four-wheel drive (4WD) vehicles via tracks which required which had to be relocated each field season due to vegetation, mostly grass, regrowth during the preceding wet season (see Section 4.2).

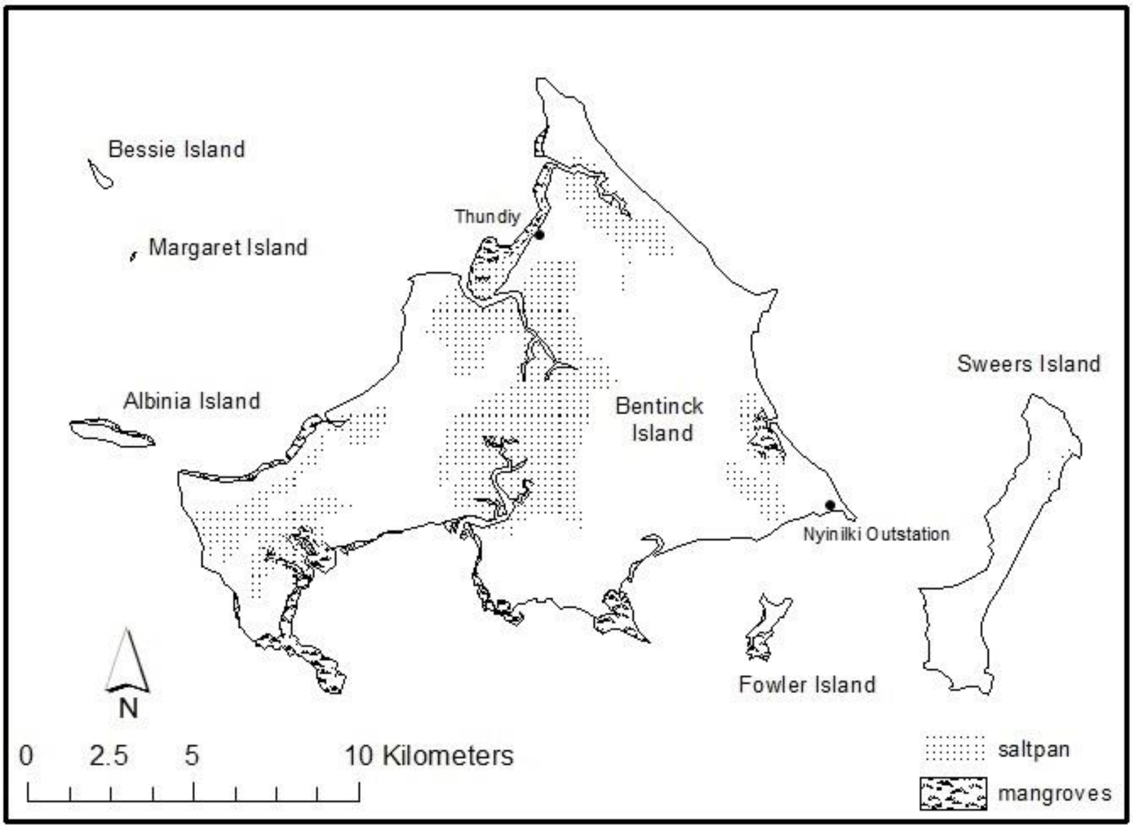

Figure 4.2 Bentinck Island showing the location of the Nyinilki outstation and the Thundiy field site.

The beach ridge, where Thundiy is located exhibits surface scatters of shell for over 4km along the crest and northwest-facing flank of the ridge. The beach ridge is bounded on either end by two creeks. Thundiy was mapped by Tindale (1962) as one of numerous named camp sites along this stretch of shore (Figure 4.3). Ground reconnaissance survey and prior excavations established that the cultural deposits present on site extend across the beach ridge and to a depth of approximately 40cm. The most prevalent surface deposits are on the seaward side of the ridge up to and just over its peak (Nagel *et al.* 2016; Peck 2016), though surface scatters of shell can be seen up to 150m inland from the line of pandanus palms which mark the extent of the tidal zone and the seaward extent of the shell deposit (see Figure 4.4). With 4km of deposits reaching up to 150m inland and to depths of 40cm the overall shell matrix could potentially comprise up to 240,000m³ of shell material.

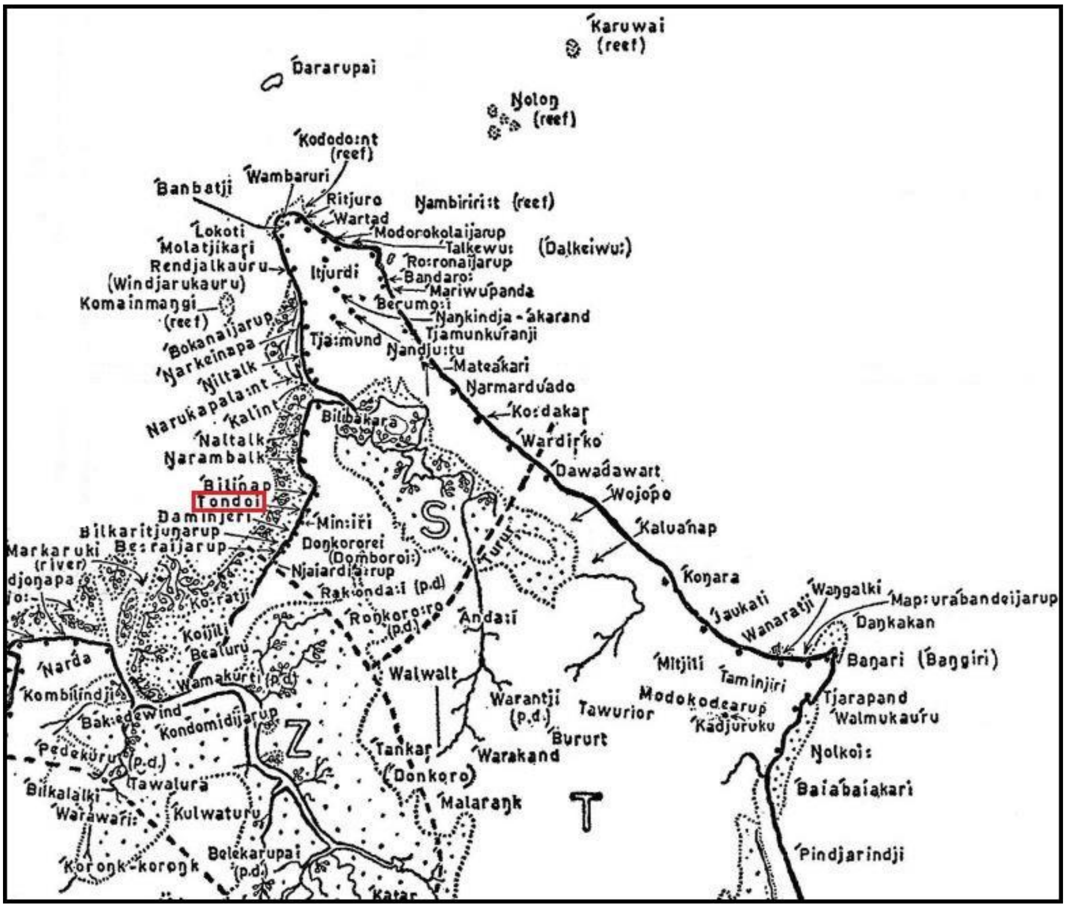

Figure 4.3 **Extract from Tindale's map of Kaiadilt place names showing the northeast tip of Bentinck Island with Thundiy (spelled Tondoi) highlighted (modified Map A, reproduced with permission of the South Australian Museum, from Tindale 1962:297).**

Figure 4.4 Thundiy shell midden and the line of pandanus palms marking the edge of the tidal zone.

The following sections detail the known environmental (Section 4.2), historical (Section 4.3), and archaeological (Section 4.4) background for Bentinck Island, with consideration as to how this information will impact the archaeological record at Thundiy and thereby the collection and interpretation of geophysical data. The site-specific methodology employed for the geophysical surveys at Thundiy is then detailed (Section 4.5) and finally the results of the surveys are presented (Sections 4.6 and 4.7) and discussed (Section 4.8).

4.2 Modern Environmental Context

The modern environmental context for the South Wellesley Islands is influenced by their location at the semi-arid margin of the monsoonal tropics. Weather patterns for this region are dominated by a wet and a dry season. The dry season is characterised by dry, cooler weather during the months of April to November with trade winds from the southeast. The wet season is characterised by hotter weather and northwest monsoon winds bringing rain, flooding and regular cyclones from December to March (see Figure 4.5).

Figure 4.5 Comparative photographs of the same two sites on Bentinck Island. On the left are photographs of the dry season and on the right the wet season; dry season photographs by Selene Kenady (July 2013), wet season photographs courtesy of Daniel Rosendahl (February 2014).

During the peak of the hot wet season in December, temperatures average a maximum of 33.7°C, while the cold dry season averages a minimum temperature of 17.6°C during its peak in July (Australian Government Bureau of Meteorology 2015a). Mean monthly rainfall varies from 346.7mm during the wet season to as little as 1.7mm in the dry season (Figure 4.6). This seasonal difference in rainfall combined with the relatively flat topography of the Wellesley Islands means large areas of Bentinck Island are prone to seasonal flooding. The highest point on Bentinck reaches a maximum of only 10m (Evans 1995:15). Extensive areas of the Island are below 5m and consist of clay-pans (or salt-pans) and mangrove forests which are inundated by peak high tides during the dry season and by seawater during the wet season: at this time the northwest monsoon winds bank up seawaters in the Gulf by as much as 2m (Tindale 1977). Between the weather and topography, fieldwork is infeasible during the wet season months from November through April.

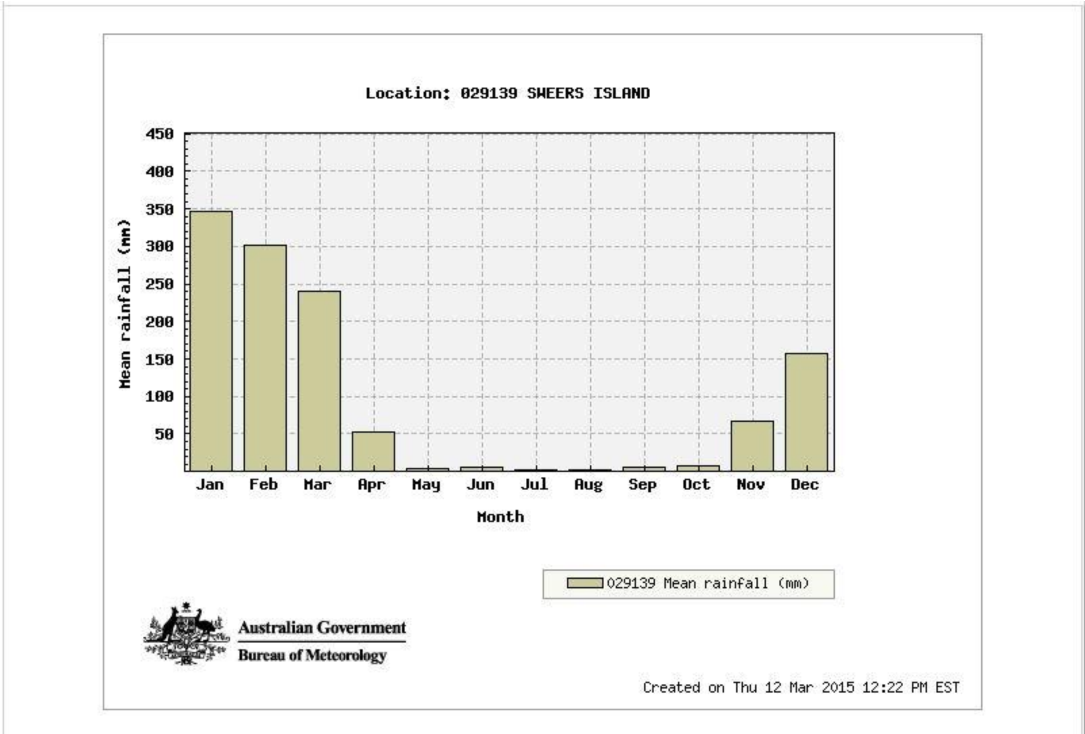

Statistics	Jan	Feb	Mar	Apr	May	Jun	Jul	Aug	Sep	Oct	Nov	Dec	Annual	Years
Mean rainfall (mm) for years 1893 to 2015	346.7	301.5	241.1	51.8	3.6	6.0	3.0	1.7	6.1	7.7	67.8	156.4	1201.6	18

Figure 4.6 Sweers Island mean monthly rainfall; based on 18 years of weather data (taken from the Australian Government Bureau of Meteorology 2015a).

Fieldwork conducted during the wet season (as pictured above in Figure 4.5) was limited to locations close to the outstation (Nyinilki) as travel by 4WD vehicle was severely limited with the tracks beyond the immediate outstation area being impassable due to flooding. Fieldwork was, in light of this, scheduled for June/July each year as these months were dry enough to make the island largely accessible and cool enough to make fieldwork physically endurable. The seasonal flooding of large areas of low-lying land can also be expected to impact upon the archaeological record. Sites are unlikely to exist in these areas as people are physically blocked, by floodwaters, from creating habitation sites for part of the year and any sites created during the dry season would subsequently be impacted by the seasonal effects of the wet season.

4.2.1 Environmental Background: Gulf of Carpentaria Sea-Levels

The Gulf of Carpentaria is characterised by its shallow waters: it is the largest tropical epicontinental (lying on the continental shelf) seaway in the world. This shallow shelf reaches a maximum depth of only 70m. The Gulf is bordered by rising sea bed on either side with the Arafura Sill to the west at 53m below present sea-level and the Torres

Strait to the east rising up to a sill only 12m below present sea-level (Reeves *et al.* 2008). Because of its characteristic shallow and relatively flat nature, the Gulf has been experienced massive environmental changes with fluctuating sea-levels. At the Last Glacial Maximum (23,000-19,000cal BP) when sea-levels were at their lowest (approximately -125m compared to modern sea-levels), the Gulf of Carpentaria would have been a large savannah plain connecting Australia to New Guinea with a very prominent lake, Lake Carpentaria.

The Gulf of Carpentaria returned to marine conditions during the Holocene when sea-levels rose by 120m. A fairly rapid transgression event began filling the Gulf around 12,200cal BP when the Arafura Sill was breached, with full marine conditions established by 10,500cal BP; the Torres Strait Sill was not breached until around 8,000cal BP (Reeves *et al.* 2008). The rising sea-levels over this period turned a set of inland hills into the Wellesley Islands. The sea-levels in the Gulf continued to rise until a high stand of approximately +2m was reached for the southern Gulf area at 6,000-8,000BP staying at this level until approximately 4,000BP (Reeves *et al.* 2008; Sloss *et al.* 2011). Dating of *in situ* oyster beds on Bentinck Island shows an age range of 4,720±40cal BP for the lower limit of the bed (+1.68 m above present sea-level) and 4,170±40cal BP for the upper limit of the oyster bed (+1.92m) (Sloss *et al.* 2011). This period of high stand is particularly relevant to the Thundiy field site as it places the site in an active foreshore zone, making it an unlikely location to find deposits exceeding 4,000-8,000cal BP (Figure 4.7).

After c.4,000cal BP gradual sea-level recession was seen until present sea-levels were reached somewhere over the past 1,000 years (Moss *et al.* 2015). Further modelling based on sediment cores taken from Bentinck Island indicate conditions changed to resemble the present at Thundiy around 1,500BP (Figure 4.8). This indicates that the shell deposits at Thundiy are unlikely to be older than 1,500cal BP, which is further supported by radiocarbon dates from the archaeological excavations (see Section 4.6.1.1).

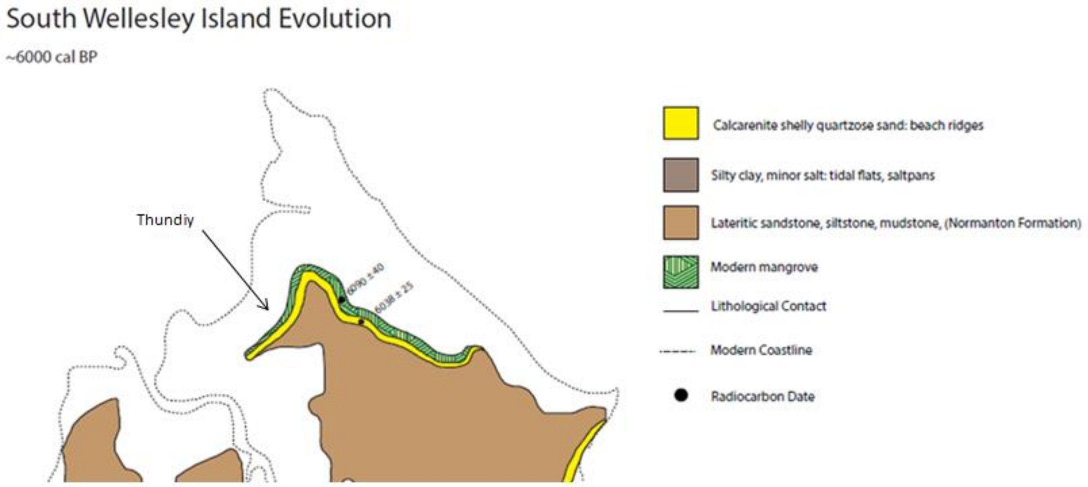

Figure 4.7 Map showing the approximate location of the present-day Thundiy field site in comparison to modelled shoreline extent at c.6,000cal BP (map prepared by Alison Sternes 2014 modified by Selene Kenady 2015).

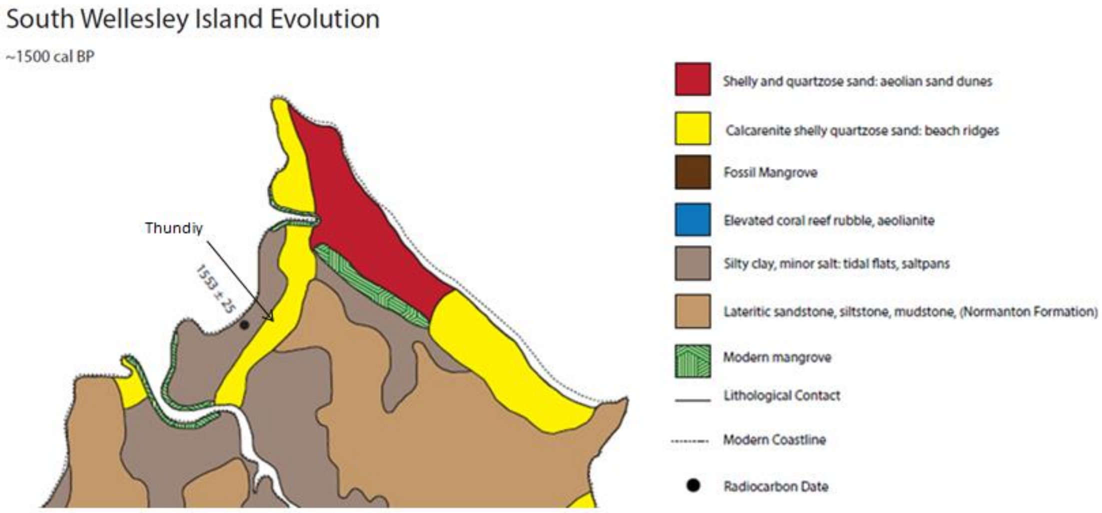

Figure 4.8 Map showing the approximate location of the present-day Thundiy field site in comparison to modelled shoreline extent at c.1,500cal BP (map prepared by Alison Sternes 2014 modified by Selene Kenady 2015).

4.3 Historical Context

The Kaiadilt have a strong link with the sea, obtaining the majority of their sustenance from the active shore zone (Tindale 1977). Kaiadilt camps were typically established on sandy beaches above the high tide mark, only being removed inland to higher ground and denser tree cover during cold winter storms from the southeast or tropical cyclones

(Tindale 1977). This practice of locating camps close to the shoreline will have resulted in the loss of sites exposed to storms and storm surges. The location of the field site, Thundiy, is sheltered from some of the worst of this weather by a stand of mangroves and pandanus palms beyond which is a broad clay-pan and a further stand of mangroves, these features have likely served as a contributing factor in the site's preservation.

The Kaiadilt employed a material culture tool-kit consisting of 28 items including rafts, spears, small fishing-nets and tools made of shell and stone (Roth 1901, 1903; Tindale 1977); for a detailed description of Kaiadilt material culture see Best (2012), Evans (1995:16-19) and Tindale (1977). Large and numerous stone-walled fish traps were also constructed in which men would spear larger fish between tides and where women would collect smaller fish left behind during low tide (Tindale 1977). These stone-walled fish traps along with the shell middens are by far the most prominent archaeological remnants on the island, making them vital resources in understanding the history of Bentinck Island and the surrounding Wellesley Islands.

Throughout their recorded history the Kaiadilt have shown a general aversion to making contact with outsiders. Historically the Kaiadilt appear to have avoided meetings with strangers unless surprised and cornered; these forced interactions would then be escaped as soon as possible (see Flinders 1802; Roth 1901). This aversion to strangers is further exhibited by the lack of evidence of interaction between the Kaiadilt and the Macassans (as would be exemplified by loan words, changes in hunting and gathering practices or genetics) even though archaeological and historical evidence show there was a Macassan presence on Sweers, Fowler and Bentinck Islands (Oertle *at al.* 2014).

Systematic contact with the Kaiadilt was not attempted by European outsiders until 1925. The Mornington Island Presbyterian Mission established communication which lasted for two years before the practice was suspended as a precaution against possible hostility. Contact by the Mission was not re-established until 1945 when friendly communication resulted in 29 Kaiadilt visiting the Mission on Mornington for a month, before being returned to Bentinck (Tindale 1962:269). This late contact between the Kaiadilt and European settlers meant the Kaiadilt lived substantially traditional lifeways until their removal from the South Wellesley Islands to the Mission on Mornington Island in 1948. Bentinck Island was then left generally vacant until 1984 when the

Kaiadilt procured a community boat in which to make visits from Mornington Island back to Bentinck (Evans 1995:42-43).

4.4 ANTHROPOLOGICAL/ARCHAEOLOGICAL CONTEXT

The first human presence on Bentinck Island (found so far) has been dated to 3,483cal BP. Analysis of excavation material and 128 radiocarbon dates (carried out by the larger research team under which the study for this dissertation was conducted) found this first sign of human occupation on Bentinck at Jarrkamindiyarrb, located on the southeast coastline of the island. Evidence for continuous occupation of Bentinck appears after 1,500BP at which point a range of sites across Bentinck and Sweers are present. There is a high representation of dates from the last 300 years with over half of the 128 dates taken from the South Wellesley Islands having median calibrated ages of <300cal BP (Memmott *et al.* 2016). Based on these dates and also from linguistic evidence, it is thought proto-Tangkic speakers were already occupying Mornington Island when sea-levels stabilised at c.2,000BP. These proto-Tangkic speakers visited the mainland and the South Wellesley Islands sporadically between c.2,000-1,500BP, before splitting into a Northern Tangkic group on Mornington Island and a Southern Tangkic group on the mainland and intervening islands. After this fission, the groups were largely independent and insular for around a thousand years. Then c.1,000BP, with the two groups having developed separate languages, a second wave of expansion from Mornington to the mainland began; resulting in the new Northern Tangkic-offshoot language spreading southwards to the mainland and to Bentinck Island, while Mornington Island itself became pre-Lardil.

Extreme climatic conditions between 800-400BP are speculated (archaeological evidence for the event has not yet been found) to have caused a very sudden change in the Northern Tangkic-offshoot language. Around this time the language becomes lexically more like Southern Tangkic while maintaining its original grammar structure. This type of linguistic change could be explained if the Northern Tangkic-offshoot language group sought refuge with the speakers of Southern Tangkic on the mainland. Under these circumstances the two language groups would have mixed and a cultural-linguistic blending would have occurred. The refugees would then have returned to their homelands with new cultural ties to the interior mainland groups and with a newly altered language (proto-Eastern Tangkic). Over time the Eastern Tangkic language group split into proto-Yangkaal-Kayardild occupying the South Wellesley Islands, Denham and Forsyth Islands and the immediate mainland, and the pre-Yangerella-Nguburindi language group occupying the mainland coastal and inland region to the south (Figure 4.9) (Memmott *et al.* 2016). Linguistic evidence indicates that cultural contact to and from the South Wellesley Islands ceased a century or two after this point at c.300cal BP. The reasons for this break are unclear but subsequently those who stayed in the Denham and Forsyth region became Yankaal speakers while those people living in the South Wellesley area became Kayardild speakers or Kaiadilt. The modern language groups and the regions they occupy are shown in Figure 4.10 (Memmott *et al.* 2016).

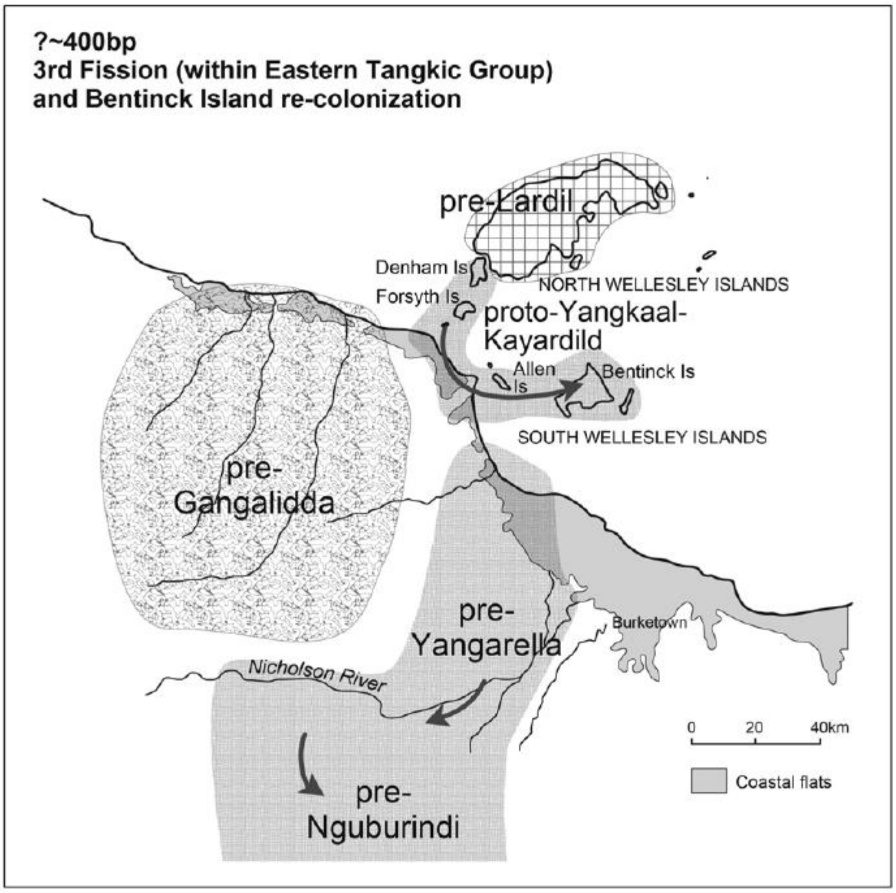

Figure 4.9 Fission of Eastern Tangkic language group (Reproduced with permission of John Benjamins Publishing Company, from Memmott *et al.* 2016:117).

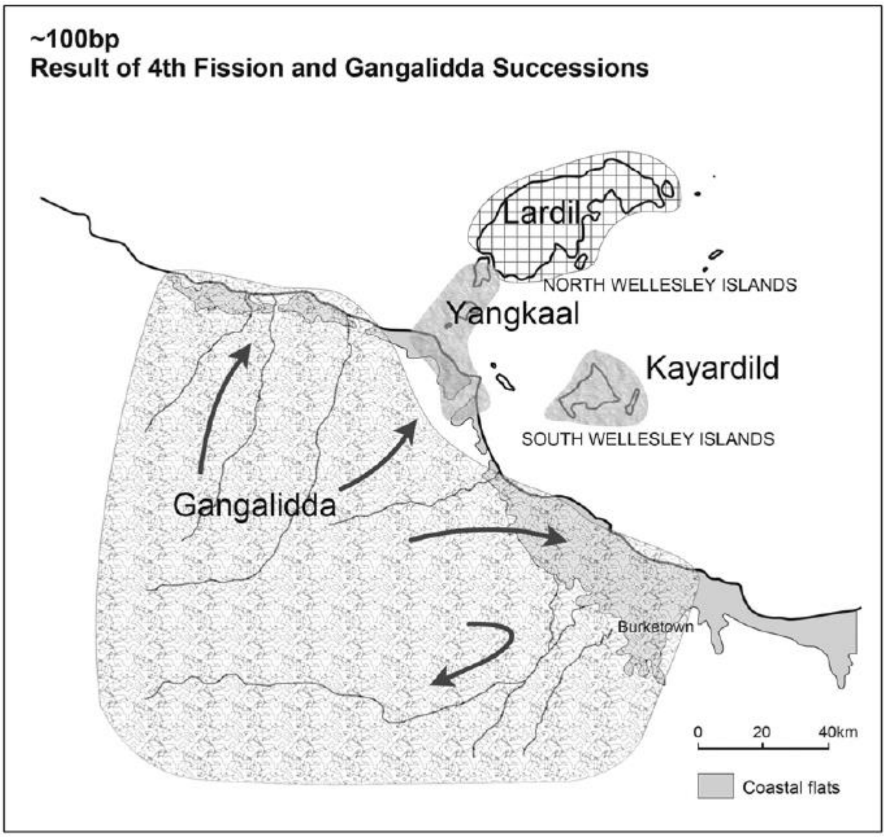

Figure 4.10 Modern language groups and the regions they occupy (Reproduced with permission of John Benjamins Publishing Company, from Memmott *et al.* 2016:118).

4.5 FIELD SITE METHODOLOGY

The large extent of the shell matrix deposits present at Thundiy makes geophysical survey a vital tool in characterising the buried shell. However the size of the site combined with its remote location means that even with geophysical surveying only a portion of the site can be investigated. With this in mind, three geophysical transects were established using a Real Time Kinematic (RTK) surveying system. Two transects (Transect A and B) were laid out side-by-side running along the ridgeline for 120m, while Transect C crossed Transects A and B running inland from the line of pandanus palms for 160m (Figure 4.11). Each transect was composed of 5m² squares. These transects were only one square (5m) wide but were more than 100m long. The squares were each assigned a unique letter and number identifier (Figure 4.12).

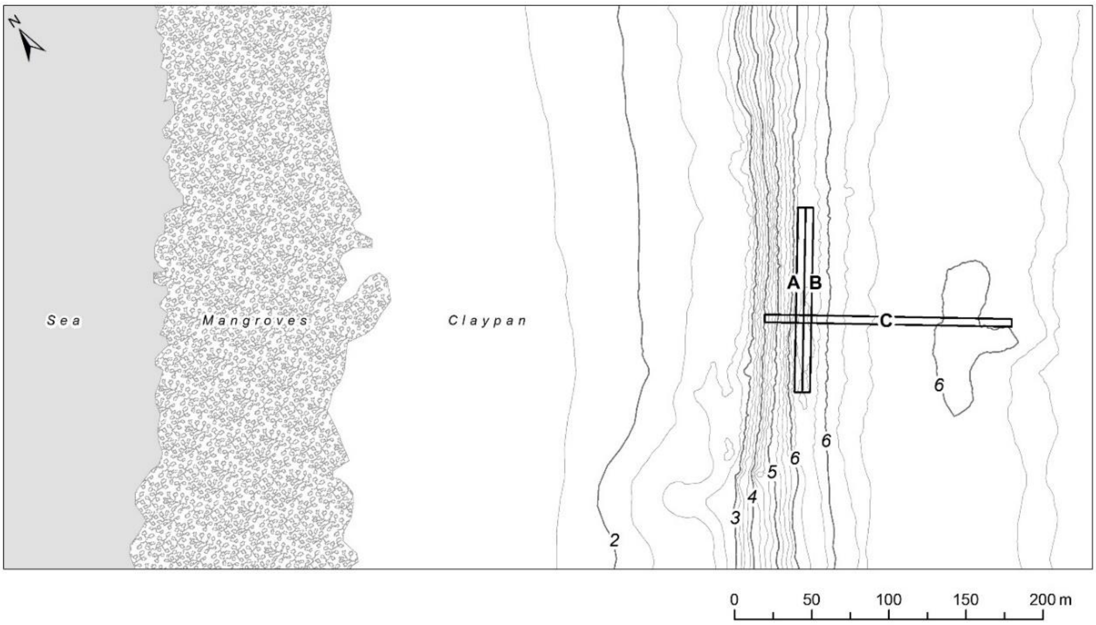

Figure 4.11 **Geophysical Transects at Thundiy (map prepared by Lincoln Steinberger and Sean Ulm 2015).**

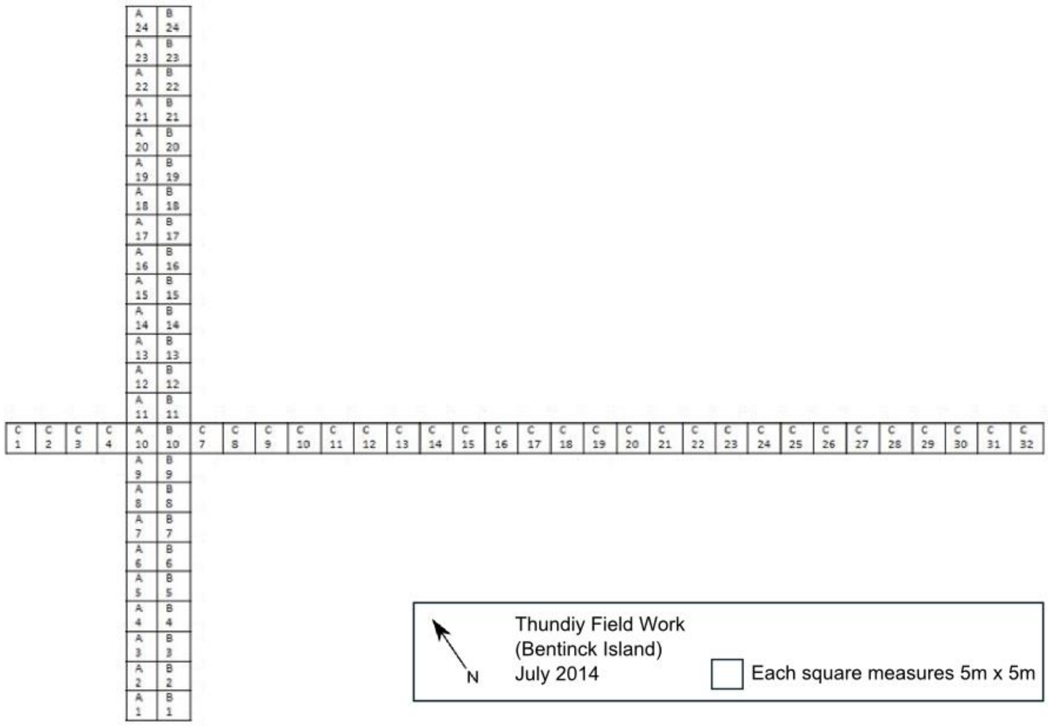

Figure 4.12 **Geophysical survey transects at Thundiy on Bentinck Island showing the unique letter and number assigned to each square.**

Previously published studies (as reviewed in Chapter 2) showed the importance of rigorous grid control, and the problems which can occur when this is not achieved. By pegging out every 5m square using the RTK detailed grids were established. The RTK was also used to place survey pegs marking the electrical resistivity grids as discussed below in Section 4.5.2. The use of an RTK system allowed for topography to be mapped at the same time as the grids were established. Prior studies (as discussed in Chapter 2) showed the negative effects of failing to properly account for topographic influence in geophysical results. This survey was designed to negate those effects by creating detailed topographic data for Thundiy using the RTK, then topographically correcting the survey results.

4.5.1 GPR Survey

GPR lines were run the full length of Transects A-B and for 155m of the 160m Transect C; the survey started 5m in from the seaward end of the transect to avoid pandanus palms. Survey lines were run 50cm apart; the 30cm wide antenna would be pulled down the middle of the first 50cm section of the Transect and then back along the middle of the next 50cm (Figure 4.13).

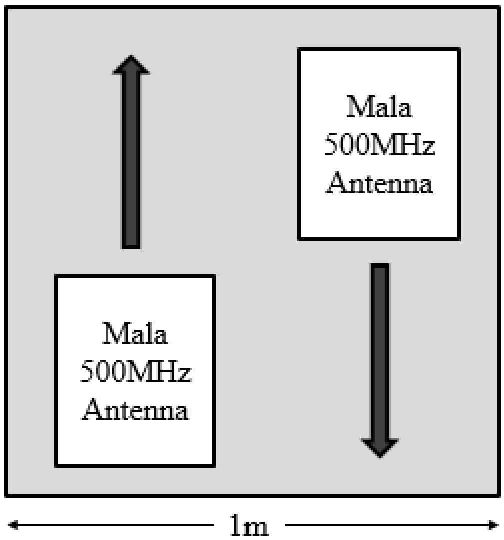

Figure 4.13 Diagram of GPR lines showing how the antenna was be situated for each line. Arrows indicate direction of travel for the antenna.

As survey guides, string lines were run every 1m to 1.5m separation along the Transects. These string lines, as well as further survey pegs (set up either as part of the main grid system, or as part of the electrical resistivity survey grids), were followed during surveying to establish straight and consistent survey lines. Fine line spacing

(0.5m) provided detailed results while the use of gridded transects in combination with the RTK provided accuracy in locating surveyed features within the ground. Surveying took place over three days. Prior to survey, the site was hand cleared using secateurs and cane knives to remove as much of the vegetation (mostly grass clumps) as possible. The remaining stubble was low enough to create a fairly smooth surface for the GPR to run over. This was done (as discussed in Section 3.3.1.1) to reduce coupling loss and coupling changes, as these would result in a reduction in signal penetration and the creation of anomalies in the data.

4.5.2 Electrical Resistivity Survey

Two long electrical resistivity survey lines were laid down the centre of Transect C to look at overall site composition. These survey lines had electrodes spaced at 1m (for a survey line of 27m) and 5m (for a survey line of 135m) and were situated at the seaward end of Transect C running over the rise of the ridge line, as this area is considered to be the main body of the shell matrix. As well as these two long survey lines, 5m square sub-grids were laid out within Transects A, B and C for the electrical resistivity. Each 5m resistivity survey grid was laid out with survey lines spaced at 1m intervals. Originally all six lines were to be surveyed, but, due to time constraints the choice was made to survey only the middle four lines (or 3m). Each electrical resistivity line was run with an electrode spacing of 25cm; with a total of 28 electrodes the lines reached to 6.75m, extending 1m beyond one end of the 5m grid and 75cm beyond the other end (Figure 4.14).

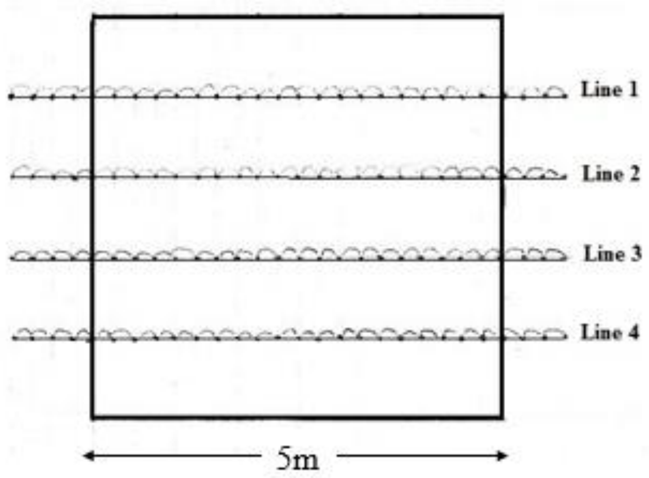

Figure 4.14 Electrical resistivity sub-grid showing placement of survey lines and electrodes.

Extending the survey lines beyond the survey grid allowed for the full 5m grid to be interpretable, as little can be gained from the edges of electrical resistivity pseudosections. Clark (1990:56) recommends extending the line of electrodes by at least one reading space beyond the desired grid to account for the way the readings are taken, as each reading falls at the midpoint of the four active electrodes. For the 25cm spacing applied throughout this study the first reading occurs 37.5cm in from the ends of the survey line.

For Transects A and B, the 5m² electrical resistivity survey grids were centred between the two transects and situated over the top of previous excavations. The excavations were 50cm square test pits laid out 50m apart. When the geophysical transects were superimposed over these excavations, electrical resistivity Grid 1 A-B was 10 transect sub-squares from Grid 2 A-B, while Grid 2 A-B fell nine transect sub-squares from Grid 3 A-B. Along Transect C four electrical resistivity surveys were conducted. These surveys were evenly spaced out along the Transect, occurring every 45m (Figure 4.15).

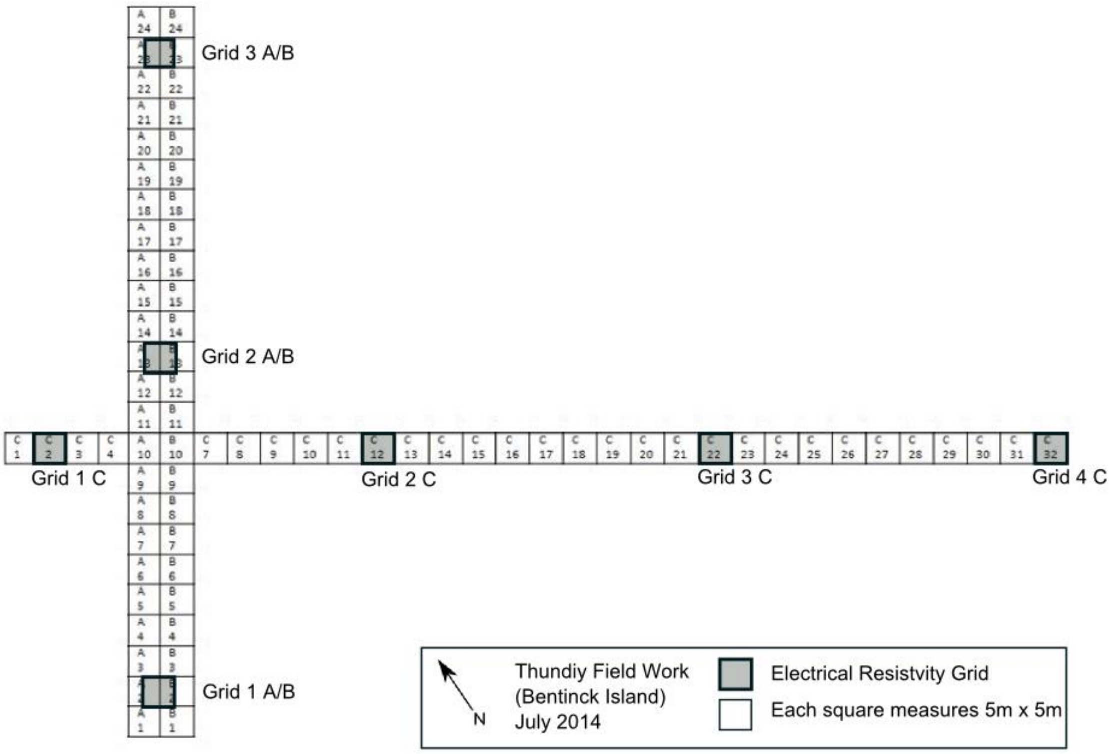

Figure 4.15 Geophysical survey transects at Thundiy on Bentinck Island, showing the location of the electrical resistivity sub-grids.

4.5.3 Ground Truthing

To maximise the information return generated by ground truthing, Hargrave (2006:274) recommends categorising anomalies to be investigated by priority and/or using a multistage approach. Anomalies are categorised based on their size, the degree of contrast and discreteness compared with the surrounding sediment, and their location and detection by multiple geophysical methods (Hargrave 2006:274). A multistage approach looks at first eliminating anomalies via less expensive and time consuming methods of inspection. The first step should be visual inspection, which is done by comparing the geophysical results with the site surface to establish if there are any obvious non-archaeological origins for recorded anomalies such as surface depressions, higher moisture content, natural rock deposits, tree roots or animal disturbances (Hargrave 2006:277). Inspection can also be conducted using a metal detector but this is site and method specific, and typically this is aimed at separating modern metal from prehistoric magnetic anomalies. Lastly, coring or shovel test pits can be used before full test excavations, but this is only recommended if the archaeologist is familiar with the natural sediment and cultural deposits present on-site in order to confirm their suitability (Hargrave 2006:278).

This study employed both a multistage approach and prioritising anomalies of interest for ground truthing. Previous excavation completed before the start of this study meant a substantial amount was already known about the chronostratigraphy of the midden deposit at Thundiy. Excavation squares had been placed along the ridge line down what was considered to be the main body of the shell deposit. The geophysical grid was placed over these squares to take advantage of the stratigraphic information they provided. Ground truthing was also undertaken at the edges of the shell matrix deposits. Two more test squares were excavated based on the geophysical results. The location of these squares were chosen based on regions of isolated low resistivity in the electrical resistivity survey results. These low resistivity anomalies were categorised as being of significant interest due to their contrast with surrounding sediment and their localised nature. Two anomalies were chosen to better understand the physical properties present on-site that were generating these low resistivity results. Originally three anomalies had been chosen for further investigation but one was quickly excluded based on a visual inspection. A tree stump with associated roots was located at the site of the third shallow, low resistance anomaly and it was concluded that the increased organic matter in this region was likely to be the source of the low resistance feature in the results. For the other two low resistance anomalies it was decided that one would undergo a 1m by 1m shovel test pit instead of 50cm by 50cm test excavation. This choice was made based on the Project Director's knowledge of the site, the Director considered the anomaly to be beyond the cultural shell matrix boundaries and therefore able to be investigated by shovel test pit. Although the anomaly was beyond the shell matrix it was still considered worth investigating to establish a better understanding of the electrical resistivity results for this area. The second anomaly was investigated via the standard 50cm by 50cm test excavation employed elsewhere on-site. The excavation and subsequent laboratory methods employed to examine the shell material are described in detail in the following section.

4.5.3.1 Excavation

A total of four excavations and one shovel test pit were conducted at Thundiy in order for this study to avoid the problems which arise from a failure to ground truth. These excavations were carried out in two stages. The first stage consisted of three 50cm by 50cm excavation squares (A, B and C). These squares were excavated in 2010 in order to assess site structure and history in the area considered to be the main body of the shell deposit (see Peck 2016). While these excavations were conducted before the commencement of this thesis, they provide vital information about the site's subsurface deposits. To utilise the information these excavations provided, the geophysical transects were established over their previous locations (Figure 4.16). The second stage of excavations (squares D and E) were undertaken in 2014 to test identified anomalies in the electrical resistivity results.

For the first round of excavation, Squares A, B and C were situated along the ridge line at 50m intervals; this area represented the densest region of shell accumulation visible at the surface. The squares were each excavated to approximately 60cm in 20 excavation units (XUs). Five points of elevation (one in each corner and one in the centre) were taken at the start and end of each XU using a dumpy level and stadia rod. Excavation forms were completed for each XU detailing the depth, the weight of the sediment removed, a Munsell Soil Color® Chart test (including Hue, Value/Chroma and description), a pH test, an associated photograph and a description of the sediment and features encountered including mapping the location of any objects removed during excavation. Objects (i.e. stone artefacts, charcoal or articulated bivalves) encountered during excavation were bagged separately, assigned a field specimen (FS) number and recorded on a FS log. The sediment removed from each XU was weighed then dry-sieved through a 2.3mm mesh. The sieving occurred at a short distance from the excavation, to prevent any air blown sediment contaminating lower XUs. Sieving was performed above a tarp, so the excavated sediment could be returned to the pit at the end and so it would not contaminate the local deposits. The sieve residue was assigned an FS number and retained, as was a sample (c.250g) of the sediment <3mm for further laboratory analyses. Each sample, object and sieve residue was double-bagged with multiple labels.

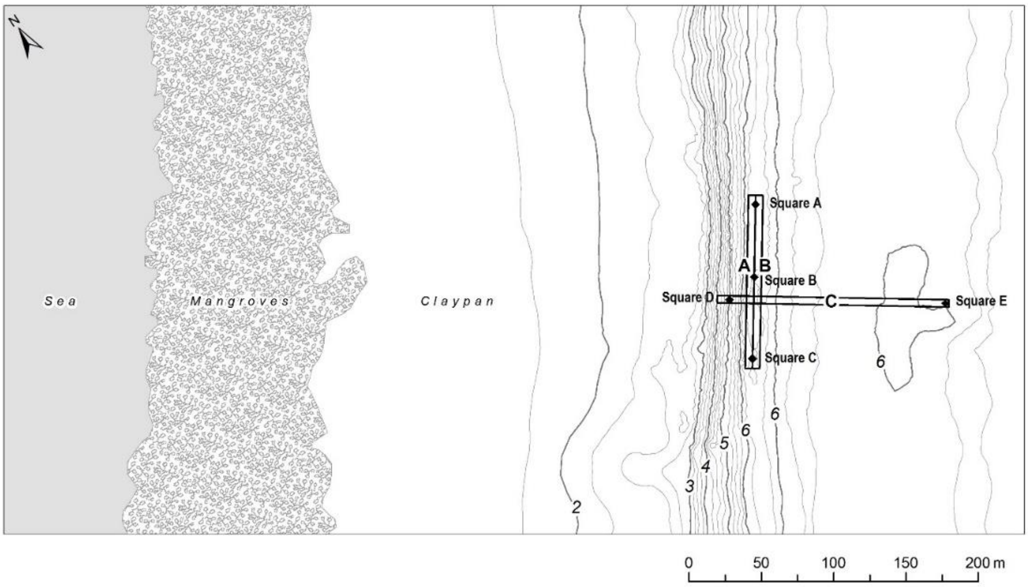

Figure 4.16 Excavation Squares A through E in relation to the Geophysical Transects at Thundiy (map prepared by Lincoln Steinberger 2015 modified by Selene Kenady 2016).

The second round of excavation consisted of Squares D and E. Square D was excavated in the same manner as Squares A-C. Square D was excavated over 17 XUs to a maximum depth of 47cm, terminating when bedrock was encountered. Square E was a 1m² shovel test pit made in a culturally sterile region at the edges of the shell matrix. Instead of employing XUs, this square was excavated by stratigraphic unit, of which there were three; excavation was discontinued at a depth of 1.15m. Samples were taken out of the pit wall starting at the surface and proceeding at 10cm intervals to 110cm, with a basal sample taken at (115cm). Objects and samples were treated the same as excavations A-D, but the sediment removed during excavation was not sieved or weighed.

4.5.3.2 Laboratory Analysis

All excavated material was analysed in the Tropical Archaeology Research Laboratory (TARL), Cairns. Sieve residue material was first wet-sieved with freshwater and air dried for at least 48 hours until completely dry before being sorted by hand (using tweezers) into generic type. These generic categories included shell, coral, stone artefacts, non-cultural stone, pumice, charcoal, pigment, crustacean carapace, bone and organic material. Shell and bone were further sorted into marine bivalve, marine gastropod, freshwater bivalve, freshwater gastropod, fish bone, and non-fish bone respectively. The sorted material was then assigned a new bag and label based on category.

Excavated shell material including fragments were identified to the lowest taxonomic level possible based on the surviving diagnostic characteristics present. The identification of shell and fish material to specific taxa was made by reference to the World Register of Marine Species (WoRMS 2014) and to Carpenter and Niem (1998). Initial basic training in recognising diagnostic characteristics was facilitated by the JCU Tropical Archaeology Research Laboratory (TARL) Shell Reference Collection as well as a laboratory manual created by Helene Peck (née Tomkins) using reference material from Claassen (1998), Colley (1990) and Starks (1901). The different taxon were then quantitatively analysed via minimum number of individuals (MNI), number of identified specimens (NISP) and shell weight per taxon. The MNI represents the minimum number of individual shellfish present in a collection, based on surviving non-repetitive diagnostic characteristics. The NISP count represents the total number of shells and shell fragments identified to a specific taxon. Shell weight per taxon is the weight of all the shell material allocated to each discrete taxa. Shell material was weighed on a Shimadzu ATY224 electronic balance to the nearest 0.1g for samples above 10g, while samples below were weighed on a Shimadzu UW2200H electronic balance to the nearest 0.0001g.

4.5.3.3 Radiocarbon Dating

Shell material from Squares A, B, C and D was sent to the University of Waikato Radiocarbon Dating Laboratory for Standard Radiometric (14C) and Accelerator Mass Spectrometry (AMS) dating. Three samples were also sent to ANSTO (Australian Nuclear Science and Technology Organisation) for AMS dating. See Table 4.1 for full details regarding the shell material for each excavation.

Radiocarbon dates obtained from shell material are affected by carbon reservoirs in the marine and estuarine environments in which the shell developed. These carbon reservoirs can vary markedly by region and can cause errors of up to several hundred years if not factored into the dating (Ulm 2006b). To enhance the accuracy of the radiocarbon dating calibrations for the shell material taken from Bentinck Island, local marine reservoir values were created for the Wellesley Islands. This was accomplished by dating live-collected shell from 1903 obtained from the Australia Museum archives (Rosendahl 2012). The shell material consisted of six articulated bivalves collected by Charles Hedley on Forsyth and Mornington Islands. Radiocarbon dates for Thundiy are reported in this thesis as calibrated dates (cal BP). Radiocarbon dates were calibrated in the University of Oxford's OxCal online radiocarbon calibration (Ramsey 2009), using the Marine 13 calibration dataset (Reimer *et al*. 2013) plus a local ΔR value of -49±102 (Rosendahl 2012).

Table 4.1 Radiocarbon dating results for Thundiy, Squares A-D.

Square	Dating Method	Laboratory Number	Shell Species	Depth (cm)	Calibrated Age in Years (cal BP)
A	C 14	Wk-32135	*Anadara granosa*	1.35	132
A	AMS	OZP-186	*Marcia hiantina*	1.35	133
A	C 14	Wk-32136	*Anadara granosa*	16.2	298
B	AMS	OZP-197	*Marcia hiantina*	1.25	104
B	AMS	Wk-34772	*Marcia hiantina*	17	510
B	AMS	Wk-28560	*Anadara granosa*	31.8	525
B	AMS	Wk-37498	*Marcia hiantina*	38.05	793
B	AMS	Wk-36175	*Marcia hiantina*	58.95	5039
C	AMS	OZP-187	*Marcia hiantina*	1.35	135
C	AMS	Wk-28561	*Anadara granosa*	31.4	747
C	AMS	Wk-36176	*Marcia hiantina*	43.2	4717
C	AMS	Wk-36177	*Gafrarium pectinatum*	58.05	4997
D	AMS	Wk-40103	*Gafrarium pectinatum*	35	5334

4.6 Field Site Results

The following sub-sections detail the results obtained from the excavation of Squares A through E (Section 4.6.1), and the geophysical surveys (see Section 4.6.2 for GPR results and Section 4.6.3 for electrical resistivity results).

4.6.1 Excavation

The results of the three original excavations (Squares A to C) were remarkably similar along the ridge. The squares were excavated to approximately 60cm and each consisted of a chronostratigraphic framework characterised by a layer of dense cultural shell at the surface overlaying natural beach ridge deposits with basal layer of consolidated beachrock material (Nagel *et al.* 2016). Figure 4.17 exhibits section photos for Thundiy excavation Squares A to C while Figures 4.18 to 4.20 show the sections diagrams for each square.

Figure 4.17 The east section photographs for Thundiy; Square A (left), B (middle) and C (right).

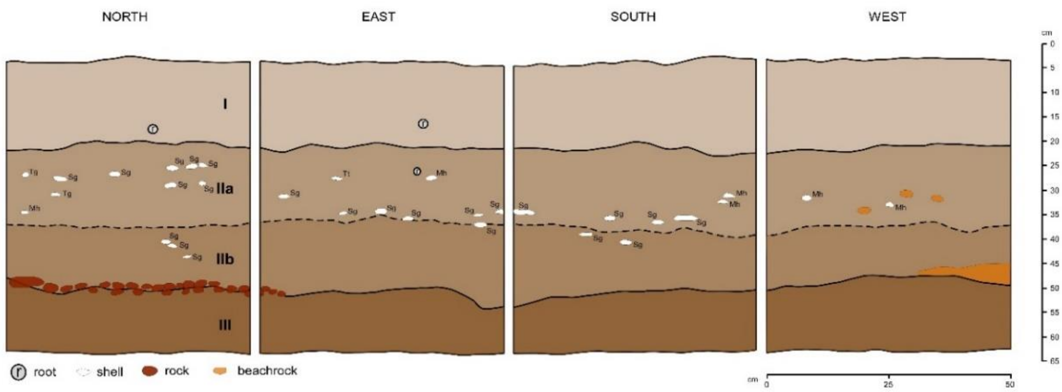

Figure 4.18 Thundiy sections diagram Square A (prepared by Michelle Langley and Sean Ulm).

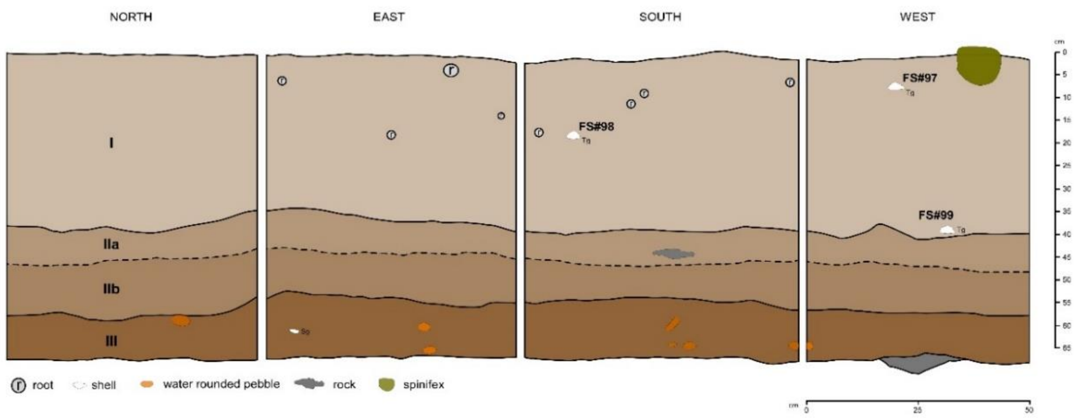

Figure 4.19 Thundiy sections diagram Square B (prepared by Michelle Langley and Sean Ulm).

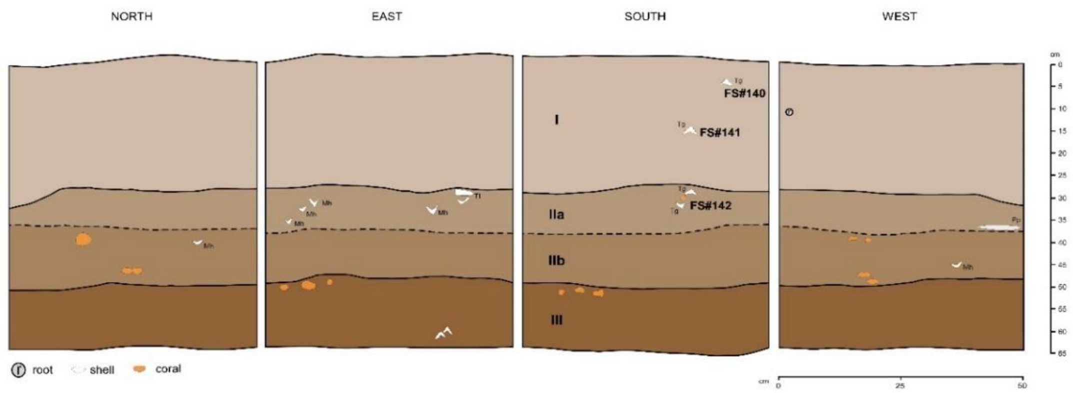

Figure 4.20 Thundiy sections diagram Square C (prepared by Michelle Langley and Sean Ulm).

Stratigraphic Unit I (SUI) represents the dense cultural shell matrix present at the surface, while SUIIa and SUIIb represent a transitional zone exhibiting a mixing of cultural shell material with underlying natural shell deposit material (Nagel *et al.* 2016). SUI exhibits well-preserved cultural shell material in a dark brown humic sediment. The midden material of SUI exhibits charcoal fragments, stone artefacts and bone fragments; this layer extends to 15cm for Square A, 35cm for Square B and 27cm for Square C. SUIIa is characterised by a continuation of the dark brown humic sediment present in the cultural matrix but with decreasing shell material present, this layer ranges in thickness from 15cm in Square A, and 5cm in Square B to 8cm in Square C (Peck 2016:127). Both SUI and SUIIa represent cultural shell midden material and are included in the volume estimates for the shell matrix (see Section 4.7). SUIIb exhibits a less humic sediment, filled with pisoliths and small (<10mm) gastropods indicative of naturally deposited beach ridge material. SUIII represents the natural underlying sediment for the site, consisting of sandy beach ridge material composed of shell grit with pebble and coral inclusions in a medium-grained siliciclastic sand (Nagel *et al.* 2016). Consolidated beachrock was found towards the base of the excavations. Beachrock is formed through consolidation of the nearshore sediments via a process of calcium carbonate cementation caused by the precipitation of carbonates in a zone with a fluctuating water table, such as a tidal zone or areas with alternations of wet and dry weather (Bird 2008:161).

The results for the squares excavated to ground truth two low resistivity anomalies (Squares D and E) were considerably different to the results obtained for Squares A, B and C. Excavation of Square D found a bowl shaped structure in the beachrock under a pisolith-rich beach ridge deposit (see Figure 4.21). The bowl-like feature in the rock was identified at 33.6cm below ground surface and continued to a depth of 55.8cm. As the interior of this bowl shaped feature matched the location, general size and shape of the low resistance anomaly being investigated (see Figure 4.35), it was concluded that it was likely to be associated with the anomaly. The basal beachrock will undoubtedly be more resistant than the overlaying sediment, which includes lower resistance features such as organic matter and added water content (both from morning dew and the estuarine water being applied to the electrodes to reduce contact resistance). The lower resistance of the overlaying sediment combined with the bowl-shaped indent in the surface of the beachrock at this specific location make it likely that the overlaying sediment is the source of the low resistance feature in the resistivity results, while the beachrock is the source of the high resistance values.

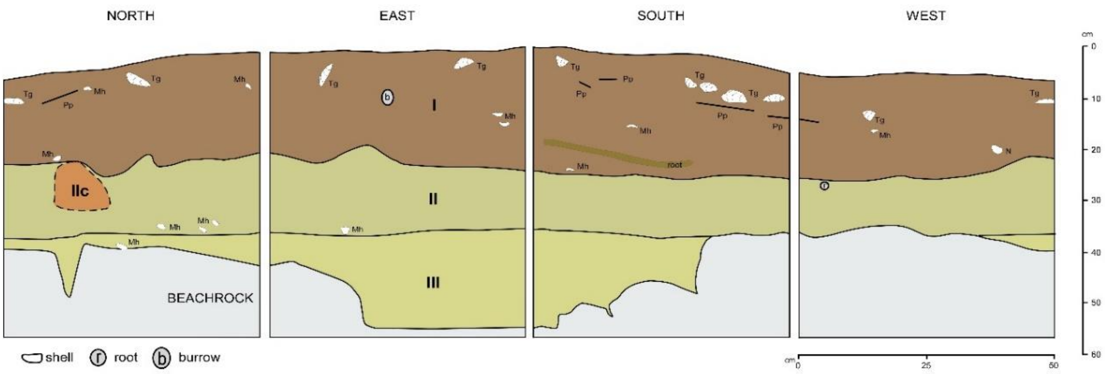

Figure 4.21 Thundiy sections diagram Square D showing the bowl-shaped depression in the beachrock (prepared by Michelle Langley and Sean Ulm).

Square E, the 1m by 1m shovel test pit, was placed beyond the end of the midden deposits. The low resistance anomaly (from 55cm to 100cm depth) identified in the electrical resistivity results (see Figure 4.36) was found to coincide with an area of abundant fine pisoliths which were retaining more moisture than the sediment above. The excavation found that from around 60cm down the pisolith numbers noticeably increased and the sediment became moist to the touch, this extended until the base of the square at 115cm (see Figure 4.22). The increased water content in these sediments will have lowered the resistance values of the sediment present and can therefore reasonably be interpreted as the source of the low resistance anomaly in the resistivity pseudosection.

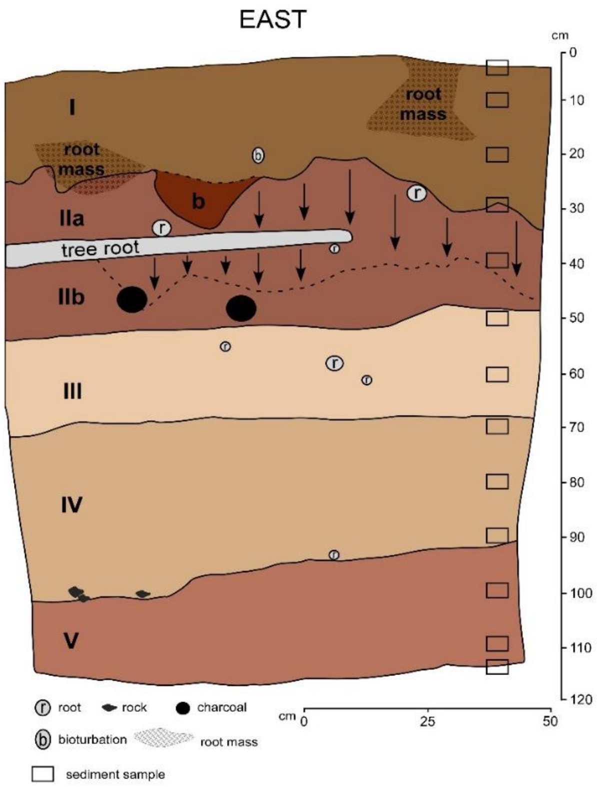

Figure 4.22 Thundiy sections diagram Square E, SUIII, IV and V were characterised by increasing pisolith numbers and moisture levels with depth (prepared by Michelle Langley and Daniel Rosendahl).

4.6.1.1 Radiocarbon Dating

Radiocarbon dating showed consistent chronostratigraphic relationships between excavations for Squares A to C. Surface deposits (SUI) dated to around 130 cal BP, with dates below ranging back to 700-800 cal BP for the cultural deposits (SUI and SUIIa). Below 40cm (SUIIb) there is a sharp stratigraphic disjunction where the cultural deposits end and the dates for the underlying natural deposits jump to 4000-5000 cal BP (see Figure 4.23). Based on these dates, the cultural shell deposits for Thundiy represent a recent initiation of cultural occupation on a much older landscape, with the natural beach ridge deposits having been formed >3,000 years prior (Nagel *et al.* 2016). The shell embedded in the beachrock of Square D gave a slightly older age of approximately 5334cal BP.

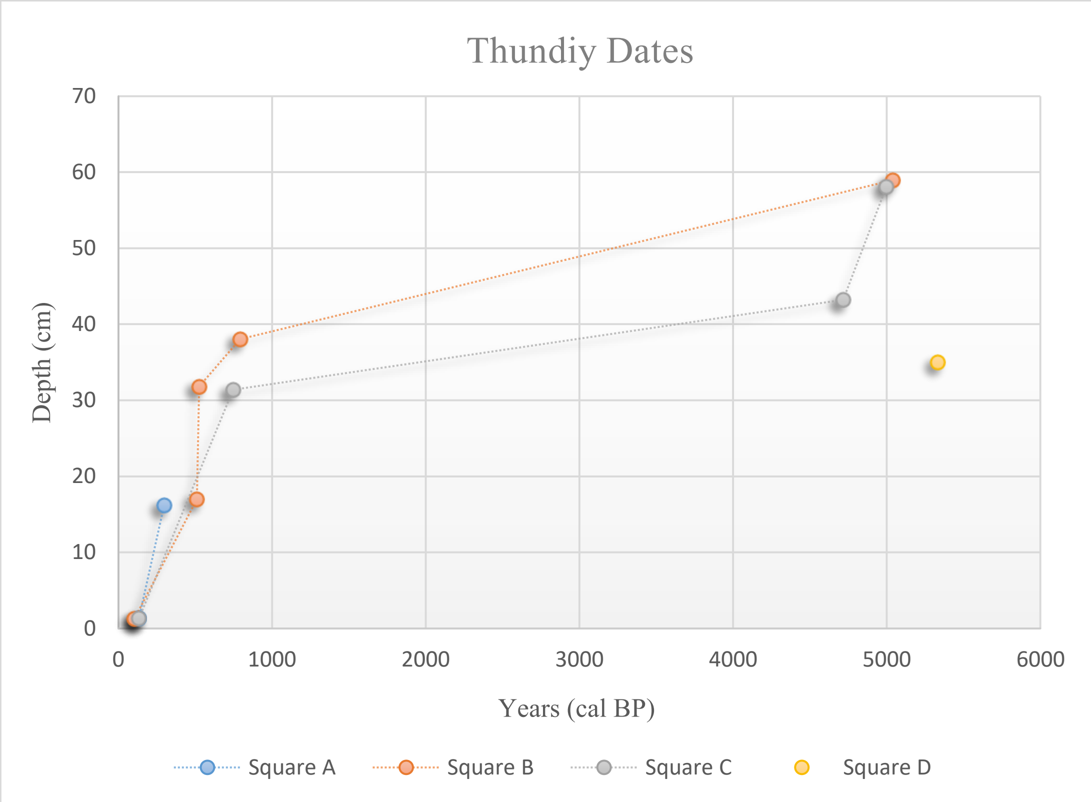

Figure 4.23 Age-depth relationship of calibrated radiocarbon ages for Thundiy from squares A, B, C and D; the Square D date represents a different age-depth relationship (being the only date over 1,000cal BP taken from below 40cm depth) as the square was excavated at the seaward base of the ridgeline where less deposits had accumulated.

4.6.1.2 Laboratory Analysis

Laboratory analysis found molluscs made up 81.7% of the sieve residue (by weight) retrieved from Square A. The sieve residue itself made up 21% (by weight) of the total mass of excavated material from the cultural units (XU1-12) of Square A. For Square B, sieve residue made up 28% of the total excavated cultural material (from XU1-13), of which molluscan shell made up 85.39%. For Square C, 27.5% of the total excavated cultural mass was retained as sieve residue (from XU1-12) of which 87.89% was molluscan shell (Peck 2016). The edible shell material for Squares A, B and C was dominated by *Marcia hiantina*. Though *M. hiantina* was found to dominate the assemblage at Thundiy, an analysis of the matrix by chronological period found the focus on particular shell species varied through time (see Figures 4.24 to 4.26). The chronological periods for this analysis were defined based on calibrated radiocarbon dates and stratigraphic units.

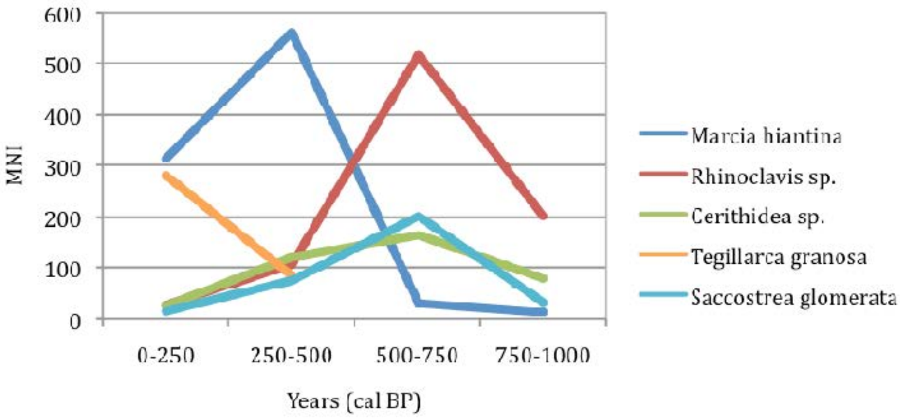

Figure 4.24 Square A, top 5 mollusc taxa by MNI per 250-year period (Peck 2016:155).

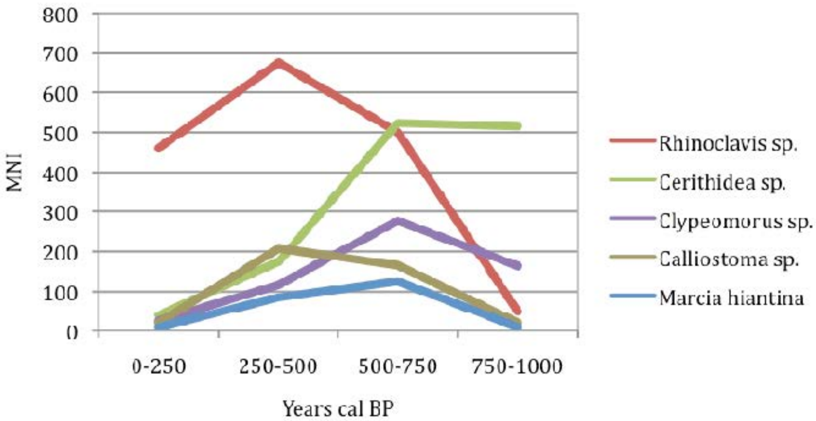

Figure 4.25 Square B, top 5 mollusc taxa by MNI per 250-year period (Peck 2016:155).

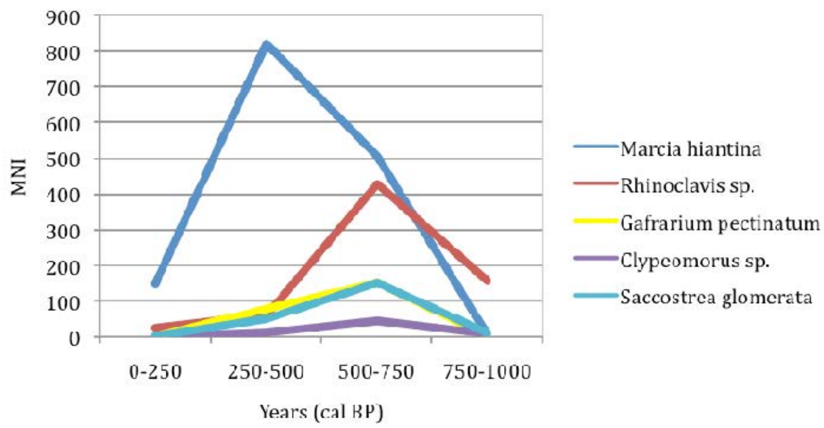

Figure 4.26 Square C, top 5 mollusc taxa by MNI per 250-year period (Peck 2016:155).

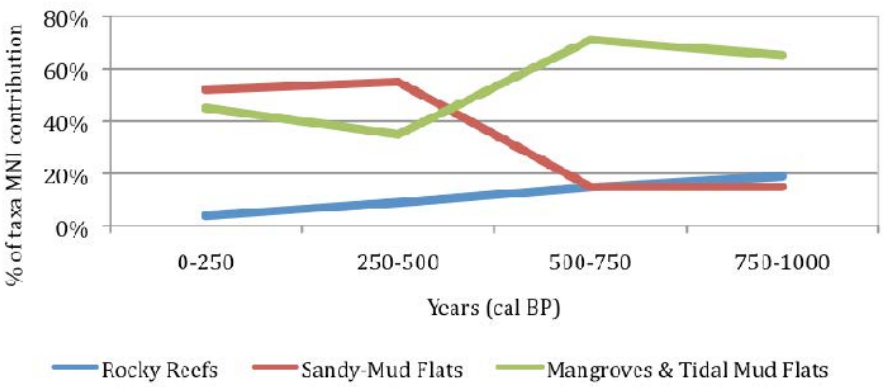

Figure 4.27 Squares A to C percentage of species by MNI collected by environmental habitat per 250-year period (Peck 2016:157).

Further analysis shows the environmental habitat from which shell species were gathered also changed through time, with species from the sandy-mud zone increasing while mangrove species decreased (see Figure 4.27). *M. hiantina*, the dominant species present in the assemblage (a sandy-mud zone species), shows an increasing percentage contribution to the overall assemblage through time though it declines in overall numbers being exploited. This trend in declining *M. hiantina* numbers is indicative of the overall trend seen at Thundiy, which indicates the site was most actively occupied during the periods covering 500-750cal BP and 250-500cal BP, with site use scaling back in the last 250 years.

4.6.2 Ground-Penetrating Radar Results

The GPR results for Transects A-B (see Figures 4.28 to 4.32) show a distinctive planar reflection of high amplitude from the surface to a depth of 60-80cm. This high amplitude response is still prevalent after *background removal* was employed during processing to minimise the horizontal banding commonly produced at the ground/surface interface in radar profiles, thus it is considered an actual subsurface feature and not just noise. This feature matches well with the cultural shell deposits documented during excavation of Squares A to C in Stratigraphic Units SUI and SUIIa. The planar reflection at the surface was therefore interpreted as representing the cultural shell matrix present on site and the base of this feature was ‘picked’ and exported to ArcGIS for the creation of volume calculations and 3D models.

In Transects A-B a separate high amplitude planar reflection off a subsurface linear interface, is visible at a depth of approximately 1.1m. This second planar reflection is located in the region of the basal beachrock present below sedimentary unit SUIII, and was interpreted as representing this feature. This reflection was also ‘picked’ and exported to ArcGIS for processing. The reflections from this planar feature were less definitive in Transect B than in Transect A. Transect A was situated on the seaward side of the ridge covering the last of the slope up to the peak of the ridge, while Transect B was situated right on the peak of the ridgeline. Perhaps the slight change in the surface angle between Transects A and B was responsible for producing a scattering of the radar waves off the subsurface planar feature, or perhaps the change in RDP was less definitive on top of the ridge.

The profiles are presented below in the Reflexw colour scale *Gray1*, with marked duplicates highlighting the interpreted anomalies. While trees were scarce on site, there were some present, and where GPR lines ran past them their roots featured prominently in the results at times obscuring or disrupting the profile below them (see also Figure 4.29). As mentioned, the two high amplitude planar anomalies in Transects A-B were interpreted to be the cultural shell matrix (producing the high amplitude response at the surface) and the beachrock present on-site (producing the deeper planar response). After processing and interpretation, the two high amplitude response features from Transects A-B were ‘picked’ and then exported to the ArcGIS software separately for processing (see Figures 4.31 and 4.32).

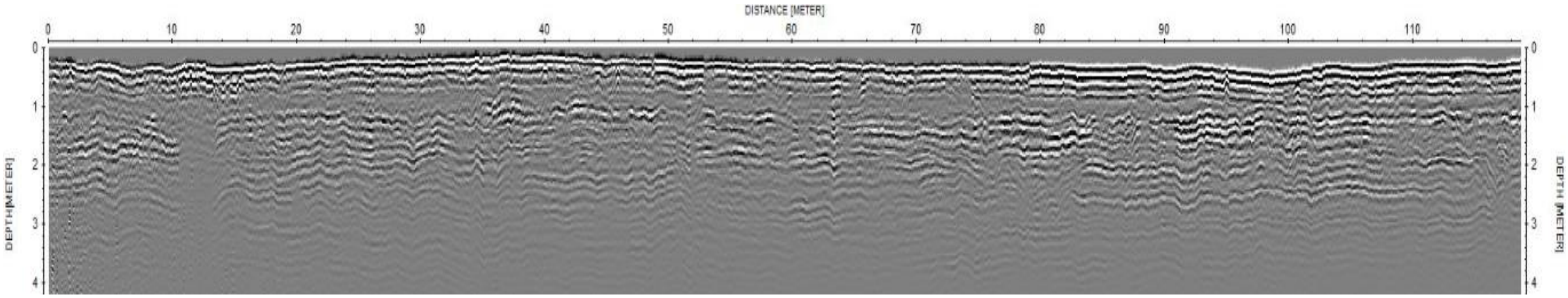

Figure 4.28 Thundiy GPR Line 4 of Transect A-B; this line was located in Transect A.

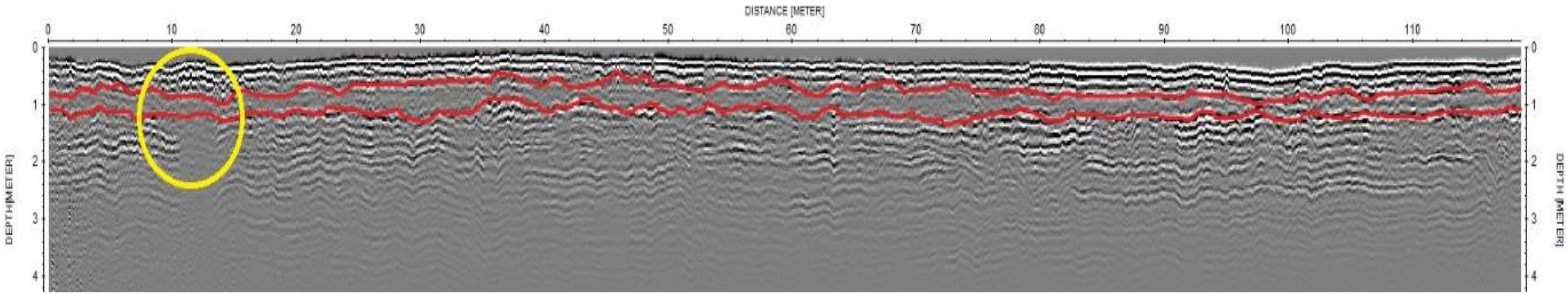

Figure 4.29 Thundiy interpreted GPR Line 4 of Transect A-B; red lines mark the two sets of distinct planar reflections at approximately 50cm and 100cm depth, while an area of prominent tree roots at the surface obscuring reflections below is circled in yellow.

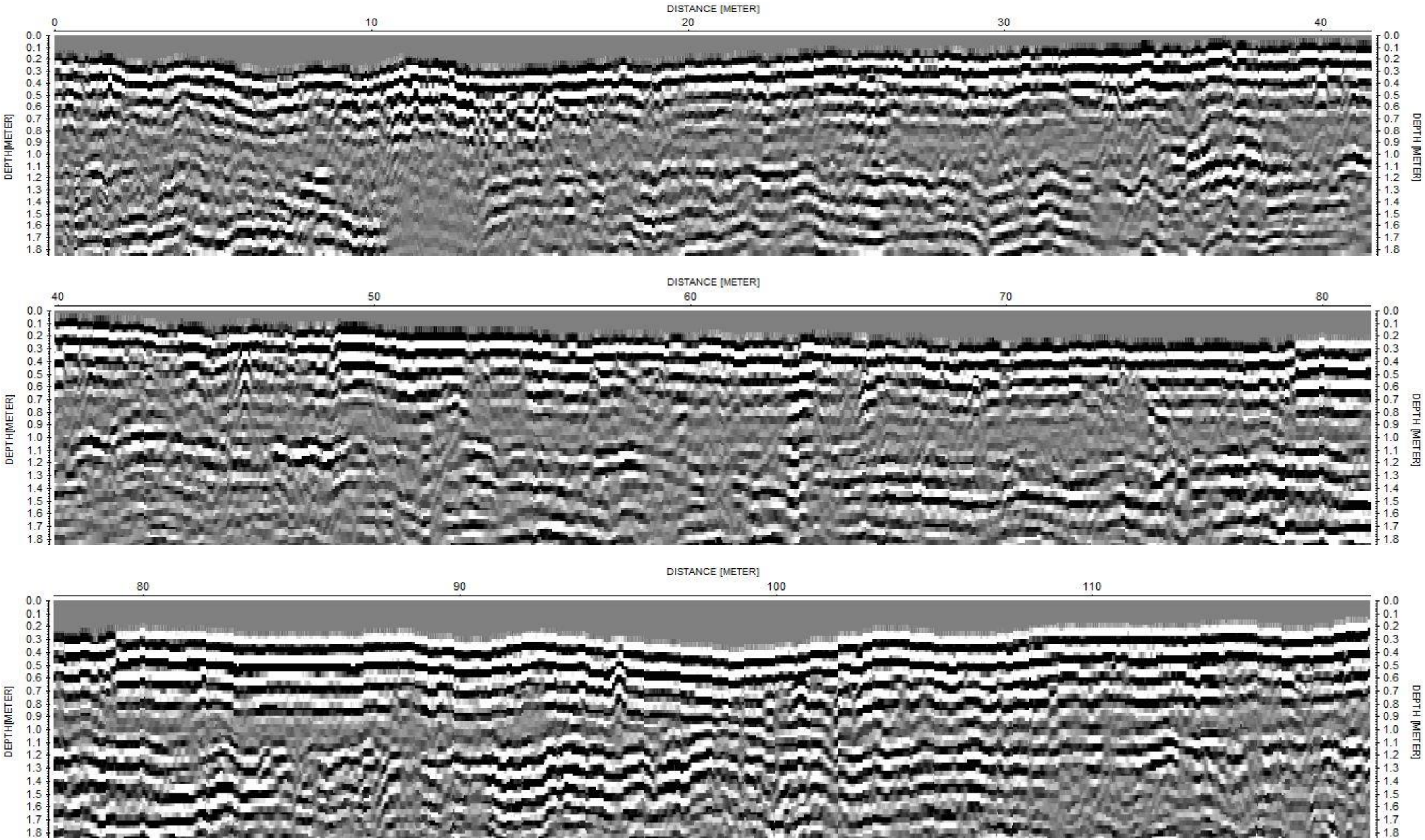

Figure 4.30 Detailed view of Thundiy GPR Line 4 of Transect A-B; 0m-40m (top), 40m-80m (middle) and 80m-120m (bottom).

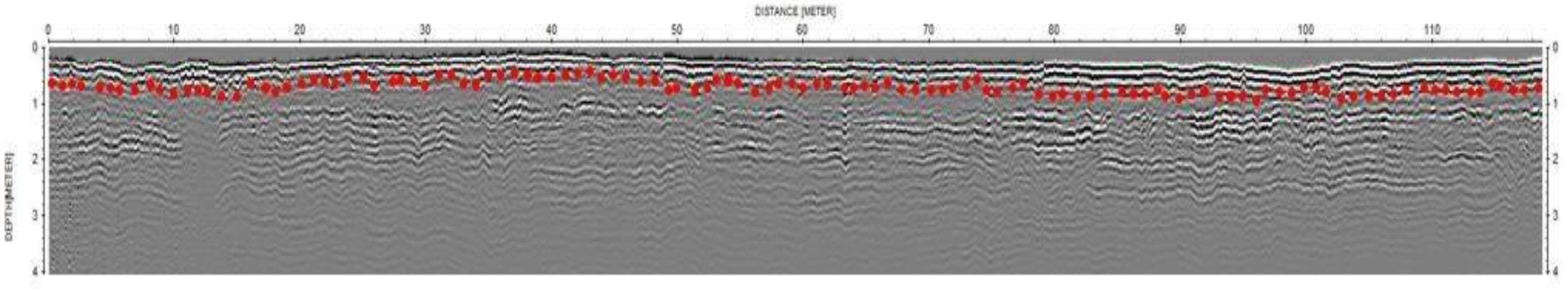

Figure 4.31 Thundiy GPR Line 3 of Transect A-B showing the 'picks' marking the lower boundary of the cultural shell deposit (original 'picks' re-marked for visibility in red). The tree root mass present from 10-12m was included in the estimation of lower boundary of the deposit.

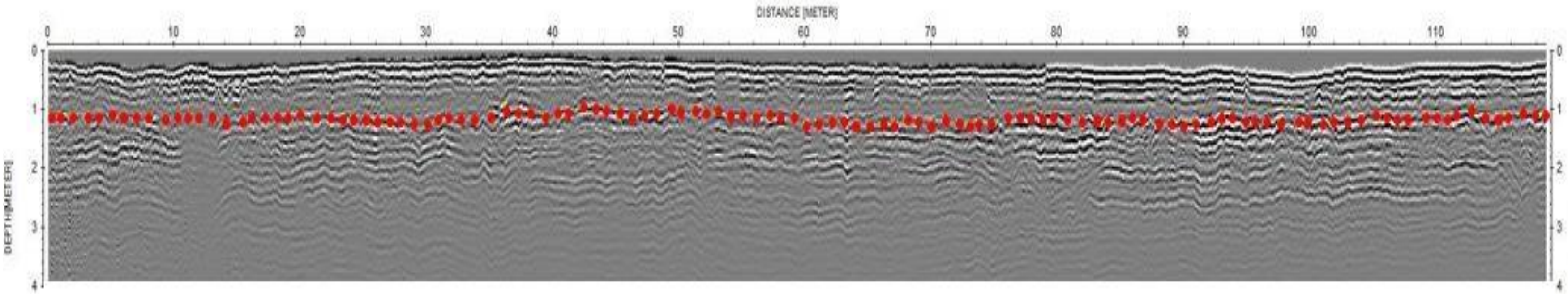

Figure 4.32 Thundiy GPR Line 3 of Transect A-B showing the 'picks' marking the upper boundary of the beachrock deposit (original 'picks' re-marked for visibility in red). Where the tree roots obscured the deposit from 10-12m the location of the deposit boundary was estimated.

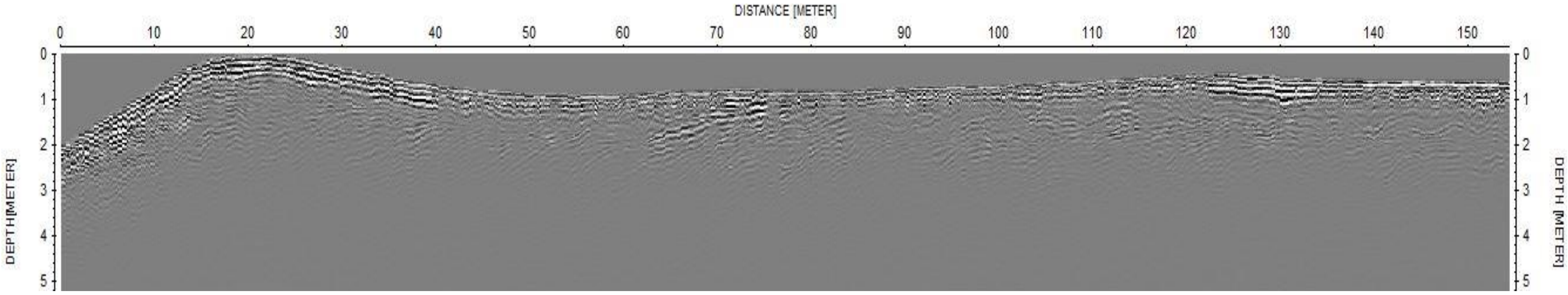

Figure 4.33 Thundiy GPR Line 1 of Transect C.

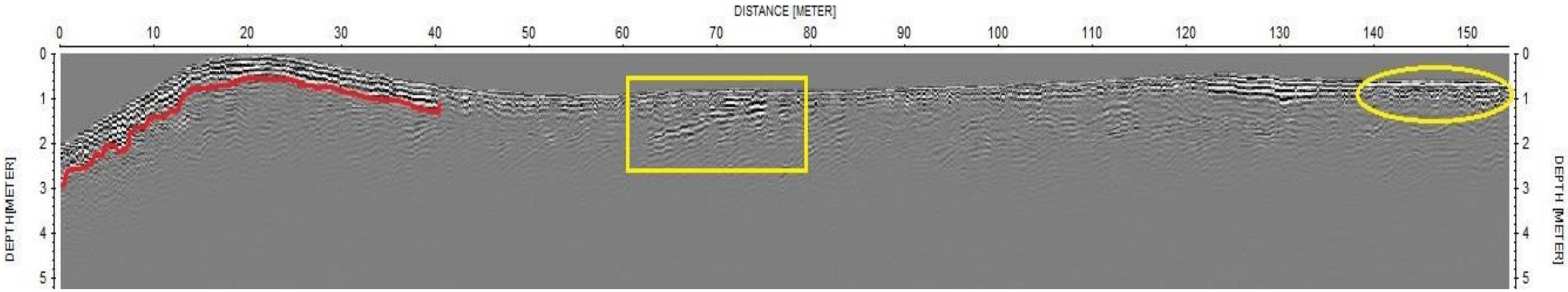

Figure 4.34 Thundiy interpreted GPR Line 1 of Transect C; a red line marks the high amplitude planar anomaly representing the shell matrix and beachrock combined, while an area of prominent tree roots at the surface is circled in yellow and the sloping planar interface interpreted as a palaeosurface is boxed in yellow.

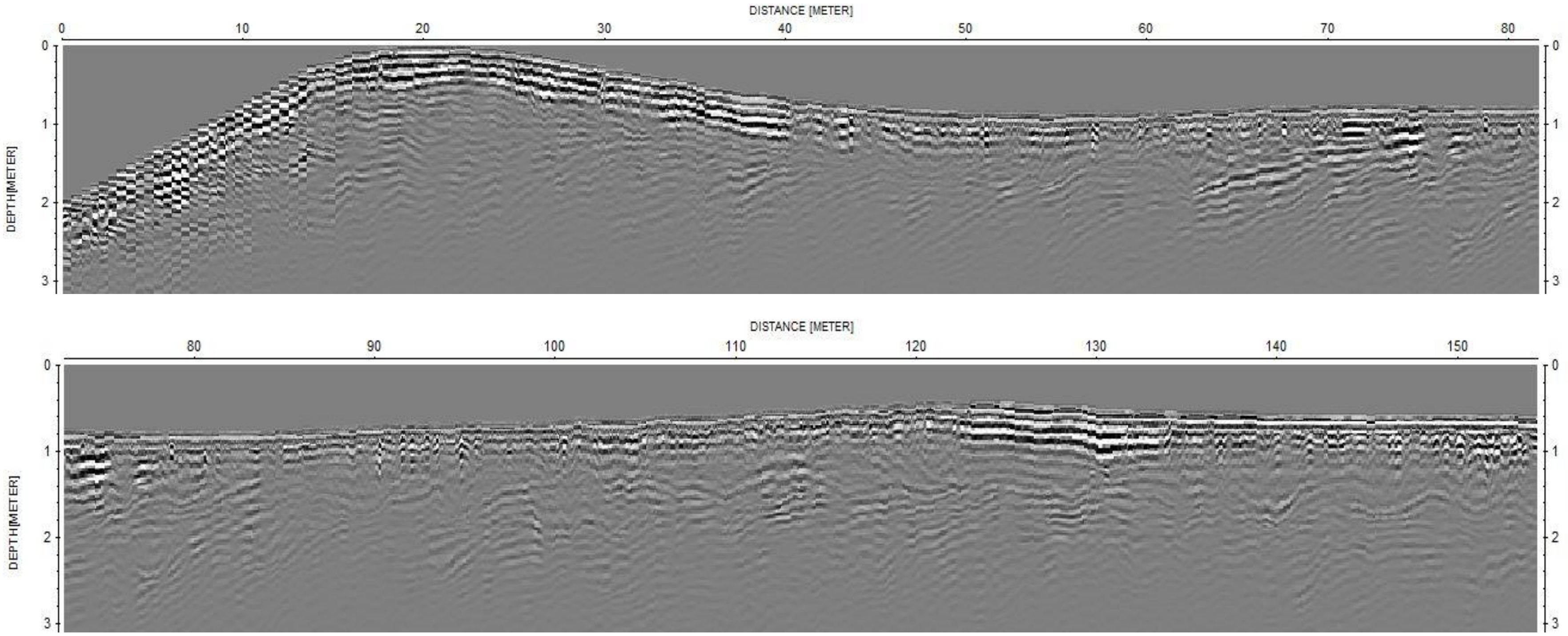

Figure 4.35 Detailed view of Thundiy GPR Line 1 of Transect C; 0-80m (top) and 80m-155m (bottom).

The results for Transect C were less distinctive. There was no clear difference in Transect C between the cultural deposits (SUI and SUIIa) and the beachrock (Below SUIII), so only a single deposit was 'picked'. The high amplitude planar response present in the results for Transect C extended to approximately 1m in depth and was interpreted as including all deposits above the beachrock, to be consistent with the interpretations of Transects A-B. The feature appeared to end at approximately 40m along the transect. Beyond this first 40m, intermittent areas of high amplitude response can been seen, particularly at 65-75m and again from 120m to the end of the profile (see Figures 4.33 and 4.35). The last 35m of high amplitude response in the profile were interpreted to be the result of tree roots as there were several large trees situated within and right next to Transect C in this region. The high amplitude response from 65-75m is more interesting however, as in this region there were no significant trees though there was a patch of denser shell material at the surface in this location. This anomaly also exhibits a sloping planar interface dipping away from the high amplitude response at the surface. This sloping interface looks like a potential palaeosurface for Thundiy, though excavation would be required to confirm this. The interface is prominently visible in the first 5 files of Transect C (or the first 2.5m of the north-eastern side) and less prominent, though still visible, for the remaining half of the transect, while the high amplitude patch at the surface is highly visible throughout all profiles for Transect C (see Appendix A).

4.6.3 Electrical Resistivity Results

The electrical resistivity struggled to make adequate contact with the highly resistant nature of the dry, sandy sediment present and as a result the data obtained was fairly inconclusive (see Figure 4.36). Dry sandy soils typically range from 80-1050Ω-m and while a reference to the resistivity range of beachrock could not be found, consolidated rocks have higher resistances than unconsolidated material; for example conglomerates range from 2,000-20,000Ω-m while sandstones range from 1-740,000,000Ω-m (Reynolds 2011:290). Due to the high resistance encountered, the results experienced high error margins. Even with significant editing during processing the results still exhibited high RMS percentages, ranging between 32% and 76% but mainly falling between 40-60%. The results from the survey grids show increased low resistivity (1-158Ω-m) at the surface as a result of the dry sandy soil being less resistant than the beachrock, combined with the estuarine water poured onto the electrodes to decrease the contact resistance. Approximately 0.5-1L of water was poured onto each electrode which caused pooling between electrodes (as they were only 25cm apart). With the two larger transect runs (down the middle of Transect C with electrodes 1m and 5m apart) these low resistivity values were averaged out of the results by the inversion.

The low resistance feature investigated via the excavation of Square D was a particularly prominent area of surface-based low resistivity (see Figure 4.37). The low resistivity anomaly investigated via Square E was not related to the surface, beginning in the profiles at a depth of 55cm. As one of the few areas of subsurface conductivity found on site, this anomaly was investigated to better understand the electrical resistivity results for Thundiy. As mentioned in Section 4.6.1, excavation found that this region of low resistivity was being caused by a pisolith rich sediment that was retaining moisture

The two longer survey lines down Transect C produced more interpretable results; see Figures 4.39 and 4.40 for the separate inversions and Figure 4.41 for the combined results. The water table can be confidently interpreted in these results, as being the source of the low resistance values at the base of the pseudosections presented in Figures 4.40 and 4.41. Saline groundwater has resistance values as low as 0.05Ω-m and for sedimentary rocks the resistivity values of pore-water present in the rock can be more important than the values of the host rock itself (Reynolds 2011:290). The close proximity of the sea (the seasonal tidal zone extends to the base of the site, only meters from the end of the profile) therefore makes it likely that the low resistance values (down to 1Ω-m) encountered below sea level in the longer survey line are regions of seawater saturated sediment and/or beachrock.

Interestingly, when the electrical resistivity pseudosections for Transect C are compared to the GPR results, a tentative correlation can be seen between the areas of higher resistance and the high amplitude planar response representing the shell matrix in the GPR results (see Figure 4.42). As evidenced by the results of Grid 1C and Square D, the higher resistance values present in the first 50m of the pseudosection are related to the beachrock. This makes it likely that the two areas of isolated higher resistance beyond the first 50m of the pseudosection are also beachrock; indicating these regions were previously nearshore zones where this rock is formed. This correlation can be seen at

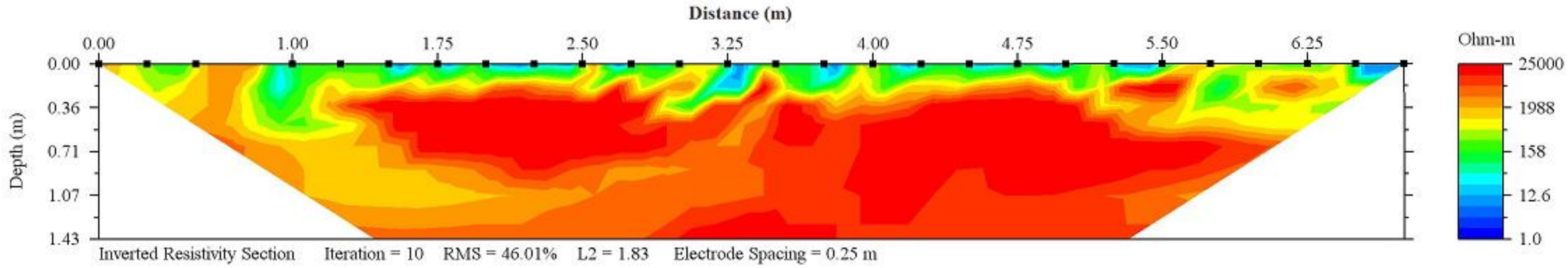

Figure 4.36 Thundiy electrical Resisitivty Grid 1A-B (Line 1) showing the highly resistant inversion results and high RMS error percentage for the resistivity surveys at Thundiy.

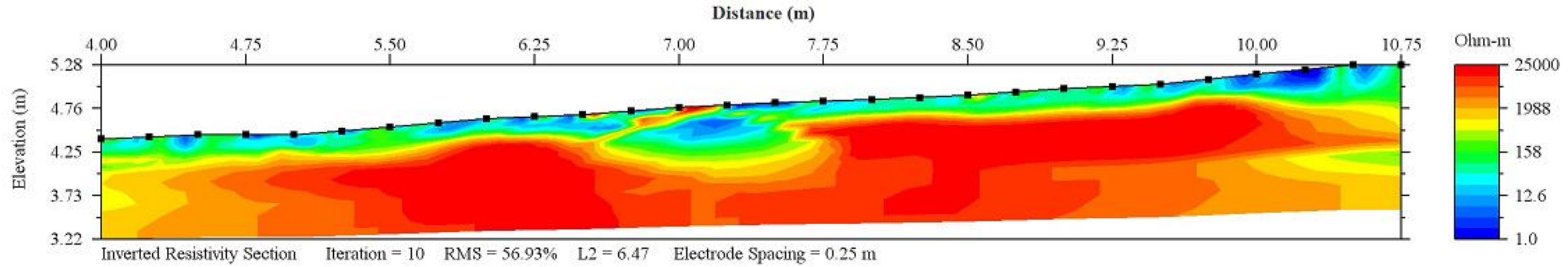

Figure 4.37 Thundiy electrical Resisitivty Grid 1C (Line 2) showing the low resistivity anomaly (at 7m) investigated via excavation Square D. Distance for this profile was altered during topographical correction and starts at 4m; this is the distance along Transect C the survey line was located.

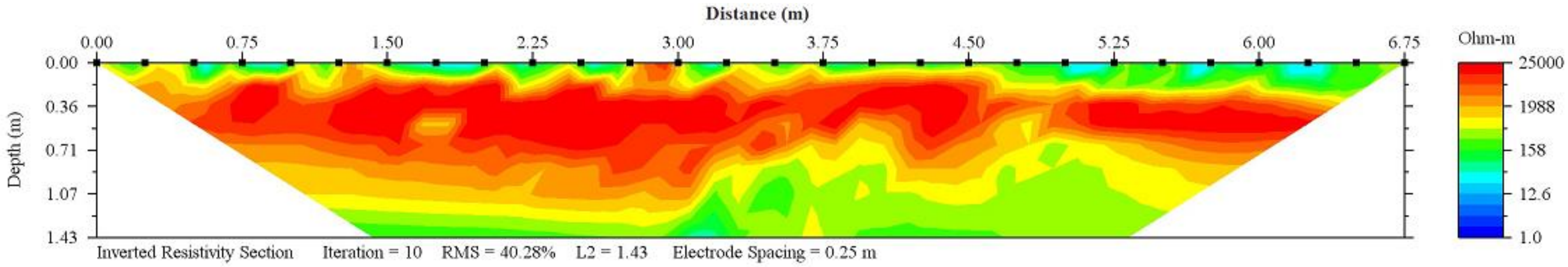

Figure 4.38 Thundiy electrical Resistivity Grid 4C (Line 3) showing the low resistivity anomaly (between 3-5m from a depth of around 50cm down) investigated via shovel test excavation Square E.

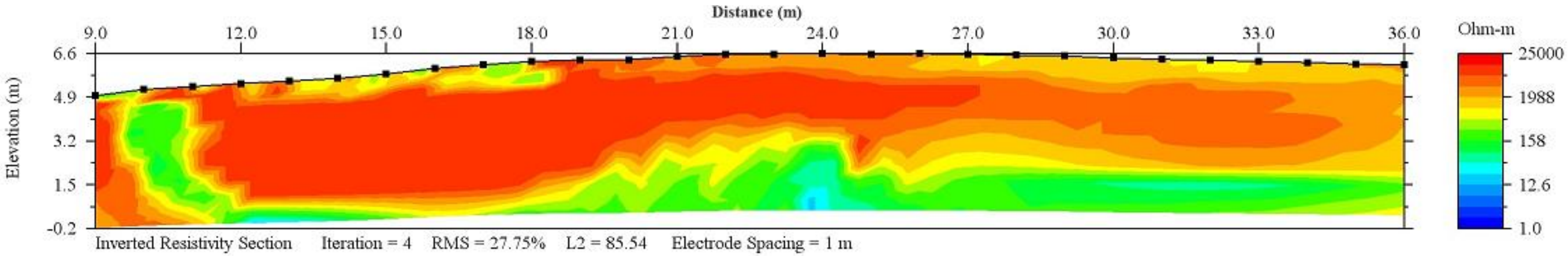

Figure 4.39 Thundiy electrical Resistivity survey line at 1m electrode spacing down the middle of Geophysical Transect C; topographically corrected with elevation based off sea level (0m being equal to sea level).

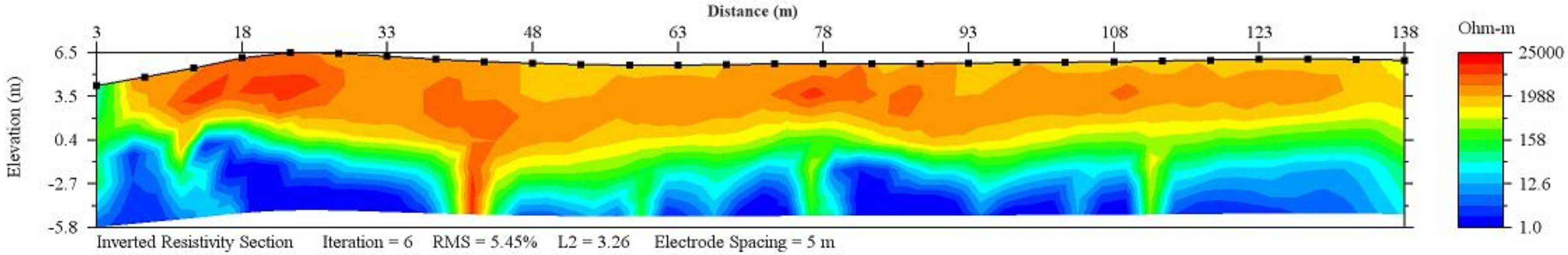

Figure 4.40 **Thundiy electrical Resistivity survey line at 5m electrode spacing down the middle of Geophysical Transect C; topographically corrected with elevation based off sea level (0m being equal to sea level).**

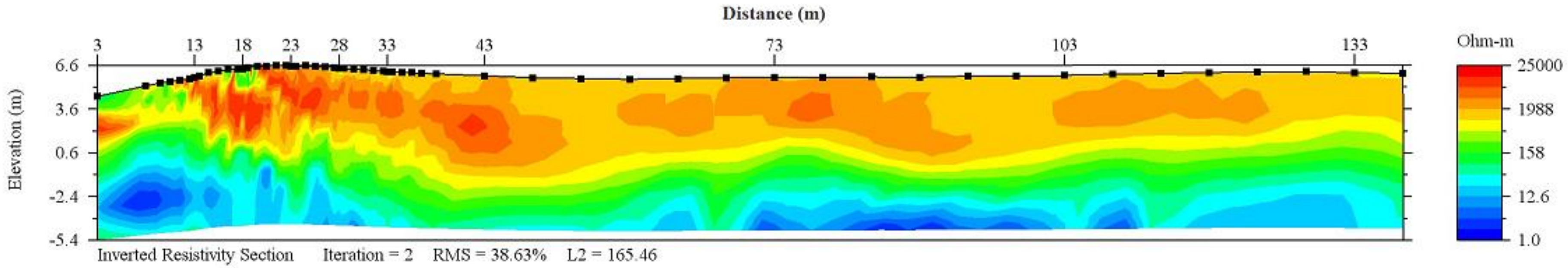

Figure 4.41 **Thundiy merged and topographically corrected 5m and 1m profiles; elevation is based off sea level (0m being equal to sea level).**

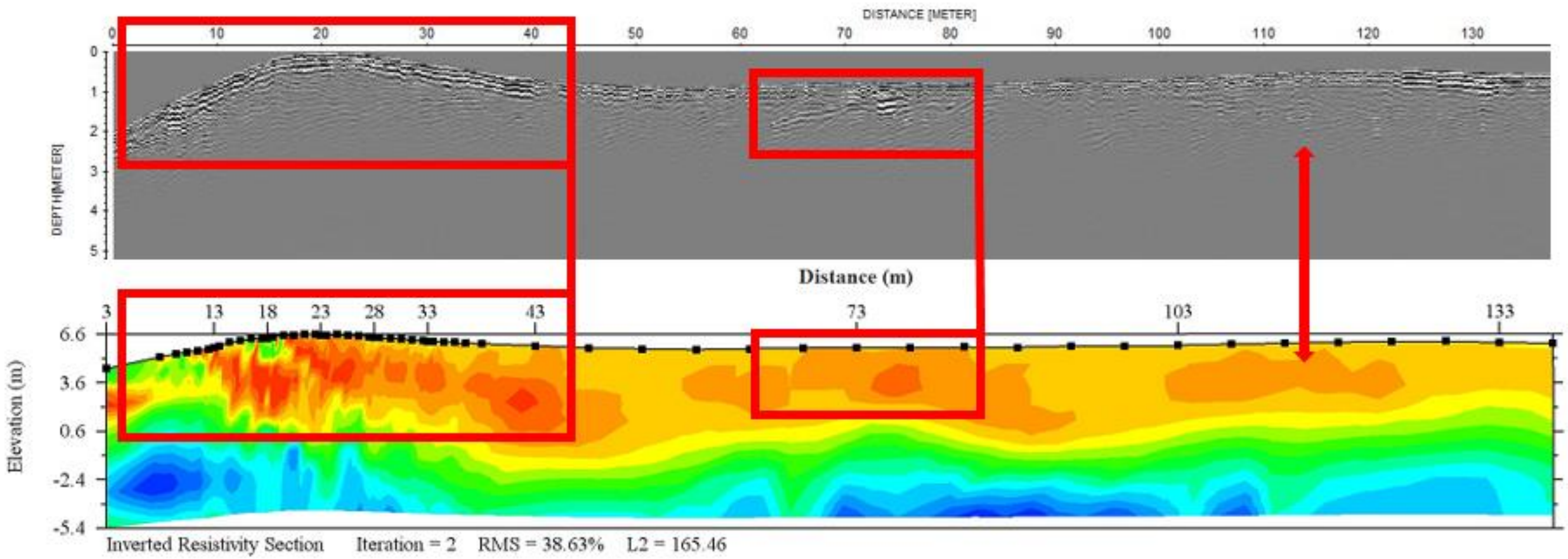

Figure 4.42 **Thundiy GPR and electrical resistivity survey lines of the middle of Transect C; highlighting (boxed in red) two corresponding areas of anomalies seen across both methods and indicating (red arrow) a third possible area of correlation.**

around 60-80m where there the high amplitude response thought to potentially represent a prior land surface and/or shell accumulation was located, and between 100-120m where an area of higher resistance can be seen in the electrical resistivity results which correlates to a region of the GPR results showing a much fainter reflection response. This reflection appears to be a possible planar feature sloping slightly shoreward similarly to the theorised palaeosurface visible between 60-80m in the survey lines. This potentially indicates another area of remanent palaeodunes although one that is not as reflective to the radar waves as the other potential palaeodune feature. The lesser reflection may be due to a change in the orientation of the dune surface causing the scattering of radar waves or it may represent a less abrupt change in the RDP values of the sediments, possibly indicating they are less consolidated or contain less shell material than the other two areas of correlating anomalies. Excavation would be required to verify these interpretations.

4.7 Three-Dimensional Mapping and Volume Results

By mapping the GPR survey results for Thundiy into ArcScene (via processing in ArcMap) a 3D model of the shell matrix deposits for Transects A, B and C was created (see Figures 4.43 and 4.44). The deposits were, as mentioned previously, separated between the cultural and natural for Transects A and B, however this was not possible for Transect C and so the deposits were mapped together. Volume estimates were also created in ArcScene (see Section 3.5.3 for details), and the total shell matrix volume for Transect C was calculated to be 108.27m³ while the total for Transects A-B was 1,104m³ with the cultural shell making up 637m³ of this larger deposit.

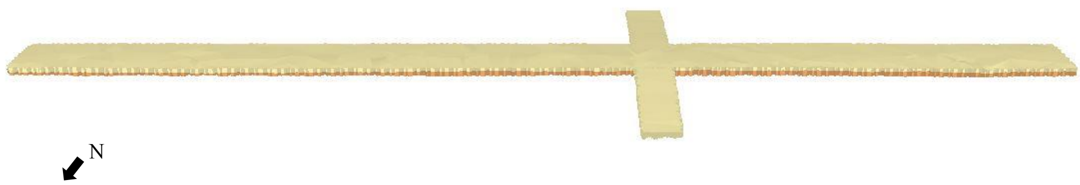

Figure 4.43 Thundiy shell matrix deposits for Transects A-B and C as viewed from the West looking to the East.

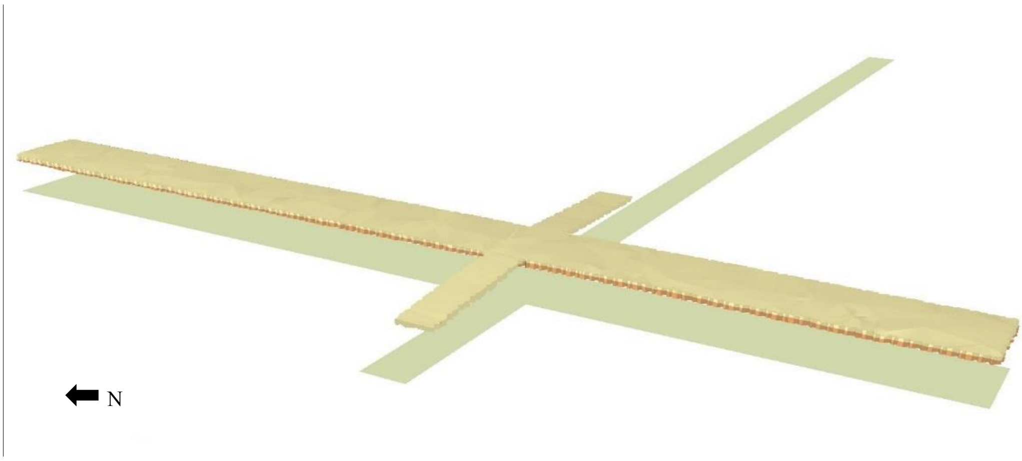

Figure 4. 44 Thundiy shell matrix deposits for Transects A-B and C as viewed from the Southwest. Underlying the deposits, the green cross underneath represents the full Transects A-B and C.

Based on the results for Transect C this would bring a total volume estimation for the larger site at Thundiy down to around 86,616m³ instead of the 240,000m³ initially estimated; as the buried matrix was found to end around 40m inland (see Figure 4.34) rather than extending the full 150m in which shell material can be seen on the surface.

In order to check these survey results against the real site conditions, the modelled volume estimates for Squares A to C were compared to the estimates produced based on the excavated material. These results are presented in Tables 4.2 and 4.3, along with the difference between the two estimates and a percentage error based on this difference (percentage error was calculated using the standard equation: actual value - experimental value ÷ actual value x 100). The cultural shell volume was calculated based on observations of the shell content, with midden material represented in SUI and SUIIa, the majority of shell was recovered by 36cm for Square A, 37cm for Square B and 30cm for Square C (Peck 2016:125). The total shell matrix for the excavation squares could only be calculated to the base of the excavations, which ended at an average of 61cm for Square A, 60.8cm for Square B, and 60cm for Square C. While the excavations for Squares A-C bottomed out in fine sandy sediments below the shell matrix (cultural and natural) they did not fully expose the beachrock thought to underlay the matrix, so these ground truthed estimates will be an underestimate of the true volume by an unknown margin. The beachrock was, however, fully exposed for Square D and here the volume calculations can be seen to match well, with a modelled volume of 0.22m³ compared with 0.23m³ for the ground truthed results. The curved basin in the beachrock in Square D meant the ground truthed volume had to be calculated by adding the volume for the top of the excavation (a rectangular prism) to the volume for the bottom of the excavation; which most closely matched half a sphere. The ground truthed volume for Square D can be expected to be close to the actual volume, but not exact, as the basin was not an exact hemisphere.

Table 4.2 Total shell matrix volume Thundiy, Squares A-D.

Thundiy Excavation	Total Shell Matrix Volume (m^3) Based on GPR Survey Results	Total Shell Matrix Volume (m^3) Based on Excavation	Modelling Compared to Ground Truthed Volume (m^3)	Error Percentage
Square A	0.22	0.15	+0.07	46% (Overestimate)
Square B	0.24	0.15	+0.09	60% (Overestimate)
Square C	0.23	0.15	+0.08	53% (Overestimate)
Square D	0.22	0.23	-0.01	4% (Underestimate)

Table 4.3 Cultural shell matrix volume Thundiy, Squares A-D.

Thundiy Excavation	Cultural Shell Matrix Volume (m^3) Based on GPR Survey Results	Cultural Shell Matrix Volume (m^3) Based on Excavation	Modelling Compared to Ground Truthed Volume (m^3)	Error Percentage
Square A	0.12	0.09	+0.03	33% (Overestimate)
Square B	0.13	0.09	+0.04	44% (Overestimate)
Square C	0.11	0.07	+0.04	44% (Overestimate)

All the modelled volume results based on the GPR survey (except the one for Square D) overestimate the deposits compared to the results calculated from the excavations. The total excavated volume for Squares A-C was further overestimated than the results for the cultural shell, but this is to be expected as it was known the excavation results were an underestimation due to the beachrock not being totally exposed. The results for Square D indicate the modelled results for the total shell matrix volume may be closer to the actual in-ground matrix than the results from Squares A-C imply.

The significant overestimation of the volume results for the cultural shell in Squares A-C indicated it was likely the ‘picks’ had been inaccurately placed on the profiles. A review of the profiles and ‘pick’ placements showed the ‘picks’ had indeed been placed on the first multiple instead of the first true reflection. Multiple reflections (or multiples) occur when the radar wave reflects back and forth between the surface and a subsurface layer (Conyers 2004:126). The volume estimate generated from the GPR survey compared to the excavation results shows the ‘picks’ were off by an average of 15cm, which due to the scale of the profile was the difference between one reflection and the next. This further implies the ‘picks’ were placed on the first multiple reflection rather than on the true shell deposit reflection. As can be seen from Figure 4.45 while this was visually a small and easy mistake to make, it had a significant impact on the results.

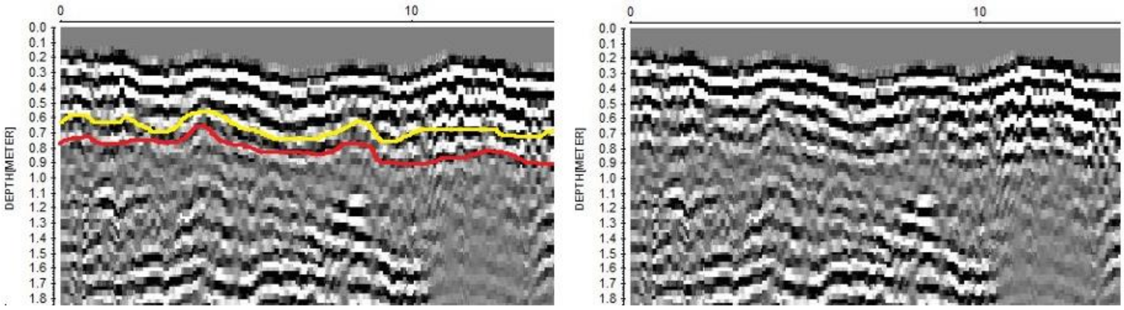

Figure 4.45 Extract of line 4 (Transects A-B) at Thundiy showing the placement of the ‘picks’ marked in red and the placement of the actual shell deposit marked in yellow. An unedited extract of line 4 is provided for visual comparison.

The ‘picks’ were recreated based on this information, and were now placed above the first multiple reflection. These results were then processed in ArcScene, with volume estimates and 3D models being created from them. The results showed a large improvement in the relation between the volume estimates generated from the GPR results and those generated from excavation. The new volume estimates exactly matched the excavation estimates from Squares B and C, while underestimating the deposits of Square A by only 11% (see Table 4.4). These new results created an overall volume estimation of 385.92m³ for the cultural shell of Transects A-B, making the total volume estimation for the cultural shell over the larger site at Thundiy 51,454.71m³. These new results produced little change in the overall 3D model of the deposits (see Figure 4.46). Though now the cultural shell layer is thinner over Transects A-B (see Figure 4.47).

Table 4.4 Re-picked cultural shell matrix volume Thundiy, Squares A-D.

Thundiy Excavation	Cultural Shell Matrix Volume (m^3) Based on GPR Survey Results	Cultural Shell Matrix Volume (m^3) Based on Excavation	Modelling Compared to Ground Truthed Volume (m^3)	Error Percentage
Square A	0.08	0.09	-0.01	11% (Underestimate)
Square B	0.09	0.09	0.0	0%
Square C	0.07	0.07	0.0	0%

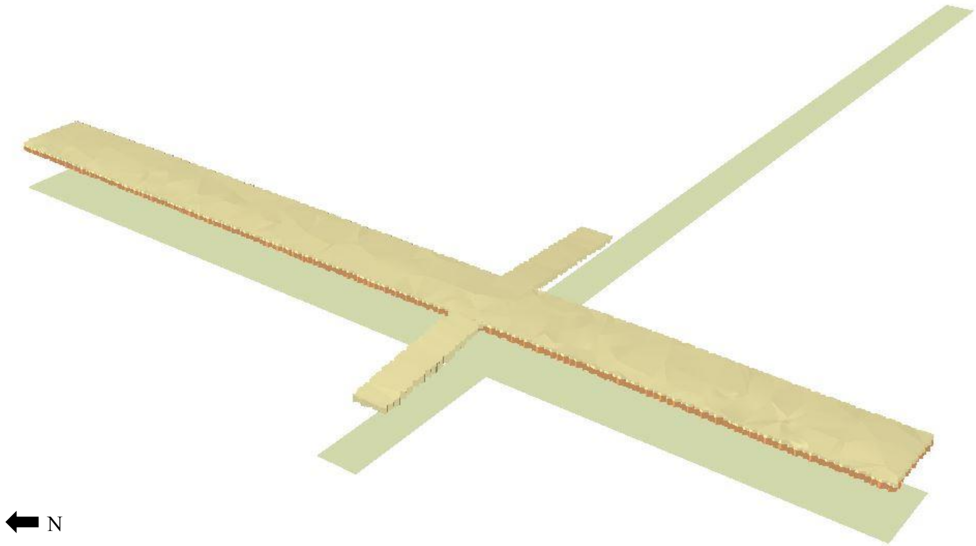

Figure 4.46 Thundiy reworked shell matrix deposits for Transects A-B and C as viewed from the South-West. Underlying the deposits, the green cross underneath represents the full Transects A-B and C.

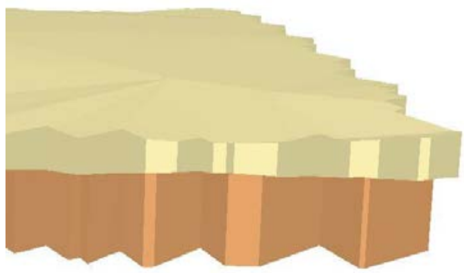

Figure 4.47 Close up of North-West corner of Transects A-B showing modelled shell matrix deposits in detail.

Confidence intervals were then calculated for the mean error percentages exhibited during modelling of the volume estimates (all confidence intervals presented have been rounded to the nearest 0.5%). Confidence intervals for the mean error were produced using the standard method of $\bar{X} \pm t\frac{s}{\sqrt{n}}$ in which the sample standard deviation (s) is divided by the square root of the sample size to create a standard error, which is then multiplied by the t value (t), obtained from a t value chart, to obtain the margin of error which is then applied to the sample mean ($\bar{X}$). For a 95% confidence level, the confidence intervals on the error margins produced by the Thundiy results are 3.5%±7% (a range of -3.5% to 10.5%) when examining the results for the corrected 'picks' and 19.5%±17% (2.5% to 36.5%) if the original misplaced 'pick' results are included. The error percentages for the total shell matrix for Squares A to C were left out of these calculations as they were not accurately ground truthed (with the excavation ending before fully exposing the beachrock). While a confidence interval could have been created directly from the volume results for Squares A to C (which would have been $0.08m^3 \pm 0.02m^3$) this was deemed inadequate for interpreting the overall volume results. However, an error range of 3.5%±7% is difficult to apply to a volume estimate. By applying the upper range of this error margin (10.5%) to the volume results produced by the modelling, a volume range which includes the true shell matrix volume should be produced. This means the true volume results for the total Grid C deposit should fall within a range of $108m^3 \pm 11.5m^3$ while the cultural shell for Grid A-B should be within $386m^3 \pm 40.5m^3$, and the total shell deposit within $1{,}105m^3 \pm 116m^3$. So the overall cultural shell for the larger site at Thundiy should fall within $51{,}455m^3 \pm 5{,}403m^3$. However, the original misplaced 'picks' show how the error values of the volume results can increase greatly. Where the volume results have not been ground truthed it would be safer to apply a confidence interval based on an error of 36.5%.

Lastly, as survey line spacing is considered to have a high impact on GPR results, different line spacings were also modelled to investigate their actual impact. For Transects A, B and C volume calculation results were generated for surveys with lines at 1m and with lines at 5m. This was accomplished by removing survey lines from the data input into ArcScene. For survey lines of 1m every other line was removed, while for surveys of 5m the start and end lines for each transect were used; these being survey lines 1, 10 and 20 for Transects A-B (Line 10 being the line between Transect A and B) and lines 1 and 10 from Transect C. The results showed only small changes, the largest being 8.5% (see Table 4.5). The 1m survey lines all decreased the volume estimate compared to the results produced by the 50cm survey lines, though this is to be expected, as with every other line being employed the final line for each transect was left out of the processing. While the results for the 5m survey lines all increased the volume estimate, with the exception of the results for the original cultural shell 'pick' placement for Transects A-B.

Table 4.5 Thundiy volume calculation results for surveys at 50cm, 1m and 5m.

Transect and Deposit	50cm Survey Results (m^3)	1m Survey Results (m^3)	5m Survey Results (m^3)	1m Survey Compared to 50cm Survey (Percentage Difference)	5m Survey Compared to 50cm Survey (Percentage Difference)
Transect C	108.27	98.90	111.82	8.5% (Less)	3% (More)
Original Transect A-B Cultural Shell	637.72	586.69	595.07	8% (Less)	6.5% (Less)
Re-Picked Transect A-B Cultural Shell	385.92	364.14	406.34	5.5% (Less)	5% (More)
Transect A-B Total Shell Matrix	1104.98	1028.77	1150.21	7% (Less)	4% (More)

4.8 Discussion

These results show the importance of employing ground truthing to interpret modelled outcomes. The significant error between the modelled volume estimates produced for the cultural shell of Transects A-B and those from excavation highlighted the existence of an error in the interpretation. By detecting this error, the 'picks' could then be revaluated and the error identified. This particular error was in interpretation, but with large and complex data sets it easily could have also been an error incorporated during conversion of the data. Detection of the error meant the results could then be reinterpreted, in this case re-picked, and the volume estimates and 3D models corrected.

Prior research papers focusing on creating volume estimates from geophysical surveys accounted for either an estimate of system error or data acquisition. System error is fairly low, with error estimates lower than 10% (Navarro *et al.* 2014; Wang *et al.* 2014; Baojuan *et al.* 2015), while data acquisition error can be large, amounting to error ranges from 20-50% (Binder *et al.* 2009; Ai *et al.* 2014), due to problems encountered during kriging interpolations because of sparse data acquisition and issues with correctly geo-locating survey lines. This case study found that when correctly interpreted the survey results can produce surprisingly accurate volume estimates. Requiring an error range of only ±10.5%, higher than, but close to the error estimates of system error created by prior publications. The significant error percentages found in this study due to interpretation error show how large errors can easily be created, and if the results were not ground truthed this error would have been difficult to detect. The results from the case study showed it would be advisable, where the results have not been ground truthed, to employ an error range of ±36.5%, a similar error value to those created by prior research experiencing data acquisition errors.

The investigation of different levels of survey detail showed little change for the homogenous Thundiy deposit. The greater change occurred for the 1m survey lines. With every other line removed (to go from 50cm to 1m line spacing) the survey missed the final line for the transects, showing it makes more of a difference for a homogenous deposit to include the edges rather than conducting a higher detailed survey. Where deposits are less homogenous the changes in survey detail may have made a more significant difference.

4.9 Summary

The geophysical surveys produced mixed results for the field site. While the shell matrix was interpretable in the GPR data, the dry sandy environment was too resistive to distinguish from the resistive shell material in the electrical resistivity results. This was a logical result for the field conditions, as much of the content of coastal sand deposits tends to be shell and coral material which will have a resistance value comparable with the shell deposits being investigated. However, even though it was a logical result it was still important to establish this result through testing. While the shell could not be differentiated from the sand in the electrical resistivity results, this testing of the array in a dry sandy environment found interpretable results for the overall site structure could be produced from larger more deeply penetrating survey lines. Overall, these field site results confirm GPR and electrical resistivity can successfully locate features of interest in relation to shell matrix sites.

The large nature of the site at Thundiy, combined with the high resolution data desired for the study, made the smaller electrical resistivity surveys inefficient due to their longer set up and running time in comparison to the GPR surveys. While the electrical resistivity needed little in the way of site preparation the survey set up and run-time were extensive, by comparison the GPR covered large areas quickly but had a greater site preparation time due to clearing of the site. Once the site was cleared, with grass clumps clipped down, it was ideal for GPR use as the large open areas meant the antenna was free of obstructions for the majority of the survey. If denser tree coverage were encountered the GPR surveys would become impractical, while the electrical resistivity surveys would become more practical especially as the added organic matter from the tree coverage should be more conductive and thus distinguishable from the highly resistive shell.

5 EXPERIMENTAL SITE: CAIRNS CAMPUS

5.1 INTRODUCTION

An experimental site was established on the Cairns campus of James Cook University in Queensland, Australia (Figure 5.1). This site was created as a control to test the accuracy of the methods employed in generating volume calculations and 3D models for the buried shell deposits. The experimental design allowed for control over the size and structure of the shell deposits being investigated. The ability to control all aspects of the experimental design allowed for the accuracy of the methods utilised to be evaluated, with the results generated from the geophysical data compared to the actual volume of shell placed into the ground. This is particularly important as prior research (see review in Chapter 2, Section 2.6) has systematically failed to compare the volume results obtained from geophysical data with real world volumes.

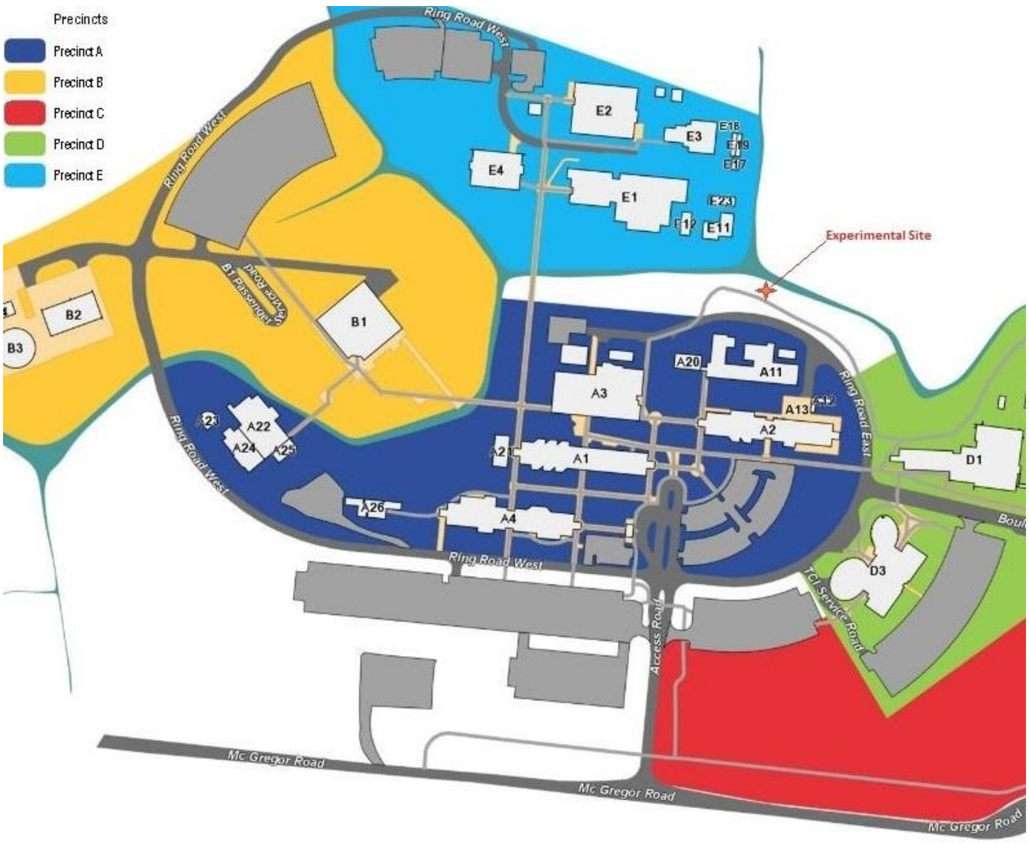

Figure 5.1 **JCU Cairns Campus Map with the experimental site location marked. Reproduced with the permission of James Cook University (modified from James Cook University: https://maps.jcu.edu.au/).**

The ability to control the conditions present in the experimental set up was also useful in determining the effects of those conditions on the GPR and electrical resistivity surveys. Two significant variables and their effect on the geophysical survey results were investigated over the course of this research. The two variables investigated were the type of sediment surrounding the shell matrix and the moisture content of that sediment; these variables are discussed in further detail in the methodology section below (see Section 5.4). Before detailing the experiment methodology, the environmental and historical context of the site will be briefly considered in Sections 5.2 and 5.3.

5.2 Environmental Context

The experimental site is located in the wet tropics. Weather patterns for this region are very similar to those for the Gulf of Carpentaria where the Thundiy field site is located; the main difference being higher rainfall patterns in the Cairns region. Like the Gulf, the weather patterns for Cairns are dominated by a wet and dry season and by similarly warm to mild temperatures. The average temperatures for Cairns range from a maximum of 31.5°C in December/January and a minimum average temperature of 17.1°C in July (Australian Government Bureau of Meteorology 2015b). Mean rainfall averages range from 451.8mm in February to 26.7mm in August (see Figure 5.2). Since the moisture content of the soil can have significant effects on the results of geophysical surveys and as heavy rainfall is a dominant feature of the weather for half the year in northern Australia, this variable and its effect on the results was investigated. Surveys were conducted under both 'wet' and 'dry' conditions so the influence of moisture levels on the survey results could be compared.

The experimental site is located immediately north of Building A11 along Atika Creek (formally Chinaman Creek) on the JCU Cairns campus. The site has been dug into the clay of the creek bank adjacent to and overhung by rainforest trees. Though the site is located approximately 10m from the creek itself, the area is not subject to flooding. The site is located on open ground with no nearby buildings adjacent to the creek buffer zone, which is a forested area either side of the creek designed to reduce erosion (see Figure 5.3). The creek channel exhibits forest with a dense canopy, this canopy shades the experimental site for a significant proportion of the day though it only minimally overhangs the site. The area of the experimental trenches is inclined by approximately 6% towards the creek (north); making it a gently inclined slope (Speight 2009:18).

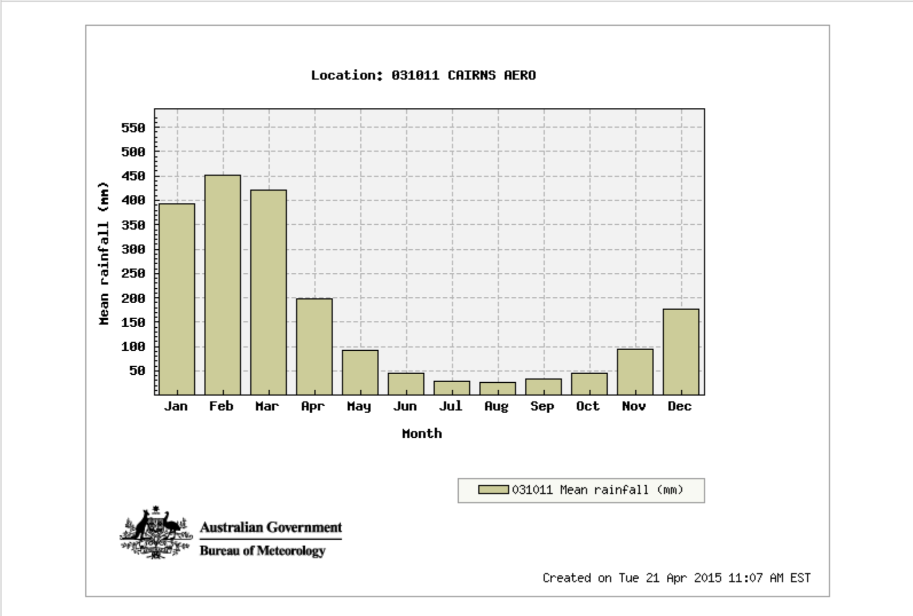

Statistics	Jan	Feb	Mar	Apr	May	Jun	Jul	Aug	Sep	Oct	Nov	Dec	Annual	Years
Mean rainfall (mm) for years 1942 to 2015	391.8	451.8	421.7	197.4	91.4	45.6	29.2	26.7	33.4	46.0	93.7	175.9	2010.7	73

Figure 5.2 Cairns mean monthly rainfall as based on 73 years of weather data spanning 1942 to 2015 (taken from the Australian Government Bureau of Meteorology (2015b).

Figure 5.3 JCU Cairns Campus Environmental Overlay aligned to north, scale provided was uninterpretable and is not included here. Experiment site location marked as a yellow star. Reproduced with the permission of James Cook University (Modified from Flanagan Consulting Group 2010:21).

5.3 HISTORICAL CONTEXT

The relatively recent construction of the Cairns Campus of JCU (site works began in 1993 while building commenced in 1994) means the ground the experiment is located in has been subject to recent large-scale disturbance. This disturbance included road works (for Ring Road East), site works for the building of the nearby postgraduate annexe (Building A11), as well as the placement of a water and sewer main (see Figure 5.4).

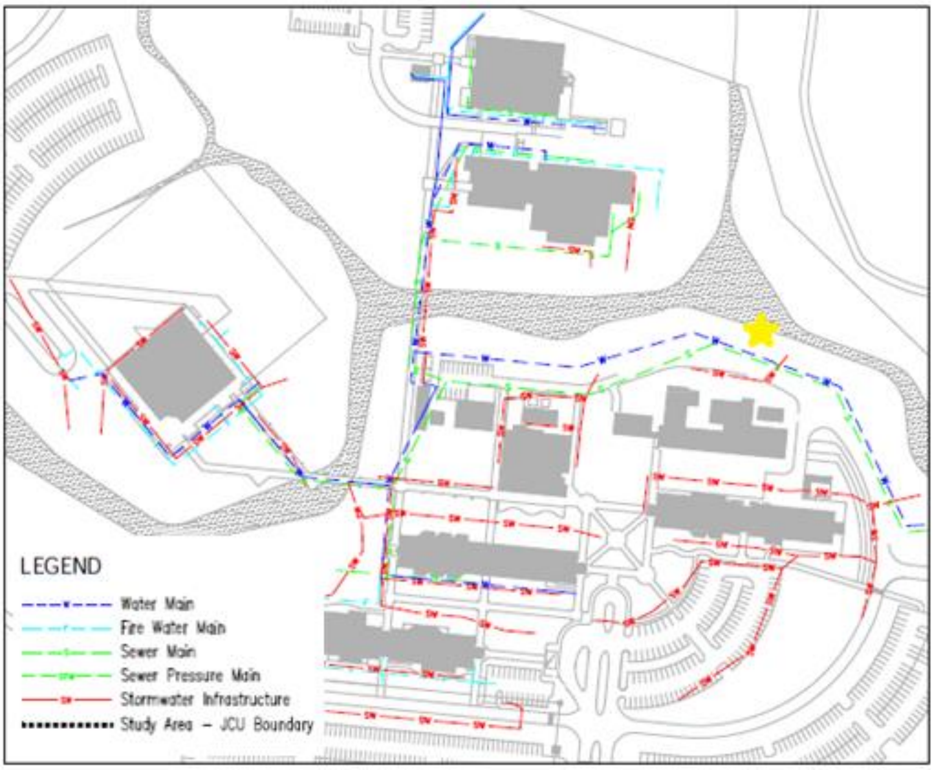

Figure 5.4 JCU Existing Services Plan, aligned to north, scale not given. Experiment site location marked as a yellow star. Reproduced with the permission of James Cook University (Modified from Flanagan Consulting Group 2011: Appendix F).

The site was subject to further disturbance when in 2000 a 4-5m saltwater crocodile and a dolphin were buried there. The animals were placed in a 1m-deep trench, cut parallel to the creek. A layer of large gravel was placed in the trench base, followed by a layer of sand topped with geotextile matting. The animals were placed in the trench, on top of the fill, wrapped in shade cloth and covered with sand and turf (the turf included a substantial base of the local clay); Figure 5.5 shows the trench fill as unearthed during the placement of Trench 1. In 2002 the dolphin was excavated and then in 2011 excavation of the crocodile started (continuing in 2012, 2013 and 2015). In 2013 experimental Trench 1 was dug into the site of the original crocodile/dolphin trench to approximately the same depth as the original trench. All the previous gravel and sand fill was removed and Trench1 was located adjacent to the remaining half of the crocodile.

Figure 5.5 Section photograph of the end walls of Trench 1 showing the prior fill.

5.4 EXPERIMENTAL SITE METHODOLOGY

The experimental site consisted of two separate 2m by 4m trenches excavated to a depth of 1m. Once excavated Trench 1 was re-filled with coarse washed sand, analogous to the environment in which archaeological shell deposits are typically found in tropical Australia, and in this sand were placed two lenses of oyster shell. Trench 1 was completed on 25 October 2013, with the first geophysical survey of the site being made on 15 August 2014. These initial survey results showed the highly resistive nature of the sand and shell made them impossible to differentiate in the electrical resistivity results. A second experimental shell matrix, Trench 2, was then constructed with an organic fill. This organic fill was designed to replicate the more conductive environments from which previous research surveys, using electrical resistivity (see Chapter 2), had produced results successfully differentiating shell material from surrounding deposits. By replicating the interpretable results generated by other studies, the current research could then employ electrical resistivity data in creating a volume estimate and 3D model of the shell matrix. To create this more conductive environment, Trench 2 was excavated by backhoe on 30 May 2015 and filled with an organic-rich garden soil mix. This new trench was placed to the west of, and aligned with, the original trench with a baulk of 2m between the two (see Figure 5.6).

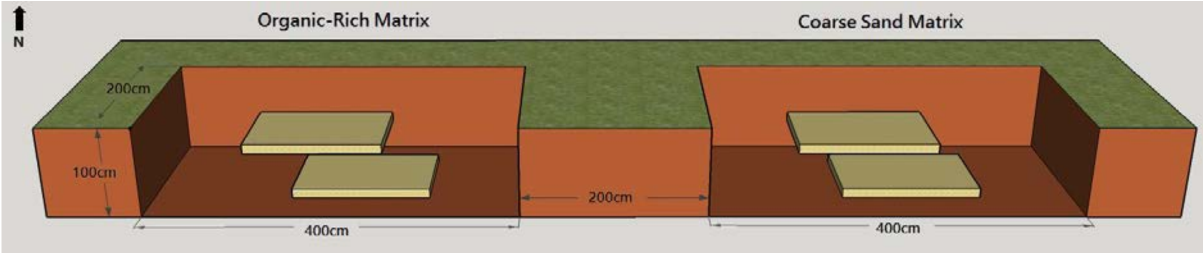

Figure 5.6 Layout of Trench 1 and 2 in relation to one another, including the location of their respective shell deposits.

The shell deposits for the experimental site consisted of oyster shell collected from two local seafood suppliers: *Cairns Ocean Products* and *Preston Fresh*. All oyster shell for the experiment was counted (establishing both MNI and NISP), weighed and then measured for volume via water displacement (Table 5.1). The oyster shells collected were an average size of 77mm in length by 47mm width and consisted predominantly of the lids or right sides, as these are discarded before sale to the public and were thus easy to collect from the retailers. The actual volume of the shell (223,340cm^3 or 0.22m^3) was established based off the water displacement method; this volume calculation does not account for total space occupied by the shell as they do not lie flat together.

Table 5.1 Total oyster shell counts for Trench 1 and 2 combined

Oyster Shell	Weight (Kg)	MNI	NISP	Litres Dispersed (L)	cm^3
Total	**406.34**	**28,539**	**28,864**	**223.34**	**223,340**

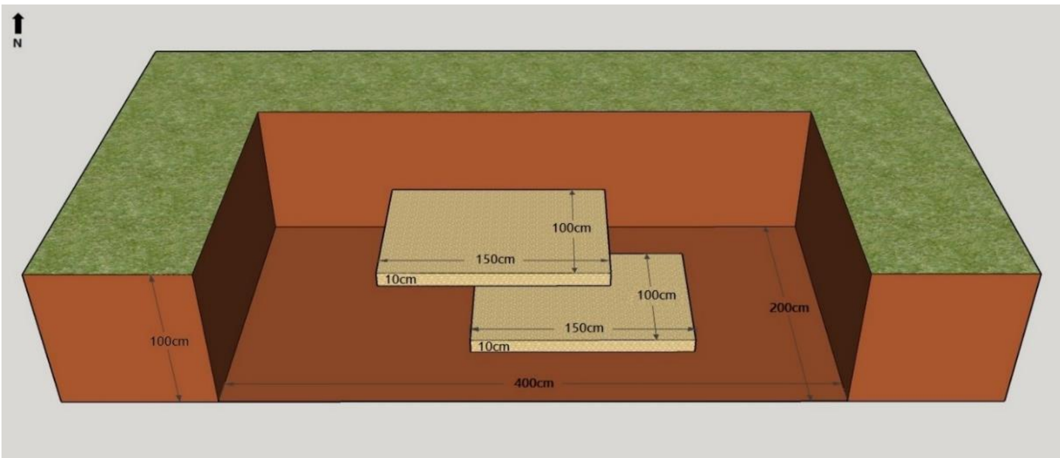

Figure 5.7 Oblique view of the shell deposits as replicated in Trench 1 and 2.

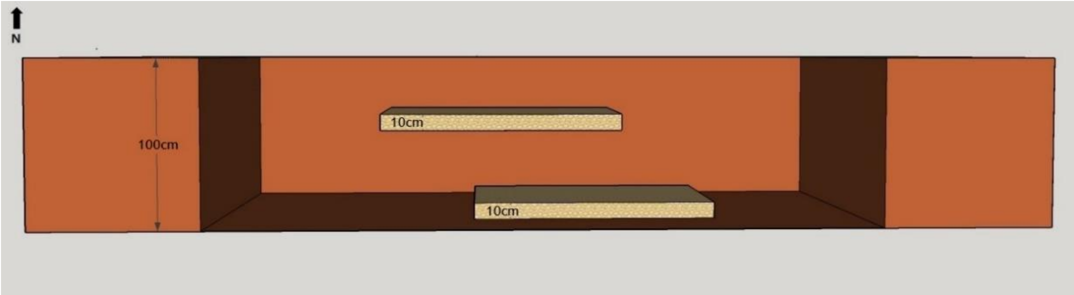

Figure 5.8 Side view detailing the shell deposits as replicated in Trench 1 and 2.

The shell was placed in two discreet layers in each trench (Figures 5.7 to 5.8). These two layers measured 1m wide by 1.5m long to an approximate depth of 10cm, making the volume of the space they occupied c.0.15m³ per layer (a total of 0.6m³). The first layer was placed directly on the basal clay of the trench, and was situated in the middle of the trench 1m in from the eastern end. The second deposit was situated an average of 42cm above the first, also in the middle of the trench but 1m in from the western end so it partially overlapped the lower deposit. Shell deposit and trench dimensions/depth were recorded with reference to a local datum via an optical dumpy level.

5.4.1 General Survey Methods

The experimental site was surveyed using strict grid control. A survey grid was established over the two trenches with survey lines running every 50cm. Each trench was surveyed separately with GPR and electrical resistivity lines beginning and ending beyond the respective trench boundaries. The survey grid was established to align with star pickets marking the corners of each trench (out of the way of geophysical survey lines), this was done so the grid could be easily relocated in the same position for replicate surveys. The low topographic relief of the site and running of the survey lines parallel to the creek bank meant only minimal topographic corrections were required for the survey profiles. GPR results were topographically corrected in Reflexw based on georeferencing data produced in ArcMap before the 'picks' were exported to ArcScene, while the 'picks' from the electrical resistivity results were topographically corrected in Microsoft Excel (based on the data produced in ArcMap) before being imported into ArcScene.

The experiment included both wet and dry season geophysical surveys. As water content has a significant effect on both GPR and electrical resistivity, running the surveys in each of the predominant weather conditions allowed for an investigation of these effects. The 'wet' surveys were conducted in the winter (the dry season) right after heavy downpours, while the 'dry' surveys also took place in winter but after a 10 day stretch of no rain. Regular rainfall over the winter months during the duration of this thesis meant a longer rain-free stretch of weather to further dry out the ground was not obtained. The water content analysis found that during these 10 days, the organic matrix of Trench 2 drained the water quicker and dried out more than the sand matrix of Trench 1 (Tables 5.3 to 5.4).

To establish the water volume present for each survey a small pit was dug into the middle of the western end of each trench from which soil cores were taken in steel bulk density rings (75mm diameter by 50mm height). Samples were taken at the surface (approximately 2cm depth as the surface was cleared first) then at 40cm and 80cm; at each depth two samples were taken. The soil cores were then weighed in the laboratory using a Shimadzu ATY224 electronic balance to the nearest 0.01g before being oven-dried for 48 hours at 105°C. Once fully dried the core was weighed again. These weights were used to create gravimetric and volumetric water content values. Gravimetric water content for this research has been expressed as a percentage: the percentage of water present per 100g of soil. Volumetric water content is the water content (also expressed as a percentage) of the total sample (Cresswell and Hamilton 2002:37-38). Creating volumetric water content values requires both gravimetric values and bulk density values. Bulk density is the ratio of the mass to total volume of a sample of dry soil, expressed as g/cm^3 (Cresswell and Hamilton 2002:36). An average of these values for each depth (2cm, 40cm and 80cm) are presented in Tables 5.3 and 5.4. For comparison, laboratory analysis was also used to create saturated and field capacity values for the sediment, each of these were conducted twice and the results averaged (Table 5.2).

Table 5.2 Gravimetric and volumetric percentages for the field capacity and saturated sediments of Trench 1 and 2.

Trench	Saturated Average Gravimetric (%)	Saturated Average Volumetric (%)	Field Capacity Average Gravimetric (%)	Field Capacity Average Volumetric (%)
Trench 1 Sediment (Sand)	24.2	33.93	3.98	5.55
Trench 2 Sediment (Organic Soil)	91.63	54.68	42.58	25.81

Field capacity as defined by the Soil Science Society of America (1997:40) is "the content of water, on a mass or volume basis, remaining in a soil 2 or 3 days after having been wetted with water and after free drainage is negligible". Saturated and field capacity values were determined by first saturating the samples from the bottom up, to remove any air from the sediment. The saturated samples were then weighed and oven dried. The field capacity samples were saturated then placed on a 1 bar ceramic suction plate (drained over 1m to create 10 kilopascals of pressure) and left to drain for approximately 48 hours before being weighed and oven dried. This is standard laboratory practice for the ceramic suction plate method (see Cresswell 2002:64-67). It is important to note how laboratory calculations of field capacity values are considered only an approximation as actual field capacity values are affected by field conditions which cannot be recreated in the laboratory (Romano and Santini 2002:727).

5.4.2 GPR Survey

GPR lines were run at the highest practical resolution with a line spacing of 25cm (Figure 5.9). With a small grid and smooth surface the highest level of survey resolution was obtainable; this level of survey detail was not practical in the field due to the rough surface on site, and was also deemed unnecessary to target a large mass of midden material. As the Mala 500MHz antenna is 30cm in diameter it was run directly down the middle of each 25cm spacing, placing the region of the recorded reflection profile approximately in the middle of each 25cm. As survey guides, string lines were run every 50cm.

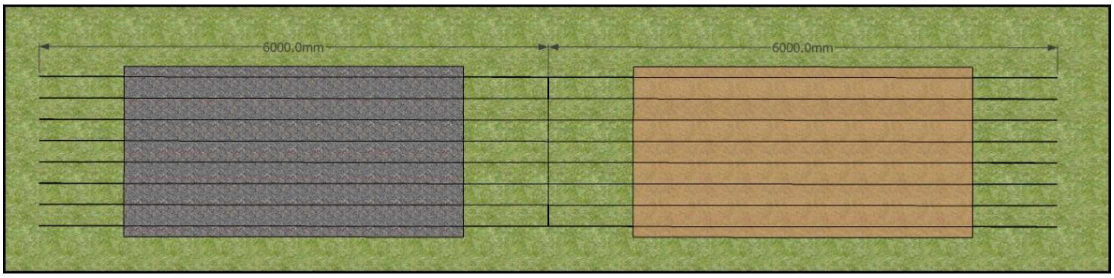

Figure 5.9 GPR survey lines for Trench 1 and 2.

The moist soil survey had to be run twice (first in July of 2015 then again in September 2015) as the profiles for the first survey were recorded with the wrong nanosecond time/depth scale. The time/depth scale displayed on the monitor became stuck at a shorter nanosecond window after the settings were opened up to a larger time window.

This error resulted in the profiles recording down to 100 nanoseconds but the time window for the files being saved with a depth scale of only 40 nanoseconds. Attempts were made to fix this in Reflexw but the results were unsatisfactory and so the GPR component of the survey was re-run after the next heavy downpour of rain had re-moistened the trenches.

After an initial survey of both trenches the GPR results for Trench 2 were found to be uninterpretable (discussed below in Section 5.5.1) and the focus of the GPR surveys was switched to Trench 1. The wet survey for Trench 1 was run with a water content slightly above the estimated field capacity for the sand fill. The 'dry' survey was run with an average water content for Trench 1 of 3.08% (see Table 5.3), less than one gravimetric percent difference from the estimated field capacity at 3.98% (see Table 5.2). However, from the 'wet' to the 'dry' survey this difference represents a 28% decrease in the average gravimetric water content; from 4.32% water per 100g of soil to 3.08%.

Table 5.3 Soil water content for GPR surveys (Trench 1).

Depth of Sample	Gravimetric Wet (%)	Volumetric Wet (%)	Gravimetric Dry (%)	Volumetric Dry (%)
2cm	4.1	6.43	2.51	3.81
40cm	4.64	6.43	3.08	4.7
80cm	4.22	6.28	3.65	5.3
Overall Average for Trench 1	**4.32**	**6.28**	**3.08**	**4.61**

5.4.3 Electrical Resistivity Survey

Trench 2 was added and surveyed in 2015 after the initial surveying of Trench 1 in August of 2014 found the electrical resistivity results produced were uninterpretable. For the experimental site electrical resistivity lines were run with an electrode spacing of 25cm, as was used during the fieldwork. Survey lines plus tape measures were laid out for the positioning of electrodes (also the same method employed for the fieldwork). Trench 1 was surveyed with four lines to confirm that none of the lines would produce interpretable results. The four lines were placed every 50cm starting 25cm in from the trench wall (Figure 5.10). Trench 2 was surveyed at a higher resolution with lines every

25cm, also commencing 25cm in from the trench wall, making a total of 7 lines (Figure 5.11); as this represented the ideal level of detail especially for a small matrix.

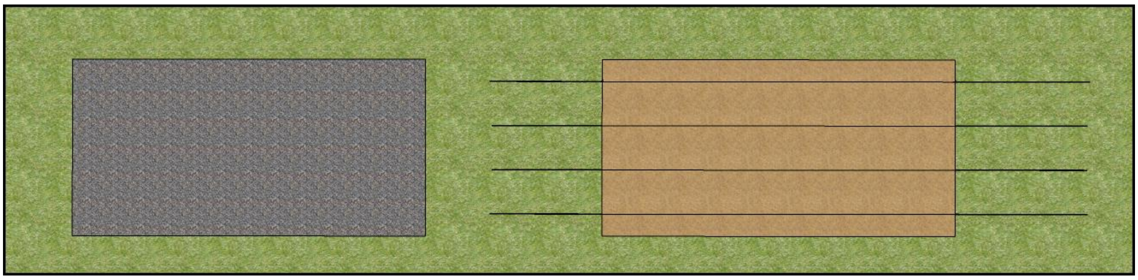

Figure 5.10 Electrical resistivity survey lines for Trench 1.

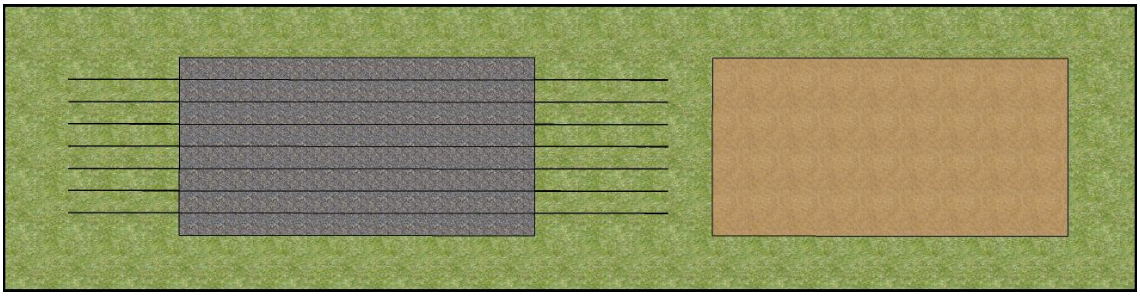

Figure 5.11 Electrical resistivity survey lines for Trench 2.

The wet survey for Trench 2 was conducted in July 2015 and as with the GPR results, was run with an average gravimetric water content (41.89%) close to the estimated field capacity (42.58%) for that matrix (see Tables 5.2 and 5.4). The dry survey was conducted in August of 2016 after a 10 day stretch of no rain. The average gravimetric water content for the trench was 18.22% which represents a 56% decrease in gravimetric water content from the wet survey.

Table 5.4 Soil water content for electrical resistivity surveys (Trench 2).

Depth of Sample	Gravimetric Wet (%)	Volumetric Wet (%)	Gravimetric Dry (%)	Volumetric Dry (%)
2cm	41	25.16	14.54	10.05
40cm	42.08	22.18	18.55	13.11
80cm	42.61	25.8	21.57	15.98
Overall Average for Trench 2	**41.89**	**24.38**	**18.22**	**13.05**

5.5 Experiment Results

The experimental site survey results are detailed below; Section 5.5.1 reports the GPR survey results while Section 5.5.2 reports the electrical resistivity survey results.

5.5.1 Ground-Penetrating Radar

The different types of fill used in Trenches 1 and 2 had as marked an effect on the GPR results as it had on the electrical resistivity results. While the sand fill of Trench 1 successfully produced interpretable visualisations of the buried shell deposit, the organic fill of Trench 2 obscured the deposit (see Figure 5.12 and Appendix C). The fill had been chosen as the most likely to be conductive, which had the adverse effect of raising the RDP to levels in which the radar waves were quickly dissipated and the GPR results rendered uninterpretable. Ideally the fill would have been conductive enough to produce a differentiation between the fill and the shell material but not to the point of obscuring the GPR results. This ideal level of conductivity should have been possible with an organic mix of soil and plant material, but the fill may have contained fertilisers not advertised in the description.

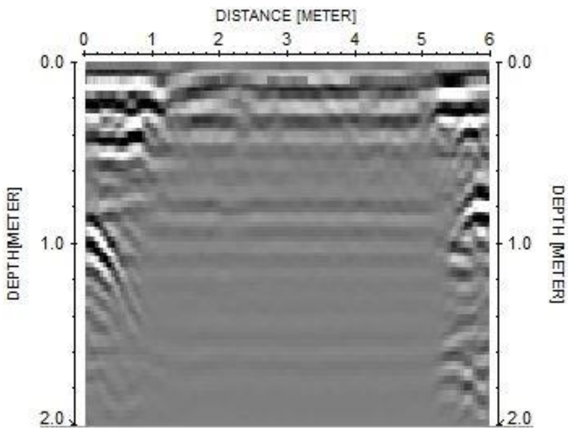

Figure 5.12 Line 5 of the GPR survey of Trench 2 showing the edges of the trench and then the fill obscuring everything in the trench and beneath it; though the bottom corners of the trench can still be seen at around 1m depth on either side of the profile.

5.5.1.1 Wet Survey Results

The wet survey results show the edges of Trench 1 at 1m and at 5m across the profile, with the corners at the base of the trench showing up at approximately 1m in depth (Figures 5.13 to 5.14). The lower layer of shell deposit is indiscernible from the base of the trench, but the upper layer of the buried shell matrix appears as a planar reflection response located in the middle of the GPR profile. The deposit can be observed starting at a depth of approximately 40cm and appearing to continue to around 50cm (Figure 5.14).

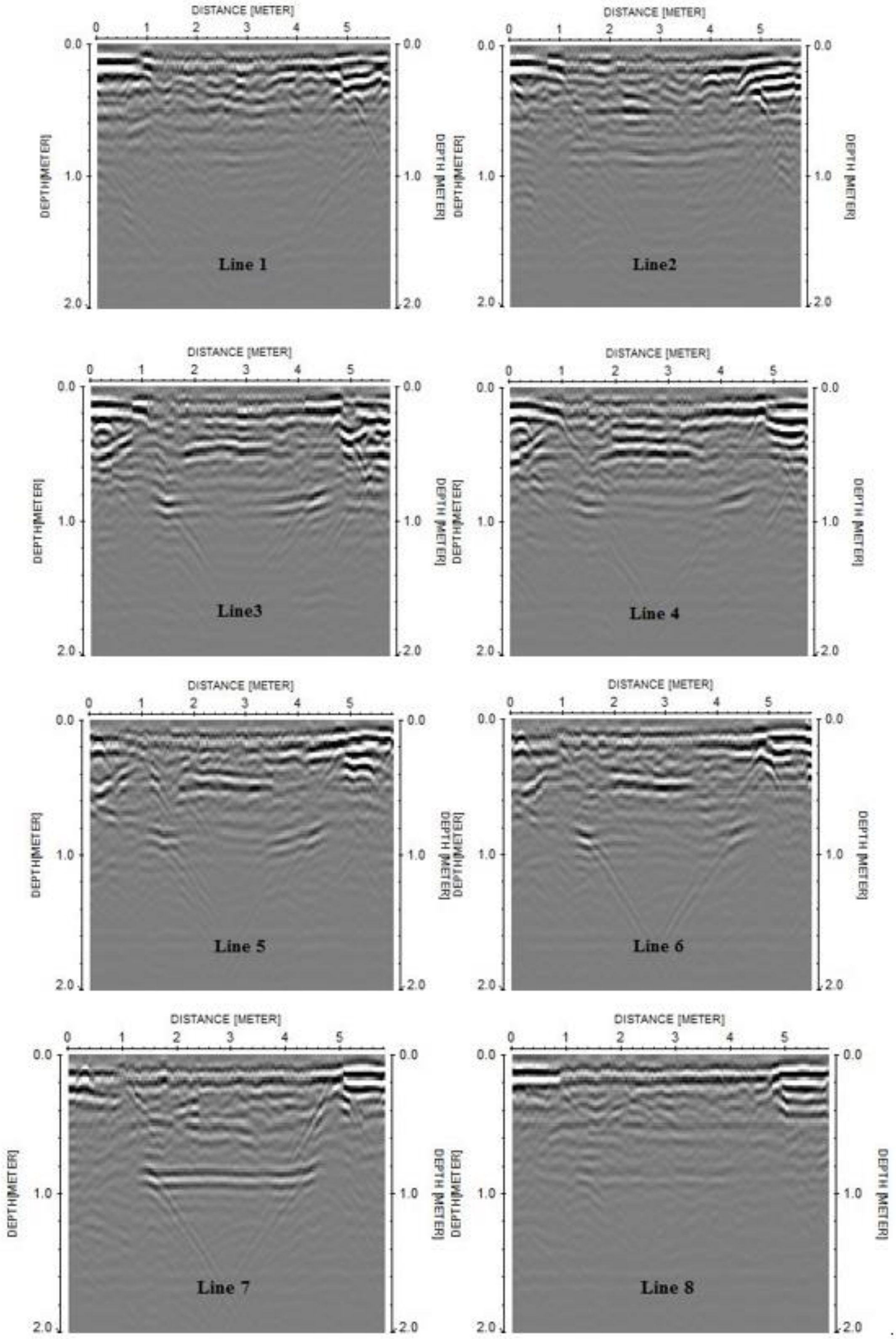

Figure 5.13 GPR wet survey lines 1 to 8.

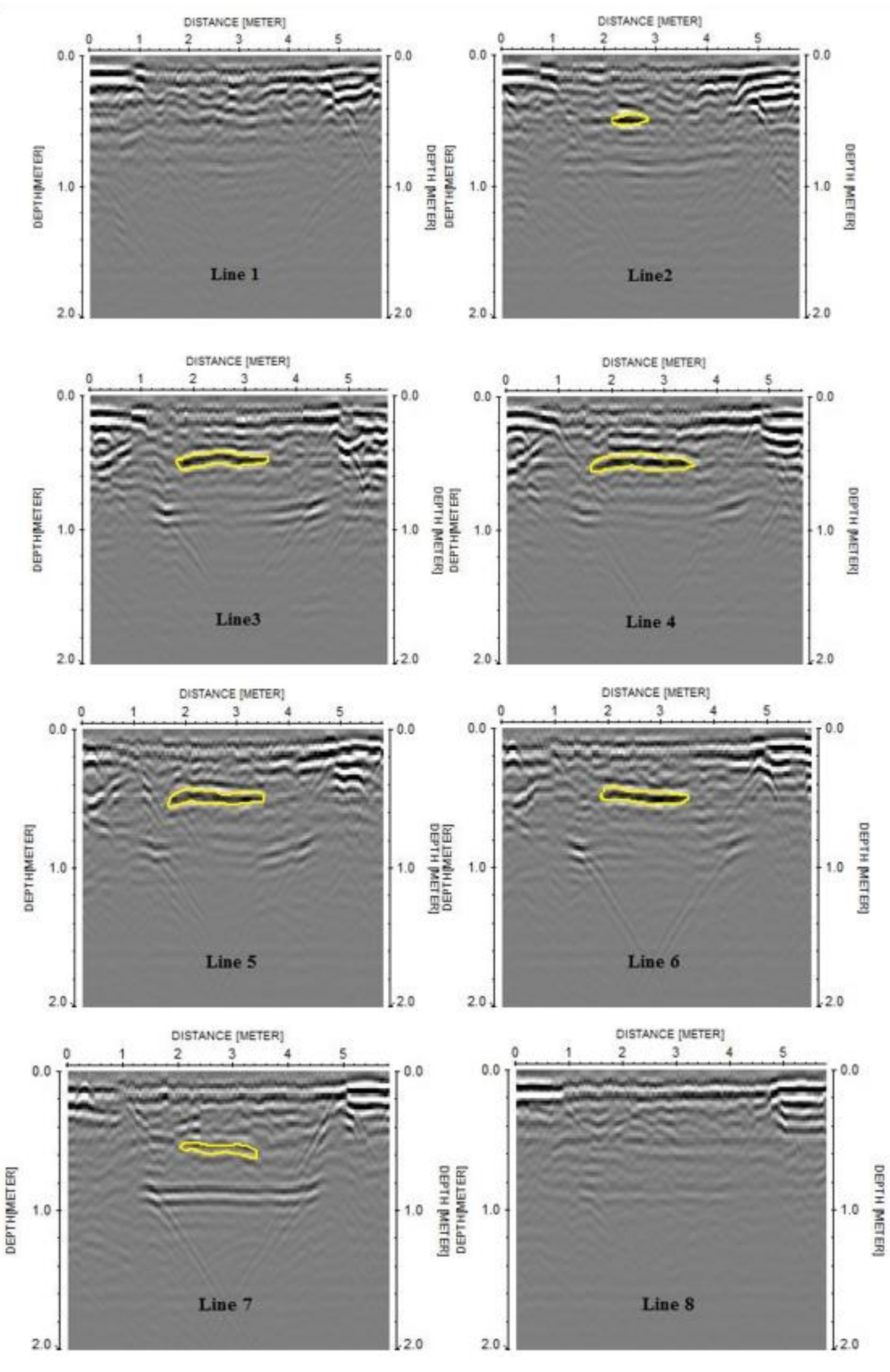

Figure 5.14 GPR wet survey lines 1 to 8 showing interpreted shell deposit circled in yellow.

Lines 1 and 8 were situated close to the trench walls, beneath which there was no shell deposit. The profiles for lines 1 and 8 illustrate this, with only the top of the trench showing up along the surface and the slightest response from the base of the trench at 1m (Figure 5.13). After processing and interpretation, the planar reflection response representing the shell deposit was 'picked' (details in Section 3.5.1). The reflection response representing the shell deposit was observable from lines 2 to 7 (Figure 5.14). The lines were interpreted with reference to their neighbouring lines so even though lines 2 and 7 exhibited less distinctive reflections than other lines they still had reflections that clearly related to the more distinctive results in lines 3 and 6. Line 4 exhibited multiple reflections (or multiples), these were not included in the 'picked' deposit as they were visually identifiable as multiples and not an actual representation of the subsurface; the upper deposit boundary for line 4 was then 'picked' with reference to lines 3 and 5. The top and bottom boundaries of the deposit for each profile were 'picked' separately and imported into ArcScene as separate files (Figure 5.15).

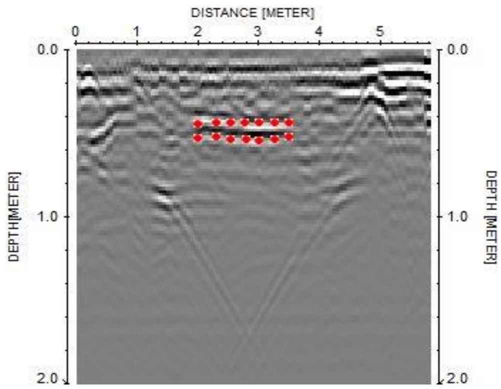

Figure 5.15 Line 6 of the GPR survey of Trench 1 showing 'picks' for both the top and bottom of the deposit.

5.5.1.2. Dry Survey Results

The dry survey results were similar to the wet results, though they were slightly more visually distinctive (Figures 5.16 to 5.17). This change may have been due to either the dryer ground or to altered screen settings for the Mala monitor. An attempt was made to re-create identical settings between surveys, but for the final survey the screen resolution had to be reset (after use by other operators) and changes to the monitor display can effect the recorded data files. This effect was previously encountered when a problem occurred (discussed in Section 5.4.2) in which the system settings differed from the display screen and resulted in the files being recorded to match the screen.

Because of this characteristic of the Mala system, it is uncertain whether the visual changes in the survey profiles was due to the Mala or to the dryer ground conditions.

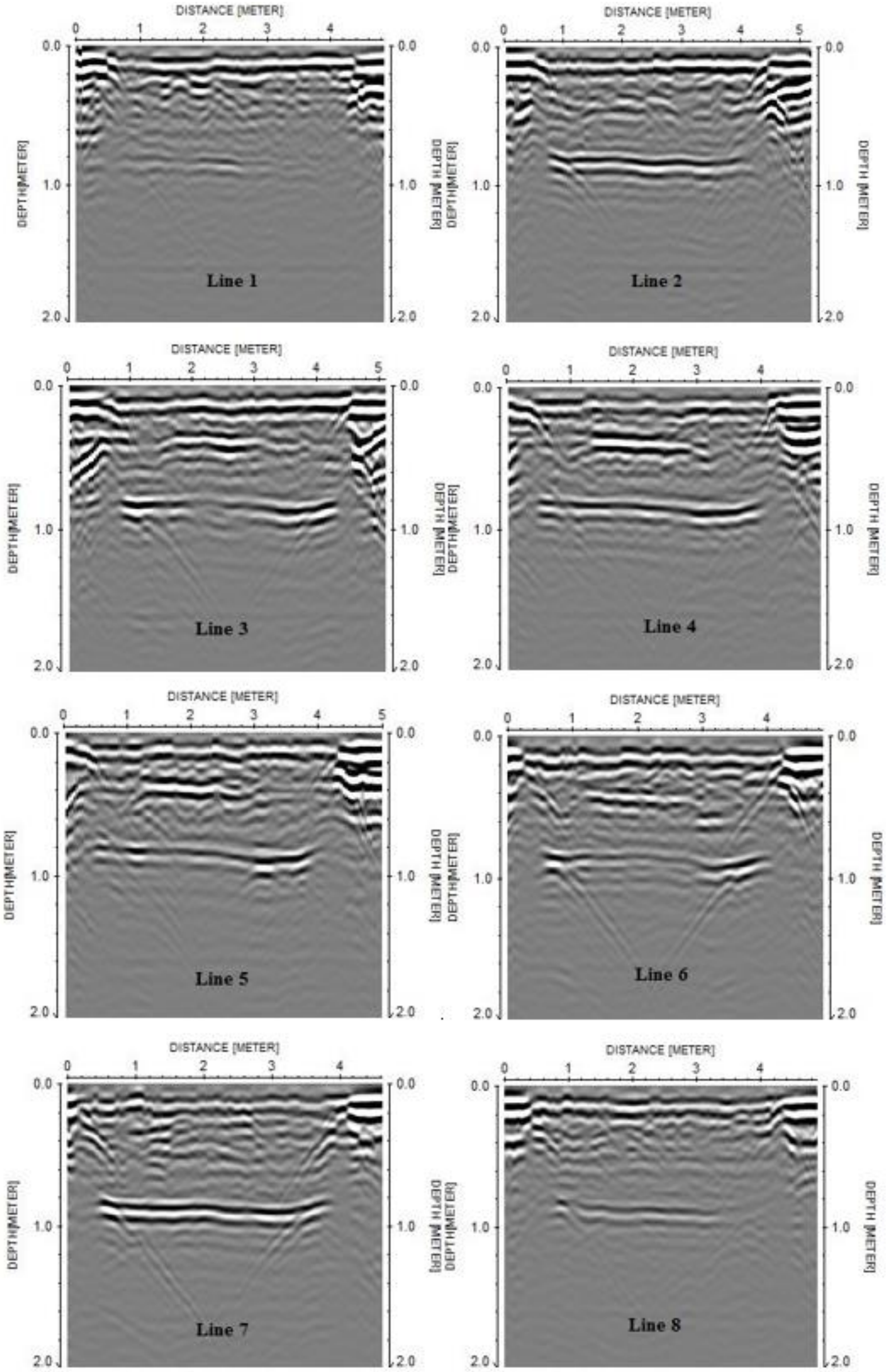

Figure 5.16 GPR dry survey lines 1 to 8.

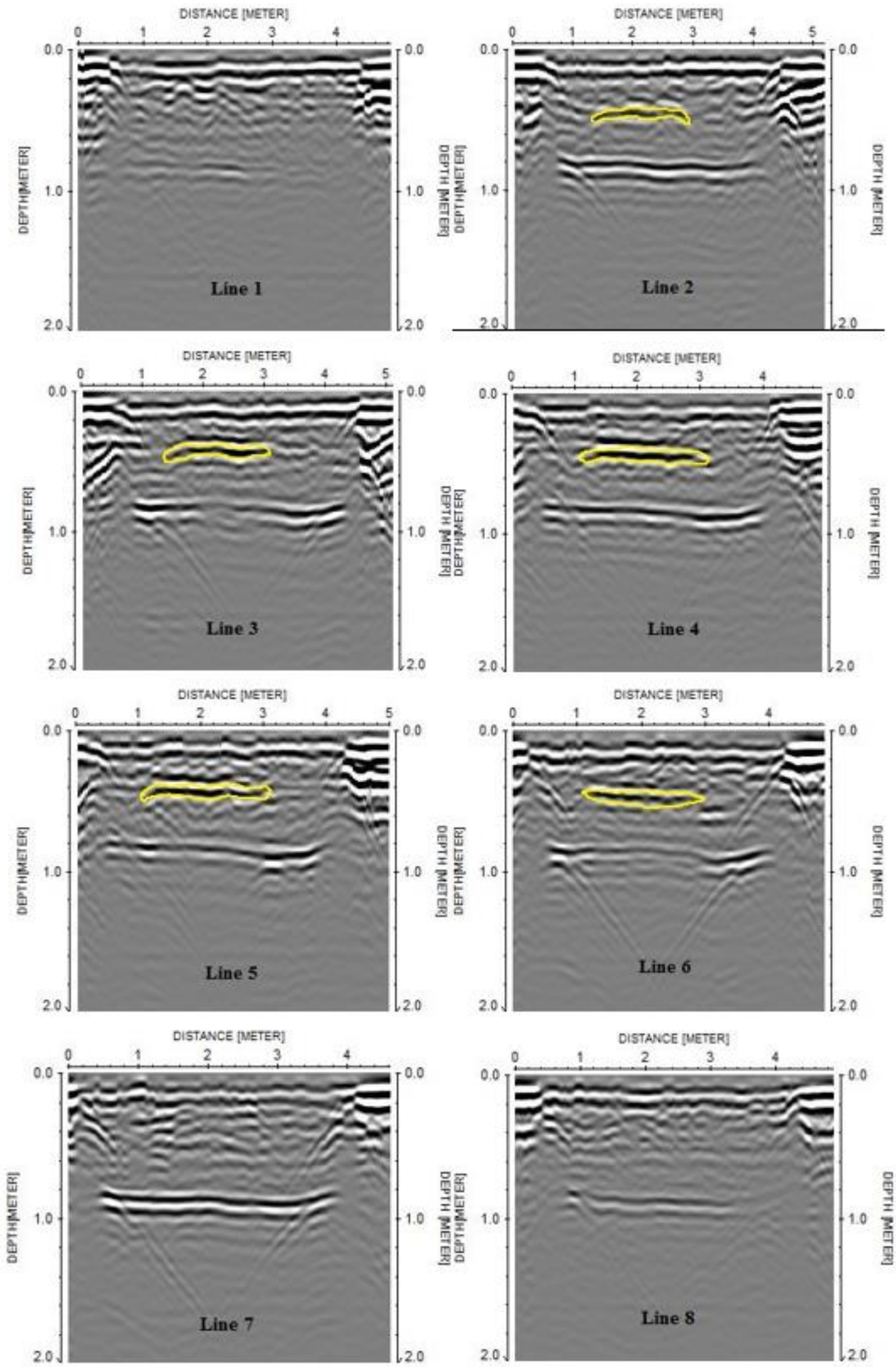

Figure 5.17 GPR dry survey lines 1 to 8 showing interpreted shell deposit circled in yellow.

The dry survey results were interpreted and 'picked' in the same manner as the wet results, though now Line 7 was considered to be uninterpretable even with reference to Line 6 (see Figure 5.17).

5.5.2 Electrical Resistivity

The electrical resistivity results for Trenches 1 and 2 varied greatly. As has been mentioned above, the results for Trench 1 (sand filled) found the sand and shell indistinguishable, while Trench 2 was set up with the express purpose of producing interpretable results by utilising a more conductive sediment matrix (garden soil). As desired, the organic fill of Trench 2 provided a conductive medium for the electrical resistivity results making the shell distinguishable from the surrounding sediment.

While the results for Trench 1 did not produce an interpretable difference between the shell and sand, the vague shape of the Trench itself is visible in the results compared to the more conductive clay around it (Figure 5.18). In Figure 5.18 the higher resistivity results of the Trench can be seen stretching from 0.75m to 5.5m along the pseudosection to a depth of 1m. This area of higher resistance varies a little amongst the different survey lines but all exhibit some distortion (see Appendix C), with the trench actually extending from 1.25m to 5.25m. The surface of the trench is reading as a more conductive area, as it did at Thundiy, due to the water poured onto the electrodes to reduce contact resistance. The GPR lines were run first for each round of surveying so their results were not affected by the additional water, and freshwater was used so that any future GPR surveys would not be adversely affected by the addition of salt.

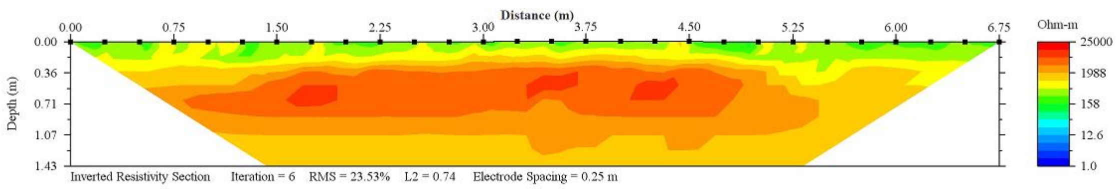

Figure 5.18 Electrical Resistivity results for Line 1 from Trench 1 showing the highly resistive shell matrix of the trench.

5.5.2.1 Wet Survey Results

Trench 2 shows up in the pseudosections as a conductive region surrounded by the more resistive clay; a reverse of the Trench 1 results. Within the trench area a more resistive patch is visible, representing the upper shell deposit, the lower deposit is indistinguishable from the clay (Figure 5.19).

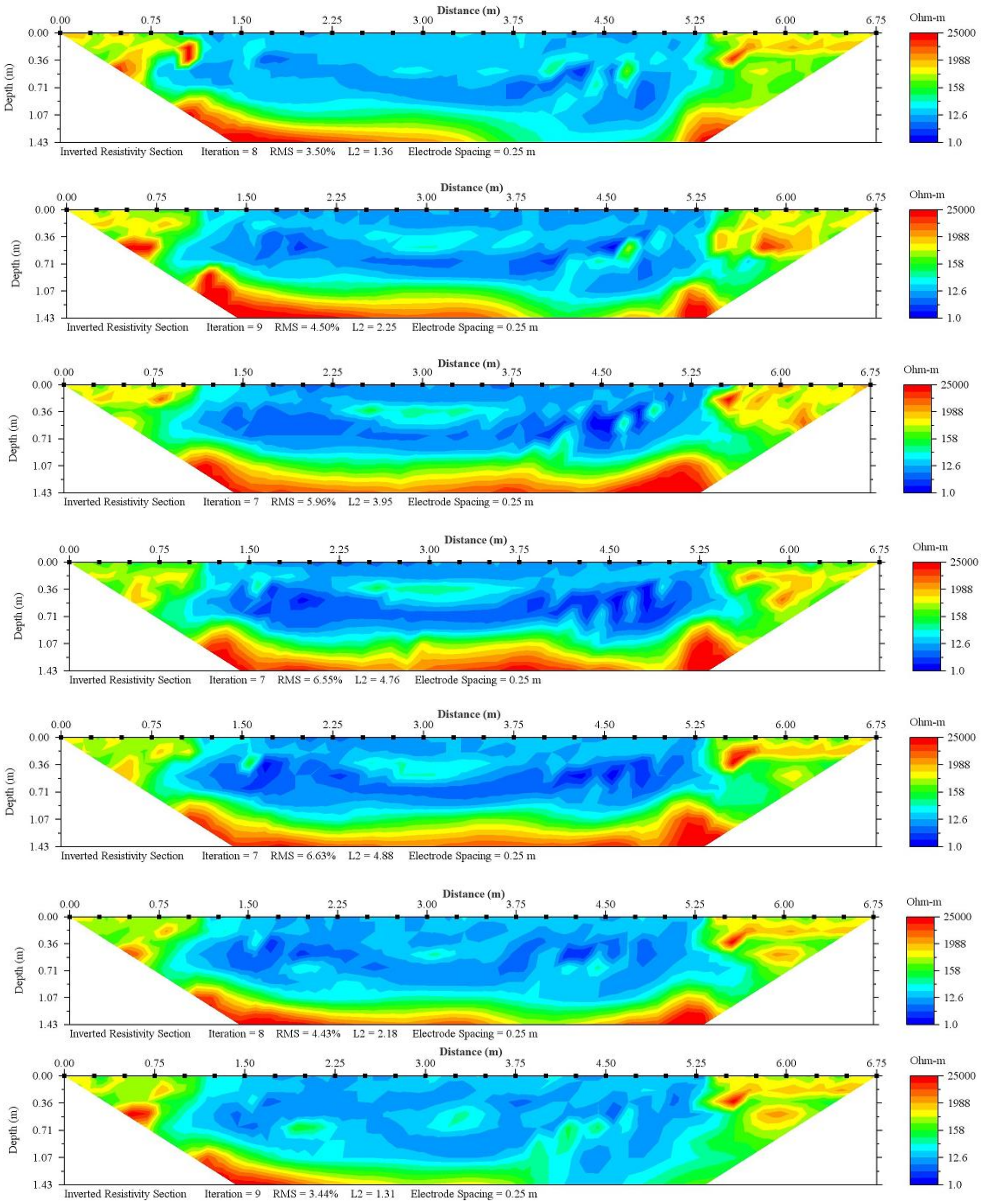

Figure 5.19 Electrical resistivity wet survey lines 1 (top) to 7 (bottom).

The pseudosections for lines 1 and 7, the first and last lines, show patches of resistance due to their proximity to the trench wall, these areas are unrelated to the shell deposit and the choice was made to disregard them as a by-product of the experimental set up.

Small areas of resistance in lines 2 and 6 were mapped as being part of the shell matrix. They were included because they related to areas of resistance mapped as shell in the adjacent lines (Figure 5.20). After processing and interpretation, the area of resistance representing the shell deposit was ‘picked’ manually (as described in Section 3.5.2). The decision was initially made to ‘pick’ only the region of higher resistance (around 158Ω-m) as shell deposit (Figure 5.21). This decision was made to isolate the highly resistive shell and reduce the amount of surrounding sediment included in the modelling. The top and bottom boundaries of the deposit were ‘picked’ separately and then imported into ArcScene as separate files.

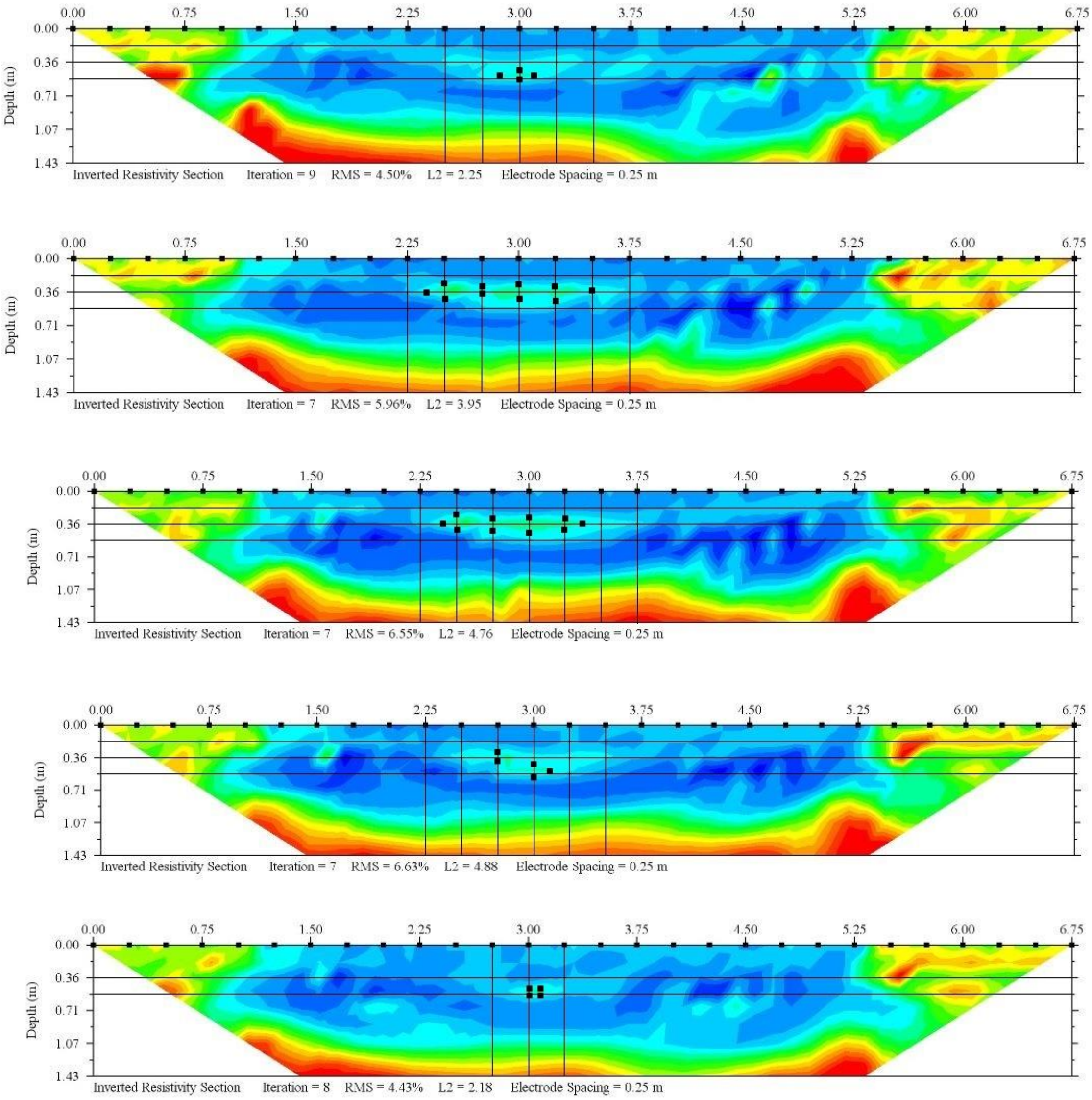

Figure 5.20 Electrical resistivity wet survey lines 2 to 6 illustrating the ‘picked’ deposit.

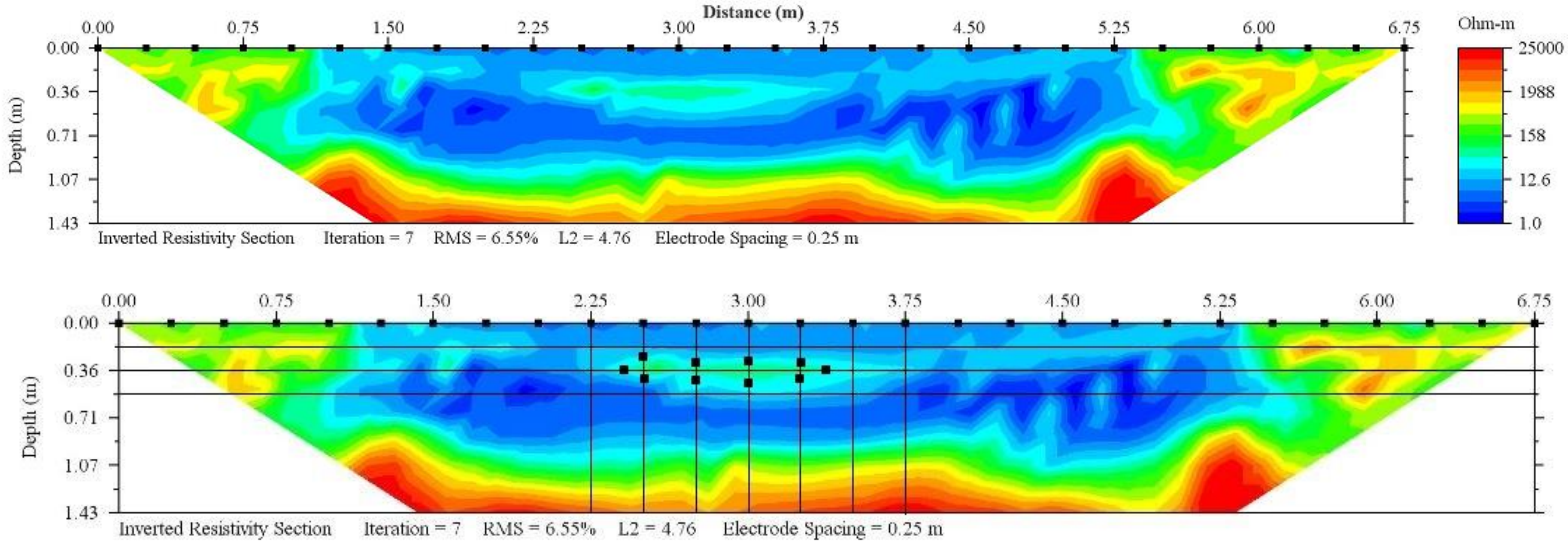

Figure 5.21 **Electrical Resistivity results for Line 4 from Trench 2 showing the grid used for establishing 'picks' as well as the 'picks' for both the top and bottom boundaries of the shell deposit. The final picks on either side of the deposit were included in both the top and bottom boundary files.**

As a comparison method, the pseudosections were then re-interpreted with the entire area of higher resistance circled and 'picked' in a second round of modelling (Figure 5.22). Instead of isolating the areas of only 158Ω-m the surrounding region of 50Ω-m was also included in the 'picks.' This would invariably create an overestimation of the deposit volume but may create a better visual 3D model for the deposit.

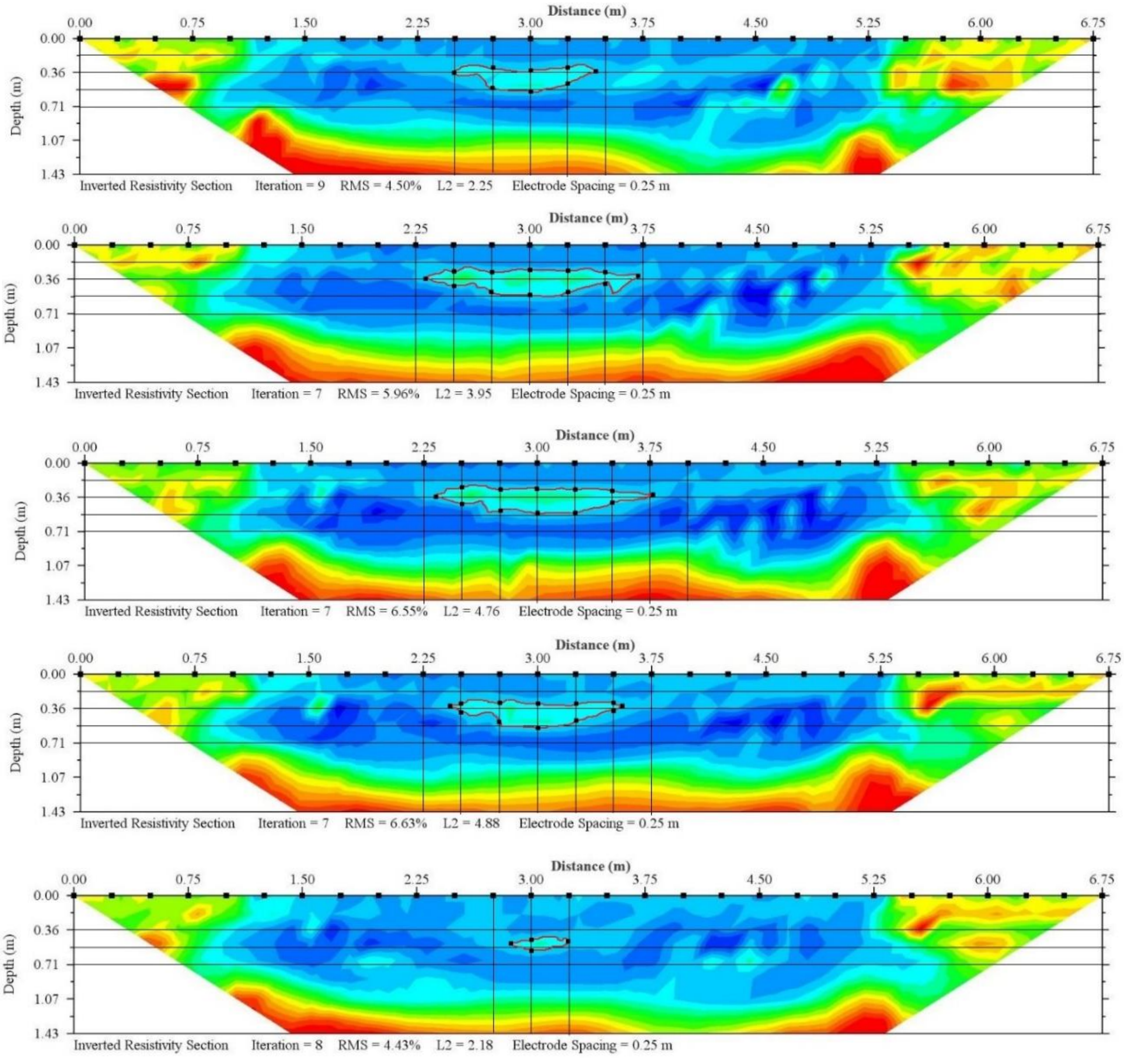

Figure 5.22 Electrical resistivity wet survey lines 2 to 6 illustrating the circled and re-picked deposit

5.5.2.2 Dry Survey Results

The dry survey results varied markedly from the wet survey (Figure 5.23).

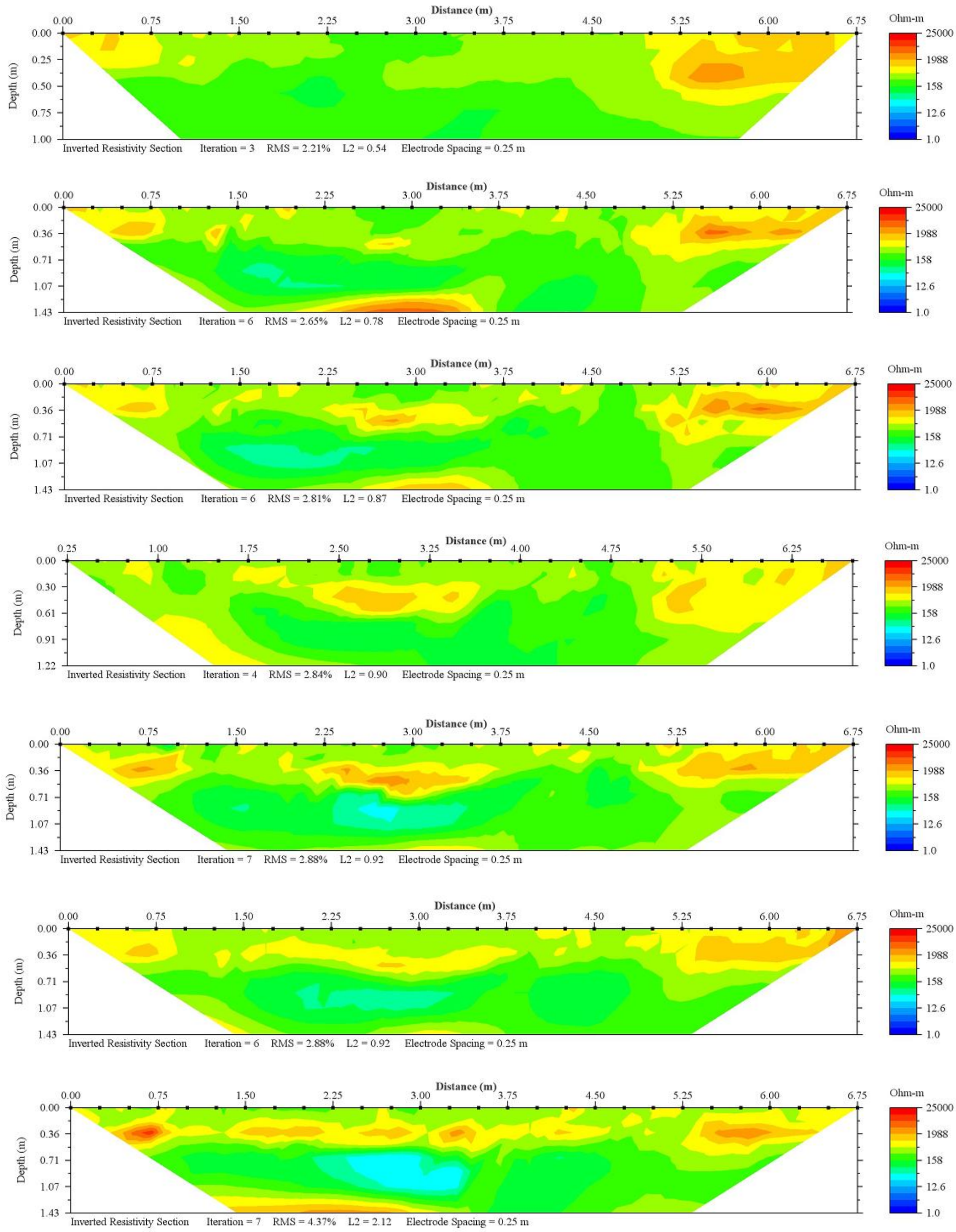

Figure 5.23 Electrical resistivity dry survey lines 1 (top) to 7 (bottom).

The ground was significantly drier and this caused more contact resistance issues. To replicate the initial survey methods used during the wet survey, fresh water was applied to the electrodes instead of salt water. This was originally done to prevent excess salt levels affecting the GPR results but became irrelevant when it was discovered that the organic mix was already too conductive for the radar waves, leading to their dissipation. The method was retained, however, in order to replicate the initial survey methods. The dry sediment, even with the application of water to the electrodes, was highly resistive and contact errors were encountered during the recording of some of the lines though RMS percentages were still low.

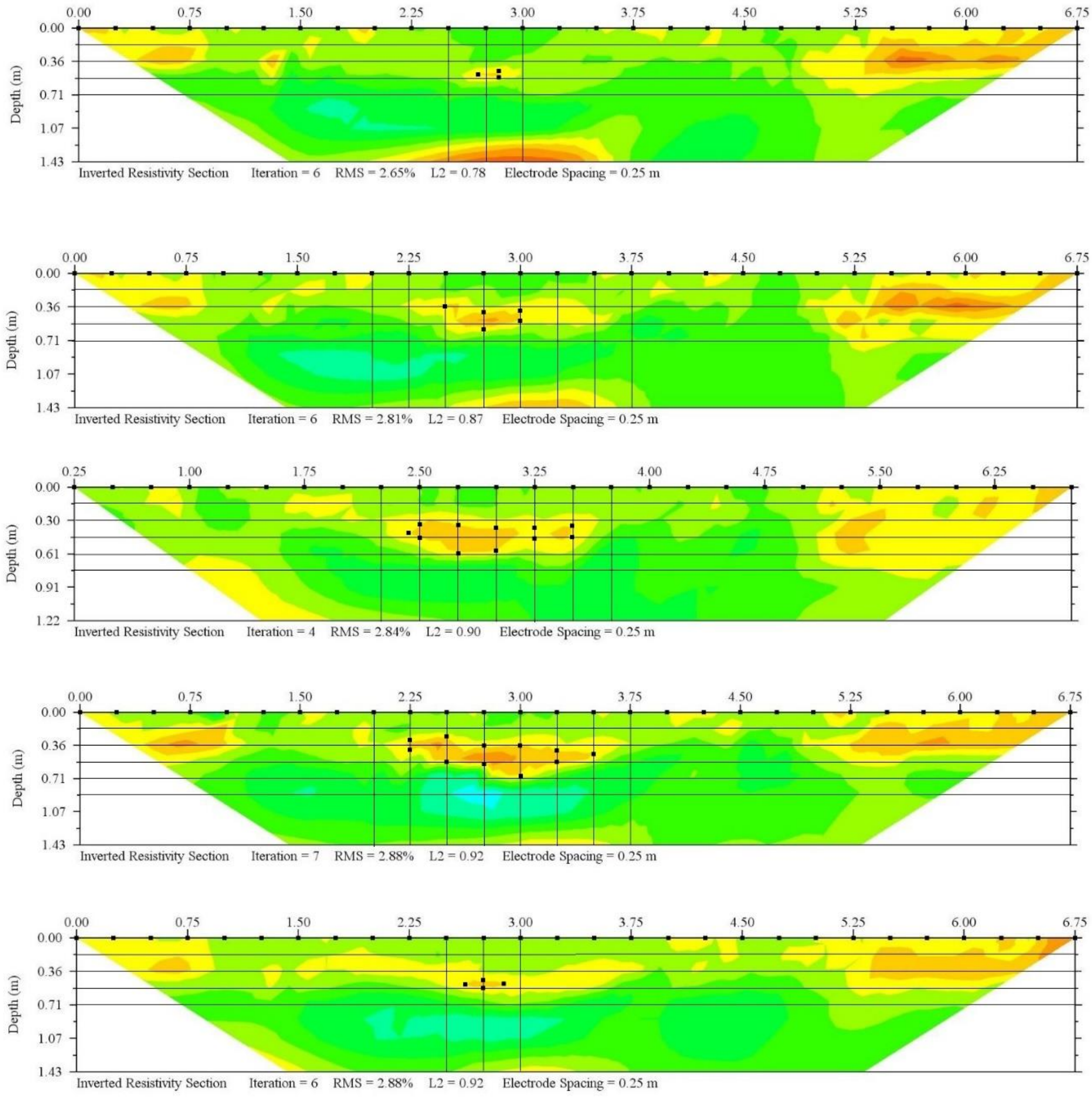

Figure 5.24 Electrical resistivity dry survey lines 2 to 6 illustrating the 'picked' deposit.

Like the wet survey results, patches of resistance in line 7 were disregarded due to the proximity of the trench wall though line 1 no longer exhibits these areas of higher resistance. The small areas of resistance in lines 2 and 6 were once again mapped as part of the shell matrix because of their relation to areas of resistance in lines 3 and 5. Like the wet survey results, the first interpretation round ‘picked’ only the areas of highest resistance (Figure 5.24) then a second round of modelling was created from ‘picks’ of the surrounding higher resistance area as well (Figure 5.25). The resistance values differed from the wet survey results, now registering as about 2,000Ω-m instead of 158Ω-m with the surrounding area at around 1,000Ω-m instead of 50Ω-m.

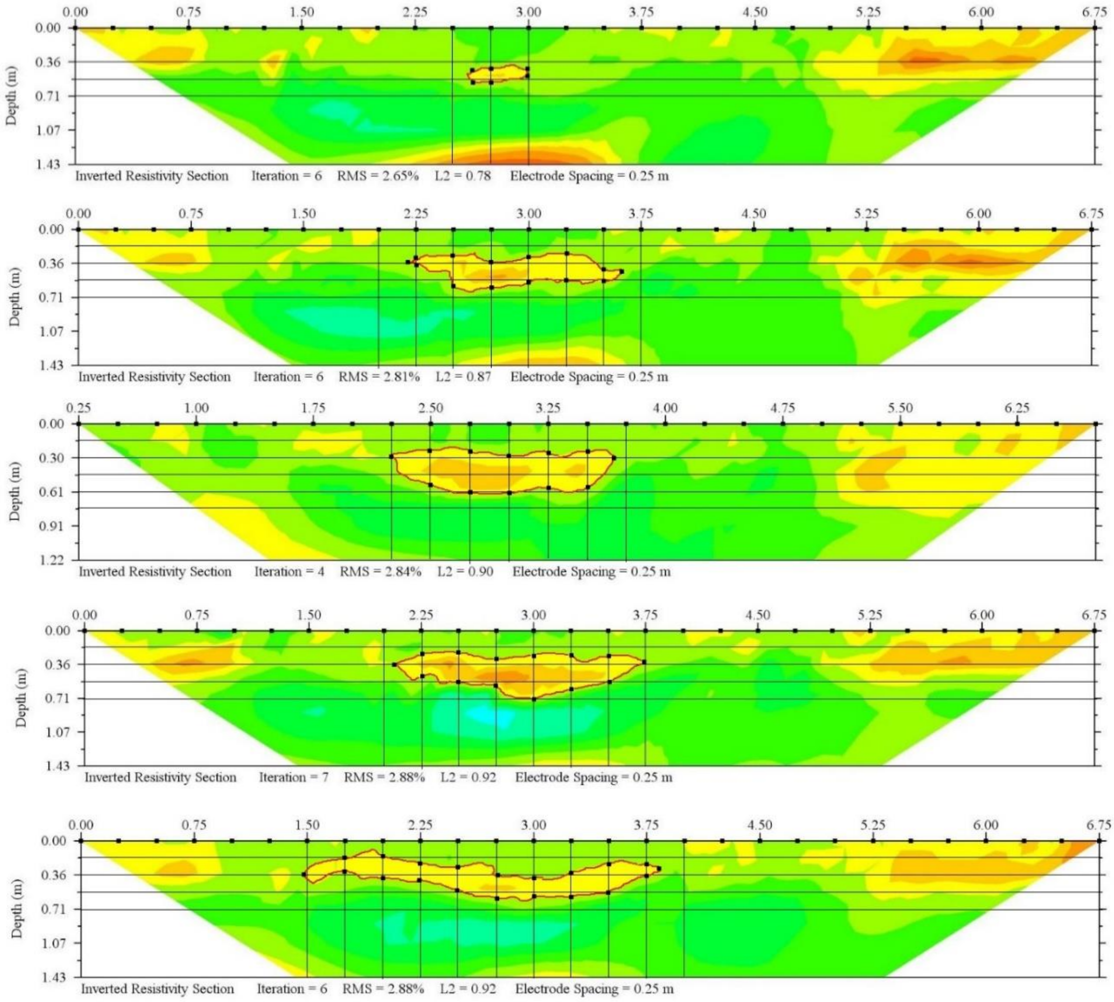

Figure 5.25 Electrical resistivity dry survey lines 2 to 6 illustrating the circled and re-picked deposit.

5.6 Three-Dimensional Mapping and Volume Results

By mapping the ‘picks’ for Trench 1 and 2 into ArcScene, 3D models of the buried shell deposits were created. The 3D models based on the GPR results for Trench 1 and the results for the first round of electrical resistivity ‘picks’ for Trench 2 are depicted in Figures 5.26 to 5.27.

Figure 5.26 Top and side view of shell matrix deposits for Trench 2 (left) and 1 (right) as modelled from wet survey results.

Figure 5.27 Top and side view of shell matrix deposits for Trench 2 (left) and 1 (right) as modelled from dry survey results.

This first round of electrical resistivity results was then compared to the second round of ‘pick’ results (Figures 5.28 to 5.29). This second interpretation round created larger 3D models that were slightly more representative of the actual in-ground deposit.

Figure 5.28 View of the top and sides of Trench 2 shell matrix deposits from electrical resistivity round two results (left) compared to round one results (right), modelled from the wet survey results.

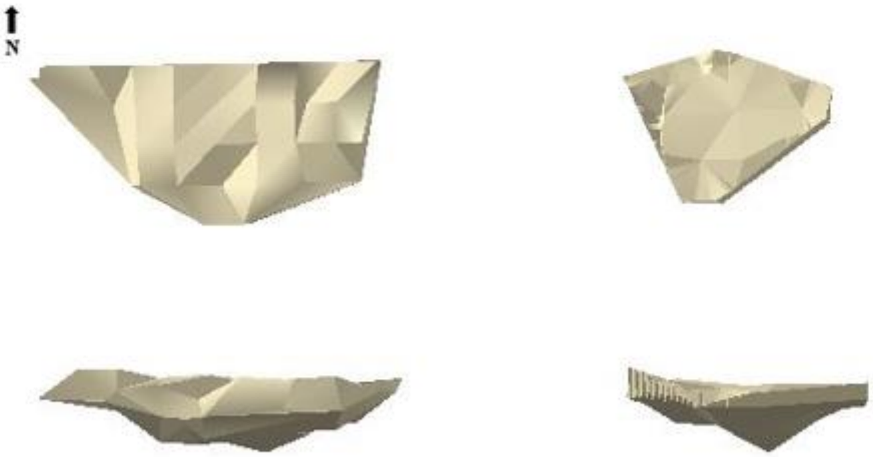

Figure 5.29 View of the top and sides of Trench 2 shell matrix deposits from electrical resistivity round two results (left) compared to round one results (right), modelled from the dry survey results.

From ArcScene, volume estimates were also calculated (Table 5.5). These geophysical volume estimates were then compared to a volume estimate based on the area the shell occupied when deposited, which came to 0.15m³. The total shell matrix volume for Trench 1, based off the GPR results, was calculated to be 0.19m³ for the wet and 0.16 m³ for the dry survey. The total for Trench 2, based off the first round of electrical resistivity 'picks', was 0.19m³ for the wet and 0.11 m³ for the dry survey. The second round of 'picks' produced estimates of 0.32 m³ for the wet and 0.17 m³ for the dry survey. With the exception of the round one electrical resistivity dry survey estimate (which was a 26% underestimate), all the volume results were overestimated.

Table 5.5 Trench 1 and 2 volume calculation results compared to volume of shell placed in the ground; for survey lines at 25cm.

Experimental Trench	Shell Matrix Volume (m³) Based on Geophysical Survey Results	Shell Matrix Volume (m³) Based on Size of Shell Deposit Placed in the Ground	Modelling Compared to Ground Truthed Volume (m³)	Error Percentage
Trench 1 (GPR) Wet	0.19	0.15	+0.04	26% (Overestimate)
Trench 1 (GPR) Dry	0.16	0.15	+0.01	6% (Overestimate)
Trench 2 Round 1 (ER) Wet	0.19	0.15	+0.04	26% (Overestimate)
Trench 2 Round 1 (ER)Dry	0.11	0.15	-0.04	26% (Underestimate)
Trench 2 Round 2 (ER)Wet	0.32	0.15	+0.17	113% (Overestimate)
Trench 2 Round 2 (ER)Dry	0.17	0.15	+0.02	13% (Overestimate)

These initial results were then compared to results produced by a survey with a 50cm transect spacing instead of the ideal 25cm. To create these 50cm survey results, every other line was removed from the processing. For the electrical resistivity only lines 2, 4 and 6 now contributed to the modelled results while for the GPR, lines 2, 4, 6 and 8 were used (though 8 had no shell deposit and did not contribute to the modelled results). These new results were then used to produce both 3D models (Figures 5.30 to 5.33) and volume estimates of the deposit (Table 5.6). The 3D models for the first round of electrical resistivity and for the GPR results are presented together in Figures 5.30 and 5.31, then the second round of electrical resistivity interpretation is compared to the first in Figures 5.32 and 5.33.

Figure 5.30 Top and side view of shell matrix deposits for Trench 2 (left) and 1 (right) as modelled from 50cm wet survey results.

Figure 5.31 Top and side view of shell matrix deposits for Trench 2 (left) and 1 (right) as modelled from 50cm dry survey results.

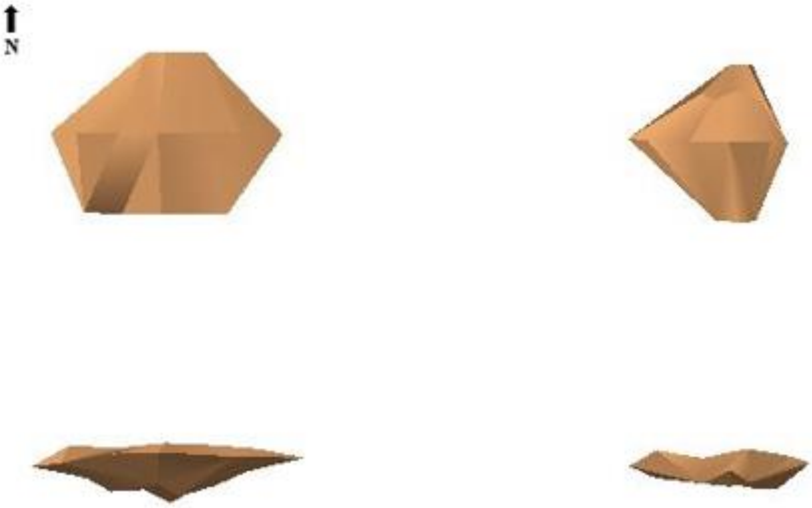

Figure 5.32 View of the top and sides of Trench 2 shell matrix deposits from electrical resistivity round two results (left) compared to round one results (right), modelled from the 50cm wet survey results.

Figure 5.33 View of the top and sides of Trench 2 shell matrix deposits from electrical resistivity round two results (left) compared to round one results (right), modelled from the 50cm dry survey results.

The volume estimate results produced from the 50cm survey vary significantly from those produced from the 25cm survey. The GPR volume estimates now closely match the in-ground deposit values; with the wet survey returning an estimate of 0.15m³ matching the actual deposit and dry survey results at 0.14m³ just slightly underestimating the deposit. Meanwhile, the electrical resistivity results now significantly underestimate the volume of the deposit for the first interpretation round and drop from a 113% to an 86% overestimate for the wet survey results in the second round of interpretation and from a 13% overestimate to a 13% underestimate for the dry survey results.

Table 5.6 Trench 1 and 2 volume calculation results compared to volume of shell placed in the ground; for survey lines at 50cm.

Experimental Trench	Shell Matrix Volume (m³) Based on Geophysical Survey Results	Shell Matrix Volume (m³) Based on Size of Shell Deposit Placed in the Ground	Modelling Compared to Ground Truthed Volume (m³)	Error Percentage
Trench 1 (GPR) Wet	0.15	0.15	0.00	0%
Trench 1 (GPR) Dry	0.14	0.15	-0.01	6% (Underestimate)
Trench 2 Round 1 (ER) Wet	0.04	0.15	-0.11	73% (Underestimate)
Trench 2 Round 1 (ER)Dry	0.07	0.15	-0.08	53% (Underestimate)
Trench 2 Round 2 (ER)Wet	0.28	0.15	+0.13	86% (Overestimate)
Trench 2 Round 2 (ER)Dry	0.13	0.15	-0.02	13% (Underestimate)

To create detailed confidence intervals for these survey results, the error percentages for all the surveys were included (wet and dry, 25cm and 50cm line spacing); all confidence intervals presented have been rounded to the nearest 0.5%. With a confidence level of 95%, the margin of error on the error experienced during surveys is 9.5%±15.5% for the GPR, 44.5%±31.5% for the first round of electrical resistivity interpretation and 56±70.5% for the second round. As with the field site results, the upper range of these error margins (25%, 76% and 126.5% respectively) will be applied as an error margin for the volume results. Meaning the true volume results for the total shell deposit should typically fall within ±25% of the estimated volume produced from GPR survey results and ±76% for electrical resistivity survey results. For example, if looking at the dry survey results for the 50cm survey the true volume of the shell deposit should fall within $0.14m^3 \pm 0.03m^3$ for the GPR and $0.07m^3 \pm 0.05m^3$ for first round of electrical resistivity results and $0.13\ m^3 \pm 0.16m^3$ for the second round. As can be seen from the first round of electrical resistivity results, this volume estimate may not always incorporate the true value.

5.7 Discussion

The base shell layer in the experimental trenches was too small to differentiate from the signal produced by the base of the trench. For the electrical resistivity the problem appeared to be that the shell and the clay, like the shell and sand, were both highly resistive and too close to differentiate. For the dry survey GPR results the reflections off the hard-packed clay appears to have obscured any reflections from the small shell mass on top of it, while the wet survey appears to have suffered from attenuation by 1m in depth. The upper shell layer in both surveys (wet and dry) probably also helped obscure the lower deposit, though they did not fully overlap.

The 3D model of the GPR results for the upper shell deposit fairly accurately represents the shape of the actual in-ground mass for both the wet and dry surveys. However, this changed when the survey lines were moved out to a 50cm spacing, with the model edges becoming distorted. The volume error rates for the GPR surveys showed fairly precise and accurate results; except for the one outlier from the wet survey of a 26% overestimate the other estimates were 6%, 0% and -6%, although the lower error percentages for the 25cm dry survey was due to line 7 being considered too difficult to interpret and not being ‘picked.’ If this region of the deposit had been interpretable the volume estimate for the 25cm survey would have been larger, creating a more significant overestimation of the deposit volume. Thus the precision of the error rates was partially due to omitting line 7 from the 25cm dry survey, which brought the volume result closer to the 50cm survey results, as they too left out line 7 (using only lines 2, 4 and 6). The volume estimates created from the 50cm transect spacing were closer to the in-ground volume of the shell with the wet survey results producing 0%

error and the dry survey at just a 6% underestimate. As mentioned though, these volume estimate results were produced from a far more distorted 3D model of the deposits.

The electrical resistivity results exhibited less accuracy in both their 3D models and their volume estimates. The 3D models showed significant distortion compared to the actual shell deposit, though the second round of modelling was better than the first. Where the entire contiguous higher resistance area was circled and 'picked' a more accurate, though still distorted, 3D model was created. The volume estimates varied significantly and showed little precision or accuracy. Though these results were not highly accurate, the 3D models and volume estimates produced did still provide valuable information about the general size and shape of the buried shell deposit, allowing for a greater understanding of the buried matrix.

The moisture content of the surrounding sediment, as theorised, was found to have a noticeable effect on the geophysical surveys. The GPR survey results were clearer and more easily interpreted under the drier survey conditions producing a better 3D model and more accurate volume estimation; though there was some uncertainty around whether this was due to the drier ground or the re-setting of the Mala monitor. As mentioned, the accuracy of the volume estimate for the dry survey was also partially due to the absence of a discernible deposit edge in the 7th survey line. The electrical resistivity survey results were more visually distinct under the wetter survey conditions, but like the GPR, they produced the more accurate modelled results under the drier ground conditions.

5.8 SUMMARY

The results of the geophysical surveys for the experimental site varied greatly by method, as they did at the Thundiy field site. Similarly to the field site the electrical resistivity could not distinguish the resistive shell material from the highly resistive sand, while the GPR clearly shows a reflection off the upper shell deposit. Conversely the garden soil mix employed as a proxy for a more conductive environment produced uninterpretable GPR data, while the electrical resistivity data showed clearly distinguishable results. Neither geophysical method could distinguish the lower shell mass from the clay substrate it lay upon.

6 DISCUSSION AND CONCLUSIONS

6.1 INTRODUCTION

The application of geophysical survey methods to archaeological research has been steadily intensifying over the past 20 years. Geophysical methods have experienced great benefits from modern technological developments with survey equipment seeing rapid improvements that have made them more affordable, accessible and easier to deploy, while producing better data. The data produced from geophysical surveys has also benefited from improved processing software which allows for more detailed analyses of the results. These improvements have led to wider and more experimental applications of geophysical surveys. With more experimental surveying, the range of archaeological site types investigated with geophysical surveys has expanded and the data produced is being applied not only to finding features of archaeological interest but also in directly addressing research questions. This current research has joined the experimental surveying trend by investigating the application of GPR and electrical resistivity surveys, with the aim of enhancing the methodology by which shell matrix sites are studied.

In this final chapter a synthesis and closing analysis of the results produced from both the Thundiy field site and the experimental site are presented (see Section 6.2), followed by an evaluation of the viability of the methods proposed in this research (Section 6.3). The chapter then concludes the current research by revisiting the aims (Section 6.4), and outlining the limitations (Section 6.5) before discussing future research directions (Section 6.6), and presenting a final summary (Section 6.7).

6.2 SYNTHESIS AND DISCUSSION OF RESULTS

The results from the GPR surveys at Thundiy and for the experimental site showed the method to be advantageous, accurately characterising buried shell deposits and providing useful information about them. The Thundiy volume estimate results for Square D and the results for the cultural shell matrix for Squares A-C were highly accurate, but only once the initial misplacement of 'picks' for Squares A-C had been fixed. The initial 'picking' for the cultural shell deposits of Squares A-C overestimated the deposit by an average of 44.6%. A review of the profiles found the 'picks' had been incorrectly placed on a multiple instead of on the reflection representing the actual change. This mistake illustrates the importance of experience: what seemed like a small difference in 'pick' placement on the profile represented a large volume overestimate in the modelled results. The full (cultural and non-cultural) shell matrix for Squares A-C also overestimated the shell deposit compared to the excavated results (by an average of 53%), but this was due to the excavation squares not fully exposing the beachrock at the base so an overestimation was expected and the accuracy of the results cannot be fully examined. For the experimental site, the GPR results overestimated the volume in the initial 25cm survey, then dropped to an underestimation for the 50cm survey lines.

The GPR results were highly accurate. The total GPR error margin on the volume estimates was only 16%±11%; this includes the erroneously placed 'picks' but discounts the full shell deposit results for Squares A-C (as they were not fully ground truthed). Without the erroneously placed 'picks' from Thundiy, the error margin falls to 6.5%±7%, however it would be advisable to apply the larger error range of 16%±11% as a more accurate representation of the true error range on the GPR volume estimates. The 3D models also closely matched the in-ground deposits, but they started to experience errors when the edges were missed in the 50cm survey results for the experimental site. This finding demonstrates that from a research perspective, higher resolution surveys are desirable.

The electrical resistivity results had the benefit of easily identifiable anomalies in the pseudosections, but were more difficult to 'pick' than the GPR results. Because of this difficulty, two different methods of 'picking' were applied to the survey results so the methods could be compared. The first round of interpretation focused on isolating only on the areas of highest resistance in the region of the shell deposit, as this was deemed to likely be the more accurate representation of the highly resistive shell. The second round of interpretation was more inclusive of the entire region of the high resistance representing the shell deposit, though this would undoubtedly include some surrounding sediment as the processing software will have blurred the boundaries between shell and organic mix during inversion. The electrical resistivity results also differed markedly between the wet and dry surveys. The resistance values for the shell deposit changed from approximately 158Ω-m in the wet survey to 2,000Ω-m in the dry. This was possibly due to retention of water between the shells during the wet survey, bringing down their overall resistance values. This difference effected the volume results, with large variations between the wet and dry survey estimates, though similar 3D models were produced throughout.

The electrical resistivity surveys produced distorted 3D models and varying levels of volume estimate accuracy. The first round of interpretation exhibited quite accurate volume estimates for the 25cm survey, but these dropped to substantial (above 50%) underestimates of the volume for the 50cm survey results. The more inclusive, second round of interpretation for the electrical resistivity results, produced better (though still distorted) 3D models than the first. This second round of interpretation vastly overestimated the shell deposit volume for the wet survey, but created quite accurate volumes estimates for the dry survey. These results imply the second round of interpretation was a more volatile method under differing ground conditions, however the difference between the 25cm and 50cm survey results was smaller and more stable for this round of interpretation than for the first round. During the second round of interpretation the difference between error results for the 25cm and 50cm surveys changed by 27 percentage points for the wet survey (representing a 12.5% drop in the volume estimate from $0.32m^3$ to $0.28m^3$) and 26 percentage points for the dry survey (representing a 23.5% drop in volume estimate). For the first round the difference between error results for the 25cm and 50cm surveys changed by 99 percentage points for the wet survey (representing a 79% drop in the volume estimate) and 27 percentage points for the dry survey (representing a 40% drop).

The electrical resistivity volume results were not as accurate as the GPR results. The total error margin on the electrical resistivity volume estimates was 50%±29%, this confidence interval includes all survey variables and interpretation rounds. The 3D models were distorted compared to the in-ground deposits, though the second round of interpretation was less visually distorted than the first. Compared to the in-ground deposits the 3D models were also slightly more distorted when produced from the 50cm survey results than when produced from the 25cm survey. Once again, this finding demonstrates that higher resolution surveys are desirable.

Due to the nature of the methods employed in this research, with points interpolated via TIN models and with deposit boundaries ‘picked’ by visual interpretation which is open to variation, the resulting 3D models and volume estimates are not a fully accurate reflection of reality. The results from this study show how volume estimates can easily become inaccurate by a significant margin due to misinterpretation or, in the case of the electrical resistivity, due to changing ground conditions (wet to dry). While inaccuracies were experienced with the volume estimates the results produced were always broadly representative of the reality of the deposits, thus providing useful information and at times even being highly accurate. The 3D models were also accurate enough to provide useful information about the deposits, with the GPR results producing highly accurate depictions of the shape and structure of the buried matrix.

The nature of the geophysical methods employed mean they will be restricted to sites where the shell deposit is characteristic enough to identify it in contrast to the surrounding sediment. This will require a deposit substantive and distinct enough from the surrounding sediments for identification in the survey results. What constitutes a distinct shell matrix will vary depending on the technique employed and the environment the shell is situated in. For GPR it is important for a significant and sudden RDP change to occur between the shell matrix and the surrounding sediment (see Section 3.3.1). Shell material is often fairly bulky compared to surrounding deposits so for most shell matrices this should not be a problem. However, as the experimental site showed, where shell deposits sit on top of a sudden and distinct RDP change (like the clay bottom of the trench or in field settings bedrock) they can be obscured in the survey results. For electrical resistivity, the shell deposits need to be located in a low Ohm-m environment so the high Ohm-m levels of the shell can be distinguished from the surrounding sediment.

6.3 Viability of Volume Calculation Method and 3D Modelling

The methods employed in this research to create the volume calculations and 3D models of the buried shell matrix are novel to shell matrix research and even fairly novel to geophysical research. Because they are novel, their viability as research methods will be considered here. In choosing the specific methodology employed for this research the first steps were to identify the geophysical survey methods best suited to meeting the aims of this study, then to source a software capable of creating the desired 3D models and volume calculations.

An extensive literature review identified GPR and electrical resistivity as the most suitable geophysical methods. The current research found GPR to be the faster method in open environments and capable of differentiating sand and shell deposits where the electrical resistivity could not. Conversely, electrical resistivity can be deployed in environments with denser vegetation and it produced interpretable results in the highly conductive organic matrix of experimental Trench 2 where the GPR could not. These outcomes show the importance of choosing the method deployed based on the soil properties and vegetation coverage of the survey location. Once the appropriate method for a given site has been chosen and survey results generated, there are several major sources of error which can affect the results of the post-processing modeling (to create 3D models and volume estimates). These sources of error can be broken into two main categories: human error and system error.

In the initial collection phase human error is an ever-present possibility. Novice practitioners to the field of geophysics are likely to make a range of mistakes regarding, for example, the array configuration or antenna chosen and the settings applied in the field. Further error can be introduced into the results by misaligning electrodes or survey lines, so strict grid control is necessary.

The system errors produced by the geophysical methods are typically small to insignificant in the data, though this error can be large if compounded by user error during the survey set up and the data processing stages. The main source of system error is introduced to the data during the process of relating the survey readings back to their real world positions. For GPR this can occur during the migration process, in which the processing software accounts for velocity changes in the subsurface which result in reflections being recorded inaccurately and adjusts these reflections back to their real world positions. In electrical resistivity this error can be incorporated into the results during the inversion process, in which the apparent resistivity readings recorded from the field are related back to the true ground resistivity values via the inversion modelling. If the surveys are run correctly and the data is processed correctly these forms of error should be negligible.

In order to create the volume estimates and 3D models of individual buried deposits required for this research, another processing software had to be sourced. While the current range of geophysical processing software for GPR and electrical resistivity allow for the creation of 3D volumes of the full survey results, they do not allow individual deposits to be isolated nor do they provide volumetric estimates for the size of deposits surveyed. To accomplish these required tasks, Esri's ArcGIS suite, including ArcMap and ArcScene, was deemed the most practical software. ArcGIS software is widely available and popular across universities. This popularity makes ArcGIS software a reliable choice, as it is a staple software which is likely to be available to the researcher, and for which there is a large support base. However, while there are extensive help forums and guides for ArcGIS software, there is little information focused on post-processing geophysical data in ArcMap and ArcScene.

The literature review conducted for this study discovered only one reference for incorporating GPR data into ArcGIS software to model the results. Kristiansen's (2013) Master's thesis was written in Norwegian and translated to English via Google Translate. Although the translation was incomplete, what was gained in terms of general procedure required to create 3D models and volume calculations of GPR data in ArcScene (via processing in ArcMap) was highly valuable as this was the only reference. The method presented by Kristiansen had to be re-established based on information gained from Esri help forums, then applied not only to the GPR data but also to the electrical resistivity data.

Further error, both human and system, can be introduced to the results during the post-processing steps. In order to single out the deposit boundaries in the geophysical results and move these data points from the GPR and electrical resistivity processing software into the ArcGIS software, a visual interpretation is required in which the user manually marks the shell matrix boundaries. This visual interpretation contributes a source of subjective error to the resulting volume calculations. As marking (or picking) the boundaries is a subjective task it is likely to vary slightly upon replication and is open to misinterpretation of results by the analyst; though by employing a consistent and experienced user there should be minimal differences between visual interpretations and less error due to incorrect interpretation. This visual interpretation is, however, the more accurate method for interpreting survey results as an experienced user is more likely to be able to accurately follow a deposit boundary and distinguish it from noise than a quantitative system could.

With the georeferencing information collected separately to the geophysical survey lines further error can also be introduced through misattribution of specific georeferenced coordinates to their corresponding survey point. With a multitude of survey files comes a multitude of georeferenced coordinates to correctly attribute, making it important to keep track of which points relate to which coordinates and to double check the work. Error in the data can also be created by the interpolation between points of the TIN models, though with detailed topographical survey data these errors should be minimal.

6.4 Aims Revisited

The current research had three stated aims presented in the form of research questions to be addressed. Each of these questions is considered here in terms of how they were answered during the course of the research.

1. Can geophysical surveys accurately delineate and map the extent of buried shell matrix deposits in northern Australian contexts?

The surveys completed at the Thundiy field site indicate the potential for geophysical surveys to map buried shell matrices in northern Australian contexts, though results will vary. The GPR surveys conducted at Thundiy exhibited clear and interpretable results, allowing for an accurate delineation of the buried shell deposit boundaries, though some trouble was experienced with multiple reflections marking the base of the cultural shell. Conversely, the electrical resistivity could not differentiate the shell from the surrounding sandy sediment at Thundiy, though it did provide interpretable results when aimed at investigating the overall site composition. The experimental site results show the potential for electrical resistivity to map shell deposits in more organic-rich sediments, but determining the boundaries of the deposit in the survey results was found to be slightly more problematic than it was for the GPR results.

2. Can volume estimates and 3D models of the buried shell matrix be created based on the data obtained from the geophysical surveys and what methods are required to do so?

This study showed that it is possible to create volume estimates and 3D models of buried shell deposits based on geophysical survey data. Research into prior efforts at estimating the volume of a buried matrix from GPR and electrical resistivity survey data highlighted methods for doing so. Of particular use was Kristiansen's (2013) Master's thesis which detailed the process of creating volume estimations and 3D models of buried matrices in ArcGIS, based on GPR survey data. The methods detailed in Kristiansen's work formed the basis of the methods employed for this research, but was expanded upon to include processing of the electrical resistivity survey data. These methods have been detailed at length in Chapter 3 (see Section 3.5.3).

3. How accurate are these models and the volume estimates created from them?

The models showed that with the appropriate level of survey detail the GPR results can accurately represent the size, shape and structure of the buried matrix. The electrical resistivity results, as mentioned above, encountered more difficulty in definitively establishing the boundaries of the deposit and thus created less accurate 3D models. The volume estimates for the GPR results exhibited a total error margin of 16%±11%, while the electrical resistivity error margin for the volume estimates was 50%±29%.

The volume estimates for both the GPR and electrical resistivity showed variability when the level of survey detail was changed. For the small deposits in the experimental site, volume estimates for the electrical resistivity results dropped by amounts varying from 12.5% up to 79%, while the GPR results dropped by 12.5% for the dry survey and 21% for the wet survey. These changes were primarily caused by a loss of accuracy in delineating the deposit boundaries when the survey lines were placed further apart. For the GPR survey these results actually brought the volume estimates closer to the in-ground volume of the shell but they created less accurate 3D models of the shape of the deposit.

The GPR results for the field site revealed a fairly homogenous deposit, so survey detail had little effect on the volume calculation results. The largest difference was a drop of just 8.5% from the 50cm survey to the 1m survey volume estimate for Grid C. Changing the survey detail from lines every 50cm to lines every 1m and 5m showed that for this homogenous deposit it was more important, in that it created less variability in the results, to include the edges of the survey area or shell midden than it was to have higher density survey lines. The results from both the field site and experimental site show the importance of incorporating the edges of the deposit, and thus indicate that a higher resolution survey is favourable as it is likely to more accurately delineate the edges of a buried matrix.

6.5 Limitations of Research

This research was limited by the application of the methods to only one field site with a comparison to one experimental site. The research could benefit from being more widely reproduced under a range of conditions. This would be particularly beneficial for the electrical resistivity results as the method could not distinguish shell from sand in the field and so there was no comparison for the experimental results. As mentioned previously (see Section 3.6) the fieldwork could also have been improved by shifting some of the focus spent on the electrical resistivity surveys into collecting extra GPR data.

6.6 Direction for Future Research

The methods developed during this research were aimed at improving the way in which shell matrix sites are investigated. While these methods were mainly developed to aid in creating appropriate sampling regimes for excavation, they could be further used to gain a greater regional understanding of shell matrix sites. Defining and characterising different site types for a region can be problematic. Part of this problem is in understanding the size, shape and character of buried deposits, which can be addressed by utilising geophysical surveys to create 3D models of the deposit. The size and shape of buried shell matrices can be quickly and efficiently established with GPR, allowing for a more time- and cost-effective strategy for comparative regional studies. By combining geophysical surveys with limited excavation from which radiocarbon dates are obtained, changes in shell midden sizes and frequency both spatially and temporally can be investigated providing insight into site formation and spatial organisation.

The creation of 3D models could also aid in conservation efforts. By creating a better understanding of the matrix present, a better conservation strategy can be generated. Geophysical surveys (particularly GPR surveys) can be used to generate 3D models of the buried matrix, identify the palaeolandscapes on which they were deposited, note features of archaeological interest within shell deposits and can also add to our understanding of shell matrices, all without destroying a vulnerable archaeological site. With their potential to enhance regional studies and aid in conservation efforts, these methods represent a practical tool for creating the foundations of community-based management plans for vulnerable shell matrix sites.

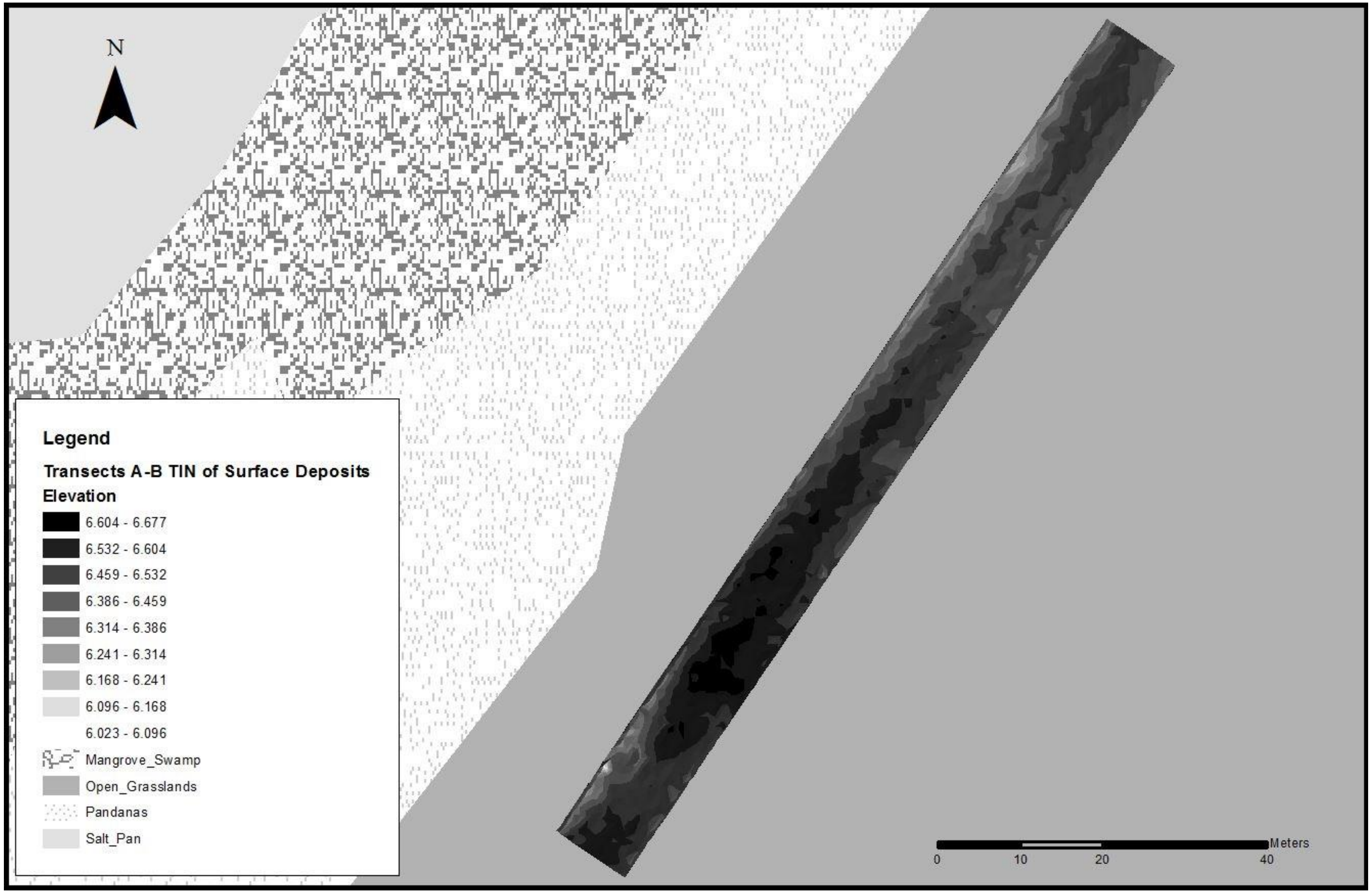

Figure 6.1 Thundiy shell deposits for Transects A and B based on GPR survey results, TIN marking the surface deposits of cultural shell is displayed (elevation is in meters above sea level).

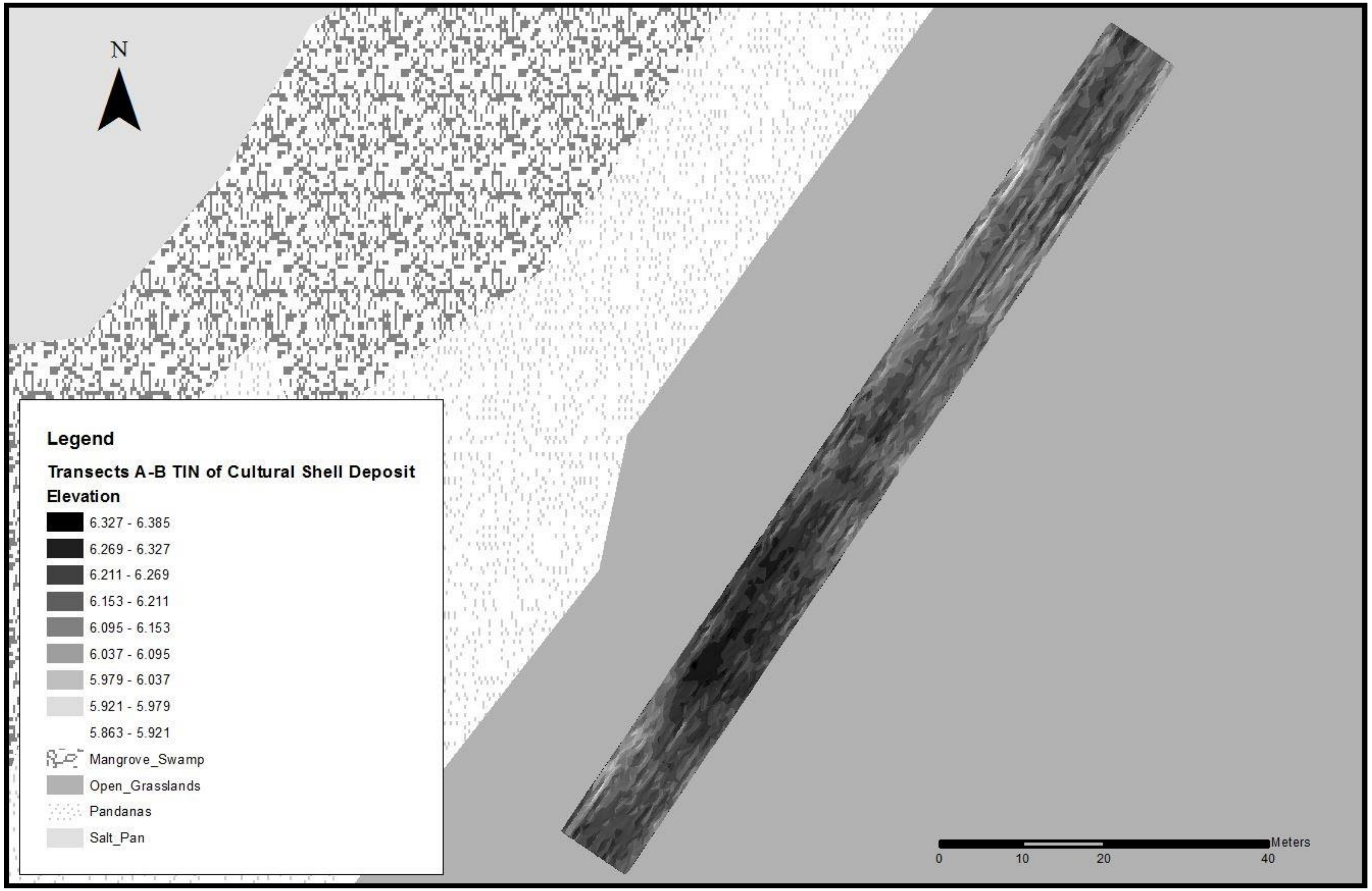

Figure 6.2 **Thundiy shell deposits for Transects A and B based on GPR survey results, TIN marking the base of the cultural shell is displayed (elevation is in meters above sea level).**

As well as the 3D models, the TIN models used to create the 3D models and the volume estimates can be mapped in relation to surrounding landscape features. These TINs provide further information about the exact spatial measurements of a shell matrix which could be used in conservation strategies. For example, Figure 6.1 depicts a TIN of the surface shell deposits at Thundiy in relation to the nearby pandanus palms and mangrove stand, while Figure 6.2 depicts the same mapped region but displays a TIN of the base of the anthropogenic shell deposits. The TINs map the precise height above sea level for different regions of the top (ground surface) and base of the anthropogenic shell matrix present at Thundiy. These maps represent a baseline from which the shell matrix at Thundiy could be monitored, for example if a cyclone caused damage to the site the degree of damage could be measured by taking new RTK readings of the ground surface, creating a new surface TIN, and comparing the new measurements to the old. Through this comparison a quantitative measure of the amount of shell matrix lost could be created. By situating the TINs in a map of the local landscape the map also allows for the tracking of landscape changes in the region of the shell matrix: if significant erosion or vegetation changes occurred the area could be re-mapped with the RTK and the results compared to previous maps allowing for a detailed monitoring of the changes.

6.7 SUMMARY

This research explored whether geophysical investigations of shell deposits could add to and aid the way we conduct shell matrix research. The aim was to conduct surveys of buried shell deposits under both field and experimental conditions, then create 3D models of the deposits and volume estimates of the shell mass. This thesis sets forth the processing steps required to map these deposits, and to create the volume estimates and 3D models. After initial processing in appropriate geophysical software programs and Microsoft Excel, Esri's ArcGIS suite of software was employed to convert the geophysical survey results into mapped models and volume estimates.

The novel methodology presented in this thesis successfully created volume estimates and visualised 3D models of buried shell matrices. Both geophysical methods produced results accurate enough, even with mistakes in interpretation, to address sampling questions and guide the placement of excavations. While these methods can provide useful information about buried shell matrices prior to excavation, it is recommended they are used in conjunction with excavation to ground truth the results. The many potential sources of error listed in Section 6.3 as well as varying ground conditions and interpretation strategies or mistakes can create significant variations in the modelled results and illustrate the importance of ground truthing so that the survey and modelled results can be compared to the reality of the deposit. When used in conjunction with excavation the methods can provide a detailed understanding of the overall population from which the excavated samples were taken, thereby improving shell matrix research. The field results also revealed how geophysical surveys can generate information regarding the palaeolandscapes on which deposits were laid. These results illustrate that despite generally held beliefs to the contrary, geophysical surveys can successfully produce information in relation to Indigenous Australian sites. There is a high level of potential benefits to be gained by applying these methods more widely in Australia.

References Cited

Advanced Geosciences, Inc. 2003 *Instruction Manual for the MiniSting™ and the Swift™*. Austin, Texas: Advanced Geosciences, Inc.

Advanced Geosciences, Inc. 2009 *Instruction Manual for EarthImager 2D: Resistivity and IP Inversion Software (Version 2.4.0)*. Austin, Texas: Advanced Geosciences, Inc.

Ai, S., Z. Wang, E. Dongchen, K. Holmen, Z. Tan, C. Zhou and W. Sun 2014 Topography, ice thickness and ice volume of the glacier Pedersenbreen in Svalbard, using GPR and GPS. *Polar Research* 33:1-8.

Ambrose, W.R. 1967 Archaeology and shell middens. *Archaeology and Physical Anthropology in Oceania* 2(3):169-187.

Annan, A.P. 2002 GPR - History, trends, and future developments. *Subsurface Sensing Technologies and Applications* 3(4):253-270.

Arias, P., M. Diniz, M. Cubas, C. Duarte, E. Iriarte, C. Salzmann, F. Teichner and L. Teira In Press Looking for the traces of the last huntergatherers: Geophysical survey in the Mesolithic shell middens of the Sado valley (southern Portugal). *Quaternary International*, Available online 3 March 2016.

Arnold, J.E., E.L. Ambos and D.O. Larson 1997 Geophysical surveys of stratigraphically complex island California sites: New implications for household archaeology. *Antiquity* 71(271):157-168.

Aspinall, A., C. Gaffney and L. Conyers 2008 Archaeological prospection - The first fifteen years. *Archaeological Prospection* 15(4):241-245.

Attenbrow, V. 1992 Shell bed or shell midden. *Australian Archaeology* 34:3-21.

Australian Government Bureau of Meteorology 2015a *Climate Statistics for Australian Locations: Sweers Island*. Retrieved 12 March 2015 from <http://www.bom.gov.au/climate/averages/tables/cw_029139.shtml>.

Australian Government Bureau of Meteorology 2015b *Climate Statistics for Australian Locations: Cairns AERO*. Retrieved 16 April 2015 from <http://www.bom.gov.au/climate/averages/tables/cw_031011.shtml>.

Bailey, G.N. 1975 The role of molluscs in coastal economies: The results of midden analysis in Australia. *Journal of Archaeological Science* 2(1):45-62.

Bailey, G.N., K. Hardy and A. Camara 2013 Shell energy: An introduction. In G.N. Bailey, K. Hardy and A. Camara (eds), *Shell Energy: Prehistoric Coastal Resource Strategies*, pp.1-6. Oxford, UK: Oxbow Books.

Balbo, A., M. Madella, I.B. Godino and M. Álvarez 2011 Shell midden research: An interdisciplinary agenda for the Quaternary and social sciences. *Quaternary International* 239(1):147-152.

Baojuan, H., L. Zhongqin, W. Feiteng, W. Wenbin, W. Puyu and L. Kaiming 2015 Glacier volume estimation from ice-thickness data, applied to the Muz Taw glacier, Sawir Mountains, China. *Environmental Earth Sciences* 74(3):1861-1870.

Barker, B. 2004 *The Sea People: Late Holocene Maritime Specialisation in the Whitsunday Islands, Central Queensland.* Terra Australis 20. Canberra: Pandanus Books, Research School of Pacific and Asian Studies, Australian National University.

Barker, R.D. 1979 Signal contribution sections and their use in resistivity studies. *Geophysical Journal International.* 59(1):123-129.

Berzins, V., U. Brinker, C. Klein, H. Lubke, J. Meadows, M. Rudzite, U. Schmolcke, H. Stumpel and I. Zagorska 2014 New research at Rinnukalns, a Neolithic freshwater shell midden in northern Latvia. *Antiquity* 88(341):715-732.

Best, A. 2012 The Aboriginal material culture of the Wellesley Islands and adjacent mainland coast, Gulf of Carpentaria: Social and environmental factors affecting variations in style. *Queensland Archaeological Research* 15:1-46.

Bevan, B.W. 2000 An early geophysical survey at Williamsburg, USA. *Archaeological Prospection* 7(1):51-58.

Binder, D., E. Bruckl, K. Roch, M. Behm, W. Schoner and B. Hynek 2009 Determination of total ice volume and ice-thickness distribution of two glaciers in the Hohe Tauern region, eastern Alps, from GPR data. *Annals of Glaciology* 50(51):71-79.

Bird, E. 2008 *Coastal Geomorphology: An Introduction*. Hoboken: John Wiley & Sons, Ltd.

Bird, M. 1995 Coastal morphodynamics and the archaeological record: Further evidence from Upstart Bay, north Queensland. *Australian Archaeology* 40:57-58.

Bird, M. 1992 The impact of tropical cyclones on the archaeological record : An Australian example. *Archaeology in Oceania* 27(2):75-86.

Bowdler, S. 1983 Sieving seashells: Midden analysis in Australian archaeology. In G. Connah (ed.), *Australian Archaeology: A Guide to Field Techniques*, pp.135-144. Canberra: Australian Institute of Aboriginal Studies.

Bowdler, S. 2014 Shell middens and mollusks. In J. Balme and A. Paterson (eds), *Archaeology in Practice: A Student Guide to Archaeological Analyses (2)*, pp.361-384. Chichester, West Sussex: John Wiley & Sons, Inc.

Cannon, A. 2000a Assessing variability in Northwest Coast salmon and herring fisheries: Bucket-auger sampling of shell midden sites on the Central Coast of British Columbia. *Journal of Archaeological Science* 27(8):725-737.

Cannon, A. 2000b Settlement and sea-levels on the Central Coast of British Columbia: Evidence from shell midden cores. *American Antiquity* 65(1):67-77.

Cannon, A. 2013 Revealing the hidden dimensions of Pacific Northwest Coast shell middens. In G.N. Bailey, K. Hardey and A. Camara (eds), *Shell Energy: Prehistoric Coastal Resource Strategies*, pp.21-34. Oxford, UK: Oxbow Books.

Carpenter, K.E. and V.H. Niem (eds) 1998 *The Living Marine Resources of the Western Central Pacific - Seaweeds, Corals, Bivalves and Gastropods Vol. 1*. Rome: Food and Agriculture Organization of the United Nations.

Ceci, L. 1984 Shell midden deposits as coastal resources. *World Archaeology* 16(1):62-74.

Chadwick, W.J. and J.A. Madsen 2000 The application of ground-penetrating radar to a coastal prehistoric archaeological site, Cape Henlopen, Delaware, USA. *Geoarchaeology* 15(8):765-781.

Cheetham, P.N. 2008 Noninvasive subsurface mapping techniques, satellite and aerial imagery in landscape archaeology. In B. David and J. Thomas (eds), *Handbook of Landscape Archaeology*, pp.562-582. Walnut Creek, CA: Left Coast Press.

Claassen, C. 1991 Normative thinking and shell-bearing sites. *Archaeological Method and Theory* 3:249-298.

Claassen, C. 1998 *Shells*. New York: Cambridge University Press.

Clark, A.J. 1990 *Seeing Beneath the Soil: Prospecting Methods in Archaeology*. London: Batsford.

Colley, S.M. 1990 The analysis and interpretation of archaeological fish remains. *Archaeological Method and Theory* 2:207-253.

Colucci, R.R., E. Forte, C. Boccali, M. Dossi, L. Lanza, M. Pipan and M. Guglielmin 2015 Evaluation of internal structure, volume and mass of glacial bodies by integrated LiDAR and ground penetrating radar surveys: The case study of Canin Eastern Glacieret (Julian Alps, Italy). *Surveys in Geophysics* 36(2):231-252.

Connah, G., P. Emmerson and J. Stanley 1976 Is there a place for the proton magnetometer in Australian field archaeology? *Mankind* 10(3):151-155.

Conyers, L.B. 2004 *Ground-Penetrating Radar for Archaeology*. Plymouth, UK: AltaMira Press.

Conyers, L.B. 2009 Ground-penetrating radar for landscape archaeology: Method and applications. In S. Campana and S. Piro (eds), *Seeing the Unseen: Geophysics and Landscape Archaeology,* pp.245-256. Hoboken: Taylor and Francis.

Conyers, L.B. 2012 *Interpreting Ground-Penetrating Radar for Archaeology*. Walnut Creek, CA: Left Coast.

Conyers, L.B. and J. Leckebusch 2010 Geophysical archaeology research agendas for the future: Some ground-penetrating radar examples. *Archaeological Prospection* 17(2):117-123.

Coutts, P.J.F. 1966 Features of prehistoric campsites in Australia. *Mankind* 6(8):338-338.

Cresswell, H.P. 2002 The soil water characteristic. In H.P. Cresswell, N.J. McKenzie and K.J. Coughlan (eds), *Soil Physical Measurement and Interpretation for Land Evaluation*, pp.59-84. Melbourne: CSIRO Publishing.

Cresswell, H.P. and G.J. Hamilton 2002 Bulk density and pore space relations. In H.P. Cresswell, N.J. McKenzie and K.J. Coughlan (eds), *Soil Physical Measurement and Interpretation for Land Evaluation*, pp.35-58. Melbourne: CSIRO Publishing.

Dalan, R.A. 2008 A review of the role of magnetic susceptibility in archaeogeophysical studies in the USA: Recent developments and prospects. *Archaeological Prospection* 15(1):1-31.

Dalan, R.A. and S.K. Banerjee 1998 Solving archaeological problems using techniques of soil magnetism. *Geoarchaeology* 13(1):3-36.

Dalan, R.A., J.M. Musser and J.K. Stein 1992 Geophysical exploration of the shell midden. In J.K. Stein (ed.), *Deciphering a Shell Midden*, pp.43-59. San Diego, CA: Academic Press Inc.

Dickson, M.E., C.S. Bristow, D.M. Hicks, H. Jol, J. Stapleton and D. Todd 2009 Beach volume on an eroding sand-gravel coast determined using ground penetrating radar. *Journal of Coastal Research* 25(5):1149-1159.

Dougherty, A.J. and M.E. Dickson 2012 Sea level and storm control on the evolution of a chenier plain, Firth of Thames, New Zealand. *Marine Geology* 307:58-72.

Erlandson, J.M. and M.L. Moss 2001 Shellfish feeders, carrion eaters, and the archaeology of aquatic adaptations. *American Antiquity* 66(3):413-432.

Evans, N. 1995 *A Grammar of Kayardild: With Historical-Comparative Notes of Tangkic*. New York: Mouton de Gruyter.

Evans, N. 2008 People of the strand: The Kaiadilt of Bentinck Island. In N. Evans, L. Martin-Chew, P. Memmott (eds), *The Heart of Everything: The Art and Artists* *of Mornington & Bentinck Islands*, pp.54-59. Fitzroy, VIC: McCulloch & McCulloch Australian Art Books.

Esri 2012 *How Surface Difference works.* Retrieved 30 October 2015 from <http://resources.arcgis.com/EN/HELP/MAIN/10.1/index.html#/How_Surface_Difference_works/00q900000019000000/>

Faulkner, P. 2008 Patterns of chronological variability in occupation on the coastal margin of Blue Mud Bay. *Archaeology in Oceania* 43(2):81-88.

Flanagan Consulting Group 2010 *Cairns Campus Master Plan 2010*. Retrieved 14 April 2015 from < https://www.jcu.edu.au/__data/assets/pdf_file/0011/38000/Cairns-Master-Plan-2010.pdf>.

Flanagan Consulting Group. 2011 *Initial Assessment Report: Proposed Designation of Land for the Purposes of Community Infrastructure James Cook University Cairns Campus. Project Number: 1829-05 R-DM0098/November 2011*. Retrieved 14 April 2015 from <http://www.jcu.edu.au/estateoffice/static/R-DM0098%20Initial%20Assessment%20Report%20Final%20_LatestReleased_1_JCU_084324.pdf>.

Flinders, M. 1814 *A Voyage to Terra Australis.* 2 Vols. London: G. and W. Nicol.

Gaffney, C. 2008 Detecting trends in the prediction of the buried past: A review of geophysical techniques in archaeology. *Archaeometry* 50(2):313-336.

Gaffney, C. and J.A. Gater 2003 *Revealing the Buried Past: Geophysics for Archaeologists.* Stroud, UK: Tempus.

Gibbs, M. and D. Gojak 2009 Remote sensing in an urban Australian setting: An example from Dr H. J. Foley Rest Park, Sydney. *Australian Archaeology* 68:45-51.

Gill, E.D. 1948 Aboriginal kitchen middens and marine shell beds. *Mankind* 4(1):249-249.

Greenwood, R.S. 1961 Quantitative analysis of shells from a site in Goleta, California. *American Antiquity* 26(3):416-420.

Gutiérrez-Zugasti, I., S.H. Andersen, A.C. Araújo, C. Dupont, N. Milner and A.M. Monge-Soares 2011 Shell midden research in Atlantic Europe: State of the art, research problems and perspectives for the future. *Quaternary International* 239(1):70-85.

Hargrave, M.L. 2006 Ground truthing the results of geophysical surveys. In J.K. Johnson, M. Giardano and K.L. Kvamme (eds.), *Remote Sensing in Archaeology: An Explicitly North American Perspective*, pp.269-304. Tuscaloosa: University of Alabama Press.

Hargrave, M.L., L.E. Somers, T.K. Larson, R. Shields and J. Dendy 2002 The role of resistivity survey in historic site assessment and management: An example from Fort Riley, Kansas. *Historical Archaeology* 36(4):89-110.

Harrison, R. 2009 The archaeology of the Port Hedland coastal plain and implications for understanding the prehistory of shell mounds and middens in northwestern Australia. *Archaeology in Oceania* 44(S1):81-98.

Henderson, W.G., L.C. Anderson and C.R. McGimsey 2002 Distinguishing natural and archaeological deposits: Stratigraphy, taxonomy, and taphonomy of Holocene shell-rich accumulations from the Louisiana chenier plain. *PALAIOS* 17(2):192-205.

Hesse, A. 2000 Count Robert du Mesnil du Buisson (1895–1986), a French precursor in geophysical survey for archaeology. *Archaeological Prospection* 7(1):43-49.

James Cook University 2015 *Cairns Campus Map*. Retrieved 17 December 2015 from <https://maps.jcu.edu.au/>.

Kristiansen, J. 2013 Fra Natur Til Kart: Veien til 3D-modellering av en isfonn ved hjelp av GIS og geofysiske metoder. Master Thesis, Faculty of Social Sciences and Technology, Norges teknisk-naturvitenskapelige universitet, Trondhiem.

Kvamme, K.L. 2003 Geophysical surveys as landscape archaeology. *American Antiquity* 68(3):435-457.

Langley, M.C., C. Clarkson and S. Ulm 2011 From small holes to grand narratives: The impact of taphonomy and sample size on the modernity debate in Australia and New Guinea. *Journal of Human Evolution* 61(2):197-208.

Larsen, B.P., S.J. Holdaway, P.C. Fanning, T. Mackrell and J.I. Shiner 2015 Shape as an outcome of formation history: Terrestrial laser scanning of shell mounds from far north Queensland, Australia. *Quaternary International*, Available online 12 August 2015.

Lourandos, H. 1997 *Continent of Hunter-Gatherers: New Perspectives in Australian Prehistory*. Cambridge: Cambridge University Press.

Lourandos, H. and B. David 1998 Comparing long-term archaeological and environmental trends: North Queensland, arid and semi-arid Australia. *The Artefact* 21:105-114.

Lowe, K. 2010 *Archaeological Site Testing along the Mississippi Gulf Coast: Cultural Resources Investigations on Hancock and Harrison Counties Mississippi.* Baton Rouge, LA: Coastal Environments, Inc.

Lowe, K.M. 2012 Review of geophysical applications in Australian archaeology. *Australian Archaeology* 74:71-84.

Martindale, A., B. Letham, D. McLaren, D. Archer, M. Burchell and B.R. Schöne 2009 Mapping of subsurface shell midden components through percussion coring: Examples from the Dundas Islands. *Journal of Archaeological Science* 36(7):1565-1575.

Memmott, P. 1982 The South Wellesley Islands and the Kaiadilt: A History and Analysis of the Significance of the Land and its People. Unpublished manuscript, Aboriginal Data Archive, School of Architecture, University of Queensland.

Memmott, P., N. Evans, R.I. Robins and I. Lilley 2006 Understanding isolation and change in island human populations through a study of indigenous cultural patterns in the Gulf of Carpentaria. *Transactions of the Royal Society of South Australia* 130(1):29-47.

Memmott, P., E. Round, D. Rosendahl and S. Ulm 2016 Fission, fusion and syncretism: Linguistic and environmental changes amongst the Tangkic people of the southern Gulf of Carpentaria, Northern Australia In J.C. Verstraete and D. Hafner (eds), *Land and Language in Cape York Peninsula and the Gulf Country*, pp.105-136. Philadelphia: John Benjamins Publishing Company.

Moffat, I., L.A. Wallis, A. Beale and D. Kynuna 2008 Trialing geophysical techniques in the identification of open indigenous sites in Australia: A case study from inland northwest Queensland. *Australian Archaeology* 66:60-63.

Morrison, M. 2013 From scatter to mound: A new developmental model for shell mound sites at Weipa. *Queensland Archaeological Research* 16:165-184.

Moss, P., L. Mackenzie, S. Ulm, C. Sloss, D. Rosendahl, L. Petherick, L. Steinberger, L. Wallis, H. Heijnis, F. Petchey and G. Jacobsen 2015 Environmental context for late Holocene human occupation of the South Wellesley Archipelago, Gulf of Carpentaria, northern Australia. *Quaternary International* 385:136-144.

Mulvaney, D.J. and J. Kamminga 1999 *Prehistory of Australia*. St Leonards, NSW: Allen & Unwin.

Nagel, T., D. Rosendahl, Q. Hua, P. Moss, C. Sloss, F. Petchey and S. Ulm 2016 Extended residence times for foraminifera in a marine-influenced terrestrial archaeological deposit and implications for palaeoenvironmental reconstruction. *Journal of Archaeological Science: Reports* 5:25-34.

Navarro, F.J., A. Martín-Español, J.J. Lapazaran, M. Grabiec, J. Otero, E.V. Vasilenko and D. Puczko 2014 Ice volume estimates from ground-penetrating radar surveys, Wedel Jarlsberg Land Glaciers, Svalbard. *Arctic, Antarctic, and Alpine Research* 46(2):394-406.

Neal, A., J. Richards and K. Pye 2002 Structure and development of shell cheniers in Essex, southeast England, investigated using high-frequency ground-penetrating radar. *Marine Geology* 185(3):435-469.

Neal, A. and C.L. Roberts 2000 Applications of ground-penetrating radar (GPR) to sedimentological, geomorphological and geoarchaeological studies in coastal environments In J.R.L. Allen and K. Pye (eds), *Coastal and Estuarine Environments: Sedimentology, Geomorphology and Geoarchaeology* pp.139-171. Bath: Geological Society.

Nishimura, Y. 2001 Geophysical prospection in archaeology. In D.R. Brothwell and A.M. Pollard (eds), *Handbook of Archaeological Sciences*, pp.543-553. New York: John Wiley.

Nowroozi, A.A., G.R. Whittecar and J.C. Daniel 1997 Estimating the yield of crushable stone in an alluvial fan deposit by electrical resistivity methods near Stuarts Draft, Virginia. *Journal of Applied Geophysics* 38(1):25-40.

O'Connor, S. 1989 Contemporary island use in the west Kimberley, Western Australia, and its implications for archaeological site survival. *Australian Aboriginal Studies* 2:25-31.

O'Connor, S. and M. Sullivan 1994 Distinguishing middens and cheniers: A case study from the southern Kimberley, W. A. *Archaeology in Oceania* 29(1):16-28.

Oertle, A., M. Leavesley, S. Ulm, G. Mate and D. Rosendahl 2014 At the margins: Archaeological evidence for Macassan activities in the South Wellesley Islands, Gulf of Carpentaria. *Australasian Historical Archaeology* 32:64-71.

O'Neil, D.H. 1993 Excavation sample size: A cautionary tale. *American Antiquity* 58(3):523-529.

Oswin, J. 2009 *A Field Guide to Geophysics in Archaeology*. Chichester, UK: Springer Berlin Heidelberg.

Otvos, E.G. 2000 Beach ridges - Definitions and significance. *Geomorphology* 32(1):83-108.

Peck, H. 2016 The Application of Ecological Models and Trophic Analyses to Archaeological Marine Fauna Assemblages: Towards Improved Understandings of Prehistoric Marine Fisheries and Ecosystems in Tropical Australia. Unpublished PhD thesis, College of Arts and Society and Education, James Cook University, Cairns.

Pluckhahn, T.J., V.D. Thompson, N. Laracuente, S. Mitchell, A. Roberts and A. Sams 2009 *Archaeological Investigations at the Famous Crystal River Site (8cI1) (2008 Field Season), Citrus County, Florida.* Tampa: The University of South Florida.

Pluckhahn, T.J., V.D. Thompson and J.W. Rink 2016 Evidence for stepped pyramids of shell in the woodland period of eastern north America. *American Antiquity* 81(2):345-363.

Pluckhahn, T.J., V.D. Thompson and B.R. Weisman 2010 Toward a new view of history and process at Crystal River (8CI1). *Southeastern Archaeology* 29(1):164-181.

Poteate, A.S. and S.M. Fitzpatrick 2013 Testing the efficacy and reliability of common zooarchaeological sampling strategies: A case study from the Caribbean. *Journal of Archaeological Science* 40(10):3693-3705.

Prinz, R., A. Fischer, L. Nicholson and G. Kaser 2011 Seventy-six years of mean mass balance rates derived from recent and re-evaluated ice volume measurements on tropical Lewis Glacier, Mount Kenya. *Geophysical Research Letters* 38, L20502.

Przywolnik, K. 2002 Coastal sites and severe weather in Cape Range Peninsula, northwest Australia. *Archaeology in Oceania* 37(3):137-152.

Ramsey, C.B. 2009 Bayesian analysis of radiocarbon dates. *Radiocarbon* 51(1):337-360.

Reeves, J.M., A.R. Chivas, A. García, S. Holt, M.J.J. Couapel, B.G. Jones, D.I. Cendón and D. Fink 2008 The sedimentary record of palaeoenvironments and sea-level change in the Gulf of Carpentaria, Australia, through the last glacial cycle. *Quaternary International* 183(1):3-22.

Reimer, P.J., E. Bard, A. Bayliss, J.W. Beck, P.G. Blackwell, C.B. Ramsey, C.E. Buck, H. Cheng, R.L. Edwards, M. Friedrich, P.M. Grootes, T.P. Guilderson, H. Haflidason, I. Hajdas, C. Hatté, T.J. Heaton, D.L. Hoffmann, A.G. Hogg, K.A. Hughen, K.F. Kaiser, B. Kromer, S.W. Manning, M. Niu, R.W. Reimer, D.A. Richards, E.M. Scott, J.R. Southon, R.A. Staff, C. Turney and J. van der Plicht 2013 IntCal13 and Marine13 radiocarbon age calibration curves 0-50,000 years cal BP. *Radiocarbon* 55(4):1869-1887.

Reitz, E.J. and E.S. Wing 2008 *Zooarchaeology*. Cambridge: Cambridge University Press.

Reynolds, J.M. 2011 *An Introduction to Applied and Environmental Geophysics*. Hoboken: John Wiley & Sons.

Rodrigues, S.I., J.L. Porsani, P.C.F. Giannini, M. Fornari, T. Atorre, P. DeBlasis and D.M.G. Ruiz 2015 Radarfacies and sedimentological analysis: Study of sedimentary substrate from an archaeological site (shell mound), southern Brazil. *The Holocene* 25(8):1257-1270.

Rodrigues, S.I., J.L. Porsani, V.R.N. Santos, P.A.D. DeBlasis and P.C.F. Giannini 2009 GPR and inductive electromagnetic surveys applied in three coastal sambaqui (shell mounds) archaeological sites in Santa Catarina state, South Brazil. *Journal of Archaeological Science* 36(10):2081-2088.

Roksandic, M., S.M.F. Mendonca de Souza, D. Klokler, S. Eggers and M. Burchell 2014 Cultural dynamics of shell-matrix sites: Diverse perspectives on biological remains from shell mounds and shell middens. In M. Roksandic, S.M.F. Mendonca de Souza, S. Eggers, M. Burchell and D. Klokler (eds), *The Cultural Dynamics of Shell-Matrix Sites*, pp.xiii-xv. Albuquerque: University of New Mexico Press.

Romano, N. and A. Santini 2002 The soil solution phase In D.L. Sparks, R.W. Weaver, J.H. Dane, and G.C. Topp (eds), *Methods of Soil Analysis: Part 4 Physical Methods*, pp.721-738. Madison, Wisconsin: Soil Science Society of America.

Rosendahl, D. 2012 The Way it Changes Like the Shoreline and the Sea: The Archaeology of the Sandalwood River, Mornington Island, Southeast Gulf of Carpentaria, Australia. Unpublished PhD thesis, School of Architecture, The University of Queensland, Brisbane.

Rosendahl, D., K.M. Lowe, L.A. Wallis and S. Ulm 2014 Integrating geoarchaeology and magnetic susceptibility at three shell mounds: A pilot study from Mornington Island, Gulf of Carpentaria, Australia. *Journal of Archaeological Science* 49:21-32.

Rosendahl, D., S. Ulm, C. Sloss, L. Steinberger, F. Petchey, G. Jacobsen, E. Stock and R. Robins 2015 Mid-Holocene Aboriginal occupation of offshore islands in northern Australia? A reassessment of Wurdukanhan, Mornington Island, southern Gulf of Carpentaria, Australia. *Quaternary International* 385:145-153

Rosendahl, D., S. Ulm and M.I. Weisler 2007 Using foraminifera to distinguish between natural and cultural shell deposits in coastal eastern Australia. *Journal of Archaeological Science* 34(10):1584-1593.

Roth, W.E. 1901 The Carpentaria blacks. *The Observer*. 24 August 1901.

Roth, W.E. 1903 *A Report from Dr. W.E. Roth, Northern Protector of Aboriginals, Home Secretary's Department, to the Under Secretary, Department of Public Lands, Queensland*, *27 June 1903.* Unpublished report prepared for the Under Secretary, Department of Public Lands, Queensland.

Rowland, M.J. and S. Ulm 2012 Key issues in the conservation of the Australian coastal archaeological record: Natural and human impacts. *Journal of Coastal Conservation* 16(2):159-171.

Rucker, D.F., G.E. Noonan and W.J. Greenwood 2011 Electrical resistivity in support of geological mapping along the Panama Canal. *Engineering Geology* 117(1):121-133.

Sambuelli, L. and S. Bava 2012 Case study: A GPR survey on a morainic lake in northern Italy for bathymetry, water volume and sediment characterization. *Journal of Applied Geophysics* 81:48-56.

Sandmeier, K.J. 2012 *Refelexw Version 7.0: Windows™ 9x/2000/XP/7-Program for the Processing of Seismic, Acoustic or Electromagnetic Reflection, Refraction and Transmission Data.* Germany: Refelexw.

Santos, V.R.N., J.L. Porsani, C.A. Mendonça, S.I. Rodrigues and P.D. DeBlasis 2009 Reduction of topography effect in inductive electromagnetic profiles: Application on coastal sambaqui (shell mound) archaeological site in Santa Catarina state, Brazil. *Journal of Archaeological Science* 36(10):2089-2095.

Scollar, I., A. Tabbagh, A. Hesse and I. Herzog 1990 *Archaeological Prospecting and Remote Sensing*. New York: Cambridge University Press.

Shenkel, J.R. 1986 An additional comment on volume calculations and a comparison of formulae using several southeastern mounds. *Midcontinental Journal of Archaeology* 11(2):201-220.

Shiner, J.S., P.C. Fanning, S.J. Holdaway, F. Petchey, C. Beresford, E. Hoffman and B. Larsen 2013 Shell mounds as the basis for understanding human-environment interaction in far north Queensland, Australia. *Queensland Archaeological Research* 16:65-91.

Sloss, C., L. Nothdruft, S. Ulm, P. Moss, J. Shulmeister, J. Reeves, D. Rosendahl and L. Wallis 2011 *Holocene Sea-Level Change in the South Wellesley Islands, Gulf of Carpentaria, Australia: A Pilot Study*. Poster to INQUAXVIII Congress, Switzerland.

Smith, A. 2001 Shell midden analysis. In T. Murray (ed.), *Encyclopedia of Archaeology: History and Discoveries.* Santa Barbara, CA: ABC-CLIO.

Soil Science Society of America. 1997 *Glossary of Soil Science Terms*. Madison, Wisconsin: Soil Science Society of America.

Somers, L. 2006 Resistivity survey. In J.K. Johnson, M. Giardano and K.L. Kvamme (eds) *Remote Sensing in Archaeology: An Explicitly North American Perspective*, pp.119-130 Tuscaloosa: University of Alabama Press.

Sorant, P.E. and J.R. Shenkel 1984 The calculation of volumes of middens, mounds, and strata having irregular shapes. *American Antiquity* 49(3):599-603.

Speight, J.G. 2009 Landform. In National Committee of Soil and Terrain (ed.), *Australian Soil and Land Survey Field Handbook*, pp.15-55. Melbourne: CSIRO Publishing.

Starks, E.C. 1901 Synonymy of the fish skeleton. *Proceedings of the Washington Academy of Sciences* 3:507-539.

Stein, J.K. (ed.) 1992 *Deciphering a Shell Midden*. San Diego: Academic Press.

Steinberg, J.M., A.M. Gontz, H. Trigg, A. Lahey, and L. Aragon 2007 *Identification of Small, Near-Surface Buried Shell Middens with Conductivity on Shelter Island, NY*. Durham, New Hampshire: The Geological Society of America. Paper No. 22(2).

Tetegan, M., C. Pasquier, A. Besson, B. Nicoullaud, A. Bouthier, H. Bourennane, C. Desbourdes, D. King and I. Cousin 2012 Field-scale estimation of the volume percentage of rock fragments in stony soils by electrical resistivity. *Catena* 92:67-74.

Thompson, V.D. 2007 Articulating activity areas and formation processes at the Sapelo Island shell ring complex. *Southeastern Archaeology* 26(1):91-107.

Thompson, V.D., P.J. Arnold, T.J. Pluckhahn and A.M. Vanderwarker 2011 Situating remote sensing in anthropological archaeology. *Archaeological Prospection* 18(3):195-213.

Thompson, V.D. and T.J. Pluckhahn 2010 History, complex hunter-gatherers, and the mounds and monuments of Crystal River, Florida, USA: A geophysical perspective. *The Journal of Island and Coastal Archaeology* 5(1):33-51.

Thompson, V.D., M.D. Reynolds, B. Haley, R. Jefferies, J.K. Johnson and L. Humphries 2004 The Sapelo shell ring complex: Shallow geophysics on a Georgia sea island. *Southeastern Archaeology* 23(2):192-201.

Tindale, N.B. 1962 Geographical knowledge of the Kaiadilt people of Bentinck Island, Queensland. *Records of the South Australian Museum* 14(2):259-296.

Tindale, N.B. 1977 Further report on the Kaiadilt people of Bentinck Island, Gulf of Carpentaria, Queensland. In J. Allen, J. Golson and R. Jones (eds), *Sunda and Sahul: Prehistoric Studies in Southeast Asia, Melanesia and Australia*, pp.247-273. London: Academic Press.

Treganza, A.E. and S.F. Cook 1948 The quantitative investigation of aboriginal sites: Complete excavation with physical and archaeological analysis of a single mound. *American Antiquity* 13(4):287-297.

Ulm, S. 2002 Reassessing marine fishery intensification in southeast Queensland. *Queensland Archaeological Research* 13:79-96.

Ulm, S. 2006a *Coastal Themes: An Archaeology of the Southern Curtis Coast, Queensland* Terra Australis 24. Canberra, ACT: ANU E Press

Ulm, S. 2006b Australian marine reservoir effects: A guide to ΔR values. *Australian Archaeology* 63(1):57-60.

Ulm, S. 2013 'Complexity' and the Australian continental narrative: Themes in the archaeology of Holocene Australia. *Quaternary International* 285:182-192.

Van Heteren, S., D.M. FitzGerald, D.C. Barber, J.T. Kelley and D.F. Belknap 1996 Volumetric analysis of a New England barrier system using ground-penetrating-radar and coring techniques. *The Journal of Geology* 104(4):471-483.

Wang, P., Z. Li, W. Wang, H. Li and F. Wang 2014 Glacier volume calculation from ice-thickness data for mountain glaciers - A case study of glacier No. 4 of

Sigong River over Mt. Bogda, eastern Tianshan, Central Asia. *Journal of Earth Science* 25(2):371-378.

Waselkov, G.A. 1987 Shellfish gathering and shell midden archaeology. *Advances in Archaeological Method and Theory* 10:93-210.

Weill, P., B. Tessier, D. Mouazé, C. Bonnot-Courtois and C. Norgeot 2012 Shelly cheniers on a modern macrotidal flat (Mont-Saint-Michel bay, France) - Internal architecture revealed by ground-penetrating radar. *Sedimentary Geology* 279:173-186.

Whittaker, F.H. and J.K. Stein 1992 Shell midden boundaries in relation to past and present shorelines. In J.K. Stein (ed.), *Deciphering a Shell Midden*, pp.25-42. San Diego: Academic Press.

WoRMS Editorial Board 2014 World Register of Marine Species. Retrieved 11 October 2014 from <http://www.marinespecies.org>.

Yde, J.C., M.K. Gillespie, R. Loland, H. Ruud, S.H. Mernild, S. De Villiers, N.T. Knudsen and J.K. Malmros 2014 Volume measurements of Mittivakkat Gletscher, southeast Greenland. *Journal of Glaciology* 60(224):1199-1207.

APPENDIX A: GPR SURVEY RESULTS FOR THUNDIY

Raw geophysical survey files can be found at: http://dx.doi.org/10.4225/28/584755108d3dc

GPR Survey Results for Transect A-B

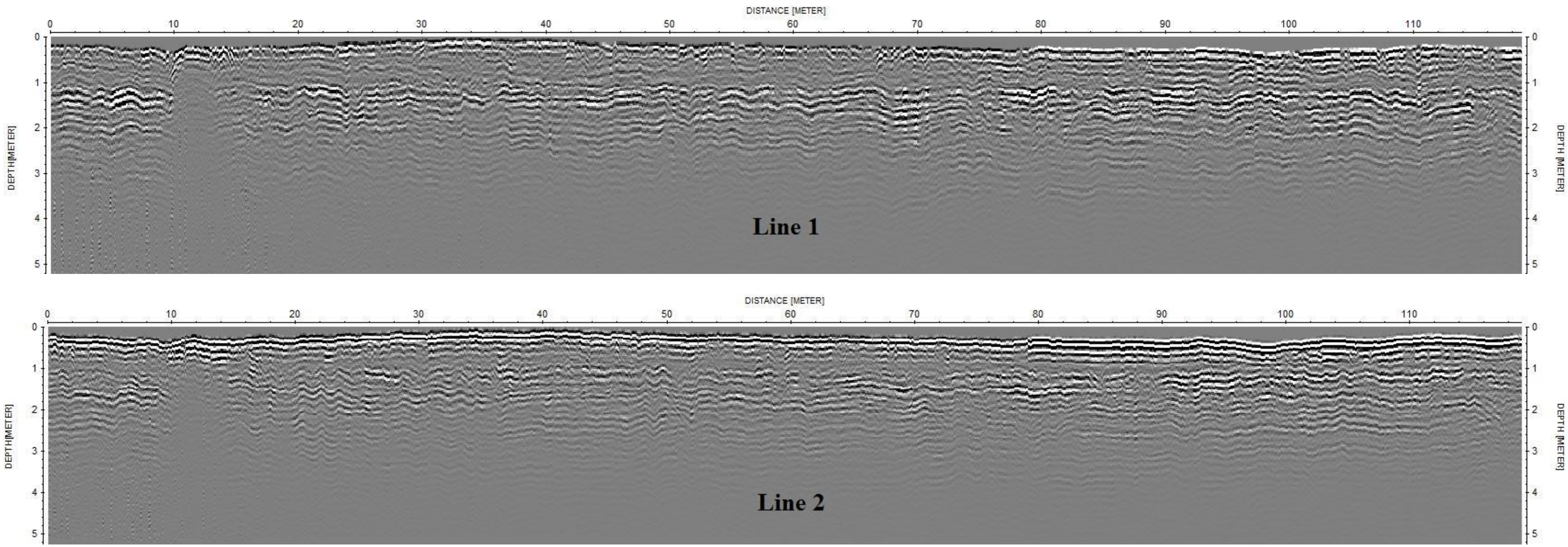

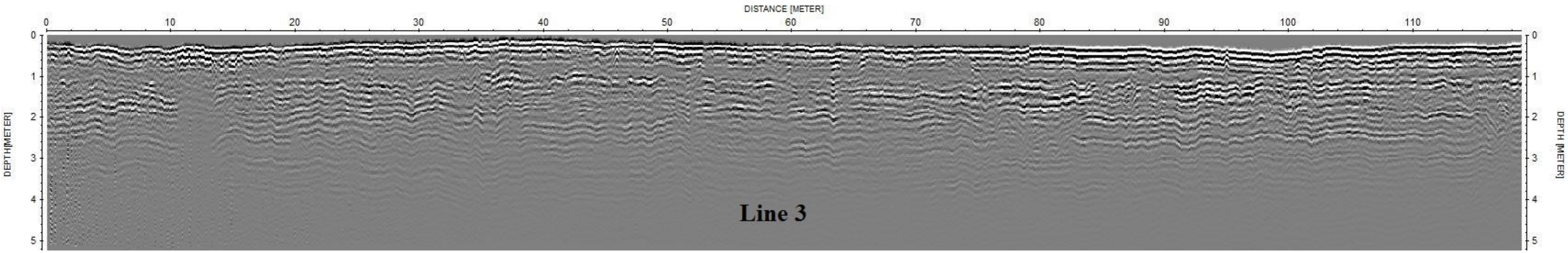
DISTANCE [METER]
0 10 20 30 40 50 60 70 80 90 100 110
DEPTH [METER]
0 1 2 3 4 5
Line 3

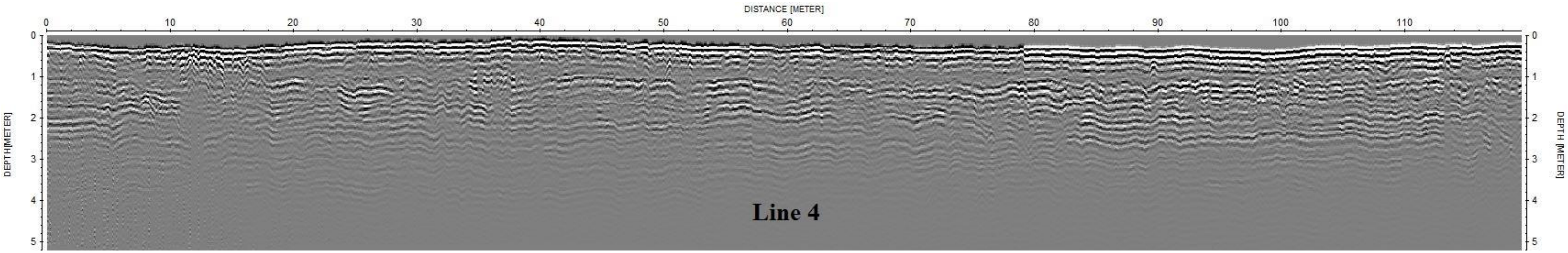
DISTANCE [METER]
0 10 20 30 40 50 60 70 80 90 100 110
DEPTH [METER]
0 1 2 3 4 5
Line 4

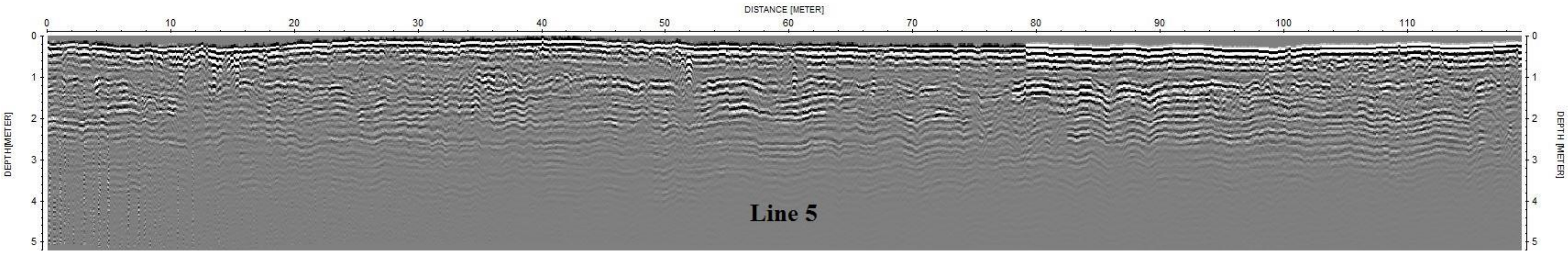
DISTANCE [METER]
0 10 20 30 40 50 60 70 80 90 100 110
DEPTH [METER]
0 1 2 3 4 5
Line 5

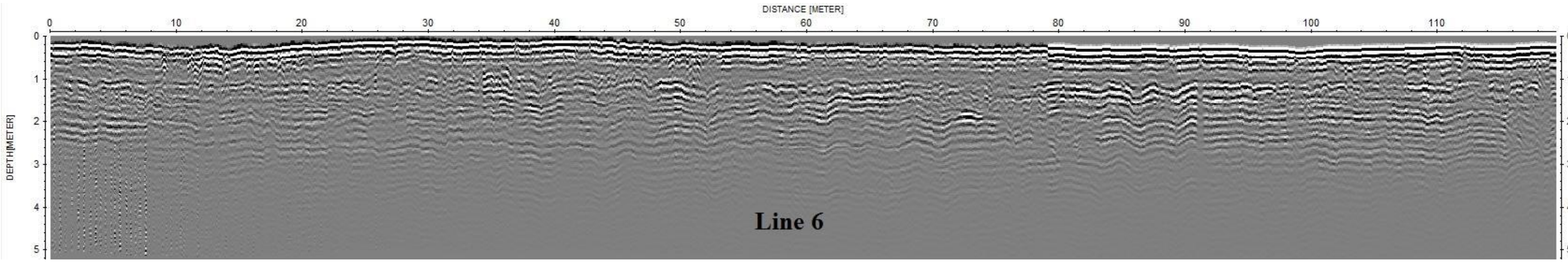
DISTANCE [METER]
0 10 20 30 40 50 60 70 80 90 100 110
DEPTH[METER]
DEPTH [METER]
0 1 2 3 4 5
Line 6

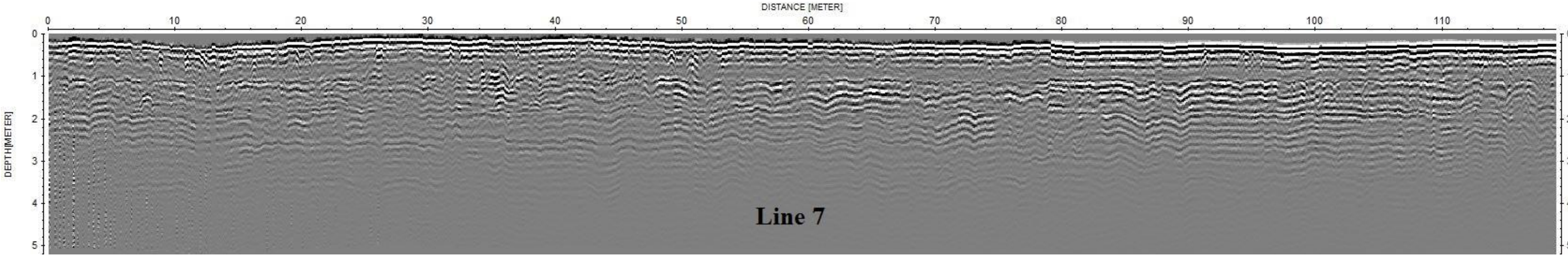
DISTANCE [METER]
0 10 20 30 40 50 60 70 80 90 100 110
DEPTH[METER]
DEPTH [METER]
0 1 2 3 4 5
Line 7

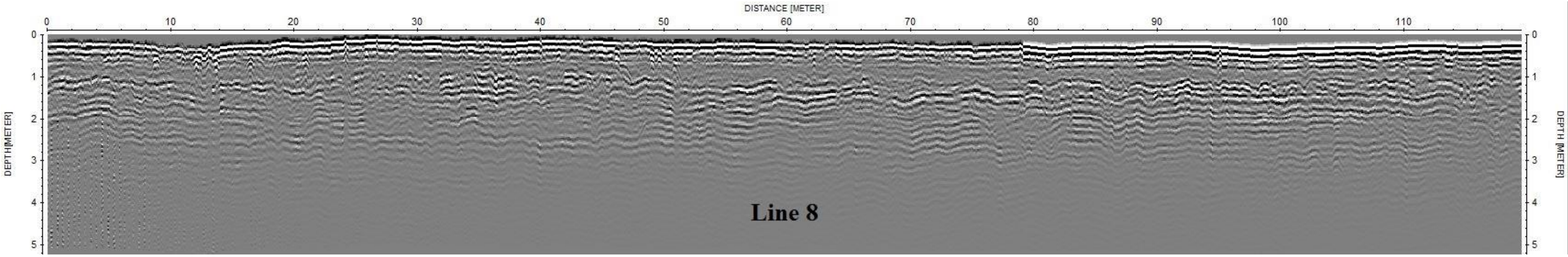
DISTANCE [METER]
0 10 20 30 40 50 60 70 80 90 100 110
DEPTH[METER]
DEPTH [METER]
0 1 2 3 4 5
Line 8

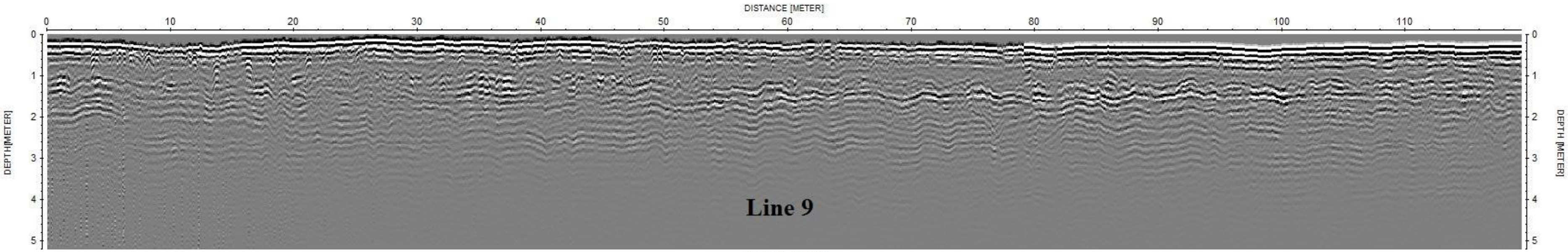
DISTANCE [METER]
0 10 20 30 40 50 60 70 80 90 100 110
DEPTH[METER]
0 1 2 3 4 5
DEPTH [METER]
Line 9

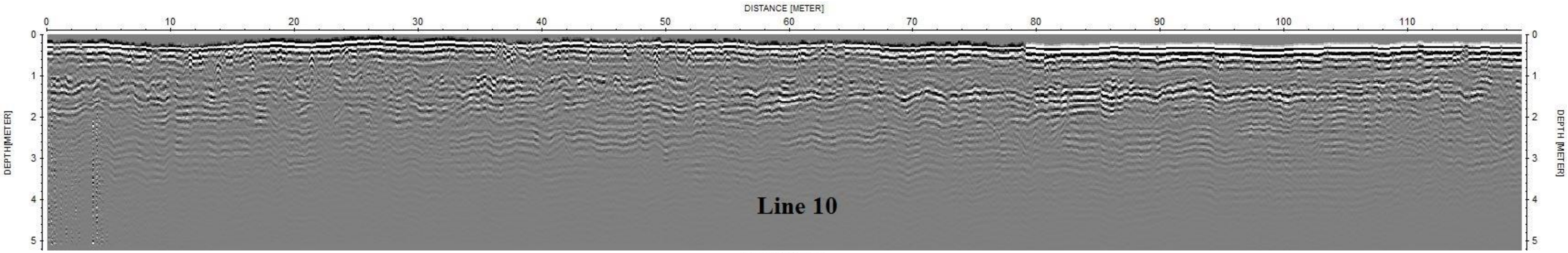
DISTANCE [METER]
0 10 20 30 40 50 60 70 80 90 100 110
DEPTH[METER]
0 1 2 3 4 5
DEPTH [METER]
Line 10

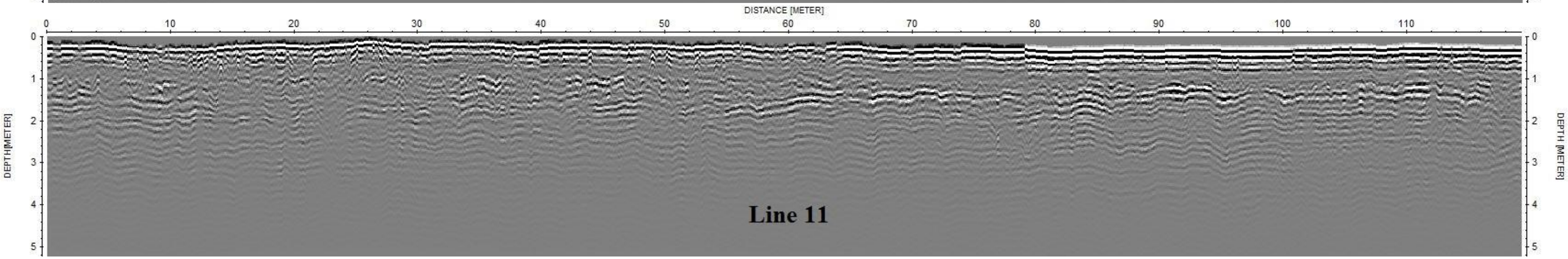
DISTANCE [METER]
0 10 20 30 40 50 60 70 80 90 100 110
DEPTH[METER]
0 1 2 3 4 5
DEPTH [METER]
Line 11

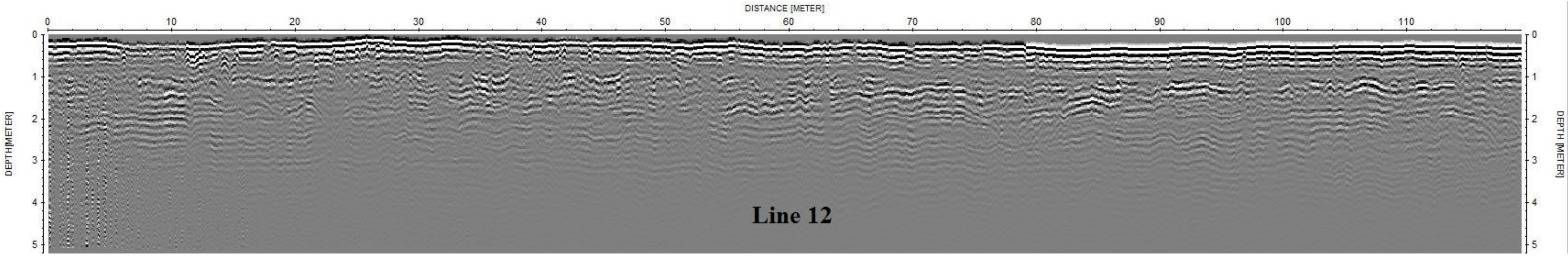
DISTANCE [METER]
0 10 20 30 40 50 60 70 80 90 100 110
DEPTH[METER]
0 1 2 3 4 5
DEPTH [METER]
Line 12

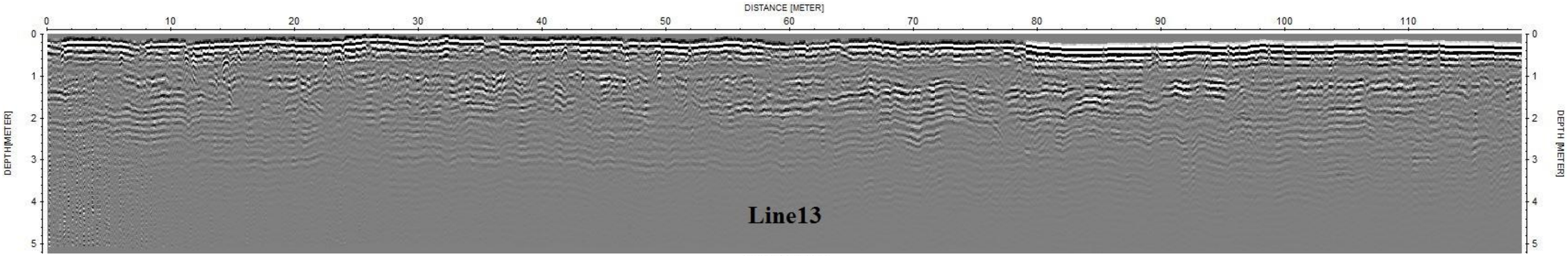
DISTANCE [METER]
0 10 20 30 40 50 60 70 80 90 100 110
DEPTH[METER]
0 1 2 3 4 5
DEPTH [METER]
Line13

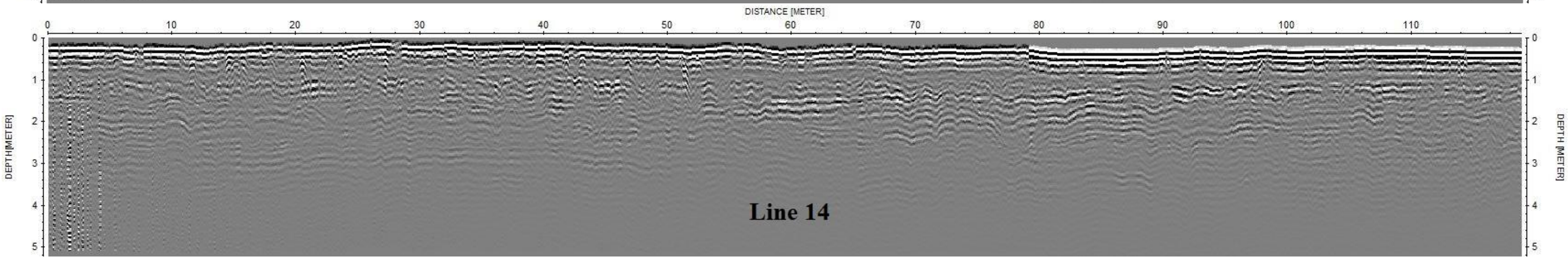
DISTANCE [METER]
0 10 20 30 40 50 60 70 80 90 100 110
DEPTH[METER]
0 1 2 3 4 5
DEPTH [METER]
Line 14

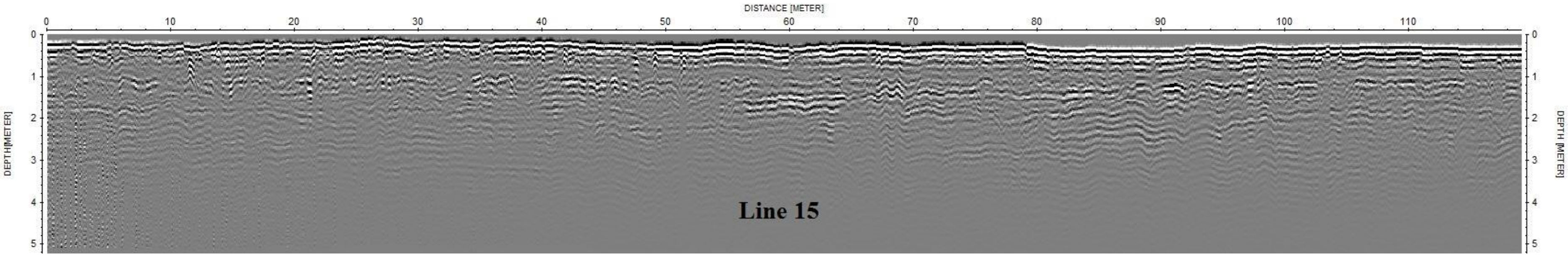
DISTANCE [METER]
DEPTH [METER]
DEPTH [METER]
Line 15

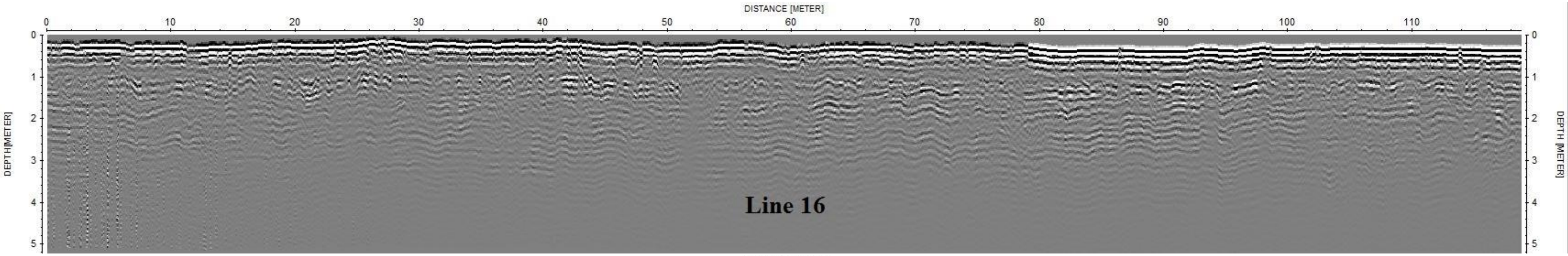
DISTANCE [METER]
DEPTH [METER]
DEPTH [METER]
Line 16

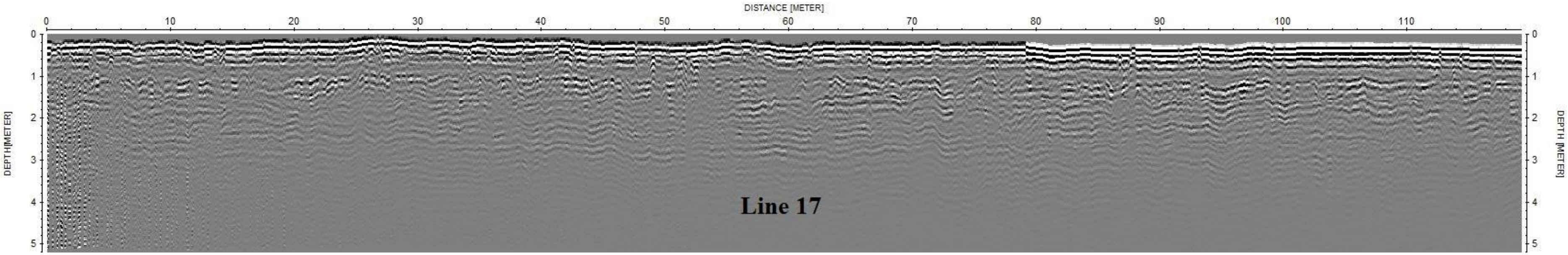
DISTANCE [METER]
DEPTH [METER]
DEPTH [METER]
Line 17

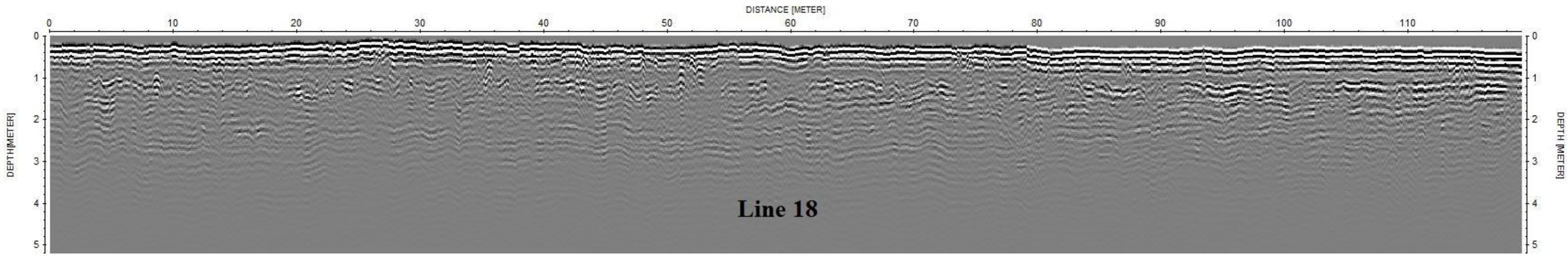
DISTANCE [METER]
DEPTH [METER]
Line 18

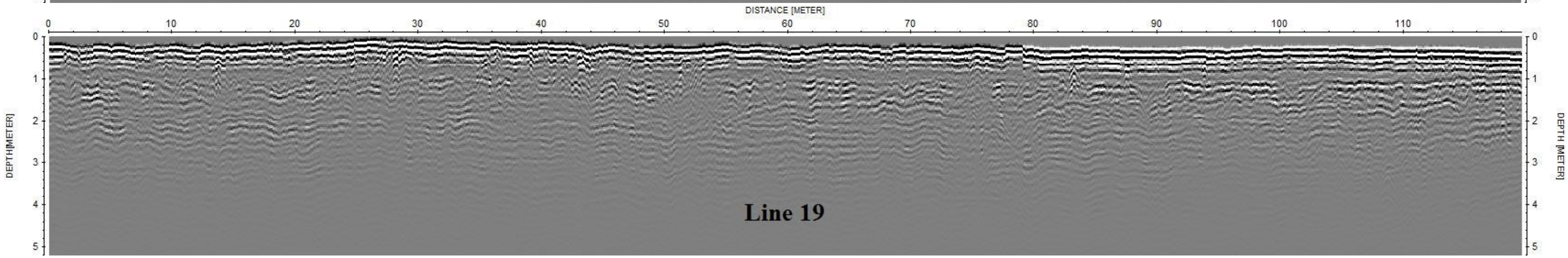
DISTANCE [METER]
DEPTH [METER]
Line 19

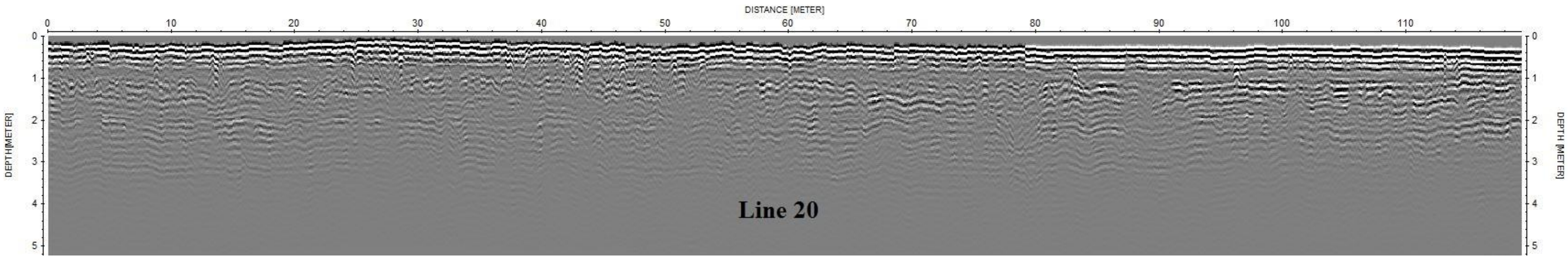
DISTANCE [METER]
DEPTH [METER]
Line 20

GPR Survey Results for Transect C

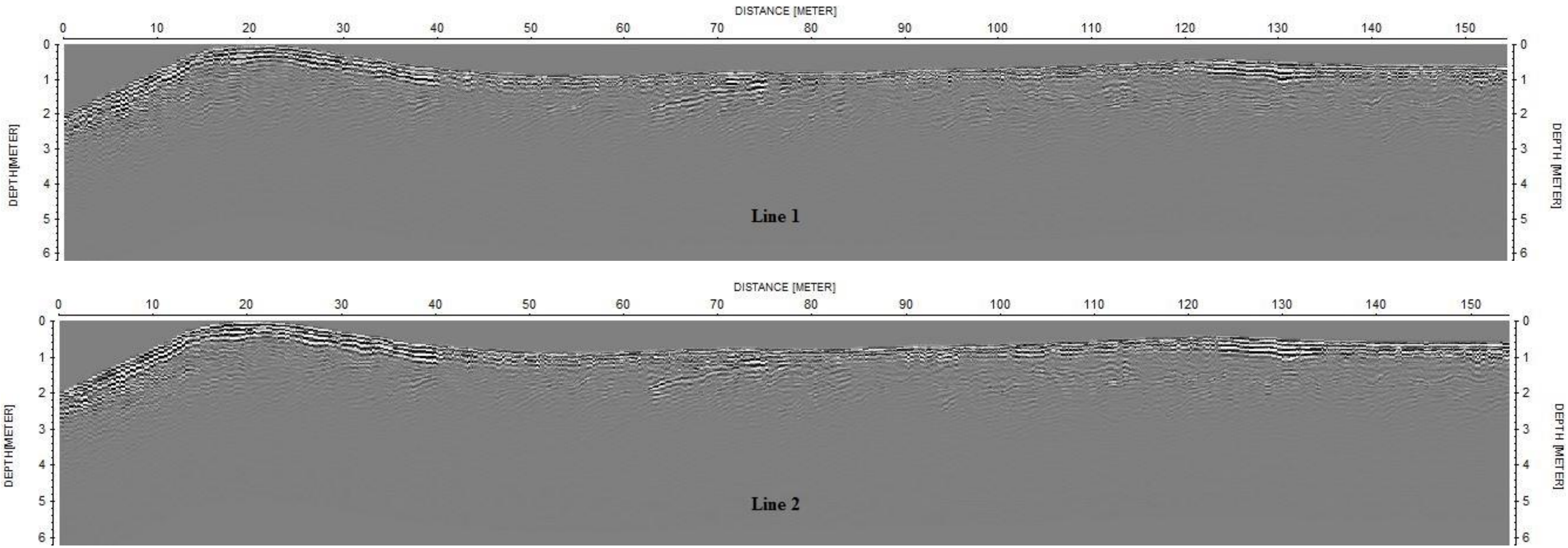

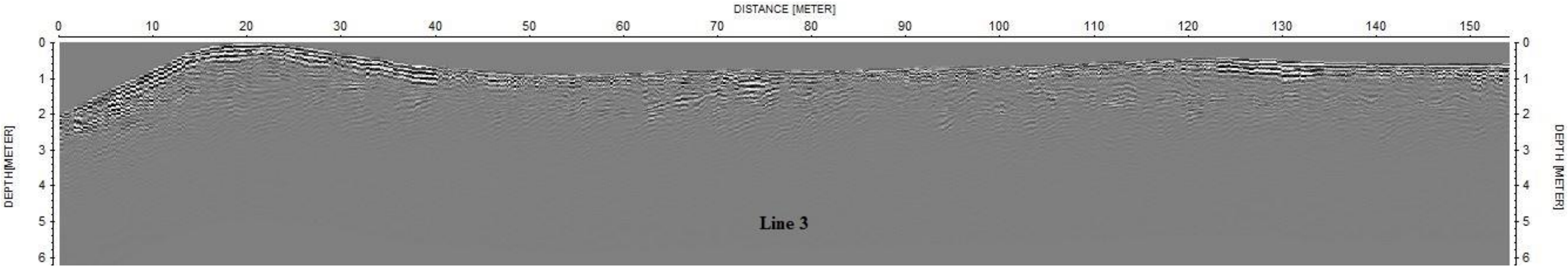
DISTANCE [METER]
0 10 20 30 40 50 60 70 80 90 100 110 120 130 140 150
DEPTH[METER]
0 1 2 3 4 5 6
DEPTH [METER]
Line 3

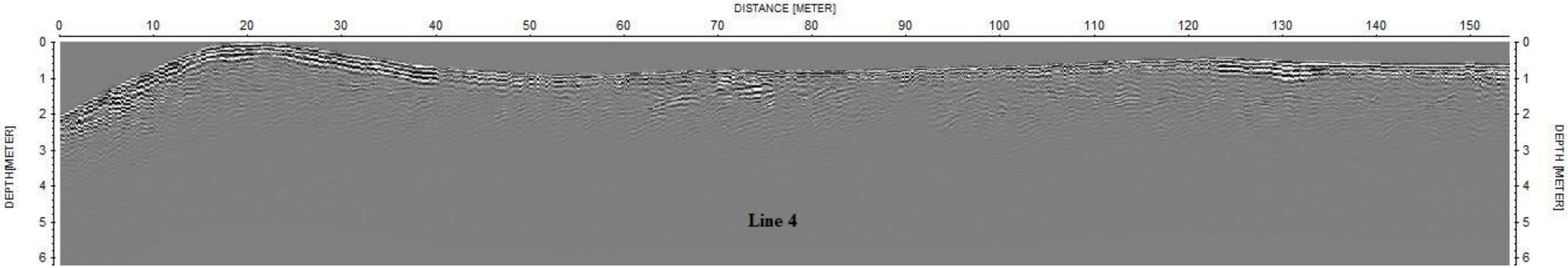
DISTANCE [METER]
0 10 20 30 40 50 60 70 80 90 100 110 120 130 140 150
DEPTH[METER]
0 1 2 3 4 5 6
DEPTH [METER]
Line 4

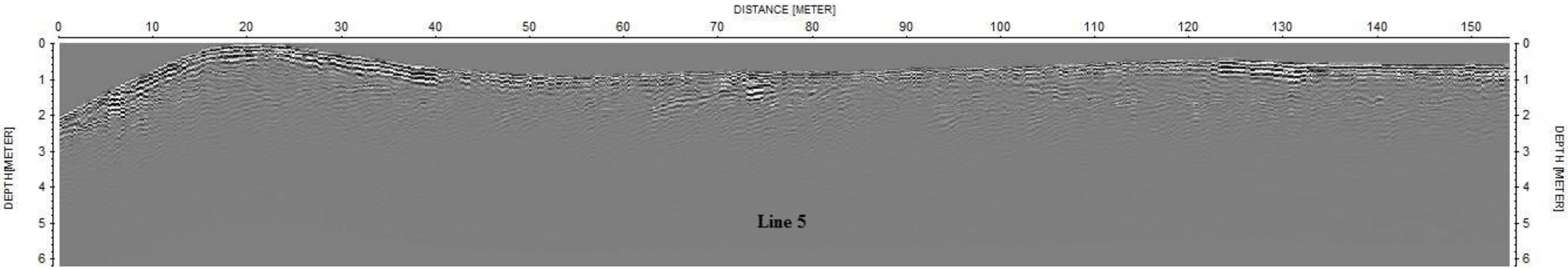
DISTANCE [METER]
0 10 20 30 40 50 60 70 80 90 100 110 120 130 140 150
DEPTH[METER]
0 1 2 3 4 5 6
DEPTH [METER]
Line 5

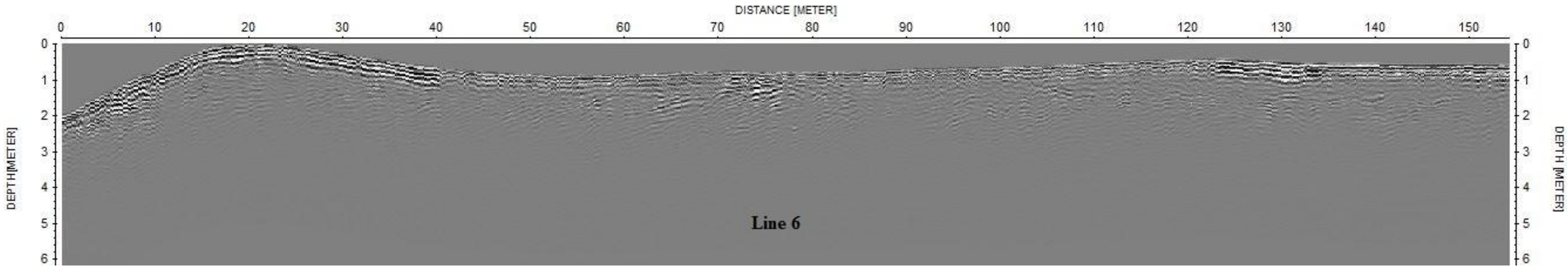
DISTANCE [METER]
0 10 20 30 40 50 60 70 80 90 100 110 120 130 140 150
DEPTH [METER]
0 1 2 3 4 5 6
Line 6
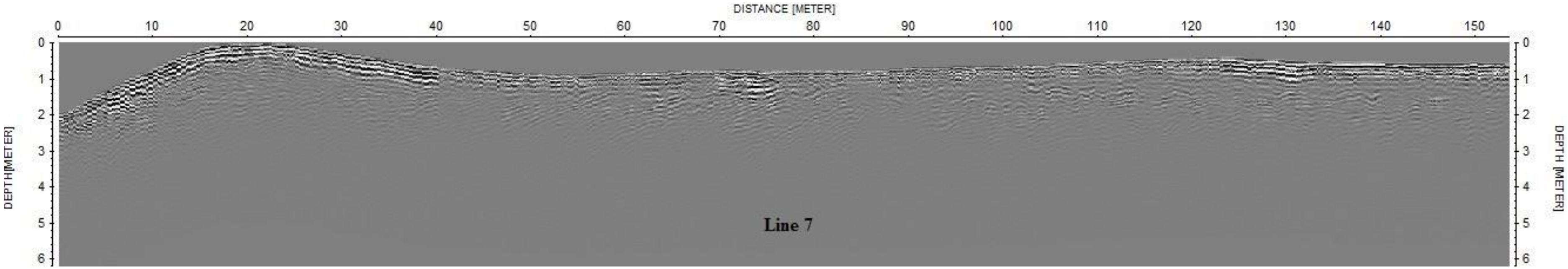
DISTANCE [METER]
0 10 20 30 40 50 60 70 80 90 100 110 120 130 140 150
DEPTH [METER]
0 1 2 3 4 5 6
Line 7
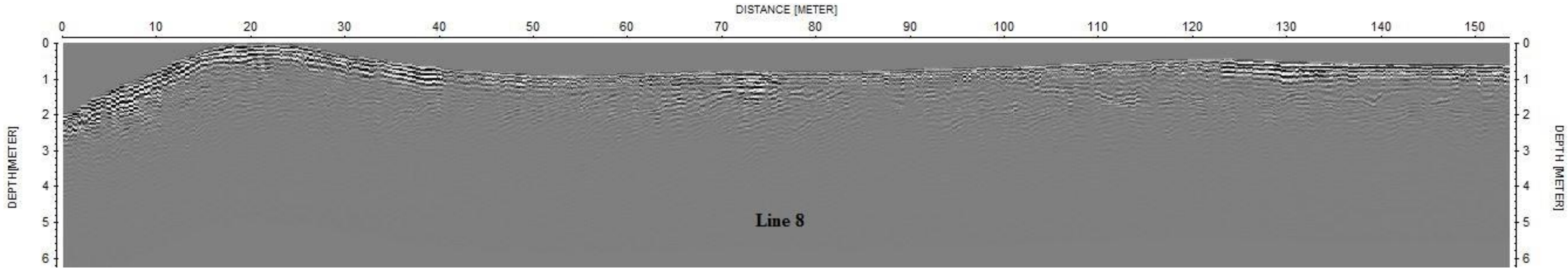
DISTANCE [METER]
0 10 20 30 40 50 60 70 80 90 100 110 120 130 140 150
DEPTH [METER]
0 1 2 3 4 5 6
Line 8

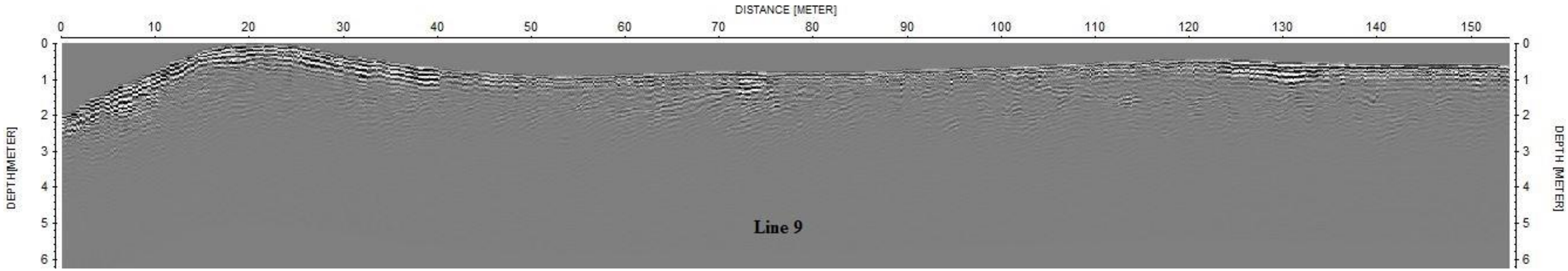
DISTANCE [METER]
0
10
20
30
40
50
60
70
80
90
100
110
120
130
140
150
DEPTH[METER]
0
1
2
3
4
5
6
DEPTH [METER]
Line 9

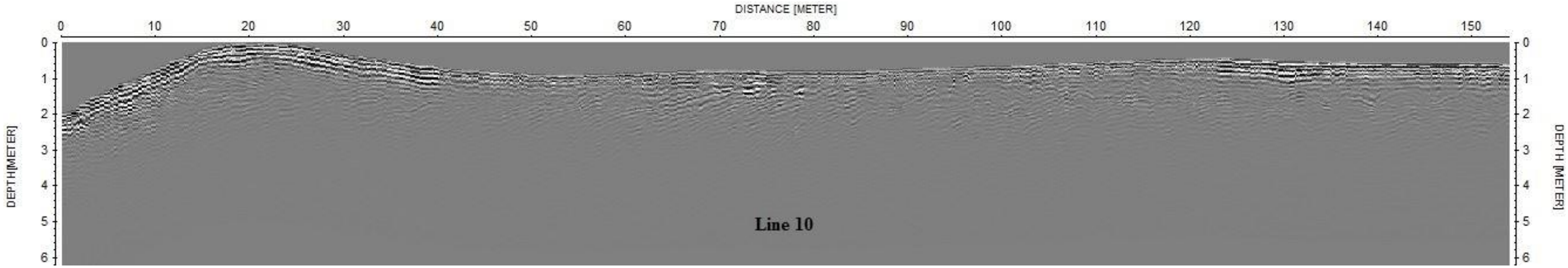
DISTANCE [METER]
0
10
20
30
40
50
60
70
80
90
100
110
120
130
140
150
DEPTH[METER]
0
1
2
3
4
5
6
DEPTH [METER]
Line 10

APPENDIX B: ELECTRICAL RESISTIVITY SURVEY RESULTS FOR THUNDIY

Raw geophysical survey files can be found at: http://dx.doi.org/10.4225/28/584755108d3dc

Sub-Survey Grid 1 From Transect A-B – Lines 1 to 4

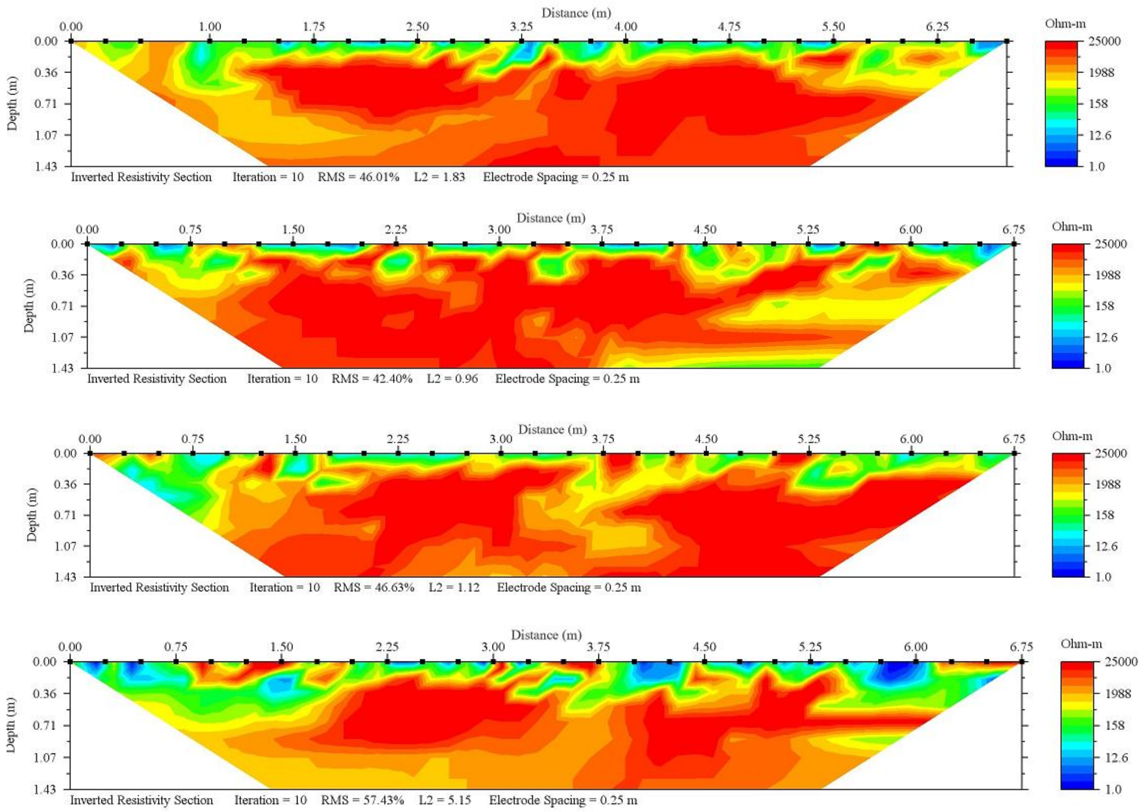

Sub-Survey Grid 2 From Transect A-B – Lines 1 to 4

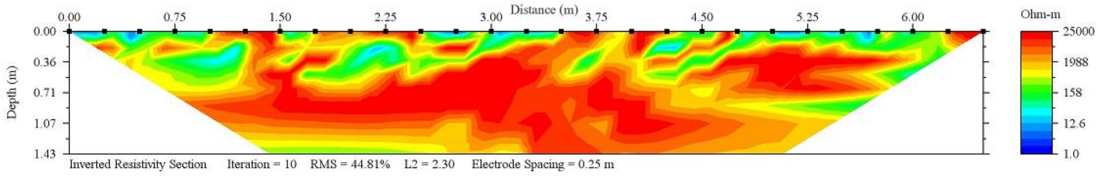

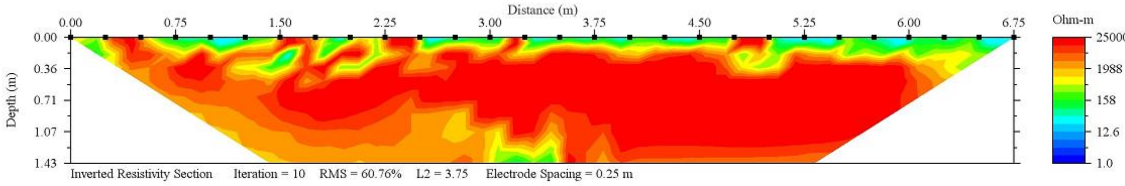

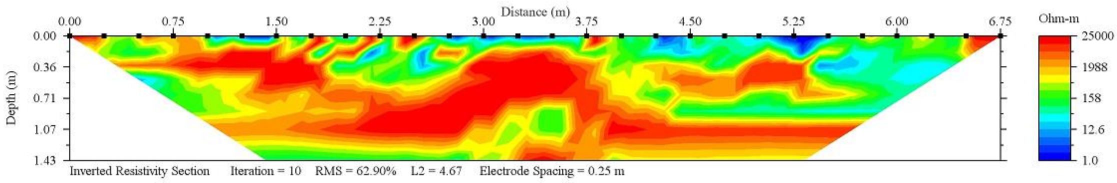

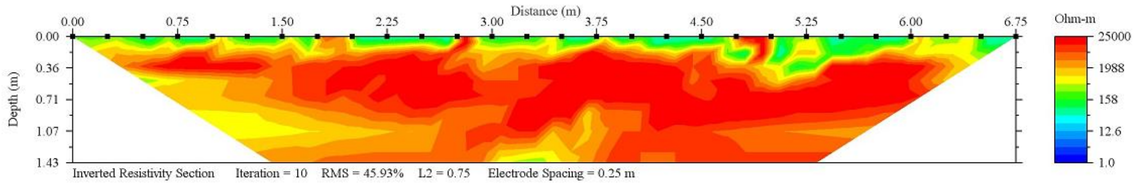

Sub-Survey Grid 3 From Transect A-B – Lines 1 to 4

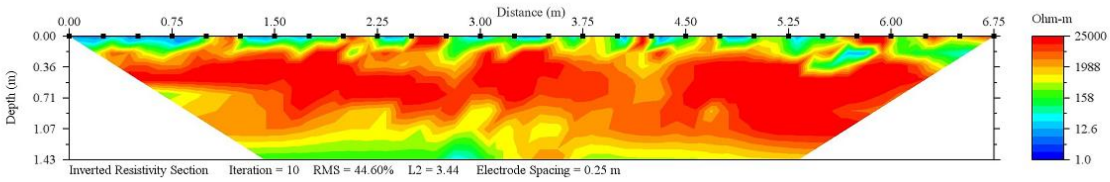

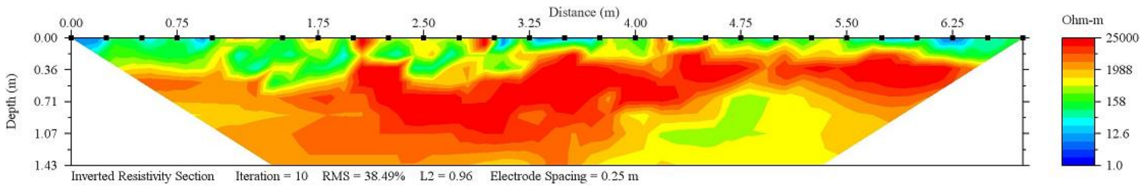

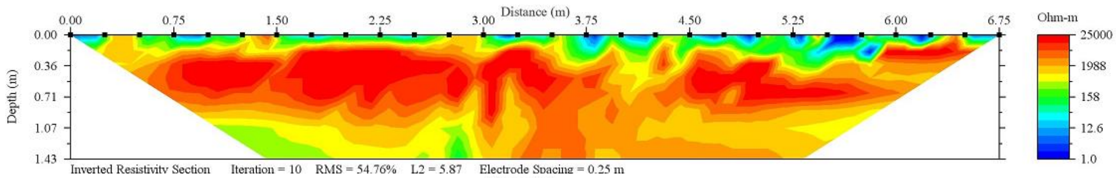

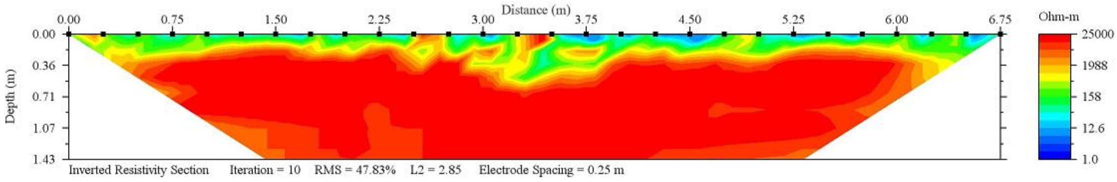

Sub-Survey Grid 1 From Transect C – Lines 1 to 4: This grid was on sloped ground so was topographically corrected.

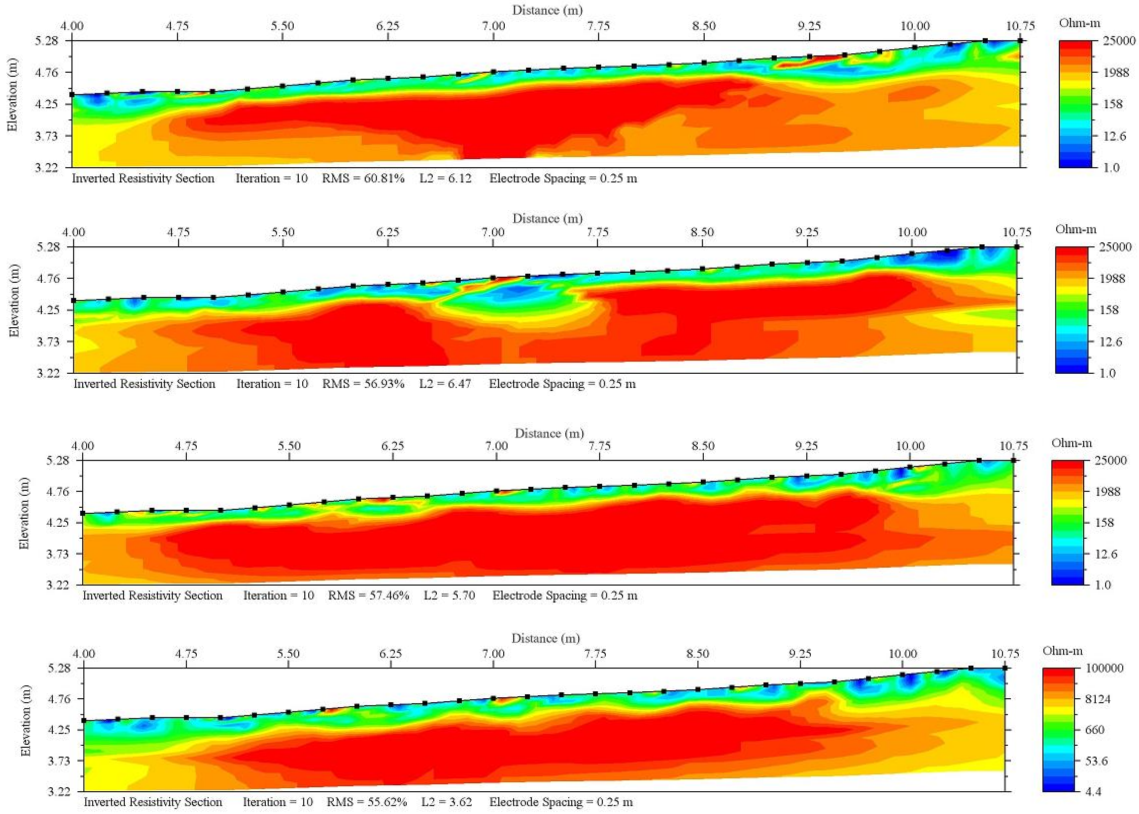

Sub-Survey Grid 2 From Transect C – Lines 1 to 4

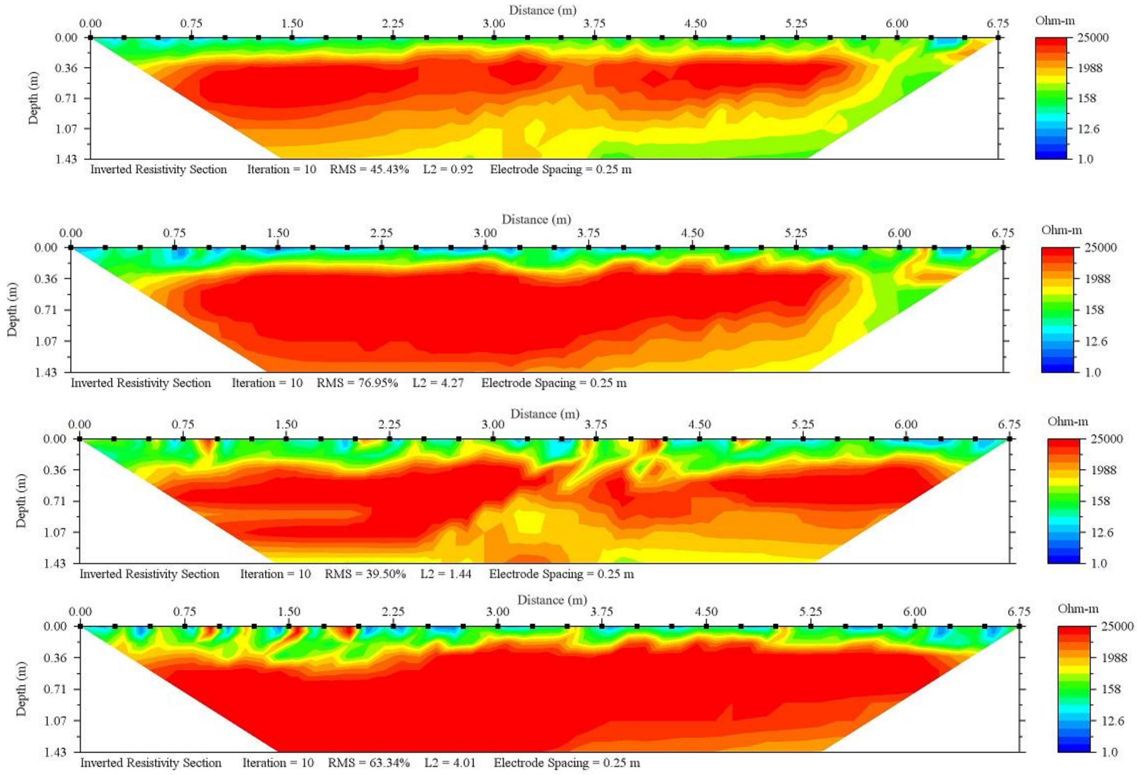

Sub-Survey Grid 3 From Transect C – Lines 1 to 4

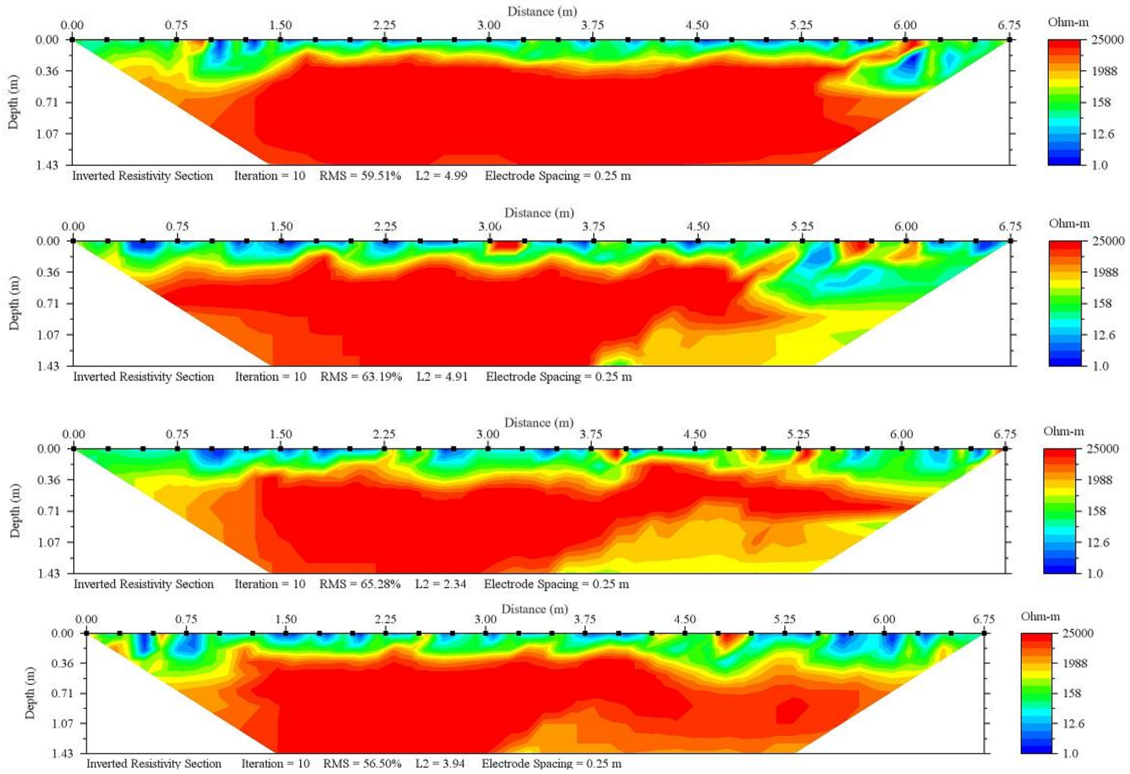

Sub-Survey Grid 4 From Transect C – Lines 1 to 4

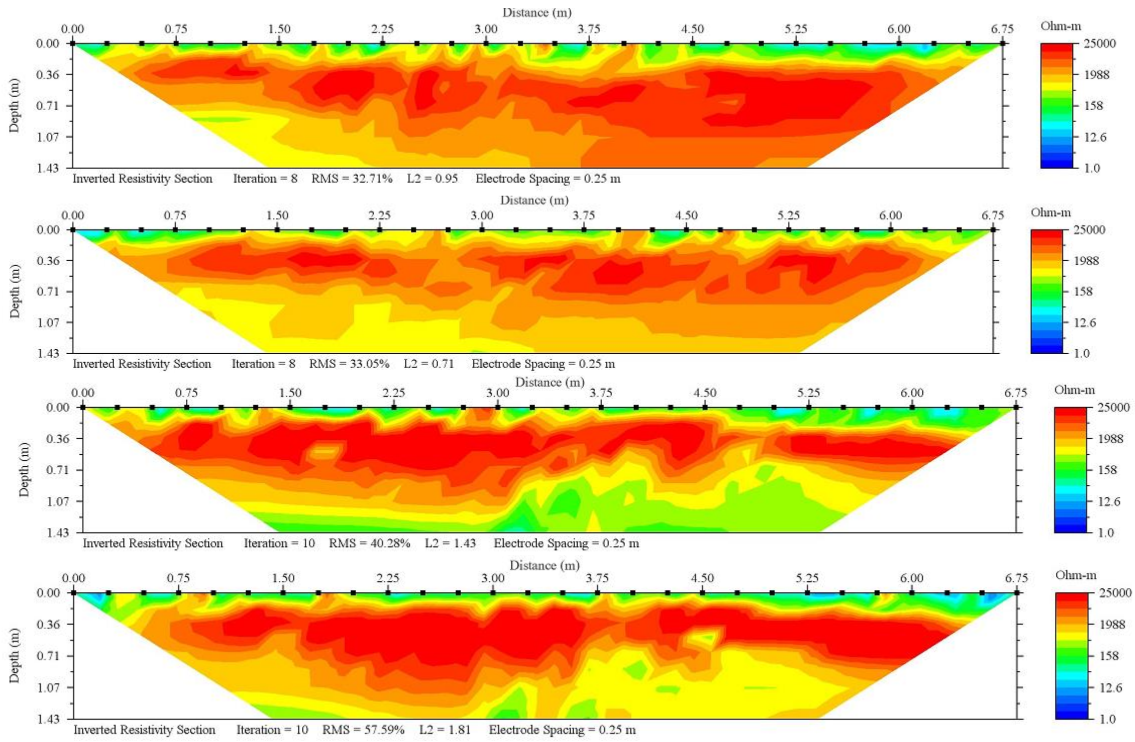

APPENDIX C: INCONCLUSIVE ELECTRICAL RESISTIVITY AND GPR SURVEY RESULTS FOR CAIRNS CAMPUS EXPERMIENTAL SITE

Raw geophysical survey files can be found at: http://dx.doi.org/10.4225/28/584755108d3dc

Electrical Resistivity Results Trench 1 – Lines 1 to 4

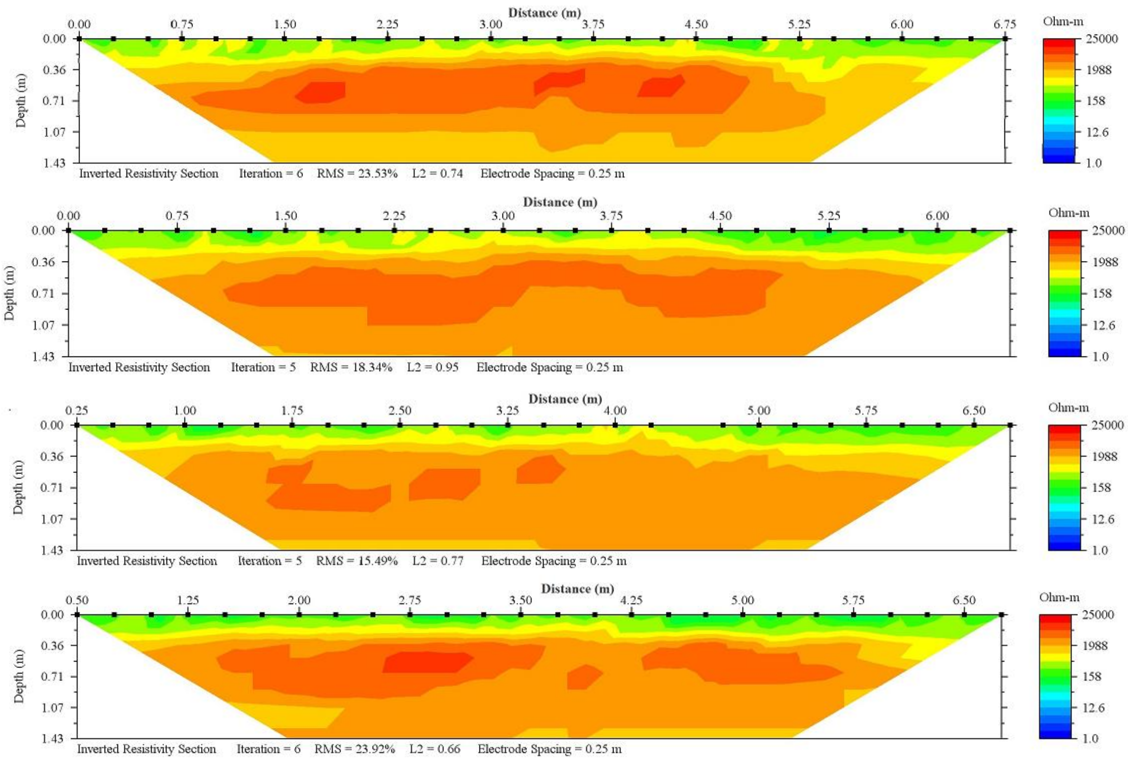

GPR Results Trench 2– Lines 1 to 8